



HAL
open science

Silica based materials for the encapsulation of β -Galactosidase

Ileana-Alexandra Pavel-Licsandru

► **To cite this version:**

Ileana-Alexandra Pavel-Licsandru. Silica based materials for the encapsulation of β -Galactosidase. Chemical engineering. Université de Lorraine, 2017. English. NNT : 2017LORR0322 . tel-01834554

HAL Id: tel-01834554

<https://theses.hal.science/tel-01834554>

Submitted on 10 Jul 2018

HAL is a multi-disciplinary open access archive for the deposit and dissemination of scientific research documents, whether they are published or not. The documents may come from teaching and research institutions in France or abroad, or from public or private research centers.

L'archive ouverte pluridisciplinaire **HAL**, est destinée au dépôt et à la diffusion de documents scientifiques de niveau recherche, publiés ou non, émanant des établissements d'enseignement et de recherche français ou étrangers, des laboratoires publics ou privés.



AVERTISSEMENT

Ce document est le fruit d'un long travail approuvé par le jury de soutenance et mis à disposition de l'ensemble de la communauté universitaire élargie.

Il est soumis à la propriété intellectuelle de l'auteur. Ceci implique une obligation de citation et de référencement lors de l'utilisation de ce document.

D'autre part, toute contrefaçon, plagiat, reproduction illicite encourt une poursuite pénale.

Contact : ddoc-theses-contact@univ-lorraine.fr

LIENS

Code de la Propriété Intellectuelle. articles L 122. 4

Code de la Propriété Intellectuelle. articles L 335.2- L 335.10

http://www.cfcopies.com/V2/leg/leg_droi.php

<http://www.culture.gouv.fr/culture/infos-pratiques/droits/protection.htm>



Collégium SCIENCES & TECHNOLOGIES
Pôle scientifique Chimie Physique Moléculaires
Ecole Doctorale SESAMES ED 412

Thèse de doctorat
Présentée pour l'obtention du titre de
Docteur de l'Université de Lorraine en Chimie
par
Ileana-Alexandra Pavel

Silica based materials for the encapsulation of **β -galactosidase**

Soutenu le 29 Novembre 2017

Membres du jury:

Rapporteurs:	Mihail Barboiu	Directeur de Recherche Institut Européen des Membranes, France
	Jordi Esquena Moret	Directeur de Recherche Institute of Advanced Chemistry of Catalonia, Espagne
Examineurs:	Vanessa Fierro	Directrice de Recherche au CNRS Institut Jean Lamour (IJL), France
	Bruno Medronho	Chargé de recherche Université de l'Algarve, Portugal
Directrice de thèse:	Andreea Pasc	Maitre de conférences (HDR) Université de Lorraine, France
Co-directeur de thèse:	Nadia Canilho	Maitre de conférences Université de Lorraine, France

Abstract

The engineering of solid dietary supplements provides several advantages in the industrial formulation of food products, in terms of its production, storage and handling. Thereby, the goal of this doctoral work is to design bio-responsive carriers for the encapsulation of an exogenous enzyme able to catalyze the hydrolysis of lactose towards simple sugar molecules. In fact, there is a consensus that the onset of symptoms characteristic of lactose intolerance are associated with lactase deficiency in the small intestine. Providing the organism with exogenous lactase is the underlying application targeted by this work through the design of silicabased materials for encapsulation.

The different types of bio-carriers developed had to overcome the simulated gastric conditions in order to release active enzyme molecules in the small intestine. Amorphous porous silica is a very good and non-toxic component affording protection versus acidic conditions, while providing controlled release. This inorganic material approved by the US Food and Drug Administration (FDA) has a relatively low cost, and presents a controlled structure (shape, size, pore diameter), as well as tunable surface chemistry.

In agreement with the main objectives, four bio-adapted encapsulation strategies were investigated as potential routes to produce solid dietary supplements for lactose intolerance treatment: (i) physical entrapment of the enzyme in pre-synthesized meso-macroporous silica materials, (ii) physical entrapment of the enzyme in low porosity silica particles coated by liposomes, (iii) encapsulation of the enzyme into thermosensitive solid lipid nanoparticles (SLNs) (iv) encapsulation of the enzyme into a biopolymer matrix coated in a mesoporous silica shell.

Resume

L'ingénierie des compléments alimentaires solides offre plusieurs avantages dans la formulation industrielle des produits alimentaires, en termes de production, stockage, et manipulation. Pour ces raisons, l'objectif de cette thèse était d'élaborer des 'cargos' bio-réactifs, permettant l'encapsulation d'une enzyme exogène capable de réaliser la réaction d'hydrolyse des molécules de lactose. Aujourd'hui il est établi que les symptômes caractéristiques de l'intolérance au lactose sont associés à une carence en lactase dans le gros intestine. Ainsi, fournir au corps humain de la lactase est l'application ciblée par ce travail, par la conception de matériaux siliciques comme support d'encapsulation.

En général, les types de cargos développés doivent surmonter les conditions gastriques pour libérer l'enzyme dans le gros intestine. La silice poreuse amorphe est un matériau inorganique non-toxique qui assure une bonne protection dans des conditions acides et permet une libération contrôlée au pH légèrement basique du colon. L'utilisation de silice amorphe poreuse permet à coût réduit d'obtenir une structure intrinsèque contrôlée (forme, taille particulaire, diamètre du pore) et une chimie de surface modifiable.

En accord avec les objectifs principaux, quatre stratégies d'encapsulation bio-adaptées ont été étudiées comme de potentiels voies pour la production de compléments alimentaires solides d'intérêt pour le traitement de l'intolérance au lactose : (i) immobilisation de l'enzyme par adsorption dans des matériaux siliciques meso-macroporeux pré-synthétisés, (ii) immobilisation de l'enzyme sur des particules de silice faiblement poreuses recouvertes par des liposomes, (iii) encapsulation de l'enzyme dans des nanoparticules de lipides solides (SLNs), (iv) encapsulation de l'enzyme dans une matrice de biopolymère recouvert d'une coque de silice mésoporeuse.

Popularized Abstract

Today smart technologies are everywhere. Most of them are related with electronics, right? But what about food? Can food be smart? Can food go beyond the necessity? What about having food that can treat, or even avoid allergies?

This PhD project is placed in the field of smart food designed to treat lactose intolerance. This investigation has been focused on the encapsulation of lactase, an enzyme or protein, that “cuts” lactose in glucose and galactose, more digestible sugars for our organism. For this, we have been working in the development of potential strategies of encapsulation of lactase in biocompatible and bio-responsive carriers. These have to protect and transport active enzyme macromolecules up to the small intestine where it can degrade the lactose molecules. Thus, the key property of these carriers is to protect the lactase from gastric pH conditions, while at the same time to release it in the small intestine. Therefore, these four main strategies were investigated: the encapsulation of enzyme in meso-macroporous silica, in thermo-responsive solid lipid nanoparticles, in a bio-polymer matrix coated with mesoporous silica shell or lactase immobilization on less porous silica beads protected by a liposome coating. All of the four are compatible in designing a route towards solid dietary supplements formulation.

This work has also perspective applications in dairy products manufacturing. So, enjoy some ice cream or some cheese and forget about lactose intolerance.

Résumé vulgarisé

Aujourd'hui les technologies intelligentes sont partout et surtout dans le domaine de l'électronique. Mais concernant la nourriture ? Peut-elle être un aliment intelligent ? Et répondre plus qu'à un besoin nutritionnel ? Que dirait-on d'un aliment traitant ou préventif des allergies ?

La thématique du sujet de cette thèse s'inscrit dans l'optique de contribuer au développement d'aliments intelligents permettant de traiter ou de soulager les personnes intolérantes au lactose. Ce travail de recherche a été focalisé sur l'encapsulation d'une lactase, autrement dit une enzyme ou une protéine, qui « coupe » le lactose en glucose et galactose qui sont des sucres plus facilement digérables pour notre organisme. Pour atteindre cet objectif, plusieurs stratégies d'encapsulation ont été étudiées afin d'obtenir des 'cargos' biocompatibles et bio-réactifs dans les conditions physiologiques. Néanmoins, le principal rôle des 'cargos' est de protéger l'enzyme du pH gastrique et de la transporter jusqu'à l'intestin petit pour qu'elle y dégrade les molécules de lactose. Ainsi, le cargo doit arriver intègre à l'intestin puis s'y désintégrer pour y libérer la lactase. C'est pourquoi, ces quatre stratégies d'encapsulation de l'enzyme ont été étudiées afin de répondre au cahier des charges : (i) encapsulation de l'enzyme dans un matériau silicique méso et macroporeuse, (ii) immobilisation dans des nanoparticules lipidiques solides, et (iii) dans une matrice bio-polymérique couverte par une coque de silice mésoporeuse ou (iv) immobilisation de la lactase sur des billes de silice faiblement poreuses protégées par une couche de liposomes. Ces méthodes d'encapsulation contribuent à l'élaboration de formulation de suppléments alimentaires solides.

Enfin, ce travail présente des perspectives d'application dans l'industrialisation de produits laitiers. Alors, appréciez une glace ou du fromage et oubliez les symptômes liés à l'intolérance au lactose.

Table of Contents

Acknowledgement	10
Abbreviations	12
General introduction	14
Introduction générale	17
Chapter 1. State-of-the-art	21
1.1. β-Galactosidase	21
1.1.1. Sources of Beta-galactosidase	21
1.1.1.1. <i>β-Galactosidases from bacteria</i>	23
1.1.1.2. <i>β-Galactosidases from fungi</i>	23
1.1.1.3. <i>β-Galactosidases from Plants</i>	24
1.1.1.4. <i>β-Galactosidases from yeast</i>	25
1.1.2. Lactose	26
1.1.2.1. <i>Lactose intolerance</i>	27
1.1.2.2. <i>Hydrolysis of lactose</i>	29
1.1.3. Techniques and matrices for immobilization	30
1.1.3.1. Methods of reversible immobilization	31
1.1.3.1.1. <i>Adsorption</i>	32
1.1.3.1.2. <i>Ionic binding</i>	34
1.1.3.1.3. <i>Hydrophobic adsorption</i>	34
1.1.3.1.4. <i>Affinity binding</i>	35
1.1.3.1.5. <i>Chelation or metal binding</i>	36
1.1.3.1.6. <i>Disulfide bonds</i>	38
1.1.3.2. Methods of irreversible immobilization	39
1.1.3.2.1. <i>Covalent immobilization</i>	39
1.1.3.2.2. <i>Entrapment</i>	41
1.1.4. Application of immobilized β-galactosidase	45
1.1.4.1. <i>Industrial application</i>	45
1.1.5. Conclusion	49
1.2. Silica-based systems for oral and food delivery	54
1.2.1. Prerequisite for oral delivery systems and food applications	55
1.2.2. Formation and origin of silica	57
1.2.2.1. Synthesis of non-porous silica nanoparticles	59
1.2.2.1.1. <i>Fumed silica nanoparticles</i>	59
1.2.2.1.2. <i>Stöber nanoparticles</i>	60
1.2.2.2. Synthesis of mesoporous silica	61
1.2.2.3. Synthesis of hybrid silica microparticles	65
1.2.2.4. Biosilica (silica diatoms)	67
1.2.3. Silica-based oral delivery systems and food applications	70
1.2.3.1. Passive release delivery systems	72
1.2.3.2. Active release delivery systems	75
1.2.3.2.1. <i>pH-controlled release</i>	75
1.2.3.2.2. <i>Enzyme-triggered release</i>	77
1.2.3.2.3. <i>pH/Enzyme-triggered release</i>	78
1.2.4. Silica health benefits and limitations	79

1.2.5. Conclusion	80
Chapter 2. Materials and Methods.....	85
2.1. Materials	85
2.1.1. Enzyme	85
2.1.2. Buffer solution	85
2.1.3. <i>In vitro</i> digestion solutions	85
2.1.4. Substrate	86
2.2. Preparation methods	86
2.2.1. Modified meso-macroporous silica supports- β -Gal _x @SiO ₂	86
2.2.1.1. Solid Lipid Nanoparticles (SLN) synthesis.....	86
2.2.1.2. Preparation of meso-macroporous silica supports	87
2.2.1.3. Preparation of modified meso-macroporous silica supports- β -Gal _x @SiO ₂	88
2.2.2. Liposomes coated silica particles (LCSP).....	89
2.2.2.1. Preparation of liposomes	89
2.2.2.2. Modification of porous silica particles (ESP)	89
2.2.2.3. Preparation of liposomes coated silica particles (LCSP)	90
2.2.3. Double emulsion type Solid Lipid Nanoparticles (SLN) synthesis	90
2.2.4. Preparation of hybrid materials	93
2.2.4.1. Preparation of hybrid alginate silica particles (ASP).....	93
2.2.4.2. Preparation of alginate core silica shell materials (SAM).....	93
2.2.4.3. Preparation of alginate particles (AP).....	93
2.3. Characterization methods	94
2.3.1. Protein Quantification Assay	94
2.3.2. Detection of enzyme and material activity	95
2.3.3. Enzyme release in simulated gastro-intestinal fluid	97
2.3.4. Dynamic light scattering.....	98
2.3.5. SAXS measurements	98
2.3.6. Nitrogen sorption analysis	99
2.3.7. Microscopy	99
2.3.8. Fourier Transform Infrared spectroscopy – FTIR.....	100
2.3.9. Thermogravimetric analysis (TGA)	100
2.3.10. Zeta potential measurements.....	101
2.3.11. DSC.....	101
Chapter 3. Physisorption on silica	103
3.1. Preferential adsorption of β-galactosidase regarding Hierarchical Meso-Macro porosity of a Silica Material	107
3.1.2. Morphology and texture of bare and enzyme-loaded silica supports.....	108
3.1.3. Interaction of β -galactosidase with the meso-macroporous material	113
3.1.4. Activity of free and immobilized enzyme into meso-macroporous silica materials.....	119
3.1.5. Conclusion.....	120
3.2 Silica-coated liposomes for β-galactosidase delivery	121
3.2.2. Characterization of bare and enzyme-loaded silica.....	122
3.2.3. Characterization of liposomes coated silica particles (LCSP).....	126
3.2.4. Enzyme activity during the immobilization and incubation	127
3.2.5. Enzyme release	128
3.2.5. Conclusion.....	132

Chapter 4. Encapsulation of β-galactosidase in responsive carriers allowing release triggered by either temperature or pH	137
4.1. Thermo-responsive food grade delivery system for the treatment of lactose intolerance	142
4.1.1. SLNs particle characterization.....	145
4.1.2. <i>In situ</i> UV-visible spectroscopy of enzyme activity	147
4.1.3. Conclusions and perspectives	157
4.2. pH-responsive hybrid silica-alginate carrier for lactose intolerance treatment.....	159
4.2.1. Particle characterization	160
4.2.2. Enzyme release in gastro intestinal simulated fluids	166
4.2.3. <i>Conclusion and perspectives</i>	168
General Conclusions and Perspectives	172
Conclusions générales et perspectives	176
Appendix 1 Techniques of characterization	180
DLS	180
Small angle X-ray scattering (SAXS).....	180
Nitrogen sorption analysis	181
Appendix 2 Shea butter technical sheet.....	185
Appendix 3 Halactase technical sheet.....	186

Acknowledgement

Firstly, I would like to thank the director of my thesis Dr. Andreea Pasc. For the three years I spent in her lab, *NANO Group of Laboratoire Structure et Réactivité des Systèmes Moléculaires Complexes (SRSMC), Unité Mixte de Recherche n°7565 of CNRS and of University of Lorraine*, she has guided my work and has supported my ideas. Her true passion for science, for chemistry and biochemistry are a true inspiration both for me and for her students. Her native curiosity has transferred into my work, offering me an enriched experience and allowing me to work on a variety of subjects, in an interdisciplinary fashion. I would particularly like to thank Nadia Canilho, my co-supervisor, for her patience and guidance that allowed me to grow as a researcher. On both a professional, as well as on a personal level I can truly say that I learned a lot from both of my supervisors. I am very grateful for the chance to be their PhD student, to be part of the SRSMC laboratory and for being included in the BIBAFOODS Marie Curie ITN. I thank Marie Curie actions, the European Union's Seventh Framework Program for research and the BIBAFOODS project (ITN 606713) for financing my work.

I would like to thank the members of the jury: Mihail Barboiu, Research Director at Institut Européen des Membranes and Jordi Esquena Moret, Research Director at Institute of Advanced Chemistry of Catalonia, who accepted to be rapporteurs, as well Bruno Medronho, Researcher (Investigador FCT) at Algarve University who accepted to be examiner. Last but not least, I would like to thank Vanessa Fierro, Research Director at CNRS, Institut Jean Lamour (IJL) the president of the jury. I truly appreciate their presence for my defense, as well as their constructive questions and comments on my work.

I thank Philippe Gros, professor at the University of Lorraine and director of the SRSMC laboratory, and Xavier Assfeld, professor at the University of Lorraine and director of the Doctoral School SESAMES for welcoming me to their respective institutions, and for always having a positive attitude.

Many thanks are also due to the many people that helped me and whom I met during this project.

From the SESAMES school, my PhD fellows, Sijin, Maxime, Philippe, Fernanda, Maciej, Hugo, Benjamin, Issam, Youssef, Timothé, Violetta, Audrey,

Sanghoon and Cheryl, I thank them for all the moments and memories we shared.

From SRSMC, Stéphane Parant and Katalin Selmeczi for their direct help in my research, and for their time, Paule Bazard for the efficiency in her work, Jean-Bernard Regnouf De Vains for allowing me to use his lab's infrastructure. Eric Dumortier, Lionel Richaudeau, Dominique Dodin and others who made me feel that I belonged to a big group (or in a big family).

Our many collaborators:

Surender Kumar Dhayal, Hans van den Brink and Martin Lund from Chr. Hansen for providing the enzyme and being great conversation partners.

Sofia Prazeres from University of Alcala for brightening the lab during her secondment. Gemma and Carnem, her supervisors, together with who we had a very fruitful collaboration in the project concerning the meso-macroporous silica.

Federico Amadei and his supervisor Dr. Tanaka from University of Heidelberg for their insight knowledge on the project concerning liposomes coted silica.

Yoran Beldengrün from IQAC-CSIC and his supervisor Jordi Esquena together with who we had a very fruitful collaboration in the project concerning pickering emulsions.

My BIBAFOODS fellows, Poonam, Maryam, Maria, Cigdem, Tomasz, Racha, Federica and Davide, I thank them for all the knowledge and fun we shared during our encounters.

I also thank to all senior researchers in the project, Tommy, Jens, Marité, Dennis, Tom, Björn, Maria, Bruno, Filipe, Carmen, Stefan and Anna, firstly for their entire contribution to the project and for always being a such pleasant and insightful company.

Last but not least, I would also like to thank my family who made the trip to see my presentation and to friends, who have been close to me and supported me all these years. Particularly, I would like to thank my husband, the chairman of ways and means, who has always been next to me, helped me, and with whom I share the love for science.

Abbreviations

α -CD: α -CD cyclodextrine
 β -gal: β -galactosidase
 β -Gal_x@SiO₂: enzyme absorbed on meso-macroporous silica
A.oryzae: *Aspergillus oryzae*
APTMS : aminopropyltriethoxysilane
AP: alginate particles
ASP: hybrid alginate silica particles
BCA: bicinchoninic acid
BCS: biopharmaceutical classification system
BET: Brunauer–Emmett–Teller
CALB: lipase B from *Candida antarctica*
CLA: colloidal liquid aphron
CLEA: Cross-linked enzyme aggregates
Ch: cholesterol
Con A: concanavalin A-enzyme
CSA: cooperative self-assembly
DDS: drug delivery systems
DLS: dynamic light scattering
DOPC: 2-dioleoyl-*sn*-glycero-3-phosphocholine
E. Coli: *Escherichia coli*
EDTA: ethylene diamine tetraacetic acid
FDA: US Food and Drug Administration
EFSA: European Food Safety Authority
EVA: ethylene vinyl acetate
Gal: galacto residue
GIT: gastrointestinal tract
Glc: Galactosyl residue
GMA: glycidyl methacrylate
GOS: Galacto-oligosaccharides
GRAS: generally regarded as safe
IMA: Immobilized Metal-Ion Affinity
IUPAC: International Union of Pure and Applied Chemistry
K.lactis: *Kluyveromyces lactis*
Kluyveromyces sp.: *Kluyveromices species*
LAB: Lactic acid bacteria
LCSP: liposomes coated silica particles
LCT: transcription mechanism
LDPE- low density polyethylene
MCM-41: **M**obil **C**omposition of **M**atter series
MPTS: Mercaptopropyl-trimethoxysilane
MSN: mesoporous silica nanoparticles
NBS: N-bromosuccinimide
NP: silica nanoparticles
NHP: Cetyl palmitate (n-hexadecylpalmitate)
NLC: nanostructured lipid carriers
NLU: neutral lactase units
OC: octyl-agarose
ONP: o-nitrophenol

ONPG: o-nitrophenyl- β -D-galactopyranoside
PBS: buffer phosphate
PC: phosphatidylcholine
PEI: polyethylenimine
PGPR: polyglycerol polyricinoleate
PMES: undec-1-en-11-yltetra(ethylene glycol) phosphate mono-ester surfactant
PsBGAL: pea seeds β -galactosidase
PU: unit of protease
RT: room temperature
SAP: alginate core silica shell particle
SAXS: Small angle X-ray scattering
SBA-15: Santa Barbara type
SBF: simulated body fluid
SDS: sodium lauryl sulfate
SGF: simulated gastric fluid
SEM: scanning electronic microscopy
SIF: simulated intestinal fluid
SLN: solid lipid nanoparticles;
subsp.: subspecies
SP: enzyme modified low porosity silica particles
TBG: tomato β -galactosidases
TEAH3: tri-ethanolamine
Thermus sp.-Thermus species
TMOS: tetramethylortosilicate
TEOS: tetraethylortosilicate
TEM-: transmission electronic microscopy
THP: trishydroxymethylphosphine
V_{max}: maximum velocity
ZnO: Native zinc oxide
ZnO-NP: Zinc oxide nanoparticles
W₁: water phase 1
W₂: water phase 2
W/O emulsion: inverse water in oil emulsion

General introduction

β -galactosidase or lactase is an enzyme naturally present in the small intestine that helps the organism to digest lactose molecules. The lactase acts as catalyst for the reaction of lactose hydrolysis, that produces simple sugars, glucose and galactose. It is now known that the majority of individuals with mild to severe symptoms of lactose intolerance present a lactase deficiency inducing an incomplete hydrolysis of the lactose. A significant fraction of global populations, around 70%, presents symptoms related to lactose intolerance. In fact, the natural production of lactase in human body gradually decreases after weaning in infancy. That is why, apart from genetically affected individuals, mainly adults develop this type of intolerance.

Consequently, lactose intolerant people avoid the consumption of dairy products. Some of them elect to take lactase supplements or to eat lactose-free foods, whose industrial production is still on the rise, notably through the use of β -galactosidases. Nevertheless, in most manufacturing processes the enzyme cannot be recovered and reused in another production cycle. On the other hand, the cost of extracting and isolating a specific enzyme remains high. As a result, the cost of producing lactose-free products is limited by the purchase price of the enzyme. Thus, one strategy is to immobilize the enzyme inside a solid support to facilitate catalyst recovery and to maintain the lactase activity along the production process. Another approach, which is underlying this work, is to introduce lactase directly into food. This method requires the encapsulation of the enzyme in a specifically designed carrier, which can be introduced as an additive during the production of any type of foods. The carrier must be compatible and responsive physiologically. In fact, as additive laws mandate, it should be food grade or above and as the oral delivery carrier, it must preserve and to protect the enzyme from the gastric pH to release it in the small intestine. This type of pH responsive carriers is usually prepared from biopolymers (e.g. zein, shellac, alginate, chitosan), from inorganic compounds like silica, or from a combination of both.

Mesoporous amorphous silica materials have been discovered in 1992. Ten years later in 2001, they started being intensively used as drug delivery

carriers, since amorphous silica had been approved as biocompatible. In fact, due to their tunable pore size, free volume and consequently large specific surface area, such a porous material offers a high uptake capacity for molecules with less than 50 nm diameter with the possibility to generate a controlled drug release system. Besides organic drugs, the porous material can also accommodate biomolecules such as enzymes. Since then, the development of sustained enzymatic catalysts is still a topic of intense investigations in very different applications (e.g. food, energy-biodiesel, pharmaceutical synthesis). The main challenges to be considered for designing supported enzyme catalysts are: retaining the native properties of the biomolecule, choosing the appropriate mode of immobilization for the intended application, and obtaining a good efficiency for the catalyst. Usually, enzyme immobilization on porous supports, either organic or inorganic, is achieved by physical adsorption (hydrogen bonding, Van der Waals interactions) or chemical adsorption through reactive linkers bonding directly the enzyme and the silica. In the perspective of increasing the enzyme loading, the life time and efficiency of the catalyst, amorphous meso-macroporous silica materials are of interest. This type of support is synthesized through a colloidal formulation. Colloidal engineering is a little explored route but in accordance with the results of this work, it appears as a promising approach to answer the challenging criteria previously announced.

In the present work, we focus on the design of biocompatible and bio-responsive enzyme carriers. Among the lactases, β -galactosidase from *Kluyveromyces lactis* source was chosen and used in this work. This enzyme is robust and a well-known catalyst for the hydrolysis of lactose in the dairy industry.

The investigation work is presented in four scientific chapters. Chapter 1 presents an overview on β -galactosidase sources and its applications. Different ways of immobilization to improve the enzyme performance are also presented and detailed. In the second part of Chapter 1, an overview of porous silica used as enzyme and drug delivery system for oral and food applications is detailed.

Chapter 2 entitled “Materials and methods” is describing in detail the experimental protocols, technics and chemicals used in this investigation.

Chapter 3 focus on the elaboration of two types of supported enzyme catalysts prepared from physical adsorption of the β -galactosidase on: (1) a meso-macroporous silica obtained through colloidal engineering is described in the first part of the chapter, and (2) a commercially available silica material, presenting low porosity, coated in a lipid bilayer for protection. In the case of the meso-macroporous material, the adsorption of the enzyme was investigated as a function of pore size and related to the specific activity within the material. The release and the catalytic efficiency, e.g. the activity of the enzyme, has been studied for liposomes coted carriers in simulated gastrointestinal fluids.

Chapter 4 presents β -galactosidase encapsulation in two different types of carriers: (1) solid lipid nanoparticles (SLNs) obtained from a double emulsion of Water/Oil/Water (W/O/W), and (2) hybrid silica-alginate particles. The SLN entrapment approach in was investigated to design a physiological thermo-responsive carrier that would free the enzyme at a certain temperature. The entrapment of β -galactosidase in hybrid silica-alginate particles strategy was investigated as a controlled release pH stimuli carrier for intestinal delivery.

The general conclusions and perspectives of future work are compiled in Chapter 5.

Introduction générale

La β -galactosidase ou la lactase est une enzyme est naturellement présente dans l'intestin grêle et participe à la digestion de molécules de lactose. La lactase agit comme un catalyseur pour la réaction d'hydrolyse du lactose, à l'issue de laquelle des sucres simples comme le glucose et le galactose sont formés. Il est maintenant connu que la majorité des individus avec des symptômes faibles à sévères d'intolérance au lactose, présentent une carence en lactase, induisant une hydrolyse incomplète du lactose. La fraction d'individu présentant des symptômes liés à l'intolérance au lactose représente 70% de la population globale. Il est avéré que la production naturelle de la lactase dans le corps humain baisse dans l'enfance après le sevrage laitier. C'est pourquoi, outre les individus affectés génétiquement, de nombreux adultes sont affectés par ce type d'intolérance.

En conséquence, les personnes intolérantes au lactose évitent la consommation des produits laitiers, mais certaines préfèrent prendre des suppléments de lactase ou manger des produits sans lactose, dont la production industrielle est en plein essor, notamment par l'usage de β -galactosidases. D'autre part, le coût d'extraction et d'isolation d'une enzyme spécifique reste élevé. De ce fait, le coût de production des produits sans lactose est limité par le prix d'achat de l'enzyme. Ainsi, une stratégie pour réduire le coût est l'immobilisation d'enzyme dans un support solide pour faciliter la récupération du catalyseur et pour maintenir l'activité de lactase durant le processus de production. Une autre approche, sous-jacente à ce travail, est l'introduction de la lactase directement dans la nourriture. Cette méthode requiert l'encapsulation de l'enzyme dans un transporteur spécialement conçu, qui peut être ajouté comme un additif durant la production de tout type de nourriture. Le transporteur doit être biocompatible et sensible au milieu physiologique du corps humain. Ainsi, comme les additifs alimentaires, la composition du transporteur il doit également être de grade alimentaire (« food grade »). Le transporteur doit aussi préserver et protéger l'enzyme du pH gastrique, pour favoriser la libération de l'enzyme dans l'intestin grêle. Un tel transporteur réactif au pH sont généralement préparés

à partir de biopolymères (e.g. zein, shellac, alginate, chitosan), de composés inorganiques comme la silice ou d'une combinaison des deux.

Les matériaux de silice amorphe ont été découverts en 1992, et dix ans plus tard, en 2001, ils ont été utilisés intensivement comme transporteurs pour les médicaments, suite à l'approbation par l' 'European Food Safety Authority' (EFSA) et la 'US Food and Drug Administration' (FDA). En effet, comme les dimensions et le volume de ces pores sont adaptables, la surface spécifique d'un matériau de silice amorphe poreux peut être importante. De ce fait, un tel support poreux présente une grande capacité de chargement pour les molécules de tailles inférieures à 50 nm. Ces matériaux poreux offrent aussi la possibilité d'une libération contrôlée des molécules encapsulées. Ainsi, le développement de catalyseurs enzymatiques est un thème d'investigation intense pour des applications très diverses (e.g. nourriture, énergie-biodiesel, synthèse pharmaceutique). Les principaux défis à prendre en considération pour fabriquer le catalyseur d'enzyme supporté sont les suivants : préserver les propriétés natives de la biomolécule, choisir une stratégie adaptée à l'application visée, et finalement obtenir une bonne efficacité catalytique. Normalement, l'immobilisation de l'enzyme sur supports poreux, organiques ou inorganiques, est effectuée par adsorption physique (liaisons d'hydrogène, interactions Van der Waals), ou par adsorption chimique de l'enzyme sur le support par liaison covalente. En perspective, pour augmenter le degré de chargement de l'enzyme dans le support, la durée de vie et l'efficacité du catalyseur formé, les matériaux de silice amorphe méso-macroporeuse présentent un fort intérêt. Ce type de support silicique est synthétisé à partir d'une émulsion qui est une dispersion colloïdale d'une phase huileuse dans l'eau et vis-versa. L'ingénierie colloïdale dans ce domaine est une voie peu explorée, mais d'après ce travail de thèse, cette approche est prometteuse pour répondre aux défis annoncés précédemment.

Ce travail est focalisé sur la conception des transporteurs biocompatibles et bio-sensibles. Parmi les lactases, la β -galactosidase extraite de la levure *Kluyveromyces lactis*, a été choisie dans ce travail. Cette enzyme

est robuste et bien connue dans l'industrie laitière comme catalyseur pour l'hydrolyse de lactose.

Ce travail d'investigation est présenté en quatre chapitres de recherche expérimentale. Le Chapitre 1 fait l'état de l'art des sources de β -galactosidase et leurs applications. D'autre part, les différentes voies d'immobilisation de l'enzyme sur des supports solides sont aussi présentées en détail. Dans la deuxième partie du Chapitre 1, fait état de la littérature portant sur la silice poreuse, utilisée comme systèmes de transport pour la libération de médicaments et d'enzymes par voie orale.

Le Chapitre 2 intitulé « Matériaux et Méthodes » décrit en détail les protocoles expérimentaux, les techniques et les composées utilisés pour mener cette recherche.

Le chapitre 3 est dédié à l'élaboration de deux types de catalyseurs supportés préparés par l'adsorption physique de β -galactosidase sur : (1) silice méso-macroporeuse obtenue par ingénierie colloïdale et (2) des billes de silice commerciales avec une faible porosité, protégées par une couche de liposomes. Dans le cas du matériel méso-macroporeux, l'adsorption de l'enzyme était étudiée en fonction de la dimension du pore et rapporté à l'activité intrinsèque du matériel. La libération, l'efficacité catalytique et l'activité de l'enzyme, ont été étudiés dans fluides gastrique et intestinal simulés pour les transporteurs enrobés par les liposomes.

Le chapitre 4 présente l'encapsulation de β -galactosidase dans deux types de transporteurs : (1) des nanoparticules lipidiques solides (NLS) obtenues par une émulsion eau/huile/eau (w/o/w), (2) des particules hybrides silice-alginate. L'approche d'emprisonnement dans des NLS était étudiées pour concevoir un système transporteur répondant à la température physiologique du corps humain facteur déclenchant la libération de l'enzyme. Quant au second systèmes, l'emprisonnement de la β -galactosidase dans des particules hybrides silice-alginate, a été étudié comme système de transport sensible au pH pour permettre une libération contrôlée de l'enzyme dans l'intestin grêle.

Enfin, les conclusions générales et les perspectives de ce travail sont exposées dans le chapitre 5.

Chapter 1. State-of-the-art

1.1. β -Galactosidase

β -Galactosidase (lactase, EC 3.2.1.23) is an enzyme that hydrolyses D-galactosyl residues from oligosaccharides, polymers and secondary metabolites. The enzyme can be used in dairy industry, in problems associated with whey disposal and lactose crystallization (sweetened and frozen dairy products) [1] or to produce prebiotics (by the production of galactooligosaccharides) [2,3]. However, because free β -galactosidase is very expensive and somewhat sensitive to external factors immobilisation is required. This makes the enzyme more economically feasible by improving its catalytic activity and allowing its reuse in batch reactors.

Enzyme identification is given by the EC number. It describes classes of enzymes catalyzing similar reactions and is a numerical nomenclature that groups enzymes based on the overall reaction that catalyzed. The EC number of β -Galactosidase means that the reaction that the enzyme catalyzes is the hydrolysis of terminal non-reducing β -D-galactose residues in β -D-galactosides.

1.1.1. Sources of Beta-galactosidase

β -Galactosidases are found in plants (peaches, apricots, almonds [4], apples, kiwis [5], tomatoes [5,6]), animal organs or in microorganisms (bacteria, fungi [7,8] and yeasts Table 1.1 .1. The enzymes produced in large (industrial) quantities are mainly obtained from *Aspergillus* sp., *Kluyveromyces* sp. and *E. Coli*.

Table 1.1 .1 Sources of β -galactosidase (adapted after [9]).

Plants	peach, apricot, kefir grains, almond, tips of wild roses, alfalfa seeds, coffee berries, beans	[4,10–12]
Animals	small intestine, brain and skin tissue	[13]
Fungi	<i>Kluyveromyces (Saccharomyces) lactis</i> , <i>Kluyveromyces (Saccharomyces) fragilis</i> , <i>Brettanomyces anomolus</i> , <i>Wingea robersii</i>	[14,15]
Bacteria	<i>Escherichia coli</i> , <i>Streptococcus thermophilus</i> , <i>Bacillus circulans</i> , <i>Bacillus steorotherphilus</i> , <i>Lactobacillus sporogenes</i>	[16][17][18][19]

Yeast *Aspergillus niger, Aspergillus oryzae, Curvularia inoegualli* [21][22][23]

The properties of β -Galactosidases, such as structure or size, varies with the source, but their specificity (hydrolysis of D-galactosyl residues) remains essentially the same. The characteristics of β -galactosidase from different sources are shown in Table 1.1 2.

Table 1.1 2. Properties of β -galactosidases from different sources.

SOURCES	OPTIMAL PH	OPTIMAL TEMPERATURE	ACTIVATORS	INHIBITORS	REF
<i>A. NIGER</i>	3.0-4.0	55-60	none	none	
<i>A. ORYZAE</i>	4-6	40-55	none	Hg ²⁺ , Cu ²⁺ , NBS ⁺ , SDS ⁺	[24]
<i>K. FRAGILIS</i>	6.9-7.3	37	Mn ²⁺ , K ⁺ , Mg ²⁺	Ca ²⁺ , Na ⁺	[25]
<i>K. LACTIS</i>	6.5-7.3	35	K ⁺ , Mg ²⁺	Ca ²⁺ , Na ⁺	[14]
<i>E. COLI</i>	7.2	40	Na ⁺ , K ⁺		[26]

*NBS: N-bromosuccinimide, SDS: sodium lauryl sulfate

Ca²⁺ ions are known to be an inhibitor for β -galactosidase. However, the enzymatic activity of β -galactosidase is not affected by the calcium ions in milk since they are bounded to casein [27]. Divalent cations, such as magnesium and manganese, may enhance the β -galactosidase activity, while monovalent cations may have a positive or negative effect depending of the origin of the enzyme [27].

The β -galactosidase enzyme exists in three forms in human intestine:

- 1- lactase found in the edge membrane of the epithelium of the small intestine (this enzyme is solely responsible for the hydrolysis of lactose);
- 2- lactase found in the lysosome of the epithelium cells of small intestine. It is also called acid β -galactosidase;
- 3- the hetero- β -galactosidase found in the cytoplasm of the epithelium cells of small intestine.

1.1.1.1. β -Galactosidases from bacteria

β -Galactosidases from bacterial sources have been widely used in food industry due to their advantages, as high activity and stability of the enzyme and ease of fermentation [28]. Lactic acid bacteria (LAB) have been the most studied and consist of *Lactobacillus delbrueckii* subsp. *bulgaricus* and *Streptococcus thermophilus* (the strains of yogurt culture). The main reasons of why they gained attention are: (i) little or no adverse effects in the consumption of some fermented dairy products by lactose maldigestion (ii) the enzyme derived from them may be used without extensive purification since they are generally regarded as safe (GRAS), (iii) the probiotic activity found for some strains, which improve the digestion of lactose [29,30].

The highest production and specific activity of β -Galactosidases was attained with *Bifidobacterium longum* CCRC 15708 strain, compared with *Bifidobacterium infantis* CCRC 14633 and *Bifidobacterium longum* B6 strains [29]. These bacteria are also used as probiotics for their potential health benefits. Bifidobacteria are present in the human and animal gut, and appear in newborns within days after birth [31]. β -galactosidase present in the colon of humans catalyses the first step of lactose fermentation. Its activity is an indicator of the capacity of colonic microbiota to ferment the lactose present in the intestine [32].

1.1.1.2. β -Galactosidases from fungi

Fungal β -galactosidases are effective in the hydrolysis of lactose present in whey (an acidic product), their optimal pH being 2.5–5.4. Fungal β -galactosidases are more sensitive to product inhibition but present the advantage of thermal stability [33]. Thermophilic β -galactosidase are one of the most robust enzymes. They present a built-in stability to temperature and other inactivation agents. They are used in industrial processing of dairy products along with heat treatment to lower the microbial contamination and obtain a sterile product [34]. In the food industry, free and immobilized enzyme forms are used. For example, β -Galactosidases from thermophile microorganisms such as *Thermus sp.* strain T2 can be used for the simultaneous soft thermal treatment and the hydrolysis of lactose [35,36].

β -galactosidase can be purified from *Aspergillus oryzae* (*A. oryzae*) RT102 strain by 2-propanol fractional column chromatography on DEAE-Sephadex A-50 and Sephadex G-200 [24]. The amino acid sequence of the enzyme includes 1005 residues with an average molecular mass of 110 kDa. The three dimensional model of *A. Oryzae* β -galactosidase shows that it is a monomeric enzyme with the active site similar with *Penicillium sp.* and *Trichoderma reesei* β -galactosidase [37]. Figure 1.1. 1. represents the three-dimensional structure of the ribbon model (A) and the catalytic center of the enzyme (B).

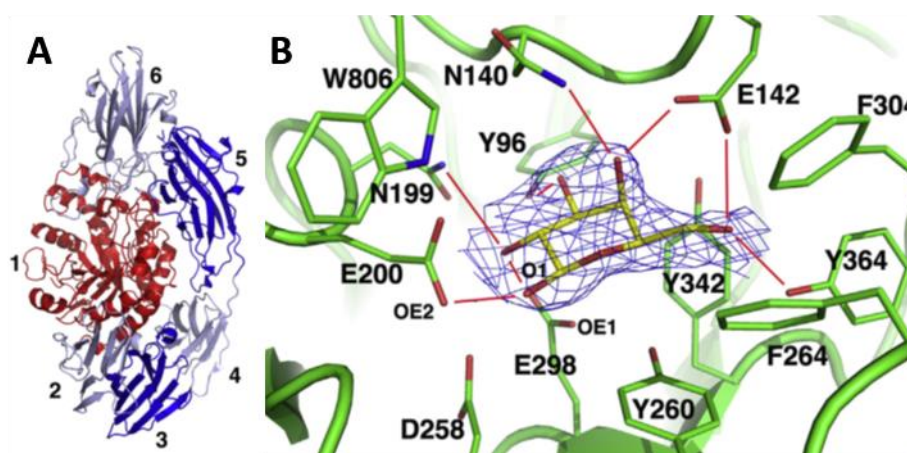


Figure 1.1. 1. The three dimensional structure of the ribbon model (A) and the catalytic center of the enzyme (B) of *A. oryzae* β -galactosidase (reproduced after [37]).

1.1.1.3. β -Galactosidases from Plants

β -Galactosidases are widely distributed in plant tissues. β -galactosidases from chickpea, radish, mung beans [38], barley, carrot [39], rice shoots [40], lupins [41], and kidney beans [42] have also been isolated, purified and characterized. Plant β -galactosidases are generally dimeric and much smaller compared with other β -galactosidases. Such enzymes have an optimal pH in the acidic range (3.5-7) [43]. Moreover, these enzymes are not only involved in the hydrolysis of lactose but also in plant growth and fruit ripening and development [38,44]. β -galactosidase activity has been reported during tomato fruit ripening (*Lycopersicon esculentum* Mill.) The cDNAs of a family of seven tomato β -galactosidase (TBG) was recognized [45]. Significant decrease in cell wall galactosyl content and the associated pectin degradation that helps with the ripening of fruit has been associated with the presence of the β -

galactosidases [46]. It has been established that β -galactosidase in papaya is responsible for the hydrolysis of its cell wall and softening of the fruit during ripening with sugar release, [47] as in the case of strawberries ripening [48]. For comparison, β -galactosidase from the cotyledons of germinated nasturtium (*Tropaeolum majus* L.) seeds is involved in *in vivo* hydrolysis of stored xyloglucan [49].

β -Galactosidase isolated and purified from plants can be used for the hydrolysis of lactose from milk. *Cicer arietinum* (chickpeas) extracted enzyme was immobilized on two different types of resins and evaluated as a cheap way to remove the lactose from milk [50]. β -galactosidase isolated from almond (*Amygdalus communis*) extracted by ammonium sulfate precipitation was used in a stirred milk batch process. This enzyme could hydrolyse 90% of lactose in milk and 94% lactose in buffer solution and whey [4]. β -galactosidase from pea seeds (PsBGAL) proved to be very unstable at low concentrations at 4°C. To work around this instability, Dwevedi et al. immobilized it on Amberlite MB-150 beads (5 μ m diameter) with glutaraldehyde. The enzyme maintained its activity for a period of 12 months at room temperature, and through its reusability cycles in lactose hydrolysis [51]. The same research group optimized PsBGAL immobilization on Sephadex and chitosan with glutaraldehyde. The new obtained catalyst presented a broad optimal working temperature and large pH intervals. The higher temperature stability and reusability propose it as suitable for industrial applications [52].

1.1.1.4. β -Galactosidases from yeast

The natural habitat of the *Kluyveromyces lactis* (*K. lactis*) yeast can be found in dairy. The β -galactosidase extracted from *K. lactis* yeast presents a good lactose hydrolysis activity. For this reason β -galactosidase from this yeast is commercially feasible and largely used in industry [53,54]. The *K. lactis* β -galactosidase forms a homo-oligomer of four identical units, a tetrameric enzyme, that was described as a dimer of dimers [55]. It is active in its tetrameric and dimeric forms [14]. The enzyme is formed of 1024 residues and have a molecular mass of 119 kDa. The monomer folds into five domains (Figure 1.1. 2. A), that contain two long insertions related to the oligomerization and

specificity. Each dimer contains two catalytic centres at the interface (Figure 1.1. 2 B).

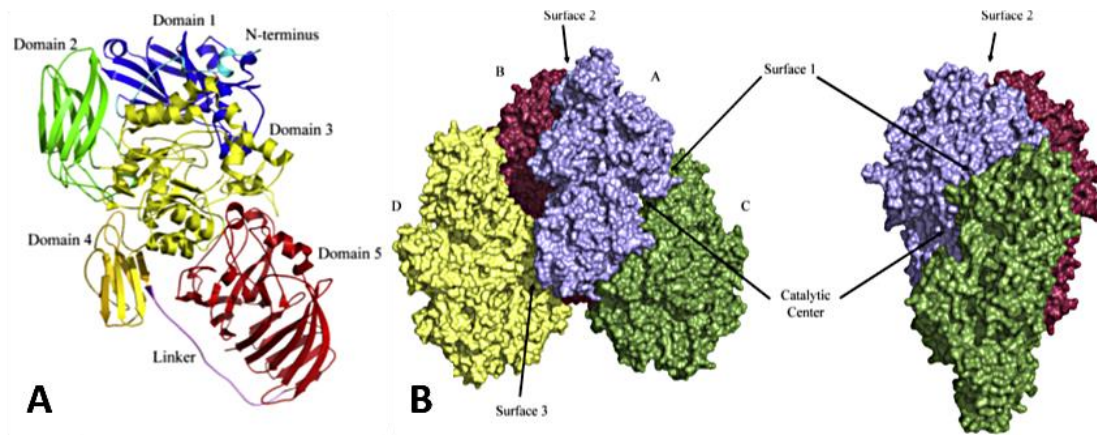


Figure 1.1. 2. Stereo view of K.Lactis- β -Gal monomer (A) Surface representation of the K.Lactis- β -Gal tetramer (B) (reproduced after [55]).

1.1.2. Lactose

The principal constituents of milk are water, fat, protein, lactose, minerals, as well as the intrace amounts pigments, enzymes, vitamins, phospholipids and gases. The main carbohydrate in milk is lactose, a disaccharide sugar with lower solubility compared to sucrose or dextrose (less than 5%). A β -(1-4) glycosidic linker joins the two monosaccharides, β -D-galactose and β -D-glucose, on the anomeric C₁ of the β -D-galactose and the C₄ of D-glucose (Figure 1.1. 3.) [56].

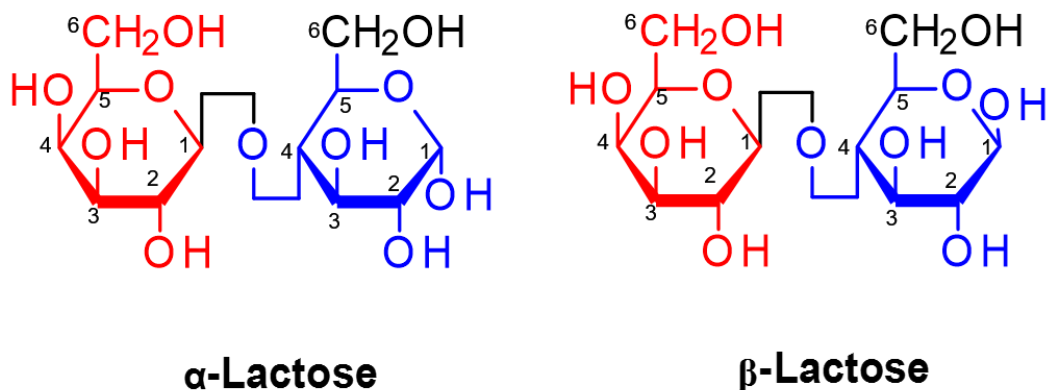


Figure 1.1. 3. α and β lactose.

In solid phase, lactose can be crystalline or amorphous. Crystalline

lactose can exist in one of two distinct forms, β -lactose and α -lactose (as monohydrate) (Figure 1.1. 3.). In milk, lactose is present in two isomeric forms β -lactose and α -lactose that are in chemical equilibrium [57].

Lactose is largely used in food industry. In yogurt, acid-coagulated dairy and some varieties of cheese the presence of lactose is crucial [58]. Isolated lactose can be used in the production of food and pharmaceutical products [59]. Galacto-oligosacchrides, lactulose, lactitol, and lactobionic acid are obtained from lactose [60].

Oligosaccharides are polymeric saccharides consisting of two to ten monomer residues (simple sugars) joined through glycosidic bonds. They can be obtained from different sources such as crops (onion, garlic) or lactose present in milk and whey (galacto-oligosaccharides) [61]. Galacto-oligosaccharides (GOS) are (galactosyl)_nlactose oligomers ($2 \leq n \leq 4$), synthesized by a transgalactosylation reaction from lactose catalyzed by β -galactosidase [62]. The reaction mechanism for the producing GOS was first proposed by Wallenfals and Malhotra, who used GOS as a growth factor for *Bifidobacterium* spp strain (have advantageous physiological effects on the host human). Owing to their roles in controlling pH in the large intestine (by promoting the production of lactic and acetic acids which limit the growth of pathogens and putrefactive bacteria [63]). The amount and composition of galacto-oligosaccharides vary with the source of enzyme, lactose concentration and the reaction conditions used in the process.

1.1.2.1. Lactose intolerance

A person unable to completely digest lactose is diagnosed with lactose intolerance. A significant fraction of global populations, of around 70%, presents symptoms related to lactose intolerance [64,65]. In fact, lactose intolerance symptoms are specifically caused by the deficiency of the β -galactosidase in the small intestine. Adults are mainly affected by lactose intolerance because the natural production of lactase in human body gradually decreases after weaning in infancy. As a result of the lack of lactase (or of the low activity of the enzyme or a diminished quantity) the hydrolysis of lactose is

incomplete. The undigested sugar pulls fluids into the large intestine, where the colonic bacteria digest the rest of the sugar, producing short chain fatty acids, gases (hydrogen, CO₂, methane). In the end, the combined osmotic effect results in the passage of acidic diarrheal stools. Lactose intolerance is described by the presence of gastrointestinal symptoms such as abdominal pain and distension, abdominal colic, bloating, flatulence, nausea or diarrhea [66].

Three types of lactose deficiency have been described: primary, secondary or congenital. Primary lactase deficiency or Late Onset Lactase Deficiency is the most common type, caused by the decline of the lactase production from infancy into adulthood, in spite of a continuous intake of exogenous lactase. Secondary lactose deficiency results from small intestine resections and diseases damaging the intestinal epithelium. Congenital occurrence is genetic and appears when two ineffective genes from parents are inherited (inability of the newborn to produce lactase) [67].

Some common tests are used to diagnose lactose intolerance: the blood test, the breath test and the endoscopy test. When the blood sugar rises above a critical threshold, subsequently to drinking a lactose-based solution, the person can be concluded as not lactose intolerant. In the breath test, the presence of hydrogen is analyzed as the concentration of hydrogen in the exhaled air increases when the lactose is fermented by the bacteria present in intestine. In the endoscopy test, the lining (mucin) of the intestine is observed and biopsied to check any damage caused by acid reflux or infection [68].

As lactose intolerant people are unable to digest milk and other dairy products, a strategy to remove the lactose from these products is required. Thus, an acidic or enzymatic lactose hydrolysis process can be applied to milk and other dairy products. The acidic method can raise some problems such as the formation of a brown colour product, protein denaturation and yield of undesirable toxic by-products (like lysino-alanine) [69]. Milder conditions of temperature and pH can be achieved by use of enzymes. However, the industrial application of the process based on the hydrolysis of the lactose with free β -galactosidase is limited due to the cost of soluble lactase.

1.1.2.2. Hydrolysis of lactose

Many research efforts have been developed to reduce or remove sugar (lactose) from dairy products. The most common way to accomplish this remains the use of β -galactosidase. Thanks to the improvements in processing techniques, hydrolyzing the lactose before packaging certain dairy products has become more prevalent. The lactose hydrolysis catalyzed by lactase mechanism was first described by Wallenfels who used β -Galactosidase extracted from *Escherichia coli* [62]. In the reaction mechanism proposed, the cysteine and the histidine residues from the active site of β -galactosidase act as proton donor and acceptor, respectively to the glycosidic linker. Cysteine contains the sulfhydryl group while histidine residue contains imidazole group acting as a proton acceptor and as nucleophile site to facilitate splitting of the glycosidic bond. Compared with E.Coli extracted enzyme, β -galactosidase from microbial sources presents two glutamic acid residues, Glu⁴⁸² and Glu⁵⁵¹ working as proton donor and nucleophile/base at the same time in the catalytic reaction [70]. The positions of the two residues in the catalytic pocket are situated in the center of each monomer of the tetrameric *K. Lactis* β -galactosidase as can be observed in Figure 1.1. 4. Residues from the domains 1, 3 and 5 surround the catalytic pocket that shapes a very narrow cavity of about 20 Å deep (see Figure 1.1. 4. A). In the dimeric arrangement, the cavities are located face-to-face within the interface. As domain 3 folds the pockets become accessible for the external substrate through a 10 Å width slot [55].

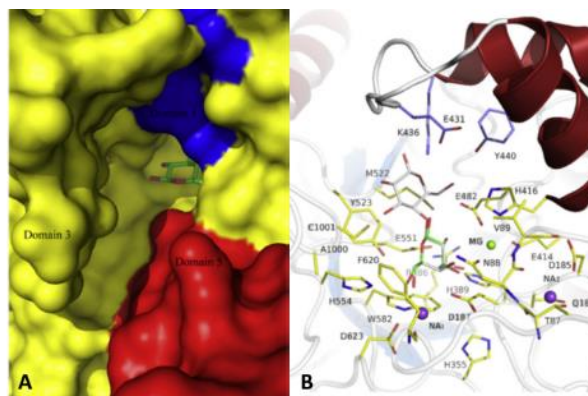


Figure 1.1. 4. (A)-Residues from 1, 3 and 5 domains building up the pocket entrance (zoomed view). (B)-Galactose bound to the active site (reproduced from [55]).

The reaction mechanism for *K. Lactis* β -galactosidase is shown in Figure

1.1. 5. In the first step of the reaction, the enzyme-galactosyl complex is formed and glucose is released. In the second step, the complex enzyme-galactosyl is transferred to a hydroxyl acceptor group (water or other saccharides). In a diluted lactose solution, water is more competitive to be an acceptor, therefore, galactose is formed and released from the active site. On the contrary, in a concentrated solution, lactose is more competitive as acceptor and binds to the enzyme-galactose complex to form oligosaccharides.

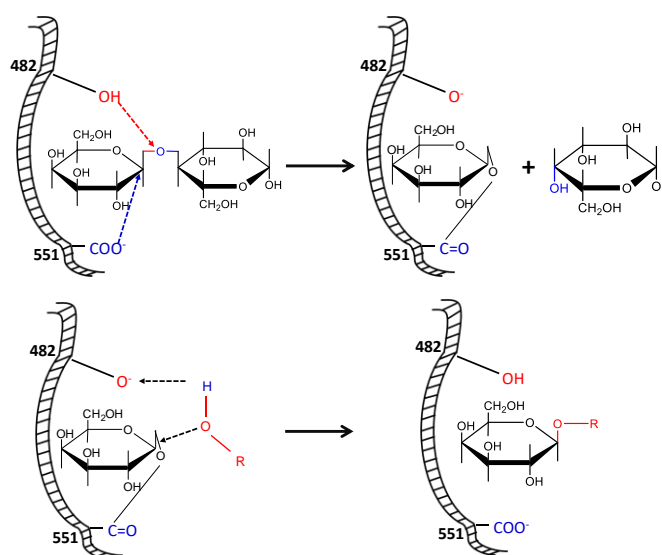


Figure 1.1. 5. Schematic mechanism of lactose hydrolysis by *K. Lactis* β -galactosidase (I) enzyme-galactosyl complex formation with the liberation of glucose, (II) enzyme-galactosyl complex transferred to an acceptor containing hydroxyl group (adapted from [70]).

1.1.3. Techniques and matrices for immobilization

The major drawback of free enzymes is their limited lifetime. External factors, such as pH, temperature, pressure, organic solvents, high ionic strength or proteases can destabilize the structure of the enzyme, leading to a decrease in their catalytic activity. Such drawbacks can be overcome by the immobilization of the enzyme. Moreover, immobilization might bring other advantages: the enzymes can be recovered and reused in a new catalytic reaction, stand longer storage, or can be released under specific conditions.

Supported enzymes might also become catalytically active in organic solvents in which the native enzymes are insoluble (eg. lipase) [71–73]. Currently, the study of solid supports suitable for enzyme immobilization is still a scientific challenge constrained by enzyme nature and target application. Furthermore, the immobilization process should also be mild, to prevent enzyme denaturation. In lactose hydrolysis, for example, the industrial process must be economically feasible, to address technical interests in milk industry. The extraction enzyme technology is still expensive, thus immobilized enzymes in food industry are in focus and the methods for the immobilization of various β -galactosidase enzymes in different solid supports were envisaged. The scientific community has also highlighted the benefit of pH and thermal stability of the biocatalyst [74].

Despite those advantages, it turns out that immobilization process can have some drawbacks, such as the loss of the enzyme activity after immobilization, mass transfer limitation (slow diffusion between the substrate in a liquid phase and the biocatalyst phase-solid), leakage of the enzyme from the matrix and cost aspect related to the implementation of the immobilization step in an industrial process [74]. According to literature, immobilization techniques can be classified in two major categories: reversible and irreversible. Irreversible methods involve the formation of the biocatalyst, while the components cannot be separated without destroying either the enzyme or the support. Reversible methods do not involve covalent bonding with the enzyme, and the enzyme can be detached from the support under gentle conditions. Chemical and physical properties of the support material including particle size, surface, porosity, functional group on the surface and morphology are important in enzyme immobilization. All these have to be considered when choosing the immobilization technique. The methods used for immobilization can also affect the kinetic parameters of the immobilized enzyme [75].

1.1.3.1. Methods of reversible immobilization

Reversible immobilization involves weak forces between the enzyme and the support, so the immobilized enzyme can be detached under gentle conditions, without destroying one of the components. The methods used are a) adsorption, b) ionic or hydrophobic binding, c) affinity binding, d) chelation

or metal binding, e) disulfite bonds. These are schematized in Figure 1.1. 6. The reversible methods for enzyme immobilization are mostly used for economic reasons:

- when the cost of the support plays an important role and the enzyme can be regenerated
- when the cost of the enzyme is high and reversible immobilization is used for the purification of the enzyme

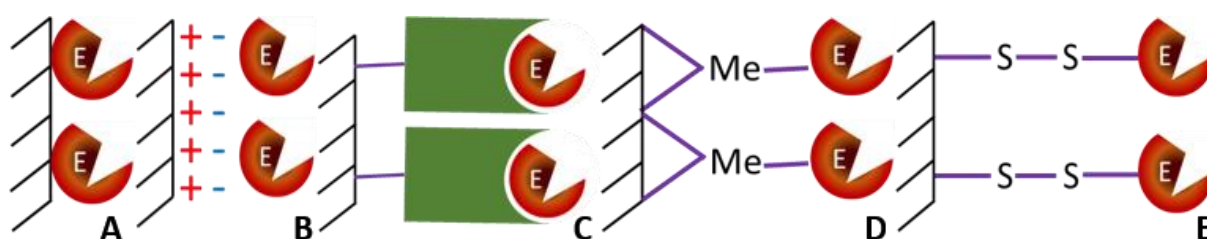


Figure 1.1. 6. Methods of reversible immobilization: (A) adsorption, (B) ionic binding/hydrophobic binding, (C) affinity binding, (D) chelation or metal binding, (E) disulfite bonds (adapted from [75]).

1.1.3.1.1. Adsorption

This method is based on the physical adsorption of enzyme on the surface of a solid support. The nature of the interactions of the enzyme with the support is usually a combination of hydrogen bonding, van der Waals forces, hydrophobic or/and electrostatic interactions depending on the chemistry of the surface. One major advantage of this method is that, usually, no reagents or a minimal modification step for the support are required, which make the procedure simple and inexpensive. In any case, this method involves weak bonds that do not prevent enzyme desorption by varying pH, temperature or in the presence of substrate.

Investigating suitable solid supports for each enzyme and for each industrial application immobilization is still a current scientific challenge. The materials employed for enzyme adsorption can be organic or inorganic.

Bone powder was used for the immobilization of *Kluyveromices fragilis* enzyme, for the removal of lactose from dairy [76]. The thermal stability of the enzyme was improved, and the material showed a 90% conversion of the

lactose present in buffered solutions, whey, whey permeate (a substitute of lactose, sweet whey powder, and/or demineralized whey powder) and skimmed milk. *K. lactis* enzyme was adsorbed on a mixed-matrix membrane containing zirconium dioxide. The maximal adsorption of the enzyme onto the membrane could be achieved under extreme parameters (temperature and pH) but it would lead to the loss of activity for the enzyme. Immobilized under the optimum parameters, the enzyme increases its activity almost 8 times [77]. Native zinc oxide (ZnO) and zinc oxide nanoparticles (ZnO-NP) were also used to immobilize the *A. Oryzae* β -Gal by simple physical adsorption mechanism. Thus, compared to the enzyme adsorbed on native ZnO, the enzyme adsorbed on ZnO-NP showed better stability against pH, temperature, galactose inhibition, better reusability and conversion of lactose in milk and whey [78]. The increased stability of the enzyme is due to the multipoint attachment of enzyme molecules to the nanomaterial that leads to limited protein unfolding.

To increase the interaction between the enzyme and the support, the specific active groups on the surface of the support can be modified. *K. lactis* enzyme was adsorbed on plasma modified cellulose acetate with ethylenediamine and 2-mercaptoethanol. Although high enzyme loading was achieved, only the thiolated membrane surface could keep a high enzymatic activity [71]. The adsorption of enzymes onto composites based on covalent coating of supports with polymers has also been proposed.

β -galactosidase from *A. oryzae* was adsorbed on with glutaraldehyde-treated chitosan for the production of galactooligosaccharides (GOS) [79] in a plug reactor, while *K. lactis* enzyme immobilized on glutaraldehyde-activated chitosan was used in a packed-bed reactor for the continuous hydrolysis of lactose and the synthesis of GOS [80]. *K. lactis* β -galactosidase was also immobilized on glutaraldehyde modified silica nanoparticles (10-20 nm) and showed an increase in the optimal pH, temperature and maximum velocity (V_{max}) in the hydrolysis of lactose [81].

1.1.3.1.2. Ionic binding

Another approach to the reversible immobilization of enzymes is based on ionic binding, the protein–ligand interactions, a principle employed in certain types of chromatography and based on ionic-exchangers. Enzyme adsorption on ion exchange supports is quick and simple method, that permits to reuse the material and it is also applicable to enzyme purification [82]. Depending of the ligand, the optimum pH and temperature of the enzyme can change.

Co-immobilization is another strategy that has been explored. For example, Peirce *et al* immobilized lipase B from *Candida antarctica* (CALB) on octyl-agarose (OC). β -galactosidase from *A. oryzae* was immobilized by ion exchange after precoating with polyethylenimine (PEI). The adsorption and desorption of β -galactosidase could be easily achieved and the OC-CALB was reused as shown in the Figure 1.1. 7 [83].

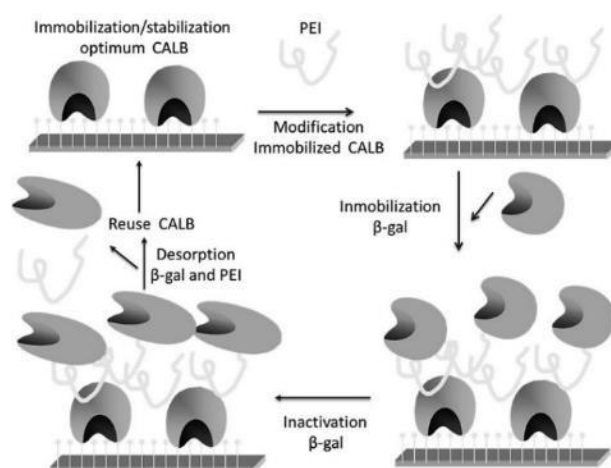


Figure 1.1. 7. Strategy of co-immobilization of Lipase B and β -galactosidase (reproduced after [83]).

1.1.3.1.3. Hydrophobic adsorption

Another chromatographic principle based on hydrophobic interactions, can be used for enzyme immobilization. The strength of interaction relies on both the hydrophobicity of the adsorbent and of the protein which varies with the change of pH, salt concentration, or temperature.

β -Galactosidase from *A. oryzae* was immobilized on colloidal liquid aphron (CLA) via hydrophobic and electrostatic interaction. The aphron is a core/shell structure in which a gas is stabilized by a layer of polymer or

surfactant. In fact, the stabilizing shell is a tri-layered domain where water is entrapped around the gas bubble between an inner and outer surfactant layer. The latter forms itself as an external electrostatic double layer (Figure 1.1. 8). 70% of β -Galactosidase was immobilized over a wide range of pH (4-10) in the shell of the CLAs. The immobilized enzyme adsorbed at the interface of the oil displayed an increase of activity compared with the free enzyme [76].

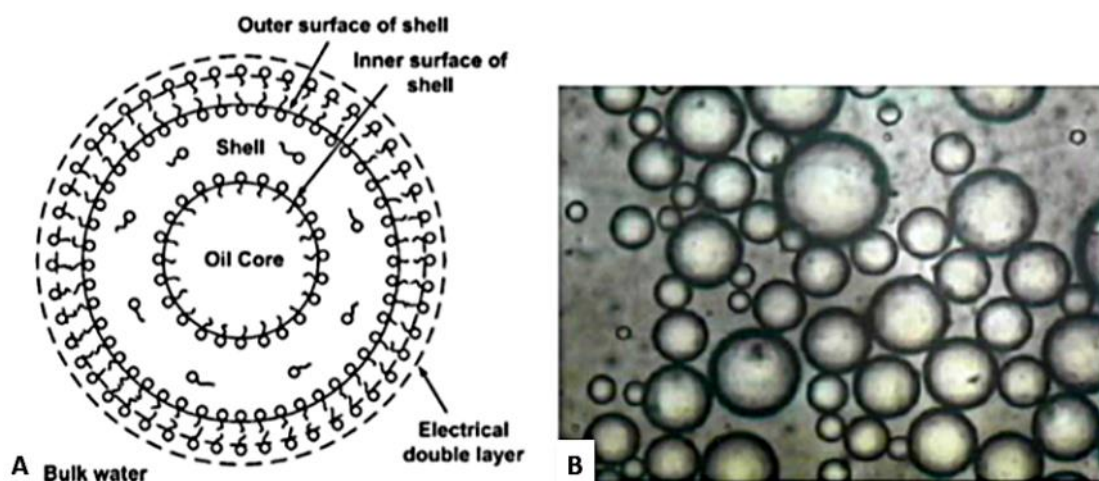


Figure 1.1. 8. Structure (a) and micrograph (b) of CLA (reproduced after [88]).

1.1.3.1.4. Affinity binding

The basis of the bioaffinity technique is the biospecific interaction between two affinity groups. The two advantages of oriented immobilization of biologically active proteins are the good steric accessibility of active binding sites (no modification/ distortion of the active site) and increase in stability.

The immobilization of glycosylate enzymes via glycosyl moieties is interesting and safe for the enzyme since the carbohydrate part does not participate in catalysis. Therefore *A. oryzae* β -galactosidase was used to form a complex with concanavalin A-enzyme (Con A) cross-linked with glutaraldehyde. The Con A complex was then entrapped in calcium alginate beads. The entrapped enzyme was more stable against various chemical and physical denaturation compared to the soluble enzyme and Con A- β -galactosidase without crosslinking entrapped in alginate [84]. Such, it could be successfully used in stirred batch process and packed bed reactor [85].

In another work of Haider *et al*, *A. oryzae* β -galactosidase was immobilized by bioaffinity adsorption on the surface of a novel support: concanavalin A layered calcium alginate–starch beads. The immobilized β -galactosidase exhibited significantly higher stability against conditions of digestive system such as pH and enzymes (salivary amylase, pepsin and trypsin) ^[86] and against external factors such as heat, urea, MgCl₂, and CaCl₂. It also presented a higher activity in the hydrolysis of lactose in whey and milk compared to the free enzyme ^[87]. Another support that was analysed under the same conditions is a polyclonal antibody bound cellulose support. The immobilized enzyme was much more stable compared to the free enzyme, and displayed a shift in pH and temperature ^[88].

K. lactis β -galactosidase was also immobilized by bioaffinity adsorption on the surface of a concanavalin A layered aluminium oxide nanoparticles support. The immobilized enzyme exhibited enhanced pH stability and broad optimum spectrum temperature compared to the soluble β -galactosidase. Immobilized galactosidase was stable against galactose inhibition and retained 85% activity after its sixth repeated use in continuous stirred tank bioreactors^[89].

1.1.3.1.5. Chelation or metal binding

Metal binding is also employed to immobilize enzymes. On the surface of organic carriers, transition metal salts or hydroxides are deposited and bound onto the matrix by coordination through nucleophilic groups. The metal salt or hydroxide is precipitated onto the support (e.g., cellulose, chitin, alginic acid, and silica-based carriers) through heating or neutralization. A part of the coordinative positions of the metals remain free to coordinate with enzyme groups. Because of steric factors, it is impossible for the matrix to occupy all coordination positions of the metal. The metal ions bounded on solid chromatographic supports absorb the enzyme through the amino acid residues that are exposed on the surface of the protein.

In order to improve the control over the formation of the adsorption sites, and improve the reproducibility, chelator ligands can be immobilized on the solid supports by means of stable covalent bonds. The metal ions are then

bound by coordination and the stable complexes formed can be used for the retention of proteins. The release of the bound proteins can then be achieved by decreasing the pH or by using competition with other, more soluble ligands. The support is subsequently regenerated by washing with a strong chelating agent such as ethylene diamine tetraacetic acid (EDTA) when desired. These metal chelated supports were named Immobilized Metal-Ion Affinity (IMA) adsorbents and have been used extensively in protein chromatography separation. This approach, using *E. coli* β -galactosidase as a model was used to test different IMA-gels with different chelated ligands (Cu^{2+} , Ni^{2+} and Fe^{3+}) as supports for enzyme immobilization [90].

A strategy to absorb large proteins has been reported by Pessla et al. Different activation degrees of amino group per gram of agarose were analysed for the purification of β -galactosidase from *Thermus sp.* strain T2 from a crude extract. The highly activated supports (40 μmol of ionic groups/g of agarose) are capable to immobilize two large β -galactosidase, with molecular size of 465 kDa (*E.coli*) and 75 kDa (*Thermus sp.*) [91] and to specifically absorbed them in the presence of 50 mM imidazole [82]. Due to the fact that large proteins have a large surface that permits long distance interactions with groups dispersed on a support, and that the interaction can be too strong, a Cu^{2+} -chelate-iminodiacetic acid-agarose support was considered. In this way, the number of enzyme bounds with the support are relatively low and the enzyme can be easily desorbed [92] –Figure 1.1. 9.

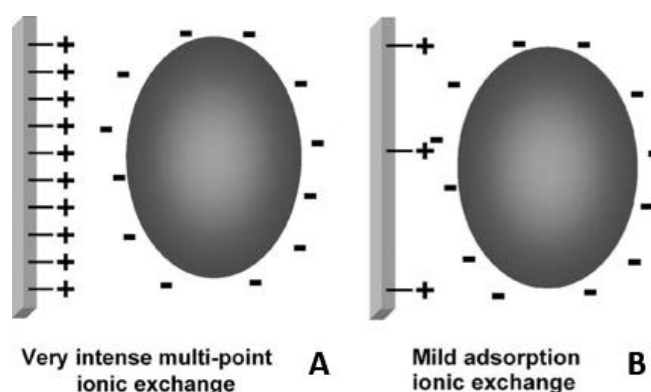


Figure 1.1. 9. Adsorption mechanism of large proteins on Cu^{2+} -chelate-iminodiacetic acid-agarose support by (A) very intense multi-point ion exchange (reproduced after [91]) and (B) mild adsorption ionic exchange (reproduced after [92])

The same group used heterofunctional epoxy Sepabeads (boronate-epoxy-Sepabeads and chelate-epoxy-Sepabeads) used to immobilize β -galactosidase from *Thermus sp.* T2 (Htag-BgaA) to decrease the inhibition. The immobilization produced small changes in the conformation of the active center, that allowed for more than a 99% hydrolysis of lactose [34].

A way to purify and immobilize the protein in a single step is to combine two techniques the epoxy groups at the surface of the matrix for enzyme immobilization and the purification by metal-chelate affinity chromatography. The *Thermus sp.* strain T2 β -galactosidase overexpressed in *E. coli* poly-His-tagged- β -galactosidase crude was immobilized with a low concentration of Co^{2+} chelating on a high epoxy groups density support. The enzyme was purified and absorbed onto the support, resulting in a very high activity and stability [93].

1.1.3.1.6. Disulfide bonds

In the case of this method, a stable covalent disulfide bond (-S-S-) is formed between the matrix and the enzyme. The reactivity of the thiol groups (-SH) from the surface of both the enzyme and the support can be controlled by pH modification. The absorption yield of this method is usually high (when the appropriate thiol-reactive

For example, β -galactosidase from *E. Coli* was reversibly attached to disulfide oxide groups introduced into thiol-containing agarose beads. The enzyme was immobilized with a yield of 90% [94,95] and the activity increased after the immobilization [96]. Due to reversibility of the disulfide bound, the enzyme can be easily detached from the support [97] and this method can be used for enzyme purification.

Introducing disulfide bonds in the enzyme structure, can increase the absorption of the enzyme on the carrier [98] or can improve the stability of the free enzyme against temperature and pH [99].

1.1.3.2. Methods of irreversible immobilization

Irreversible immobilization involves strong interactions between the enzyme and the support. The enzyme cannot be detached without destroying either the structure of the enzyme (and by default the activity), either the support. The irreversible enzyme immobilization methods are: covalent immobilizations (A), entrapment in gels (B) and fibers (C), microencapsulation (D) and chemical aggregation (E) as schematized in Figure 1.1. 10.

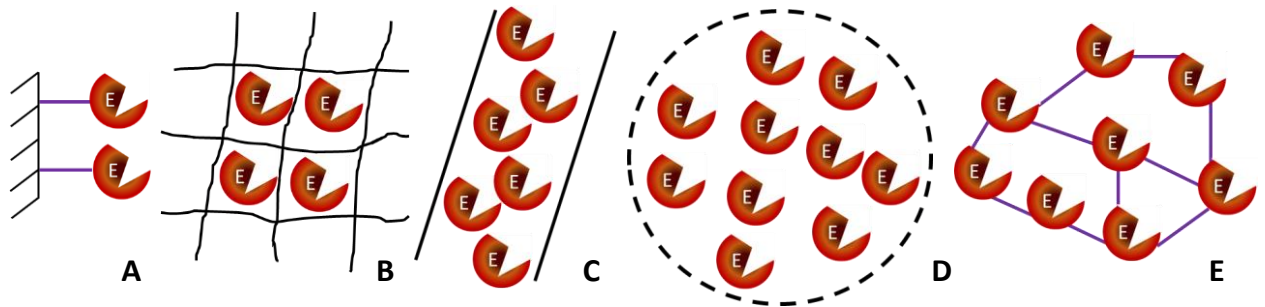


Figure 1.1. 10. Irreversible methods of immobilization: covalent immobilizations (A), entrapment in gels (B) and fibers (C), microencapsulation (D) and chemical aggregation (E) (adapted from [75]).

1.1.3.2.1. Covalent immobilization

Covalent immobilisation methods lead to irreversible and sustainable biocatalysts and prevent the leakage of enzyme, covalently bonded to the support. However, covalent coupling may induce drastic changes in the enzyme conformation, when it occurs near the active site ^[100] or reduce enzyme flexibility at high bonding density to the support ^[101]. Therefore, the support and the spacer must be carefully chosen. The covalent immobilization can be divided in two main classes: i) post functionalization of the matrix and ii) in situ functionalization of the matrix during the synthesis.

Usually the covalent immobilization is used to increase the stability ^[102,103] and the reusability of an enzyme, or to change the optimal pH and temperature when the biocatalyst is used in a reactor (see more in subchapter Industrial application)

For example, β -Galactosidase from *A. oryzae* was immobilized in Nylon membranes grafted with glycidyl methacrylate (Nylon/GMA) via diazotization (through tyrosine residues of the enzyme) and via condensation (through

multipoint attachment with arginine residues of the support). Both techniques lead to the increase of the K_m values ^[104]. It should be noticed that diazotization method was more efficient in a bioreactor under non-isothermal conditions^[105]. On the same support (Nylon/GMA), the influence of the spacer length between the enzyme and the support (hexamethylenediamine, ethylenediamine or hydrazine) was analyzed. With the increase of the spacer length, the optimum pH, temperature and the apparent K_m . decreased. But all membranes showed good results in non-isothermal bioreactors ^[106].

Moreover, the same enzyme was also covalently attached to cotton cloth activated by tosylchloride and used for the production of galacto-oligosaccharides ^[107]. Thus, the enzyme changed its reactivity, from the hydrolysis of lactose (into glucose and galactose) to the trans-glycosylation of lactose to galacto-oligosaccharides.

To obtain double reactivity of the enzyme, *Talaromyces thermophilus* CBS β -galactosidase was covalently attached to Eupergit C (macromolecular beads of acrylic polymer) and the resulting material was used for the removal of lactose at high temperature as well as for the formation of galacto-oligosaccharides. ^[108]. For the same application *K. lactis* ^[109] and *A. Oryzae* ^[110] were immobilized on magnetic polysiloxane-polyvinyl alcohol composite.

Immobilized enzymes might become resistant to glucose inhibitions. This phenomenon was observed with a β -galactosidase from the thermophilic microorganism, *Thermus* sp. strain T2, immobilized on trishydroxymethylphosphine (THP) activated silica-alumina support ^[35].

For the reuse of the enzyme, Elnashar et al ^[111] covalently attached *A. Oryzae* enzyme with glutaraldehyde on natural biopolymers i.e. carrageen coated chitosan. The material showed thermal stability and conferred pH and temperature improvements, also providing good reusability to the enzyme.

Crosslinking (or chemical aggregation) is based on the formation of covalent bonds between enzymes molecules, leading to three-dimensional structures. Thus, there is no requirement for a support. Crosslinking is generally combined with other methods, mostly to stabilize and prevent the enzyme leakage during the crosslinking. Glutaraldehyde is the most common

cross-linker. It can be used to chemically aggregate the enzyme ^[112] to be linked with the support as aggregates, or to lock the enzyme onto the support after absorption ^[113].

Gaur et al. compared aggregation by cross-linking with two other techniques (adsorption on celite and covalent coupling to chitosan) for the synthesis of GOS with *A. oryzae* β -gal. Cross-linked enzyme aggregates (CLEA) were efficient in lactose hydrolysis with a yield of 78% monosaccharide in 12h ^[114].

Crosslinked with glutaraldehyde, concanavalin A-Celite 545 immobilized *A. oryzae* β -galactosidase was compared with the adsorbed enzyme and with the free enzyme. The covalent immobilized enzyme showed better resistance to product inhibition (glucose and galactose) and increased efficiency in hydrolyzing lactose from milk and whey in batch processes ^[115]. N-terminal α -amines and lysine ϵ -amines from *K. lactis* enzyme were covalently attached to amino-modified polyethylene film with glutaraldehyde. The as-modified film with stood heat treatment in the presence of an ionic denaturant with a high enzyme retention, suggesting that the material can be used in food active packaging ^[116].

1.1.3.2.2. Entrapment

Entrapment is defined as physical confinement of enzymes or cells in an environment where the substrate is able to penetrate, and the enzyme cannot escape. This method differs from covalent binding or cross-linking since the enzyme does not bind to the matrix. This entrapment mode can be classified in five major types: lattice, microcapsule, liposome, membrane and reverse micelle ^[117]. The entrapment can be made in organic, inorganic or hybrid matrices.

For β -galactosidase immobilization, the lattice method (microencapsulation) is mostly used. In that case, the enzyme is entrapped in a matrix of natural or synthetic polymers. The most popular one is alginate, a natural polysaccharide that forms hydrogels by ionotropic gelation with a divalent metal cation such as Ca^{2+} -Figure 1.1. 11.

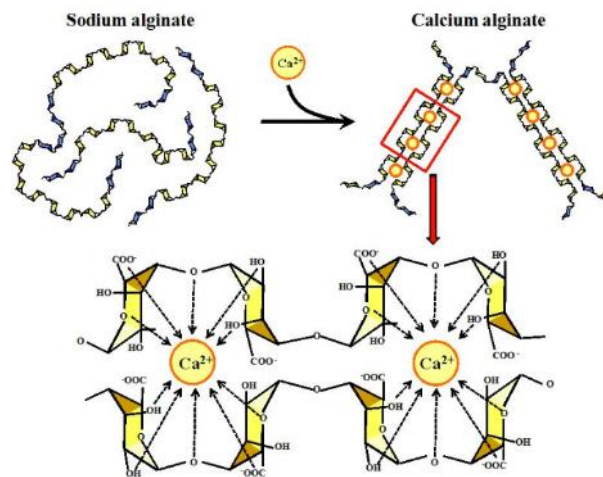


Figure 1.1. 11. Structure of alginate and its binding with calcium cations (reproduced after [118]).

Mammarella et al. entrapped *K. fragilis* β -Galactosidase in alginate-carrageenan hydrogel beads of 2.4 mm [119]. It was observed compared with other ions (Na^+ , Mn^{2+} , Mg^{2+} , Ca^{2+}) the K^+ ions have the most beneficial effect on enzyme activity [120]. K-carrageenan, along with the K^+ ions increased the enzyme activity. Combined with gelatin, alginate was used to immobilize *A. oryzae* in fibers hardened with glutaraldehyde. The fibers were formed by pumping a solution of β -galactosidase, alginate, gelatine, glycerol and sodium acetate buffer through a syringe into a solution of CaCl_2 solution prepared in calcium acetate buffer (pH 5.3) containing glutaraldehyde. The immobilized enzyme showed good storage stability (for 35 days without activity decrease) and was more stable at high pH and temperature, compared with the free enzyme [121].

On the other hand, Taqieddin et al. [122] entrapped enzyme in a liquid or solid core alginate and a chitosan shell microcapsule technology to encapsulate β -galactosidase. Ba^{2+} crosslinked alginate was more efficient (100% enzyme entrapped) compared with Ca^{2+} (only 60% efficiency). Ca^{2+} ions present an inhibitor effect for the enzyme as shown in Table 1.1 2.

Gelatin-based films with β -galactosidase from *A. oryzae* were elaborated to immobilized enzyme to extend the stability of the protein in dried films state. The film and the enzyme activity were stables up to 36° C and a relative humidity of 75% [123]. The resulting dry films might fit with industrial requests in

terms of stability, handling, storage, and transportation of functional proteins in a cost-effective manner.

Synthetic polymers forming hydrogels are also attractive for enzyme immobilization. For example, the polyvinylalcohol (PVA) gel is interesting for its innocuous character, biocompatibility, low toxicity, good long-term and mechanical stability and low biodegradability. Batsalova et al entrapped fungal β -galactosidase in PVA cryogel beads and the enzyme gained thermal stability compared to the free enzyme. The latest retaining 70% of activity at 50°C and 5% at 60°C [124]. β -galactosidase from *A. oryzae* was immobilized in lens-shaped PVA capsules (LentiKats). The immobilized enzyme showed stability after 35 repeated batch runs and during 14 months storage [125].

For the digestion of lactose in milk, dried liposomes containing β -galactosidase were prepared. In the presence of bile salts, the lysis of liposomes is efficient and the entrapped enzyme is released in the stomach for the “in situ” digestion of the lactose [126]. Rodríguez-Nogales et al. [65] [127] optimized the entrapment of β -Galactosidase from *E. Coli* in cholesterol-phosphatidylcholine (Ch:PC) liposomes. The dehydration-rehydration vesicle method was used in order to create the liposomes. The enzyme concentration, pH, type and time of sonication, the ratio Ch:PC, and sucrose concentration (as cryoprotectant) were optimized as well.

Another approach to encapsulate enzyme is the “fish-in-net” method. This method implies a direct interaction between the silica precursor and enzyme. The enzyme (fish) is trapped in the silica network (net). This method is useful for the prevention of bacterial contamination when the β -galactosidase and lysozyme enzymes are co-immobilization. A silica matrix that contained entrapped β -galactosidase from *A. oryzae* was modified with covalently bound lysozyme (Figure 1.1.13). Both enzymes were active, and the materials were used to treat milk. This resulted in bacterial cell viability dramatically decreased when used in the industrial process. Thus, the rate of lactose hydrolysis was improved and a good storage and operational stability was reached during the reuse of the catalyst support in the industrial production of low lactose milk [128].

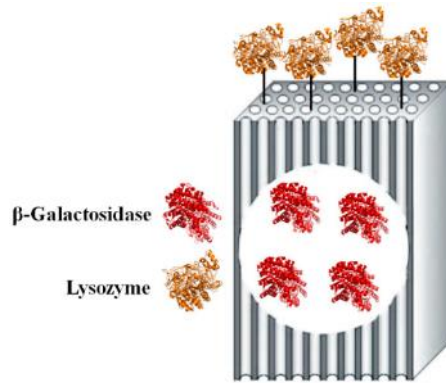


Figure 1.1. 12. Fish in net approach for co-immobilization of two enzymes (reproduced after [128])

Hybrid matrices may combine the advantages of both organic and inorganic materials.

The latest materials were synthesized by impregnation of mesoporous silica particles (MCM-41) with an alginic acid solution that contained β -galactosidase from *K. fragilis*, followed by the biopolymer gelation with CaCl_2 . The hybrid material exhibited a higher stability upon ageing compared to a pure alginate gel [129].

The development of food containing β -galactosidases is challenging, since enzymes can lose their activity through pH and temperature changes, during processing, but also after ingestion over gastrointestinal transit. Recently, encapsulation of β -galactosidases within hydrogel microbeads was proposed as an alternative to protect it in different pH and thermal conditions. The encapsulated enzyme couldn't be protected by the acid-induced or thermal-induced loss of activity, but had higher activity compared with the free enzyme at mild pH (> 4) and temperature ($< 50^\circ\text{C}$) conditions [130]. Silica nanoparticles were also suggested as a protective matrix for β -galactosidases [131]. Silica is the most used support for gastro-intestinal release as shown in the Chapter 1.2. The enzyme was encapsulated in silica nanoparticles aggregates. Compared with porous hydrogel microbeads, the silica particles were able to provide an efficient protection for a wide range of pH (2-11) where the enzyme retained the same activity. This system also protected the enzyme from thermal inactivation for up to 70°C .

Enzyme immobilization has attracted a lot of attention. From the binding to a support to encapsulation into a matrix, enzyme immobilization is used to improve the enzymes' performance. Organic and inorganic materials were used, both with their own strengths and weaknesses. Hybrid materials are promising materials since they can potentially have the advantages of both.

1.1.4. Application of immobilized β -galactosidase

Hydrolysis of lactose to glucose and galactose by β -galactosidase would overcome some of the industrial application limitations of whey and milk, lactose has a poor solubility, insufficient sweetness and generates lactose intolerance problems. There are basically two ways to use the enzyme, in soluble enzyme form for batch process or as an immobilized enzyme in continuous operation. The possibility of reusing the enzyme in a continuous industrial process could make the cost of enzyme immobilization profitable [68].

1.1.4.1. Industrial application

β -galactosidase is sometimes used in alcohol containing beverages, but its main application is in the production of milk and fermented milk products such as yoghurt and cheese. Low lactose milk and dairy products gives chance to lactose intolerant people to consume these products. Another reason to decrease the lactose content in dairy products is the prevention of lactose crystallization in ice cream, frozen milks, whey and condensed milk. In respect to the mentioned points, limiting lactose in food processing can improve some technological and sensorial quality of dairy foods, by increasing the digestibility, softness and creaminess.

In the cheese industry, the whey represents a waste product, which causes several economic and environmental problems. Hydrolysis of lactose present in whey converts whey into very useful sweet syrup, which can be used in the dairy [132], baking and soft drinks industries [117]. After hydrolysis, the whey can be used as cattle food resource or even to develop new free lactose products [133]. This organic waste can also be used as an available substrate for microbial cell cultivation [134,135].

Another important aspect to the dairy industry is that the hydrolysis of lactose by β -galactosidase can lead to the synthesis of oligosaccharide and galactooligosaccharides. They can be produced from D-lactose via by glycosyl transfer catalyzed by the enzyme β - galactosidase. Galactooligosaccharides are prebiotics, and are not usually digested in the small intestine, but fermented by colonic bacteria in the large intestine. This could lead to changes in the colonic ecosystem in favor of some bacteria, such as bifidobacteria, which may have health benefits, including protection against certain cancers and lowering of cholesterol levels [136]. The structures of some oligosaccharides obtained from lactose are presented in Table 1.1 3.

Table 1.1 3. Structures of some oligosaccharides obtained from lactose [137] .

Disaccharides	β-D-Gal (1\rightarrow6)-D-Glc β-D-Gal (1\rightarrow6)-D-Gal β-D-Gal (1\rightarrow3)-D-Glc β-D-Gal (1\rightarrow2)-D-Glc β-D-Gal (1\rightarrow3)-D-Gal	allactose galactobiose
Trisaccharides	β -D-Gal (1 \rightarrow 6)- β -D-Gal (1 \rightarrow 6)-D-Glc β -D-Gal (1 \rightarrow 6)- β -D-Gal (1 \rightarrow 4)-D-Glc β -D-Gal (1 \rightarrow 6)- β -D-Gal (1 \rightarrow 6)-D-Gal β -D-Gal (1 \rightarrow 3)- β -D-Gal (1 \rightarrow 4)-D-Glc β -D-Gal (1 \rightarrow 4)- β -D-Gal (1 \rightarrow 4)-D-Glc β -D-Gal (1 \rightarrow 6)- β -D-Gal (1 \rightarrow 6)- β -D-Gal (1 \rightarrow 4)-D-Glc β -D-Gal (1 \rightarrow 6)- β -D-Gal (1 \rightarrow 3)- β -D-Gal (1 \rightarrow 4)-D-Glc β -D-Gal (1 \rightarrow 6)- β -D-Gal (1 \rightarrow 4)-D-Glc	6'digalactosyl-glucose 6' galactosyl-lactose 6' galactotriose 3' galactosyl-lactose 4' galactosyl-lactose
Tetrasaccharides	β -D-Gal (1 \rightarrow 6)- β -D-Gal (1 \rightarrow 6)- β -D-Gal (1 \rightarrow 4)-D-Glc β -D-Gal (1 \rightarrow 6)- β -D-Gal (1 \rightarrow 3)- β -D-Gal (1 \rightarrow 4)-D-Glc β -D-Gal (1 \rightarrow 3)- β -D-Gal (1 \rightarrow 6)- β -D-Gal (1 \rightarrow 4)-D-Glc	6'digalactosyl-lactose
Pentasacchride	β -D-Gal (1 \rightarrow 6)- β -D-Gal (1 \rightarrow 4)-D-Glc	6'trigalactosyl-lactose

Gal-galacto, Glc- Galactosyl

Various reactors with different configurations and varying the operation conditions (like temperature and pH) were used for the enzymatic hydrolysis of lactose from either milk/whey or pure lactose (Table 1.1.4.). As the price of the process is determined by the cost of the enzyme, a continuous industrial production that involves the reuse of a single batch of enzyme can be

considered [107,138]. The direct addition of the soluble enzyme by recycling it through a membrane separation processes or the use of immobilized enzymes are technically feasible. Compared to the free β -galactosidase, its immobilization offers numerous advantages. The supported catalyst can be used in batch or in a continuous process, it simplifies enzyme removal from the reaction mixture, and affords a rapid termination of the reactions and a better control on product formation [87,139,140]. The β -galactosidase enzyme immobilized reactors have been extensively studied. Enzyme-membrane systems (EMR) [141], hollow-fiber reactors (HFRs), fluidized-bed reactors (FBRs) [142], packed-bed reactors (PBRs) [119,143,144], and stirred-tank reactors (STRs) are the main reactors used in lactose hydrolysis [145]. They all present advantages and disadvantages. Commonly, the stirred-tank reactors (batch procedure) using free enzyme, in batch operation mode are used in commercial applications [140]. Although, it is simple and easy to control, it has couple of disadvantages related to high enzyme content and labour cost [146]. Compared with the batch procedure, β -galactosidase immobilized onto highly activated supports in packed-bed reactors, allows for the continuous reuse of the biocatalyst improving the global yield. This technique also has some drawbacks, the enzyme can lose the activity due to the multipoint immobilization and the diffusion can be limited by the support. The bioreactor configuration with a suitable membrane (MBR) displays some advantages: it is facile, low relative costs and inexpensive adjusting hydromonics with a high packing density (large specific surface per unit of mass) [147,148]. The enzyme can be absorbed [149] or chemisorbed [150] onto the bioreactor membrane and the lactose conversion is accomplished in a single step with high yields. The main advantages of MBR method are the preservation of the native kinetic properties of the free enzyme and the possibility of working in homogeneous solutions in presence of the substrate. The major disadvantages of this configuration are the clogging of ultra-filtration membranes with milk proteins and the increased risk of microbial contamination, especially during prolonged operation times at ambient temperatures. By operating the system at relatively high temperatures and using deproteinated substrates (whey permeate) these drawbacks can be partially eliminated [151].

Numerous hydrolysis systems have been investigated (with some examples shown in Table 1.1.4) using different types of reactors and different immobilization strategies (as discussed previously). However, the scaling up process has been applied only to a few of them and even fewer have been applied on an industrial or semi-industrial level. For instance, only couple of companies such as, Centrale del Latte of Milan, Cooperative Butter Factory and Snow Brand are using immobilized β -galactosidase for the production of dairy products [152].

Table 1.1 4. Hydrolysis of lactose by immobilized β -galactosidase under different operating conditions.

SOURCE OF β -GALACTOSIDASE	SUPPORT USED FOR IMMOBILIZATION	SOURCE OF LACTOSE	OPERATING CONDITIONS	REACTOR	CONVERSION (%)	REF
K. FRAGILIS	Porous silanized glass modified with glutaraldehyde	Whey permeate	pH 6, 50°C, reactor	batch and recycling packed-bed	86-90	[134]
K. FRAGILIS	Silica-alumina	Milk buffer	pH 7, 40°C	batch	99%	[133]
A. ORYZAE	Cross-linked poly(vinyl alcohol)/natural polysaccharide chitosan	Lactose and milk whey	pH 5, 50-60°C	Fixed bed	95%	[153]
THERMUS SP T2	Sepa beads	Novo buffer	pH 6.5, 50°C	batch	99%	[34]
K. FRAGILIS	Cellulose beads	Milk and whey	pH 6.6, 50°C	Batch and fluidized bed	>80% in whey and 7% in milk	[142]
E. COLI	Magnetic poly (GMA-MMA)	Lactose	pH 7, 35°C	Fixed bed, flow rate 20 mL/h for 60 h	88%	[154]
K.LATIS	Magnetic polysiloxane-polyvinyl alcohol	Skimmed milk	pH 6.5, 25°C	Batch and stirred	90%	[109]
A. ORYZAE	Lens-shaped polyvinyl capsules	lactose	pH 4.6, 45°C	Batch and stirred	100%	[125]
A. NIGER	Concanavalin A layered hybrid beads calcium alginate-starch	Whey, milk	pH 4.8, pH 6.6, 37°C		≈80%	[87]
E.COLI	Polypropylene spirally membrane		pH 6.8, 40°C	Bioreactor	90%	[155]

1.1.5. Conclusion

β -Galactosidase is one of the most used enzymes in food dairy processing, with an array of applications, from technological and environmental to nutritional and quality control. Mainly, the enzyme has two main functions: the hydrolysis of lactose from milk products for the production of free/low lactose dairy products to be consumed by lactose intolerant people and the production of galactosylated products by transgalactosylation reaction. β -Galactosidase enzymes are extracted from various sources, from plants (peaches, apricots, almonds, apples, kiwis, tomatoes), animal organs or from microorganisms (bacteria, fungi, yeasts). Depending on the natural source, β -Galactosidase is active at different pH levels and at various temperatures. β -Galactosidase enzymes from plants have an optimal pH between 3.5-7, from fungi between pH 2.5–5.4, from animal cells between 6-7, from bacterial and yeast sources between pH 6.5–7.5.

To increase the enzyme reusability, thermal stability and pH tolerance, β -Galactosidase enzymes have been immobilized on both organic (e.g. alginate, chitosan, cotton) and inorganic (e.g. silica, carbon) supports. Different immobilization methods have been used, from reversible immobilization (adsorption, ionic or hydrophobic binding, affinity binding, chelation or metal binding, disulfite bonds), that involves weak forces between the enzyme and the support, to irreversible immobilization (covalent immobilizations, entrapment in gels and fibers, microencapsulation, chemical aggregation), that involves strong interactions between the enzyme and the support.

Moreover, immobilized systems can provide better enzyme activity and confer a tuneable reactivity (either the hydrolysis of lactose to glucose and galactose, either to the production of oligosaccharides).

Immobilized β -galactosidase enzymes have been researched in different reactors for the continuous hydrolysis of lactose from whey, milk or different buffers. Enzyme-membrane systems, hollow-fiber reactors, fluidized-bed reactors, packed-bed reactors, and stirred-tank reactors are couple of reactors examples used in lactose hydrolysis.

Bibliography

- [1] S. S. Asraf, P. Gunasekaran, **2016**.
- [2] A. Gosling, G. W. Stevens, A. R. Barber, S. E. Kentish, S. L. Gras, *Food Chem.* **2010**, *121*, 307–318.
- [3] B. Rodriguez-Colinas, L. Fernandez-Arrojo, A. O. Ballesteros, F. J. Plou, *Food Chem.* **2014**, *145*, 388–394.
- [4] T. Haider, Q. Husain, *J. Sci. Food Agric.* **2007**, *87*, 1278–1283.
- [5] G. S. Ross, R. J. Redgwell, E. A. MacRae, *Planta* **1993**, *189*, 499–506.
- [6] A. T. Carey, K. Holt, S. Picard, R. Wilde, C. A. Tucker, C. R. Bird, W. Schuch, C. B. Seymour, U. K. A. T. C, E. A. Macrae, et al., **2017**, 1099–1107.
- [7] M. T. Flood, M. Kondo, *Regul. Toxicol. Pharmacol.* **2004**, *40*, 281–292.
- [8] Z. Nagy, T. Kiss, A. Szentirmai, S. Biró, *Protein Expr. Purif.* **2001**, *21*, 24–9.
- [9] M. L. Richmond, J. I. Gray, C. M. Stine, *J. Dairy Sci.* **1981**, *64*, 1759–1771.
- [10] P. Prunus, D. H. Lee, S. Kang, S. Suh, J. K. Byun, **2003**, *15*, 68–74.
- [11] S. Gulzar, *Am. J. Plant Sci.* **2012**, *3*, 636–645.
- [12] K. Itoh, T. Toba, T. Itoh, S. Adachi, *Lett. Appl. Microbiol.* **1992**, *15*, 232–234.
- [13] J. C. Ball, L. G. Puckett, L. G. Bachas, *Anal. Chem.* **2003**, *75*, 6932–6937.
- [14] M. Becerra, E. Cerdán, M. I. G. Siso, *Biotechnol. Tech.* **1998**, *12*, 253–256.
- [15] J. Fiedurek, J. Szczodrak, *Acta Microbiol. Pol.* **1994**, *43*, 57–65.
- [16] J. LEDERBERG, *J. Bacteriol.* **1950**, *60*, 381–392.
- [17] M. V. R. RAO, S. M. DUTTA, *J. Food Sci.* **1981**, *46*, 1419–1423.
- [18] R. a Daniel, J. Haiech, F. Denizot, J. Errington, *J. Bacteriol.* **1997**, *179*, 5636–5638.
- [19] H. Hirata, T. Fukazawa, S. Negoro, H. Okada, *J. Bacteriol.* **1986**, *166*, 722–727.
- [20] Y. M. Han'guk San'op Misaengmul Hakhoe., J. C. (Ildong P. C. L. . S. (Korea R. R. L. Lee, Y. J. Choi, H. C. (Korea U. S. (Korea R. D. of G. E. Yang, *San'op Misaengmul Hakhoe Chi.*, Han'guk San'op Misaengmul Hakhoe, **2001**.
- [21] K. M. Nevalainen, **1981**, *41*, 593–596.
- [22] S. Nizamuddin, a Sridevi, G. Narasimha, *African J. Biotechnol.* **2008**, *7*, 1096–1100.
- [23] N. A. Zagustina, A. S. Tikhomirova, *Biokhimiia* **1976**, *41*, 1061–6.
- [24] Y. Tanaka, T. Horiuchi, *J. Biochem.* **1975**, *77*, 241–247.
- [25] R. R. MAHONEY, J. R. WHITAKER, *J. Food Biochem.* **1978**, *1*, 327–350.
- [26] M. C. Crescimbeni, V. Nolan, P. D. Clop, G. N. Marin, M. A. Perillo, *Colloids Surf. B. Biointerfaces* **2010**, *76*, 387–96.
- [27] J. Garman, T. Coolbear, J. Smart, *Appl. Microbiol. Biotechnol.* **1996**, *46*, 22–27.
- [28] C. Picard, J. Fioramonti, A. Francois, T. Robinson, F. Neant, C. Matuchansky, *Aliment. Pharmacol. Ther.* **2005**, *22*, 495–512.
- [29] C. G. Vinderola, J. A. Reinheimer, *Food Res. Int.* **2003**, *36*, 895–904.
- [30] T. Vasiljevic, P. Jelen, *Innov. Food Sci. Emerg. Technol.* **2002**, *3*, 175–184.
- [31] K. Arunachalam, *Nutr. Res.* **1999**, *19*, 1559–1597.
- [32] A. Jain, Y. Gupta, S. K. Jain, *J. Pharm. Pharm. Sci.* **2007**, *10*, 86–128.
- [33] M. . Boon, A. E. . Janssen, K. van 't Riet, *Enzyme Microb. Technol.* **2000**, *26*, 271–281.
- [34] B. C. C. Pessela, C. Mateo, M. Fuentes, A. Vian, J. L. García, A. V. Carrascosa, J. M. Guisán, R. Fernández-Lafuente, *Enzyme Microb. Technol.* **2003**, *33*, 199–205.
- [35] M. Ladero, M. T. Perez, A. Santos, F. Garcia-Ochoa, *Biotechnol. Bioeng.* **2003**, *81*, 241–252.
- [36] M. Ladero, G. Ruiz, B. C. C. Pessela, A. Vian, A. Santos, F. Garcia-Ochoa, *Biochem. Eng. J.* **2006**, *31*, 14–24.
- [37] M. M. Maksimainen, A. Lampio, M. Mertanen, O. Turunen, J. Rouvinen, *Int. J. Biol. Macromol.* **2013**, *60*, 109–115.
- [38] S. C. Li, J. W. Han, K. C. Chen, C. S. Chen, *Phytochemistry* **2001**, *57*, 349–359.
- [39] H. Konno, K. Katoh, **1992**.
- [40] H. Konno, H. Tsumuki, **1993**, 40–47.
- [41] M. S. Buckeridge, J. S. G. Reid, **1993**, 502–511.
- [42] S. Biswas, A. M. Kayastha, R. Seckler, *J. Plant Physiol.* **2003**, *160*, 327–37.
- [43] G. Simos, T. Giannakouros, J. G. Georgatsos, **1989**, *28*, 2587–2592.
- [44] A. Carrillo-López, A. Cruz-Hernández, A. Cárabez-Trejo, F. Guevara-Lara, O. Paredes-López, *J. Agric. Food Chem.* **2002**, *50*, 1681–1685.
- [45] D. L. Smith, D. A. Starrett, K. C. Gross, *Plant Physiol.* **1998**, *117*, 417–423.
- [46] I. K. Kang, S. G. Suh, K. C. Gross, J. K. Byun, *Plant Physiol.* **1994**, *105*, 975–9.
- [47] H. Lazan, S. Y. Ng, L. Y. Goh, Z. M. Ali, *Plant Physiol. Biochem.* **2004**, *42*, 847–853.
- [48] D. L. Smith, K. C. Gross, *Plant Physiol.* **2000**, *123*, 1173–1184.
- [49] M. Edwards, J. L. Bowman, I. C. M. Deagll, J. S. G. R. li, *J. Biol. Chem.* **1988**, *263*, 4333–4337.
- [50] W. Tu, S. Sun, S. Nu, X. Li, *Food Chem.* **1999**, *64*, 495–500.
- [51] A. Dwevedi, A. M. Kayastha, *J. Agric. Food Chem.* **2009**, *57*, 682–688.
- [52] A. Dwevedi, A. M. Kayastha, *Bioresour. Technol.* **2009**, *100*, 2667–2675.
- [53] C. S. Kim, E.-S. Ji, D.-K. Oh, *Biochem. Biophys. Res. Commun.* **2004**, *316*, 738–43.

- [54] S. R. Tello-Solís, J. Jiménez-Guzmán, C. Sarabia-Leos, L. Gómez-Ruiz, A. E. Cruz-Guerrero, G. M. Rodríguez-Serrano, M. García-Garibay, **2005**, 10200–10204.
- [55] A. Pereira-Rodríguez, R. Fernández-Leiro, M. I. González-Siso, M. E. Cerdán, M. Becerra, J. Sanz-Aparicio, *J. Struct. Biol.* **2012**, *177*, 392–401.
- [56] G. D. Miller, J. K. Jarvis, L. D. McBean, National Dairy Council., *Handbook of Dairy Foods and Nutrition*, CRC Press, **2007**.
- [57] P. SCHUCK, A. DOLIVET, *Brazilian J. Chem. Eng.* **2002**, *19*, 397–402.
- [58] P. Walstra, T. J. (Tom J. . Geurts, J. T. M. Wouters, *Dairy Science and Technology*, CRC/Taylor & Francis, **2006**.
- [59] V. H. Holsinger, *Physical and Chemical Properties of Lactose*, **1997**.
- [60] M. G. Gänzle, G. Haase, P. Jelen, *Int. Dairy J.* **2008**, *18*, 685–694.
- [61] † C. A. Hsu, ‡ and S. L. Lee, † C. C. Chou*, **2007**, DOI 10.1021/JF063126+.
- [62] K. Wallenfels, O. Prakash Malhotra, *Adv. Carbohydr. Chem.* **1962**, 239–298.
- [63] I. Y. S. Rustom, M. I. Foda, M. H. López-Leiva, *Food Chem.* **1998**, *62*, 141–147.
- [64] T. M. Bayless, E. Brown, D. M. Paige, *Curr. Gastroenterol. Rep.* **2017**, *19*, DOI 10.1007/s11894-017-0558-9.
- [65] J. M. Rodríguez-Nogales, A. D. López, *Int. Dairy J.* **2006**, *16*, 354–360.
- [66] P. S. Panesar, R. Panesar, R. S. Singh, J. F. Kennedy, H. Kumar, *J. Chem. Technol. Biotechnol.* **2006**, *81*, 530–543.
- [67] M. B. Heyman, *Pediatrics* **2006**, *118*, 1279–1286.
- [68] Q. Husain, *Crit. Rev. Biotechnol.* **2010**, *30*, 41–62.
- [69] R. Sinha, C. Radha, J. Prakash, P. Kaul, *Food Chem.* **2007**, *101*, 1484–1491.
- [70] Z. Quinn Z.K, C. Xiao Dong, *Biochem. Eng. J.* **2001**, *9*, 33–40.
- [71] H. A. Gulec, *Colloids and Surfaces B-Biointerfaces* **2013**, *104*, 83–90.
- [72] A. M. Klibanov, *Nature* **2001**, *409*, 241–246.
- [73] P. V. Iyer, L. Ananthanarayan, *Process Biochem.* **2008**, *43*, 1019–1032.
- [74] B. Brena, P. González-Pombo, F. Batista-Viera, *Immobil. Enzym. Cells Third Ed. Methods Mol. Biol.* **2013**, *1051*, 1–11.
- [75] N. Carlsson, H. Gustafsson, C. Thörn, L. Olsson, K. Holmberg, B. Åkerman, *Adv. Colloid Interface Sci.* **2014**, *205*, 339–60.
- [76] S. B. Lamb, D. C. Stuckey, *Enzyme Microb. Technol.* **1999**, *26*, 574–581.
- [77] P. Jochems, Y. Satyawali, S. Van Roy, W. Doyen, L. Diels, W. Dejonghe, *Enzyme Microb. Technol.* **2011**, *49*, 580–8.
- [78] Q. Husain, S. A. Ansari, F. Alam, A. Azam, *Int. J. Biol. Macromol.* **2011**, *49*, 37–43.
- [79] D.-C. Sheu, S.-Y. Li, K.-J. Duan, C. W. Chen, *CEUR Workshop Proc.* **2014**, *1225*, 41–42.
- [80] M. P. Klein, L. P. Fallavena, J. da N. Schöffner, M. A. Z. Ayub, R. C. Rodrigues, J. L. Ninow, P. F. Hertz, *Carbohydr. Polym.* **2013**, *95*, 465–70.
- [81] M. L. Verma, C. J. Barrow, J. F. Kennedy, M. Puri, *Int. J. Biol. Macromol.* **2012**, *50*, 432–7.
- [82] B. C. C. Pessela, C. Mateo, M. Filho, A. Carrascosa, R. Fernández-Lafuente, J. M. Guisan, *Enzyme Microb. Technol.* **2007**, *40*, 242–248.
- [83] S. Peirce, J. J. Virgen-Ortiz, V. G. Tacias-Pascacio, N. Rueda, R. Bartolome-Cabrero, L. Fernandez-Lopez, M. E. Russo, A. Marzocchella, R. Fernandez-Lafuente, *RSC Adv.* **2016**, *6*, 61707–61715.
- [84] T. Haider, Q. Husain, *Int. J. Biol. Macromol.* **2007**, *41*, 72–80.
- [85] T. Haider, Q. Husain, *Chem. Eng. Process. Process Intensif.* **2009**, *48*, 576–580.
- [86] T. Haider, Q. Husain, *Int. J. Pharm.* **2008**, *359*, 1–6.
- [87] T. Haider, Q. Husain, *Int. Dairy J.* **2009**, *19*, 172–177.
- [88] T. Haider, Q. Husain, *Biochem. Eng. J.* **2009**, *43*, 307–314.
- [89] S. A. Ansari, Q. Husain, *J. Mol. Catal. B Enzym.* **2011**, *70*, 119–126.
- [90] B. Brena, L. Ryden, J. Porath, *Biotechnol. Appl. Biochem.* **1994**, *19*, 217–231.
- [91] B. C. C. Pessela, M. Fuentes, C. Mateo, R. Munilla, A. V. Carrascosa, R. Fernandez-Lafuente, J. M. Guisan, *Enzyme Microb. Technol.* **2006**, *39*, 909–915.
- [92] B. C. C. Pessela, R. Torres, M. Fuentes, C. Mateo, R. Munilla, A. Vian, A. V. Carrascosa, J. L. Garcia, J. M. Guisán, R. Fernandez-Lafuente, *J. Chromatogr. A* **2004**, *1055*, 93–98.
- [93] B. C. C. Pessela, C. Mateo, A. V Carrascosa, A. Vian, G. Rivas, C. Alfonso, M. Guisan, R. Ferna, *Biomacromolecules* **2003**, *4*, 107–113.
- [94] F. Batista-Viera, M. Barbieri, K. Ovsejevi, C. Manta, J. Carlsson, *Appl. Biochem. Biotechnol.* **1991**, *31*, 175–195.
- [95] K. Ovsejevi, C. Manta, F. Batista-Viera, in *Methods Mol. Biol.*, **2013**, pp. 89–116.
- [96] K. Ovsejevi, B. Brena, F. Batista-Viera, J. Carlsson, *Enzyme Microb. Technol.* **1995**, *17*, 151–156.
- [97] F. BATISTA-VIERA, M. CARMEN, J. CARLSSON, *Appl. Biochem. Biotechnol.* **1994**, *44*, 1–14.
- [98] K. Ovsejevi, V. Grazú, K. Cuadra, F. Batista-Viera, *Enzyme Microb. Technol.* **2004**, *35*, 203–209.
- [99] A. Rico-Díaz, M.-E. Álvarez-Cao, J.-J. Escuder-Rodríguez, M.-I. González-Siso, M. E. Cerdán, M. Becerra, *Sci. Rep.* **2017**, *7*, 45535.
- [100] M. Di Serio, C. Maturo, E. De Alteriis, P. Parascandola, R. Tesser, E. Santacesaria, *Catal.*

- Today* **2003**, 79–80, 333–339.
- [101] J. Pedroche, M. del Mar Yust, C. Mateo, R. Fernández-Lafuente, J. Girón-Calle, M. Alaiz, J. Vioque, J. M. Guisán, F. Millán, *Enzyme Microb. Technol.* **2007**, 40, 1160–1166.
- [102] M. J. Hernaiz, D. H. G. Crout, *Enzyme Microb. Technol.* **2000**, 27, 26–32.
- [103] P. Torres, F. Batista-Viera, *Molecules* **2017**, 22, 284.
- [104] M. M. El-masry, a De Maio, P. L. Martelli, R. Casadio, a B. Moustafa, S. Rossi, D. G. Mita, *J Mol Catal B-Enzym* **2001**, 16, 175–189.
- [105] A. De Maio, M. M. El-Masry, Z. H. Abd El-Latif, M. Portaccio, U. Bencivenga, D. G. Mita, *J. Mol. Catal. - B Enzym.* **2001**, 16, 191–204.
- [106] A. De Maio, M. M. El-masry, P. De Luca, V. Grano, S. Rossi, N. Pagliuca, F. S. Gaeta, M. Portaccio, D. G. Mita, **2003**, 21, 253–265.
- [107] N. Albayrak, S.-T. Yang, *Biotechnol. Bioeng.* **2002**, 77, 8–19.
- [108] P. Nakkharat, H. Dietmar, *Appl. Biochem. Biotechnol.* **2002**, 98–100, 311–318.
- [109] D. F. M. Neri, V. M. Balcão, M. G. Carneiro-da-Cunha, L. B. Carvalho Jr., J. A. Teixeira, *Catal. Commun.* **2008**, 9, 2334–2339.
- [110] D. F. M. Neri, V. M. Balcão, R. S. Costa, I. C. A. P. Rocha, E. M. F. C. Ferreira, D. P. M. Torres, L. R. M. Rodrigues, L. B. Carvalho, J. A. Teixeira, *Food Chem.* **2009**, 115, 92–99.
- [111] M. M. M. Elnashar, M. A. Yassin, *Appl. Biochem. Biotechnol.* **2009**, 159, 426–437.
- [112] Q. Z. K. Zhou, X. Dong Chen, *J. Food Eng.* **2001**, 48, 69–74.
- [113] M. Portaccio, S. Stellato, S. Rossi, U. Bencivenga, M. S. Mohy Eldin, F. S. Gaeta, D. G. Mita, *Enzyme Microb. Technol.* **1998**, 23, 101–106.
- [114] R. Gaur, H. Pant, R. Jain, S. K. Khare, *Food Chem.* **2006**, 97, 426–430.
- [115] S. A. Ansari, Q. Husain, *Food Bioprod. Process.* **2012**, 90, 351–359.
- [116] J. M. Goddard, J. N. Talbert, J. H. Hotchkiss, *J. Food Sci.* **2007**, 72, 1–6.
- [117] Z. Grosová, M. Rosenberg, M. Rebroš, *Czech J. Food Sci.* **2008**, 26, 1–14.
- [118] K. Kashima, I. Masanao, in *Adv. Desalin.*, **2012**, pp. 3–36.
- [119] E. J. Mammarella, A. C. Rubiolo, *J. Mol. Catal. B Enzym.* **2005**, 34, 7–13.
- [120] E. J. Mammarella, **2001**, 142.
- [121] A. Tanriseven, Ş. Doğan, *Process Biochem.* **2002**, 38, 27–30.
- [122] E. Taqieddin, M. Amiji, *Biomaterials* **2004**, 25, 1937–1945.
- [123] L. Zhang, A. Otte, M. Xiang, D. Liu, R. Pinal, *Molecules* **2015**, 20, 17180–17193.
- [124] K. Batsalova, K. Kunchev, Y. Popova, A. Kozhukharova, N. Kirova, **1987**, 227–230.
- [125] Z. Grosová, M. Rosenberg, M. Rebroš, M. Šipocz, B. Sedláčková, *Biotechnol. Lett.* **2008**, 30, 763–767.
- [126] C. K. Kim, H. S. Chung, M. K. Lee, L. N. Choi, M. H. Kim, *Int. J. Pharm.* **1999**, 183, 185–193.
- [127] J. M. Rodriguez-Nogales, A. Delgadillo, *J. Mol. Catal. B Enzym.* **2005**, 33, 15–21.
- [128] H. Li, S. Li, P. Tian, Z. Wu, Z. Li, *Molecules* **2017**, 22, DOI 10.3390/molecules22030377.
- [129] T. Coradin, J. Livage, *Comptes Rendus Chim.* **2003**, 6, 147–152.
- [130] Z. Zhang, R. Zhang, L. Chen, D. J. McClements, *Food Chem.* **2016**, 200, 69–75.
- [131] Z. Wu, Z. Wang, B. Guan, X. Wang, Y. Zhang, Y. Xiao, B. Zhi, Y. Liu, Z. Li, Q. Huo, *New J. Chem.* **2013**, 37, 3793.
- [132] L. Domingues, N. Lima, J. A. Teixeira, *Process Biochem.* **2005**, 40, 1151–1154.
- [133] M. Ladero, A. Santos, F. García-Ochoa, *Enzyme Microb. Technol.* **2000**, 27, 583–592.
- [134] J. Szczodrak, *Acta Biotechnol.* **2000**, 10, 631–637.
- [135] R. Rech, M. A. Z. Ayub, *Process Biochem.* **2007**, 42, 873–877.
- [136] S. Chockchaisawasdee, V. I. Athanasopoulos, K. Niranjana, R. A. Rastall, *Biotechnol. Bioeng.* **2005**, 89, 434–443.
- [137] R. R. Mahoney, *Food Chem.* **1998**, 63, 147–154.
- [138] A. Axelsson, G. Zacchi, *Appl. Biochem. Biotechnol.* **1990**, 24–25, 679–693.
- [139] G. Mantioli, F. F. De Moraes, G. M. Zanin, *Acta Sci. - Heal. Sci.* **2003**, 25, 7–12.
- [140] X. Li, Q. Z. K. Zhou, X. D. Chen, *Chem. Eng. Process. Process Intensif.* **2007**, 46, 497–500.
- [141] S. Novalin, W. Neuhaus, K. D. Kulbe, *J. Biotechnol.* **2005**, 119, 212–218.
- [142] I. Roy, M. N. Gupta, *Process Biochem.* **2003**, 39, 325–332.
- [143] A. R. Özdural, D. Tanyolaç, I. H. Boyaci, M. Mutlu, C. Webb, *Biochem. Eng. J.* **2003**, 14, 27–36.
- [144] C. R. Carrara, E. J. Mammarella, A. C. Rubiolo, *Chem. Eng. J.* **2003**, 92, 123–129.
- [145] E. Jurado, F. Camacho, G. Luzón, J. M. Vicaria, *Bioprocess Biosyst. Eng.* **2005**, 28, 27–36.
- [146] G. M. Rios, M. P. Belleville, D. Paolucci, J. Sanchez, *J. Memb. Sci.* **2004**, 242, 189–196.
- [147] A. N. Genari, F. V. Passos, F. M. L. Passos, *J. Dairy Sci.* **2003**, 86, 2783–2789.
- [148] N. Vasileva, Y. Ivanov, S. Damyanova, I. Kostova, T. Godjevargova, *Int. J. Biol. Macromol.* **2016**, 82, 339–346.
- [149] S. CURCIO, V. CALABRO, G. IORIO, *J. Memb. Sci.* **2006**, 273, 129–142.
- [150] N. Diano, V. Grano, S. Rossi, U. Bencivenga, M. Portaccio, U. Amato, F. Carfora, M. Lepore, F. S. Gaeta, D. G. Mita, *Biotechnol. Prog.* **2004**, 20, 457–466.
- [151] D. G. Hatzinikolaou, E. Katsifas, D. Mamma, A. D. Karagouni, P. Christakopoulos, D. Kekos, *Biochem. Eng. J.* **2005**, 24, 161–172.
- [152] P. S. Panesar, S. Kumari, R. Panesar, *Enzyme Res.* **2010**, 2010, 1–16.
- [153] S. Rejikumar, S. Devi, *Int. J. Food Sci. Technol.* **2001**, 36, 91–98.

- [154] G. Bayramoglu, Y. Tunali, M. Y. Arica, *Catal. Commun.* **2007**, *8*, 1094–1101.
- [155] N. Vasileva, Y. Ivanov, S. Damyanova, I. Kostova, T. Godjevargova, *Int. J. Biol. Macromol.* **2016**, *82*, 339–346.

1. 2. Silica-based systems for oral and food delivery ¹

Silicon dioxide (SiO₂) or silica, is abundantly distributed in the earth's crust in the form of silicate minerals, and is a component in plants, cereals and fruits [1]. Human body also contains silicon in its skeleton, heart, muscles, blood vessels, skin, hair and nails, ligaments of cartilage [2]. Living organisms such as siliceous sponges have an amorphous skeleton generated by an enzyme, the silicatein [3].

From robust industrial solids to soft biocompatible materials, silica has a range of properties that can be tuned according to the design applications, through wet or thermal processes. Mesoporous materials with high surface areas and pore volumes [4] are obtained through sol-gel process, by far the most used synthetic route. Highly ordered pores with hexagonal or cubic arrangements can be obtained with tunable sizes in the range of 2 to 50 nm [5]. Moreover, the presence of silanol groups (Si-OH) on the inner and outer surface of the material facilitates its chemical functionalization by specific groups related to the desired application. Such chemical properties make those materials suitable for adsorption of pollutants, polymer filler, and catalyst applications [6]. Beyond those applications, nanomedicine is also of high interest. Drug delivery and bio-imaging are topics in which the use of amorphous silica is becoming popular especially because of its biocompatibility and capacity to uptake poorly soluble drugs. There are more and more sophisticated targeted silica carriers that are stimuli-responsive multifunctional platforms to allow both diagnostic and therapy, known as theranostic approach. In the food sector, silica can be employed as catalysts for the synthesis of bioactive molecules and nutrients [7], as sensors [8] or as carriers for the formation of functional food [9]. "Functional food" refers to the food or food component that can offer beyond basic nutrition some health benefits [10].

Nowadays, significant efforts are made in respect to developing smart drug delivery systems (DDS) for different administration routes, including the

¹ This subchapter is based on the review: R.Diab, N. Canilho, *J.A.Pavel*, F.B.Haffner, M.Girardon and A. Pasc, "Silica-based systems for oral delivery of drugs, macromolecules and cells"-Advances in Colloid and Interface Science-In press [26]

oral one. Indeed, the oral administration is still the most comfortable and efficient for the patient, although the passage through the gastrointestinal barrier remains challenging. Before being approved as nontoxic and biodegradable, silica was already used as excipients in medicine and food additives (E551). More recently, according to the US Food and Drug Administration (FDA) and the European Food Safety Authority (EFSA), amorphous forms of silica and silicates are generally recognized as safe for oral delivery of ingredients in amounts up to 1500 mg per day [11].

In this context, the aim of this chapter is to give an extended overview on the latest advances of the use of silica for oral delivery including drugs, proteins, hormones, cells (probiotic bacteria) and enzyme. They can be used in the elaboration of functional food or in oral pharmaceutical dosage forms.

1.2.1. Prerequisite for oral delivery systems and food applications

Noninvasive, accessible, simple and economical, the oral administration remains at the top of the prescribed and over-the-counter medications over the world. Therefore, it is not surprising that whenever possible, clinicians prefer to prescribe oral dosage forms instead of parenteral ones which are not only invasive but require medical interventions and occasionally hospitalization. Several intravenous-to-oral route conversion programs were implemented in hospitals aiming to reduce infection risks inherent to the intravenous administration, to reduce medication costs and to improve patients' compliance [12–16].

Great research efforts have been dedicated to the development of oral dosage forms that might substitute/limit the use of parenteral forms. Nevertheless, the design of drug products for the oral route remains challenging. Indeed, the passage through the gastrointestinal tract (GIT) is harsh on drugs, which will encounter several barriers before reaching the systemic circulation. Several factors are involved: i) the gastric pH that is as low as 1 in fast conditions; ii) the presence of hydrolytic enzymes in the gastric and intestinal juices; iii) the intestinal drug efflux by *P*-glycoprotein pumps localized

in enterocytes' apical membranes; and iv) the premature drug catabolism by the hepatic and/or intestinal cytochrome P450 [17].

The success of this passage depends partially on the drug's own physicochemical properties such as water solubility, molecular weight, partition coefficient [18] and also on the delivery system. The design of ODDS could be adjusted to ensure other functions beyond the protection of the payload from its premature degradation. In this respect we can mention:

- i) the **gastro-retention** sought for different purposes, e.g. to achieve a local action in the stomach, to enhance the absorption of drugs within a narrow window or even to enhance the stability of unstable drugs in the intestinal juice [19];
- ii) the **gastro-resistance** of drugs that are subjected to degradation in the severe gastric environment or conversely, to protect the gastric mucus against drugs' irritant effects;
- iii) the **sustained release** aiming a reduction in dosing frequency and therefore improving the patients' compliance;
- iv) the **triggered release** to a specific site, e.g. targeting a high drug amount directly on specific cells in the colon;
- v) the **mucoadhesion** on the intestinal epithelium allowing the increase of the intestinal residence time, and thus a longer time for drug absorption;
- vi) an **enhancement of the dissolution rate** of drugs of class II and IV (according to the biopharmaceutical classification system).

The above-mentioned functions of ODDS could be reached by using appropriate formulations from the wide range of ingredients nowadays available. For instance, polysaccharides, e.g. chitosan, cellulose, starch and their derivatives, alginates, pectin, and acacia gum; proteins, e.g. albumin, gelatin and gliadin; polymethacrylates bearing quaternary ammonium groups (Eudragit[®] RS/ Eudragit[®] RL) are all mucoadhesive polymers allowing the close contact of payloads with the intestinal epithelium for extended periods of time. Moreover, in the formulation of hydrophilic matrices, micro- and nanoparticulate DDS, these polymers form swellable networks enabling the

sustained diffusion of drugs. Furthermore, these polymers are able to promote paracellular transport through the intestinal epithelium by producing a transient opening of the tight junctions between the enterocytes ^[20,21] .

The gastro-resistance becomes possible thanks to pH-sensitive polymers such as, cellulose acetato-phthalate and Eudragit[®] L or Eudragit[®] S. The unique feature of these polymers is the presence of carboxylic groups (–COOH). In the acidic gastric juice where the pH is below the pKa of carboxylic acid groups (≈ 4), the protonated form (water insoluble) is predominant, which constitutes a physical barrier against drug release. In the intestinal juice, the pH is higher than 4, which induces polymer deprotonation, dissolution and thus allowing drug release.

The enhancement of the dissolution of poorly soluble drugs is carried out using a variety of materials. For instance, lipids such as monoglycerides, triglycerides, glycerophospholipids and middle- and short-chains fatty acids are used in the formulation of lipophilic matrix tablets, self-microemulsified DDS, solid lipid nanoparticulate DDS and nanostructured lipid carriers, among others. It is noteworthy to mention that middle- and short-chains fatty acids are able to reversibly destabilize the tight junctions of the epithelium, and thereby enhancing intestinal permeability of the loaded drug ^[22,23].

On top of this properties, for food applications, the effect of silica on product appearance, mouth feel, texture, flavor and shelf live should be minimum or compatible with the food matrix ^[24].

1.2.2. Formation and origin of silica

Silica can be classified in two main categories, crystalline (*i.e.* quartz, cristobalite, tridymite or calcinated diatomite) or amorphous, as a function of the connectivity between the tetrahedral units and of the long-range periodicity in the network. Figure 1.2. 1 illustrates typical differences of periodicity between an amorphous silica bulk and cristobalite, chosen as example of crystalline silica. In both cases, the bulk of silica is composed of SiO₄ tetrahedral units that form siloxane rings of different Si–O sizes. The size of the silica rings present on the silica surface generally ranges from flexible 12-membered rings to

strained 4-member Si–O rings, and the distribution of such siloxane rings generally depends on the calcination/activation temperature of silica [25]. At the surface, various kinds of silanols can be found; they can be classified as isolated (non-H-bonded), geminal, vicinal, and interacting (H-bonded) silanols (Figure 1.2. 1). In the case of crystalline silica, such as cristobalite, only three kind of silanols can be found at the surface: geminal (for 001 termination), vicinal (for 101 termination) and isolated silanols (for 111 termination) while in the case of amorphous silica, all kinds of silanols are present (Figure 1.2. 2). This property explains the highest reactivity of amorphous silica surface vs crystalline ones. Moreover, depending on the reaction conditions, such as temperature or condensation degree, the -OH density at the surface of the material can be tuned between less than 1 to 7 -OH/nm².

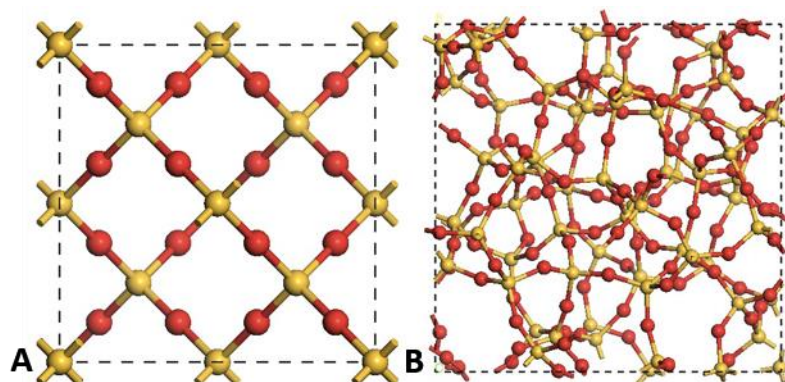


Figure 1.2. 1. Unit cells of bulk structures of (A) crystalline (ex. β –cristobalite) 7.16 x 7.16 x 7.16 Å³ unit cell, containing 8 SiO₂ units and (B) amorphous SiO₂, 14.32 x 14.32 x 14.32 Å³ unit cell, containing 64 SiO₂ units (reproduced from [25]).

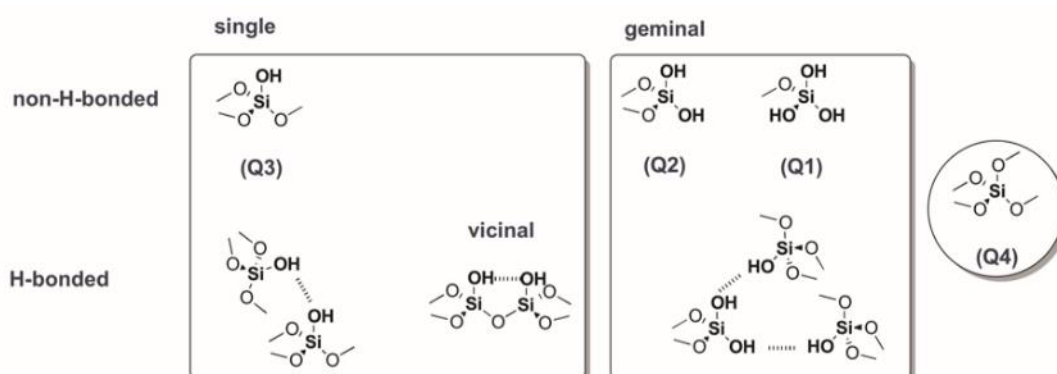


Figure 1.2. 2. Types of silanol and silica bridges (reproduced from [26]).

In oral drug delivery and food applications, only amorphous silica should be considered, due to its lower toxicity and increased dissolution in biological

fluids. Amorphous silica can be classified in natural (biosilica, e.g. diatomite) and synthetic (Figure 1.2. 3). In the last category, various forms of silica were defined depending for example on the process: wet, *i.e.* silica-gel, precipitated and colloidal silica and thermal, *i.e.* fused and fumed silica.

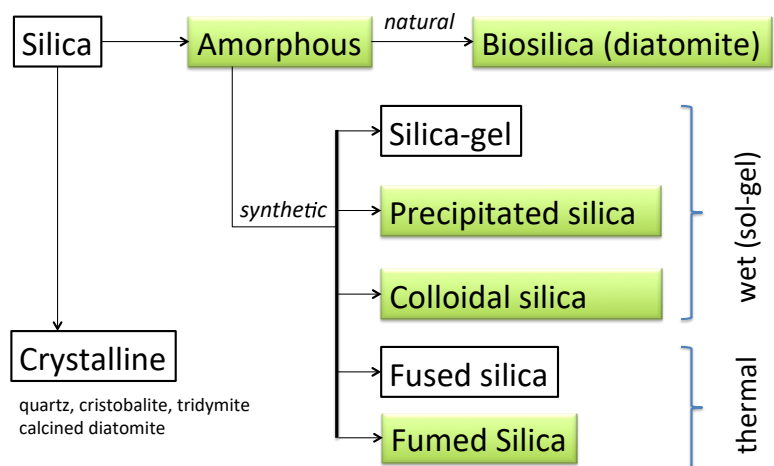


Figure 1.2. 3. Classification of various forms of silica.

There are four types of silica-based materials used as oral delivery systems and smart foods: (1) non-porous silica nanoparticles (fumed and Stöber nanoparticles), (2) mesoporous silica nanoparticles, (3) mesoporous silica based materials, (4) biosilica, e.g. diatoms. Payload materials can be obtained either by post silica synthesis or by one pot synthesis. These materials can be likewise obtained at low temperatures, which is compatible with the manipulation of drugs, biomolecules [27] or cells [28].

1.2.2.1. Synthesis of non-porous silica nanoparticles

1.2.2.1.1. Fumed silica nanoparticles

Amorphous fumed silica is manufactured through a flame-synthesis technology in which silicon tetrachloride (SiCl₄), playing the role of the silica precursor, is vaporized in an oxygen-hydrogen flame. The spontaneous and quantitative hydrolysis reactions with oxygen and hydrogen result in SiO₂. The flame temperature reaches between 1200 to 1600 °C allowing the formation of viscous droplets of amorphous silicon dioxide, so-called primary particles, which collide and fuse together building up stable aggregates. The primary particle sizes are around 3 to 50 nm while the aggregates are of 200 to 500 nm.

The dimensional criteria and the hydrophilic and hydrophobic character dictate the grade of the fumed silica [29,30].

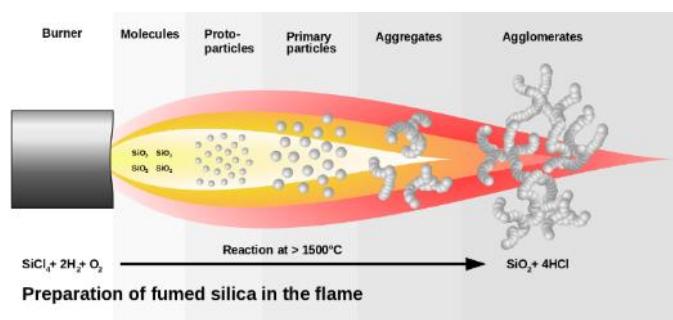


Figure 1.2. 4. Flame pyrolysis of silicon tetrachloride in electric arc (reproduced form [31]).

AEROPERL® 300 Pharma (particle size of 30 μm) is used in the formulation of Hesperidin, an oral delivery carrier [33]; hydrophilic Aerosil 380 (particle size of 7 nm) is used to stabilize Pickering emulsions as to lipid-based oral delivery systems (ODS) [34–37]. Aerosil ® 200 was used to immobilize food ingredients as essential oil components (carvacrol, eugenol, thymol and vanillin) and their antimicrobial activity was tested into pasteurized milk inoculated with *L. innocua* [40].

1.2.2.1.2. Stöber nanoparticles

Fumed silica is manufactured at high temperatures, but in 1968 Stöber reported an affordable wet chemistry pathway to produce in laboratory conditions non-porous colloidal particles with controlled size. This route remains today the most used synthetic approach to prepare monodisperse silica nanoparticles (SiNP). It is a sol-gel process wherein typically tetraethylorthosilicate molecules follow hydrolysis and condensation reactions providing precursor species and the necessary supersaturation for the formation of particles. The reactive media contains ammonia as a basic catalyst for the hydrolysis reaction. In such process, the diameter of silica particles is controlled by the relative contribution of nucleation and growth processes. This synthetic way allows to produce individual silica particles with diameters ranging from 50 nm to 2 μm [32].

This type of synthetic non-porous silica is largely used in oral applications due to their chemical stability and intrinsic hydrophilicity, which are appropriate for biological environments. Andreani *et al.* associated insulin to SiNP and they coated them with mucoadhesive polymers such as chitosan or PEG aiming the oral delivery of insulin [33,34].

1.2.2.2. Synthesis of mesoporous silica

Since 1990, porous synthetic amorphous silica materials have been widely used in various applications, especially as catalyst [35] or absorbents, but also as drug carriers [9,36–40]. The porosity of materials can be classified according to IUPAC into three categories: macroporous (> 50 nm), mesoporous (2 to 50 nm) and microporous (< 2 nm). So far, mesoporous silica materials are synthesized from either micelles of surfactants by cooperative self-assembly (CSA) or from surfactant liquid crystals templates through the transcription mechanism (LCT) [41,42] (Figure 1.2. 5). In both pathways, the silica source hydrolyses and then polycondenses around the structure-directing agent leading to a hybrid gel, called mesophase. Nevertheless, the two mechanisms differ by the concentration of surfactant in the synthesis media. At high surfactant concentration liquid crystals are formed, thus hydrolysis and polycondensation of a silica source leads to a mesostructured material templated by the liquid crystalline phase. In the case of the cooperative self-assembly mechanism

Figure 1.2. 6, the surfactant concentration is low but usually above the critical micellar concentration. During the polycondensation of the silica, the micelles grow to finally form an inorganic mesostructured silica-surfactant composite, also called mesophase. The mesoporosity is released after surfactant removal, either by calcination or by solvent extraction [43].

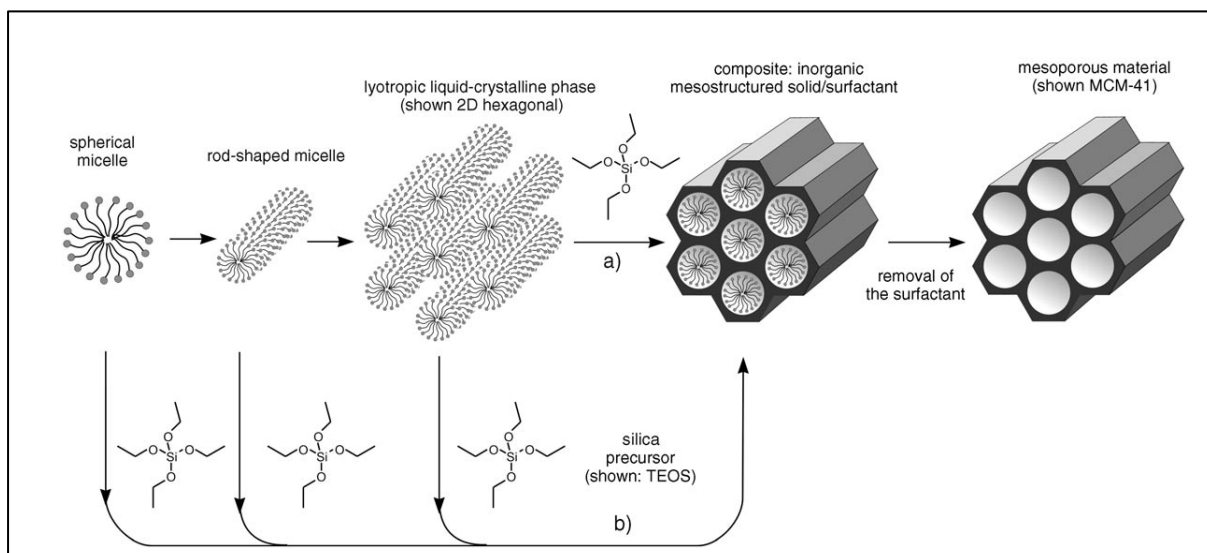


Figure 1.2. 5. Formation of mesoporous materials by structure-directing agents: a) true liquid-crystal template mechanism, b) cooperative liquid crystal template mechanism (reproduced from [41]).

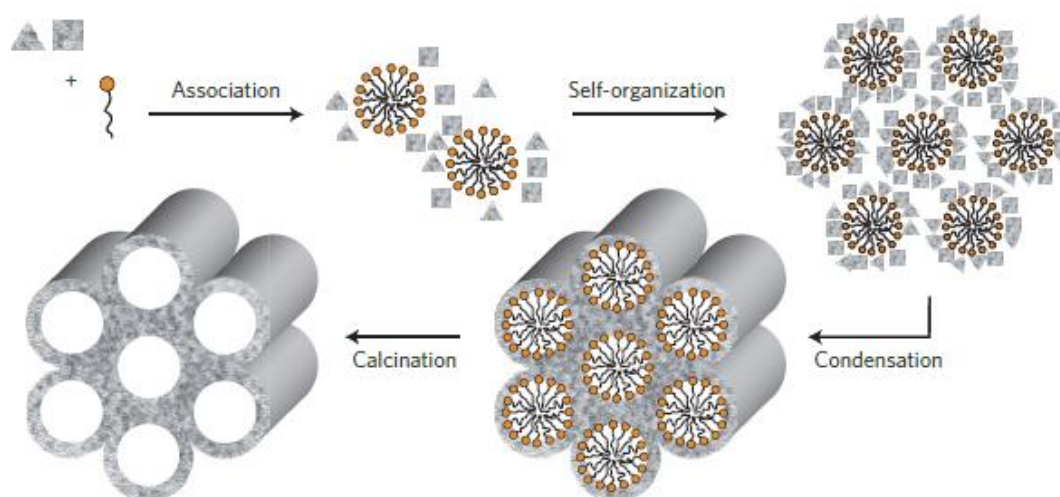


Figure 1.2. 6. cooperative self-assembly mechanism (reproduced from [44])

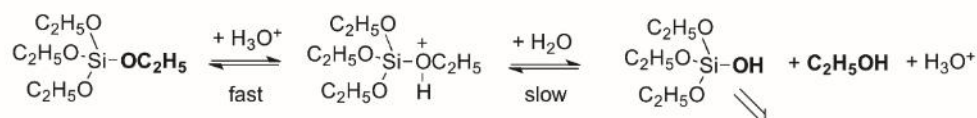
Nevertheless, obtaining mesoporous materials with highly ordered porosity is not trivial. In fact, intimate interactions between the organic template and the silica must take place during the hydrolysis and the polycondensation of the silica mesophase as shown in Figure 1.2. 5 and in

Figure 1.2. 6. The main factors influencing the material structuring are the experimental conditions (pH^[45], temperature, aging time), the type of silica precursor, the surfactant nature, its concentration and the molar ratio between the surfactant and the silica source that have a direct impact on the hydrolysis,

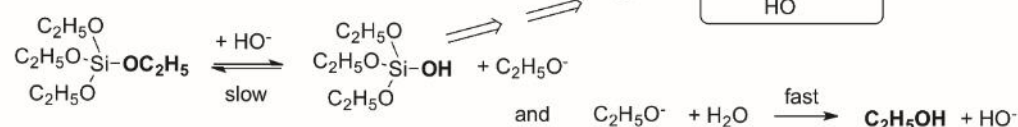
condensation, and dissolution reactions [46]. Pore size can also be tuned by the diameter of the micelles that depends on the surfactant molecular weight, the bigger the micelles the larger the pore sizes. The micelles can also be swollen by organic solvents [47]. The porogens (or surfactant) can be either non-ionic [48], cationic [49] or anionic [50,51]. Food grade directing agents, such as polyglycerol esters of fatty acids [52], myristic acid ester of pentaglycerol [53], and oleic acid [54] have also been employed. Each template has a specific interaction with the silica source, which is in most of the cases an alkoxy silane, such as tetramethylortosilicate (TMOS) or tetraethylortosilicate (TEOS). Alkoxy silanes release methanol or ethanol as reaction by-products that might compromise the hybrid silica/surfactant self-assembly or could be detrimental to proteins or cells, if directly entrapped during the sol-gel synthesis [55]. The formation mechanism of the silica scaffold and the release of ethanol during the hydrolysis/condensation reaction from TEOS are outlined as an example below.

Hydrolysis

acid-catalyzed reaction

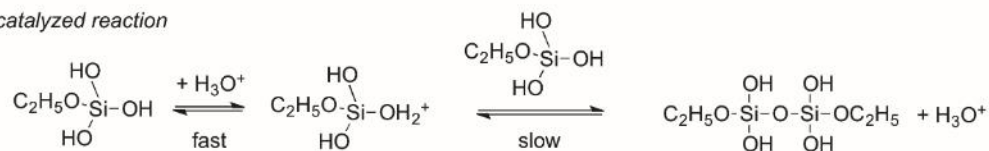


base-catalyzed reaction

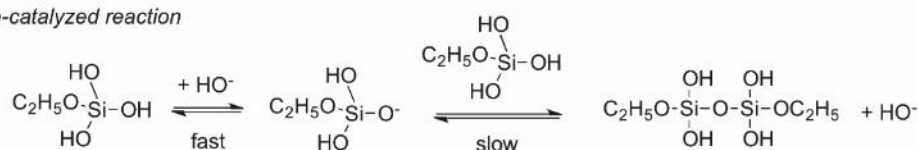


Condensation

acid-catalyzed reaction



base-catalyzed reaction



To avoid possible toxic by-products, acidified aqueous sodium silicate solutions can be used to perform the synthesis in appropriate pH conditions

with respect to the entrapped biocompound [56,57]. A food grade alternative is rice husk ashes [58,59]. The pH and the salts content are drastically influencing the charge density of silica and the ionic strength of the media during the synthesis. The temperature also has an important effect either in helping the formation of the hybrid structure or in dissolving it. However, the sol-gel process can occur at temperatures below 40°C, which makes it compatible with biomolecules or cells^[28]. The aging time and pH are also influencing the properties of the resulting silica material, in terms of texture, morphology and mesopores structuring. During the aging step, the silica precursor is hydrolysed and starts to condense to form a gel, which strength and stiffness increase with the degree of siloxane crosslinking. At low pH, the hydrolysis of alkoxy silane is faster than at high pH, but the condensation is slower. It should be also noted that TMOS is hydrolysed faster than TEOS [43,60].

Since the 90's, many new synthetic amorphous mesoporous materials have been created with 1D, 2D or 3D pore channel arrays, different pore sizes, specific areas and even with nanoparticulate morphologies. In fact, silica nanoparticles (SiNP) are an excellent candidate for their conjugation with drug, biomolecules or cells [28] in the sense that (i) SiNP possess residual silanol groups (Si-OH) at their surface which can be functionalized by different organic groups [61] (ii) these materials can be synthesized at low temperature, which is compatible with the manipulation of biomolecules [27], (iii) SiNP present large surface areas which allows high interactions with drugs [62], (iv) SiNP can act as drug reservoirs by possessing high porosity and allowing efficient drug loading [63], and (v) the material is known to be biocompatible for *in vivo* applications [64], (vi) SiNP are not subjected to microbial attack [65].

The most used mesoporous silica nanoparticles (MSN) in drug or bio-encapsulation are MCM-41 and SBA-15. The synthesis of MCM-41 (**M**obil **C**omposition of **M**atter series) involves liquid crystal templating using commonly cetyl trimethylammonium bromide (CTAB) that leads to a 2D hexagonal pore channel array with 3.6 nm in size. The diameters of MCM-41 nanoparticles can be controlled ranging from 25 to 100-150 nm [66-70]

The SBA-15 (**S**anta **B**arbara type) is also largely used as biocarrier. This type of mesoporous silica material is prepared by cooperative self-assembly with a pluronic surfactant, P123, a non-ionic block co-polymer. The pore channels adopt also a 2D hexagonal packing with a diameter varying from 6 to 10 nm depending on the synthesis conditions [5,71].

1.2.2.3. Synthesis of hybrid silica microparticles

The discovery of the previously described synthetic routes opened up the frontiers for the preparation of nanoparticulate or microparticulate silica materials with hierarchical porosity, such as meso-macroporous materials.

Our group prepared such materials by using a silica precursor and dispersions of solid lipid nanoparticles in a micellar solution (Figure 1.2. 7), [72–74]. The formation of the silica matrix is based on a dual templating mechanism, combining self-assembly mechanism of surfactant micelles (Tween 20, Tween 40 or Pluronic P123) with transcription mechanism of solid lipid nanoparticles. Depending on the reaction conditions, the morphology of the final material can be tuned to capsules or to block matter (Figure 1.2. 7, left). The size of the mesopores is strongly dependent on the nature of the surfactant in excess, 3 nm (Tween 20), 5 nm (Tween 40) or 9 nm (Pluronic P123), whereas the size of the macropores depends only on the size of SLN (250 ± 150 nm). The macroporous void was clearly evidenced by TEM (Figure 1.2. 7 right). The organization degree of the silica wall depends on the surfactant: only wormlike mesoporous capsules were obtained with Tween 20, and hexagonally ordered microdomains embedded in wormlike mesoporous silica capsules were obtained with Tween 40. Hexagonally ordered silica with circularly ordered mesoporosity could be achieved with Pluronic block copolymer P123.

Using the same strategy, core-shell microparticles were prepared with a core of solid lipid nanoparticles and a mesostructured silica shell. By encapsulating curcumin in the solid lipid nanoparticles before the silica formation, hybrid core-shell materials were obtained after drying, without any further washing step [75].

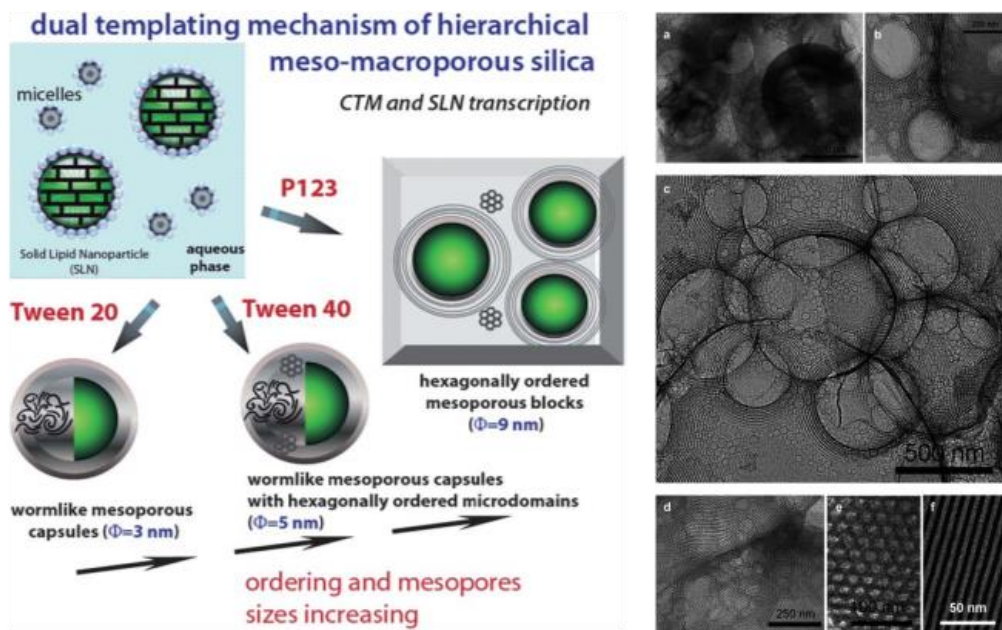


Figure 1.2. 7 (Left) Schematic representation of hierarchical meso-macroporous silica obtained through a dual templating mechanism combining self-assembly mechanism with micelles of Tween 20, Tween 40 and P123 and SLN transcription; (Right) TEM micrographs of meso-macroporous silica obtained from SLN dispersions with P123 at various temperatures: 100°C (a and c), 70°C (b) and 40°C (d-f) (reproduced from [74]).

Core-shell microparticles containing an ionogel as core and a silica shell could be also obtained in a two steps synthesis (Figure 1.2. 8). In the first step, the probiotic bacteria *Lactobacillus rhamnosus* GG and sodium alginate were electrospayed over a calcium bath leading to alginate beads of about $220 \pm 15 \mu\text{m}$ (Figure 1.2. 8). In a second step, the microgels were dispersed in an aqueous solution containing Tween 40 as porogen, APTMS (aminopropyltrimethoxysilane) and TMOS (tetramethoxysilane) as silica sources. The hydrolysis of both precursors and their co-condensation resulted in core-shell microparticles. Moreover, due to the presence of the surfactant, mesoporosity could be introduced into the silica shell during the mineralization process. When encapsulating living matter, the porosity is essential to allow bidirectional diffusion of nutrients and metabolites in and out of the beads, which in our case resulted in proliferation of the bacteria under confinement. The mild synthesis conditions of the mineralization step were not detrimental to bacteria and allowed their encapsulation while maintaining a good viability (more than 8 log/mL). The release studies simulating the gastrointestinal conditions showed that the bacteria encapsulated in the alginate-silica microparticles had a superior survivability in comparison to free bacteria or even with bacteria encapsulated only in alginate beads [76].

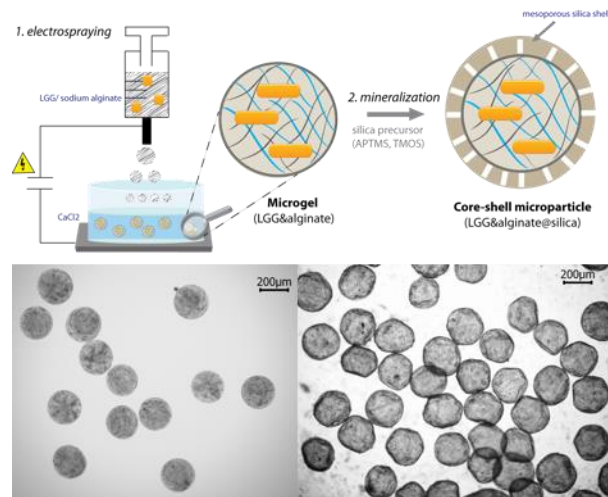


Figure 1.2. 8. (Top) Schematic representation of the general procedure leading to core-shell microgels. (Bottom left) Optical microscopy micrograph of wet LGG&alginate beads recovered by ionogelation of the electrospayed polymeric solution containing the bacteria and (bottom right) of wet core-shell LGG&alginate@silica microparticles (reproduce from [76]).

Both curcumin and LGG encapsulated materials can be used for food applications.

1.2.2.4. Biosilica (silica diatoms)

Silicon is abundantly distributed in nature and has key functions, such as being a micronutrient for plants, or a key element in the production of stable structures, essential to all living organisms. Two typical examples of biosilica are: the porous skeleton of diatoms [77] and the glass spicules of siliceous sponges [78]. Silica diatoms, have been already investigated for oral delivery applications [79,80].

Diatoms are considered to be harmless due to their amorphous silica structure [81]. Food grade diatomaceous earth has been approved in USA to feed animals and there are already several human grade diatomite silica microparticles products in the market in Europe and Australia (e.g. SiLaLive) [82]. These intricate silica-based systems were used to build-up complex oral carriers whose synthesis and applications are summarized in Table 1.2. 1.

Table 1.2. 1. Selected examples of silica-based oral delivery systems [26].

Delivery system	Silica source	Payload	Coating	Encapsulation method	Release mechanism	<i>In vitro/in vivo/ex vivo</i> studies	Ref
Non porous silica nanoparticles							
Stöber NPs	TEOS	Insulin	PEG 6000 PEG 20000	Physisorption of insulin to pre-synthesized uncoated silica nanoparticles- subsequent coating with PEG	Passive diffusion	<i>Ex vivo</i> permeation studies using everted rat intestine	[33]
Stöber NPs	TEOS	Insulin	Chitosan	Physisorption of insulin in chitosan solution to pre-synthesized uncoated silica NPs	Passive diffusion	<i>In vitro</i> studies of NP interactions with porcine mucin	[34]
Mesoporous silica particles							
MCM-48	Ludox AS40	Ibuprofen Erythromycin	-	Physisorption by immersion	Passive diffusion	<i>In vitro</i> drug release in a simulated body fluid (pH 7.7-7.4)	[91]
<i>Ja3d</i> MSN SBA-15 silica	TEOS/MPTS nf	Itraconazole	-	Physisorption by immersion	Passive diffusion	<i>In vitro</i> drug release in a simulated gastric fluid (pH 1.2)	[89]
SBA-15 and MCM-41 functionalized with amino group	nf	Bisphosphonates	-	Electrostatic interaction between drug's phosphate group and silica's amine group at pH 4.8	Passive diffusion at pH 7.4	<i>In vitro</i> drug release in phosphate buffer pH 7.4	[92]
MCM41 nanoparticles	nf	Rhodamine B	α -CD, adamantly ester	Physisorption	Porcine liver esterase triggered	<i>In vitro</i> hydrolysis in HEPES buffer pH7.5	[93]
MCM48	TEOS/APTES	Silfalizine	Succinylated soy protein isolate	Physisorption and coating	pH/enzyme triggered	<i>In vitro</i> drug release in simulated GIT fluid at pH 1.2, 5., 7.4	[94]
Hybrid silica microparticles							
Core-shell (SLN- mesostructured silica)	TMOS	Curcumin	-	1. encapsulation of curcumin in SLN by emulsification/sonication; 2. Sol-gel	Passive diffusion	<i>In vitro</i> drug release in a simulated GIT fluid (pH 1.2-7.4)	[75]
Core-shell (alginate silica)	TMOS/ APTMS	LGG	-	1. preparation of LGG/alginate microgels by electrospraying, 2. mineralization	Erosion of silica shell	<i>In vitro</i> drug release in a simulated GIT fluid (pH 1.2-7.4)	[76]
Spherical mesocellular foam	hydrophilic fumed silica	Insulin	Eudragit L30D- 55 Eudragit L100	Physical adsorption by immersion	pH triggered	<i>In vitro</i> drug release in simulated GIT fluid at pH 1.2 and 6.8	[95]
Diatom silica microparticles							
Diatom silica	fossile	Indomethacin/ Gentamicin	-	Physisorption	Passive diffusion	<i>In vitro</i> drug release in simulated intestinal fluid at pH 7.2	[96]
Diatom silica	fossile	Mesalamine/ prednisone	-	Physisorption	Passive diffusion	<i>In vitro</i> drug release in a simulated GIT fluid (pH 1.2-7.4)	[82]

Table 1.2. 2. Selected examples of silica-based food delivery systems.

Delivery system	Silica source	Payload	Coating/Capped	Encapsulation method	Release mechanism	Release studies	Ref
Non porous silica nanoparticles							
Stöber NPs	TEOS	resveratrol	PMES	Physisorption	Passive diffusion	<i>In vitro</i> drug release in phosphate buffer pH 7.4	[97]
Mesoporous silica particles							
MCM-41	TEOS	resveratrol	-	Impregnation, solid-state method	Passive diffusion	<i>In vitro</i> drug release in phosphate buffer pH 7.4	[98]
MCM-41	TEOS	Vitamin B2	polyamine 3-[2-(2-aminoethylamino)ethylamino]propyl-trimethoxysilane).	Physisorption by immersion	pH and salts triggered	<i>In vitro</i> release in a pH containing different anions	[39]
Hollow microspheres, SBA-15	TEOS	Vitamin B3 precursor	-	Covalent grafting method	pH trigger	<i>In vitro</i> release in a simulated gastric fluid (pH 1.2)	[52]
MSNs	TEOS	Vitamin C	-	Physisorption	Burst release at basic pH	<i>In vitro</i> drug release in SGF(pH 1.2), SIF (7.4), SBF(7.4)	[99]
MCM41 micropart	TEOS/ TEAH3	Folic acid	-	Impregnation	pH triggered	Yoghurt <i>in vitro</i> drug release in a simulated GIT fluid (pH 2, 4, 7.5)	[100]
Mesoporous silica mesoparticles	TEOS	Curcumin	-	Entrapment	Passive diffusion	<i>In vitro</i> release at physiological pH	[101]
Mesoporous silica mesoparticles	TEOS	oligophenol	-	Entrapment	Passive diffusion	<i>In vitro</i> release at physiological pH	[101]
Mesoporous silica mesoparticles	TEOS	Trans-β-Carotene	-	Entrapment	Passive diffusion	<i>In vitro</i> release at physiological pH	[101]
SBA-15	TEOS/APTES	Vitamin E	LDPE	Impregnation	Passive diffusion	Migration tests in olive oil	[102]
MCM-41	SiO ₂	Quercetin	-	Kneading method	Passive diffusion	Diffusion through a semi-permeable cellulose membrane	[103]
SBA-15, Syloblock	TEOS	α-tocopherol	LPDE, EVA	Physisorption	Passive diffusion	Migration tests in ethanol	[104]
MCM-41	TEOS/TEAH3	Garlic extract	Polyamines and hydrolyzed starch on nylon-6	Physisorption	Pancreatic or pH triggered	Electrochemical studies in aqueous solution at pH 7 or 2	[105]

MPTS : Mercaptopropyl-trimethoxysilane ; APTMS : aminopropyltriethoxysilane, SLN: solid lipid nanoparticles; α-CD cyclodextrine

PMES: undec-1-en-11-yltetra(ethylene glycol) phosphate mono- ester surfactant ,SGF: simulated gastric fluid , SIF: simulated intestinal fluid, SBF simulated body fluid

TEAH3:tri-ethanolamine,LDPE: low density polyethylene, EVA: ethylene vinyl acetate

1.2.3. Silica-based oral delivery systems and food applications

Single or multiple drug substances can potentially be loaded in the same dosage form, making mesoporous silica materials a versatile tool for combination of therapies [4]. The special architecture of mesoporous silica offers an efficient protection for biomolecules which are subjected to lysis by the gastrointestinal juices [33]. The protection related mechanism may consist in a confinement or a steric hindrance that would protect the loaded biomolecule inside the pores from the action of catalytic enzymes [83].

The wide range of pore sizes offer the possibility to load in silica matrices a large variety of drugs [84], macromolecules [33], genes [85,86], or even cells [87]. Furthermore, pore size monitoring could be used in the obesity treatment[88] or in the adjust the release kinetics adjustment [89,90].

The highly porous structure of silica makes it an ideal candidate as a DDS floating matrix intended to achieve a certain gastro-retention. Mesoporous silica nanoparticles mixed with sodium bicarbonate and cellulose derivative polymer were used for the preparation of floating tablets of curcumin and captopril, as hydrophobic and hydrophilic model drugs, respectively. The obtained tablets showed an extensive floating behavior over 12 hours of gastro-retention [106]. Highly porous calcium silicate [107] and aluminum silicate [108] were also successfully used for the preparation of floating DDS containing repaglinide and methotrexate, a combination of a hypoglycemic agent with poor absorption in the upper intestinal tract and an antineoplastic agent with a short half-life of 2 hours, respectively.

The principal issues related to oral drug delivery, *i.e.* solubility and intestinal permeability [109], could be addressed by the implementation of mesoporous silica materials in the development strategies of ODDS. The poor solubility of BCS class II, such as celecoxib [110], fenofibrate [111] and telmisartan [112], and BCS class IV such as furosemide [113], could also be reversed following their encapsulation in mesoporous silica DDS. It is noteworthy that the design of ordered mesoporous silica into nanoparticulate

DDS result in a higher intestinal permeability due to enhanced cell uptake and reduced drug efflux [112].

Mesoporous silica has been used not only for drugs delivery applications, but also for the encapsulation of food ingredients to improve molecules stability and bioavailability. Vitamins are nutrients essential for humans that are not produced by the body. They have a low activity in the presence of metal ions, ultraviolet light and heat. Water-soluble vitamins as riboflavin (vitamin B2) [39,114], niacin (vitamin B3)[52], and ascorbic acid (vitamin C) [99] or oil-soluble vitamins as β -carotene (precursor of vitamin A) [101] and α -tocopherol (vitamin E) [102,115] were immobilized on silica for food applications. Phytochemicals as polyphenols (from wine [116]), quercetin [103,117], resveratrol [97,98] or curcumin [101] that have antioxidant activity, organosulfurs with antibiotic activity [105], glucosinolates that have antibacterial efficacy [118] were immobilized in silica to improve their properties. Another class of food ingredients that were encapsulated in silica are bioactive peptides [119–122].

Silica-based ODDS were classified according to their payloads release mechanisms in the GIT, which in turn depends on the employed loading strategy [26]. Different methods (Figure 1.2. 9) such as one-step condensation (one-pot encapsulation), immersion method, impregnation method or supercritical CO₂ method, incipient wetness impregnation method, hot melt can be used for the loading of porous silica. After the loading, the pores can be capped with molecular ensembles to confer the carriers a stimuli response [9].

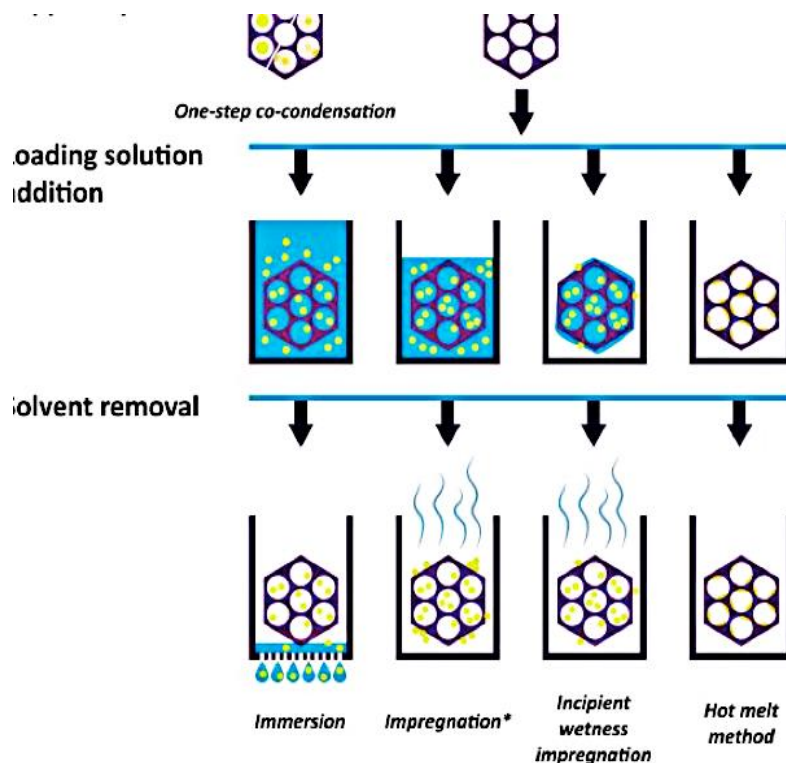


Figure 1.2. 9. Schematic representation of different loading methods (reproduced from [123]).

Generally speaking, the physically adsorbed drugs are more likely to be released by diffusion; whereas the covalently-linked counterparts to be released by interactions with internal and external triggers, e.g. hydrolysis by digestive or gut enzymes, increased ionic strength and/or pH variation along the GIT, external magnetic field action [26], among others as showed in the Figure 1.2. 9 and summarized is Table 1.2. 1 and Table 1.2. 2.

1.2.3.1. Passive release delivery systems

As presented above, the synthesis of ordered-porous silica could be controlled, by varying the reaction parameters and the structure directing agent (template), with the aim to obtain materials with different morphologies, pore sizes, ordering and volume and displaying various surface properties. These features were found to determine both drug loading and passive release.

Several studies highlighted a relationship between release kinetics and pore sizes [89,91] pores shape [124], particle size [112,125], or hydrophilicity [126].

Pore size is an important factor, not only to ensure the loading of the molecules inside the pores but also to release it [127]. Mellaerts et al. studied the influence of four different types of SBA-15, a mesoporous silica material having hexagonally-ordered pores, on the release kinetics of itraconazole, an anti-fungal agent with a very poor aqueous solubility [89]. The pore size varied from 4.5 to 9.0 nm, and the pore volume ranged from 0.42 to 0.80 cm³·g⁻¹. The release performance of materials loaded with 10 wt% of itraconazole was assessed in a simulated gastric fluid at pH 1.2. It was found that the larger the material pore size and volume, the faster the release rate. To explain these findings, the authors suggested: i) more rapid influx and a competitive absorption of water in the wider mesopores, and ii) breaking up intermolecular interactions between in drug crystals due to their separation onto the SBA-15 surface [89]. Allyl isothio-cyanate (AITC), an antimicrobial, used principally in foods as a flavoring agent, was encapsulated in MCM-41 and SBA-15 [118,128,129]. The pore size and distribution influences the desorption, as 65% of the compound was burst release form the SBA-15 system in the first 12 hours.

On the other hand, Balas et al. developed a DDS based on mesoporous silica intended for the oral delivery of bisphosphonates, an anti-osteoporotic drug with poor bioavailability. For this purpose, they used two silica materials, with hexagonally ordered mesopores, SBA-15 and MCM-41. Unexpectedly, it was found that the release rate from SBA-15 (pore size 9.0 nm) was slower than that from MCM-41 (pore size 3.8 nm). Additionally, the loading efficiency on SBA-15 was smaller than that on MCM-41. These findings were explained by the higher surface area of MCM-41 (1157 m² g⁻¹) with respect to that of SBA-15 (719 m² g⁻¹) and that the release was rather a surface-dependent phenomenon [124].

The size of the DDS is also an important feature and has to be carefully considered. Zhang et al. designed mesoporous silica micro- and nanoparticulate as ODDS for telmisartan [112]. The performed release studies, in an enzyme-free simulated intestinal fluid (SIF) pH 6.8, showed an increase in the release rate when the particle size was decreased down to the nanometer range. The authors explained this finding by the shorter channel length and then the shorter diffusion distance to be crossed by the guest

molecule before reaching the release medium. Similarly, Aerts et al. studied the influence of particle size on the drug release behavior from amorphous microporous silica materials [125] and they found that the smaller the particle size, the faster the release.

Alteration of the silica surface hydrophilicity (by methylation of Si-OH) is another way to control the passive diffusion of the guest drug [126]. The digestive fluids influx could be reduced inside the inner channels and this way, the drug dissolution/degradation could be delayed.

In 2011, Aw et al. proposed silica microcapsules from diatoms as new carrier for oral delivery of therapeutics, namely indomethacin and gentamicin^[96]. The first one is a widely used and poorly soluble anti-inflammatory drug and the second is a highly water-soluble cationic aminoglycoside antibiotic widely used in therapeutic implants to prevent bacterial infections. Typical structural features of diatom silica microparticles (DSMs) used in this study are: diameters between 4 and 6 μm ; length between 10 and 20 μm , with regularly spaced rows of pores with a diameter of approximately 400–500 nm. Drug molecules can be loaded on both internal and external surface of the material. Controlled release over 6–7 h for both drugs were achieved in sink conditions and the results proved that those DSM meet requirements for extended oral dosage.

More recently, Zhang et al. have evaluated the potential of DSMs for the delivery of mesalamine and prednisone, two commonly prescribed drugs for gastrointestinal diseases [82]. DSMs used in this study were cylindrical, with 10–20 μm in length and ca.10 μm in diameter, with well-defined pores of 300–500 nm). *In vitro* release studies showed no difference in release kinetics for free and encapsulated mesalamine. However, prednisone showed a clear sustained release after loading in DSMs). In overall, the study showed that DSMs have a low cytotoxicity on Caco-2, HT-29, HCT-116 cells and Caco-2/HT-29 co-cultured cells, at concentrations up to 1000 mg/mL. Both drugs undergo a controlled release under simulated gastro-intestinal conditions and an enhanced permeability across Caco-2/HT-29 co-culture monolayers. The results thus demonstrate that DSMs can be considered as a non-cytotoxic biomaterial with a high

potential to improve the mesalamine and prednisone bioavailability by sustaining the drug release and enhancing drug permeability.

1.2.3.2. Active release delivery systems

The large silica surface covered by silanol group Si-OH offers a unique opportunity to design smart DDS. Indeed, silanols can be easily functionalized leading to delivery systems with programmed drug release as a function of either (i) internal signals, e.g. pH variation [130], glucose [131–133] or catabolic or bacterial enzyme availability [93], [94] or (ii) external stimuli, e.g. temperature [134], irradiation [135], magnetic field [136], etc. Herein, are described and presented (Figure 1.2. 10) stimuli-responsive silica-based systems.

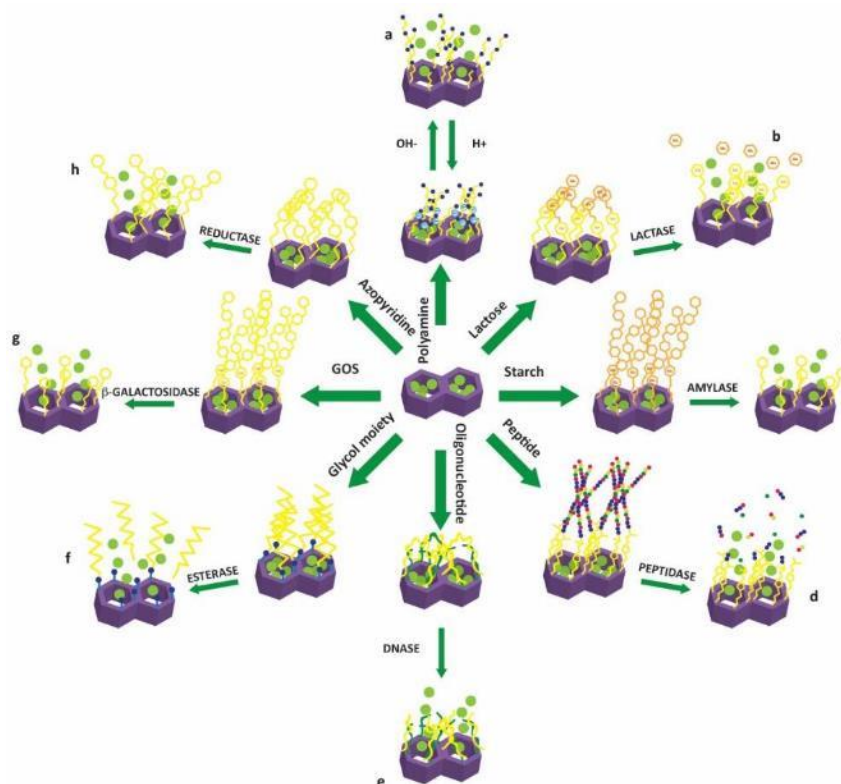


Figure 1.2. 10. Molecular gates and trigger responses for pore-capped silica materials (reproduced from [123]).

1.2.3.2.1. pH-controlled release

pH-sensitive silica-based carriers represent an interesting alternative for the oral delivery of peptides and proteins, or for vitamins protecting them from the GIT proteolytic

environment. To do so, the design might consist in coating the particles with a weak acid that remains insoluble in the highly acidic gastric juice forming a physical barrier. This physical barrier prevents the diffusion of proteases and the acidic juice into the matrix as well as the diffusion of the guest-substance to the external medium. The stability of the coating decreases when the pH increases. Therefore, the determination of the release site in the GIT depends upon the acid pKa.

Pettit et al. developed a silica-based carrier for vaccine oral delivery. After the antigen immobilization on silica beads, a coating with myristic acid, a food additive, was performed [130]. The authors reported that the developed carrier provided an almost entire protection of the loaded antigen (nearly 100% of protein recovery) after 1 hour-exposition to protease K 500 μ U at 37 °C and 4 hour-exposition to a simulated gastric fluid (SGF). According to the reported findings, the coating with myristic acid remained intact at pH 3.6 and pH 5, where no release of was detected. The antigen release started at pH 8.8 and was sustained during 24 hours. Importantly, the antigen secondary structure was conserved during the loading and after the release, as confirmed by circular dichroism spectroscopy [130].

Qu et al. elaborated silica-based nanoparticulate system for the oral delivery of glucagon like-peptide 1 (GLP-1), a glucose-regulating enteroendocrine-derived hormone. The authors used Areosil® 200 non-porous silica nanoparticles, on which GLP-1 was adsorbed and subsequently coated with Eudragit® L100, a gastro-resistant polymer with mucoadhesion properties [137]. The release kinetics was assessed *in vitro* at pH 1.0 and 7.4 in phosphate buffer solutions. A faster release was observed at pH 7.4 than in acidic conditions confirming the protective effect of the pH-sensitive polymer layer.

Recently, our group reported core-shell microcapsules (MC-CU) based on solid lipid nanoparticles (SLNs) and mesoporous silica intended for the oral delivery of a poorly soluble model drug, *i.e.* curcumin [75]. Curcumin is a food yellow pigment extracted from *Curcuma longa*. The low absorption when administrated orally limits its antioxidant, anti-inflammatory and anti-carcinogenic activity. In these systems, curcumin was first entrapped in SLNs, which were subsequently mineralized using TMOS as silica source. According to *in*

vitro studies, the resulting hybrid system behaves as a gastro-resistant delivery system. Interestingly, MC-CU were shown to be readily taken up by Caco-2 cell line, an *in vitro* intestinal epithelium cell model. These results demonstrated the potential of this delivery platform for enhancing both drug solubility and intestinal permeability.

Pérez-Esteve et al. developed a functional food enriched with folic acid based on pH-sensitive mesoporous silica [100]. Folic acid was encapsulated in amine-functionalized silica matrix with the aim to enhance its bioavailability by hindering its premature release and degradation in the stomach. Instead, folic acid was progressively released in the intestine where it is completely absorbed. Indeed, at low pH, amine groups are protonated hence promoting Coulombic repulsions due to closely located ammonium groups. Consequently, in low pH silica pores are blocked. The progressive increase of the pH after the pyloric passage decrease the ratio of protonated “blocked gates” allowing a sustained release of the payload.

1.2.3.2.2. Enzyme-triggered release

The design of these systems is based on the principle of pore-capping of silica materials with a cleavable gate (Figure 1.2. 10). A multitude of link types could be designed between the gate and the pore in order to be readily cleavable by predefined enzyme. The variety of the enzymes present in the gastro-intestinal track can lead to the developed of sophisticated gate-controlled release silica nanocarriers triggered at a specific site (stomach, intestine, colon). Bernandos et al. [138] developed a simple gate-controlled release silica nanocarriers triggered by enzymatic hydrolysis. The synthesis of this system was based on loading of the guest molecule ($[\text{Ru}(\text{bipy})_3]\text{Cl}_2$ -as model molecule) by physical adsorption inside the pores of mesoporous silica (MCM-41) than the surface was modified with a lactose derivative (β -D-galactose and β -D-glucose monosaccharides linked through a β 1 \rightarrow 4 glycosidic bond). The hydrogen bonding interactions between the disaccharides keep the cargo inside. The researchers showed the release of the loaded molecule from the silica nanocarriers following its exposition to β -galactosidase, the enzyme present in the brush-border in the intestine, as a proof of

concept. Another capped molecule that is used and hydrolyzed by β -galactosidase is alkylgluconamine derivative of a galacto-oligosaccharide [139].

Food ingredients as starches that are hydrolyzed by pancreatin [138], avidin (a white yolk protein) [140] and modular peptide [141] that are cut by protease, cytosine-phosphodiester-guanine oligodeoxynucleotide [142], or oligodeoxynucleotides [143] triggered by deoxyribonuclease were also used to prepare enzyme-triggered release silica systems.

1.2.3.2.3. pH/Enzyme-triggered release

Popat *et al.* designed mesoporous silica nanoparticles displaying both pH and enzyme responsiveness and thus a release profile depending upon its location in the GIT [94]. The matrix used for this system is based on amino-modified MCM-48 displaying a cubic bicontinuous pore structure. A coating with succinylated soy protein isolate (SSPI), a hydrophobic polymer stable in acidic pH media (with isoelectric point at pH 5) and a modified food component, was carried out (Figure 1.2. 11). The coating choice, as presented by the authors, was explained in terms of: i) stability due to the covalent attachment between the SSPI's carboxylic group and the silica's amine group; ii) insolubility in acidic media; iii) susceptibility of the succinylated protein towards the proteolytic enzymes in the small intestine. The authors conducted *in vitro* release studies in SGF (pH 1.2) containing pepsin and in SIF, (pH 7.4) in the presence or absence of pancreatin, in order to check the performance of their developed system. According to their results, the drug release was successfully tuned and took place only in SIF in a slow and sustained pattern over 48 hours. Importantly, the release rate was doubled when pancreatin was added to the SIF.

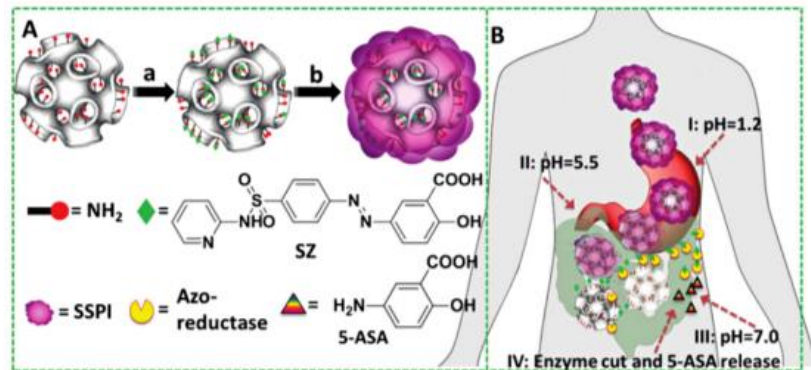


Figure 1.2. 11. Schematic representation of (A) synthesis of MSN–NH₂– SZ@SSPI. a: SZ is loaded into amino functionalized MCM-48 (MSN–NH₂) to form MSN–NH₂–SZ, b: coating of SSPI using amide chemistry leads to MSN–NH₂–SZ@SSPI. (B) Oral delivery and site-dependent programmable release of SZ into 5-ASA in the GIT from MSN–NH₂–SZ@SSPI (reproduced from [94]).

1.2.4. Silica health benefits and limitations

Silica is found everywhere on the planet, present in the earth's crust, in water but also in a great number of living organisms. Silica is considered as “Generally Recognized as Safe” by FDA regulations and an authorized additive in Europe as E-551 class [144]. Synthetic amorphous silica has been used for many years in food industry as a beer and wine clarifying agent, to thicken pastes, as a carrier agent for flavoring and aromas or as an anticaking agent [145] to maintain the flow properties of powder products. As a natural product silica is found in beverages (water, beer and coffee) and food (cereals and vegetables). The mean daily intake of dietary silicon as silica were estimated to be 19 and 40 mg in adult women and men, respectively [146].

To be used in food as smart delivery devices, silica materials should overcome some sociological, toxicological, technological legal and semantic limitations [9]. Silica is not considered harmful for humans, but before considering adding to the food or to used as oral delivery system some parameters such as size distribution, particle size [147–149] and shape [150], mass, reactivity, solubility, chemical composition and surface properties [151,152] should be taken into account [10,153]. Particle size of the silica can change the functionality [154], the particles they are more easily decomposed with the decrease of the diameter [155]. To date, the process for the synthesis functionalization and loading of mesoporous silica is developed in the lab and the scaled-up for an industrial application

is underdeveloped due to the high productions cost [9]. Another technological problem for the transition of silica from the lab to industry is the compatibility of these carriers with the food [24].

1.2.5. Conclusion

This chapter highlights the emerging interest of silica-based delivery systems in oral delivery and food industry of drugs, biomolecules or cells accounting for the design of new functional foods containing probiotic bacteria. The carriers can be synthesized through two routes: (1) encapsulation of payloads in pre-synthesized silica or (2) one-pot encapsulation and silica formation. Indeed, silica can be obtained through the sol-gel process at low temperature (<40°C), which makes it compatible with the manipulation of temperature-sensitive drugs, peptides, proteins and more particularly, cells. Porosity can be easily imprinted into silica materials through the use of structure-directing agents or soft templates. Therefore, materials with large surface areas and pore volumes can be obtained as well as materials that exhibit high drug loading capacity. Pore sizes can be tuned in the range of 2-50 nm in the case of mesopores, and from hundreds of nm to tens or hundreds on microns in the case of macropores. The residual silanol groups at the surface of silica can be also functionalized allowing high interactions with drugs. Overall, the porosity of silica materials can be tailored as a function of the size and properties of the payload. The most sophisticated functionalization strategies have been elaborated to control drug delivery kinetics at the appropriate site with zero premature release along with preventing undesired side effects. The researchers can play freely to build up fascinating and efficient multifunctional carriers.

The long history of use of silica and silicates in food and drug products for the oral route without allegedly harmful effects over the last 50 years has demonstrated their safety. The main degradation product of silica, *i.e.* orthosilicic acid, is not toxic and is rapidly eliminated by the kidneys [149] or by fecal excretion [148]. However, when administrating silica via routes other than the oral one, it was found to be less tolerated or even toxic.

Bibliography

- [1] D. Napierska, L. C. J. Thomassen, D. Lison, J. a Martens, P. H. Hoet, *Part. Fibre Toxicol.* **2010**, *7*, 39.
- [2] K. R. Martin, *Met. Ions Life Sci.* **2013**, *13*, 451–473.
- [3] W. E. G. Müller, X. Wang, *FEBS J.* **2012**, *279*, 1709.
- [4] A. M. Chen, M. Zhang, D. Wei, D. Stueber, O. Taratula, T. Minko, H. He, *Small* **2009**, *5*, 2673–2677.
- [5] D. Zhao, J. Feng, Q. Huo, N. Melosh, G. Fredrickson, B. Chmelka, G. Stucky, *Science* **1998**, *279*, 548–52.
- [6] A. Sayari, S. Hamoudi, Y. Yang, *Chem. Mater.* **2005**, *17*, 212–216.
- [7] C. Márquez-Alvarez, E. Sastre, J. Pérez-Pariente, **2004**, *27*.
- [8] A. Bernardos, L. Kourimska, *Czech J Food Sci* **2013**, *31*, 99–107.
- [9] E. Pérez-Esteve, M. Ruiz-Rico, R. Martínez-Mañez, J. M. Barat, *J. Food Sci.* **2015**, *80*, 2504–2516.
- [10] T. Bech-Larsen, K. G. Grunert, *Appetite* **2003**, *40*, 9–14.
- [11] FDA, **2009**, www.accessdata.fda.gov/scripts/fcn/gras_notices/GR.
- [12] M. T. Zamin, M. M. Pitre, J. M. Conly, *Ann. Pharmacother.* **1997**, *31*, 564–570.
- [13] K. M. Kuper, *Intravenous to Oral Therapy Conversion*, **2008**.
- [14] M. A. Fischer, D. H. Solomon, J. M. Teich, J. Avorn, *Arch. Intern. Med.* **2003**, *163*, 2585–2589.
- [15] A. Åsberg, A. Humar, H. Rollag, A. G. Jardine, D. Kumar, P. Aukrust, T. Ueland, A. A. Bignamini, A. Hartmann, *Clin. Infect. Dis.* **2016**, *62*, 1154–1160.
- [16] J. M. Cyriac, E. James, *J Pharmacol Pharmacother* **2014**, *5*, 83–87.
- [17] K. S. Pang, *Drug Metab. Dispos.* **2003**, *31*, 1507–1519.
- [18] R. Panchagnula, N. S. Thomas, *Int. J. Pharm.* **2000**, *201*, 131–50.
- [19] B. N. Singh, K. H. Kim, *J. Control. Release* **2000**, *63*, 235–259.
- [20] K. Sonaje, K. J. Lin, M. T. Tseng, S. P. Wey, F. Y. Su, E. Y. Chuang, C. W. Hsu, C. T. Chen, H. W. Sung, *Biomaterials* **2011**, *32*, 8712–8721.
- [21] G. Singh, R. S. Pai, *Drug Deliv.* **2016**, *23*, 532–539.
- [22] B. Aspenström-Fagerlund, L. Ring, P. Aspenström, J. Tallkvist, N. G. Ilbäck, A. W. Glynn, *Toxicology* **2007**, *237*, 12–23.
- [23] B. Aspenström-Fagerlund, B. Sundström, J. Tallkvist, N. G. Ilbäck, A. W. Glynn, *Chem. Biol. Interact.* **2009**, *181*, 272–278.
- [24] E. Pérez-Esteve, L. Oliver, L. García, M. Nieuwland, H. H. J. de Jongh, R. Martínez-Mañez, J. M. Barat, **2014**.
- [25] A. Comas-Vives, *Phys. Chem. Chem. Phys.* **2016**, *18*, 7475–82.
- [26] R. Diab, N. Canilho, I. A. Pavel, F. B. Haffner, M. Girardon, A. Pasc, *Adv. Colloid Interface Sci.* **2017**, DOI 10.1016/j.cis.2017.04.005.
- [27] C. Kneuer, M. Sameti, E. G. Haltner, T. Schiestel, H. Schirra, H. Schmidt, C. M. Lehr, *Int. J. Pharm.* **2000**, *196*, 257–261.
- [28] C. F. Meunier, P. Dandoy, B. L. Su, *J. Colloid Interface Sci.* **2010**, *342*, 211–224.
- [29] H. Barthel, L. Rosch, J. Weis, *Organosilicon Chem. 11* **1996**, 761–778.
- [30] H. Barthel, M. Heinemann, M. Stintz, B. Wessely, *Chem. Eng. Technol.* **1998**, *16*, 169–176.
- [31] “Battery Fumed silica, Resin Fumed silica, Silicone Rubber Fumed silica-Minmetals East Industrial,” can be found under <http://www.hjsil.com/aboutus/Technology/>, **n.d.**
- [32] W. Stöber, A. Fink, E. Bohn, *J. Colloid Interface Sci.* **1968**, *26*, 62–69.
- [33] T. Andreani, C. P. Kiill, A. L. R. de Souza, J. F. Fangueiro, L. Fernandes, S. Doktorovová, D. L. Santosa, M. L. Garcia, M. P. D. Gremião, E. B. Souto, et al., *Colloids Surfaces B Biointerfaces* **2014**, *123*, 916–923.
- [34] T. Andreani, M. Leonardo, L. Esteban N., R. de S. Ana Luiza, K. Charlene P., F. Joana F., G. Maria L., G. Palmira D, S. Amélia M., S. Eliana B., *Eur. J. Pharm. Biopharm.* **2015**, *93*, 118–126.
- [35] C. T. Kresge, M. E. Leonowicz, W. J. Roth, J. C. Vartuli, J. S. Beck, *Nature* **1992**, *359*, 710–712.
- [36] A. Popat, S. B. Hartono, F. Stahr, J. Liu, S. Z. Qiao, G. Qing (Max) Lu, *Nanoscale* **2011**, *3*, 2801.
- [37] M. Vallet-Regí, A. Rámila, R. P. Del Real, J. Pérez-Pariente, *Chem. Mater.* **2001**, *13*, 308–311.
- [38] M. Vallet-Regí, F. Balas, D. Arcos, *Angew. Chemie - Int. Ed.* **2007**, *46*, 7548–7558.
- [39] A. Bernardos, E. Aznar, C. Coll, R. Martínez-Mañez, J. M. Barat, M. D. Marcos, F. Sancenón, A. Benito, J. Soto, *J. Control. Release* **2008**, *131*, 181–189.
- [40] É. Pérez-Esteve, A. Fuentes, C. Coll, C. Acosta, A. Bernardos, P. Amorós, M. D. Marcos, F. Sancenón, R. Martínez-Mañez, J. M. Barat, *Microporous Mesoporous Mater.* **2015**, *202*, 124–132.
- [41] F. Hoffmann, M. Cornelius, J. Morell, M. Fröba, *Angew. Chem. Int. Ed. Engl.* **2006**, *45*, 3216–51.
- [42] Y. Wan, D. Zhao, *Chem. Rev.* **2007**, *107*, 2821–2860.
- [43] A. E. . Palmqvist, *Curr. Opin. Colloid Interface Sci.* **2003**, *8*, 145–155.
- [44] S. H. Tolbert, *Nat. Mater.* **2012**, *11*, 749–751.
- [45] R. K. Iler, *J. Colloid Interface Sci.* **1980**, *75*, 138–148.
- [46] C. . Brinker, *J. Non. Cryst. Solids* **1988**, *100*, 31–50.
- [47] M. Kruk, L. Cao, *Langmuir* **2007**, *23*, 7247–7254.

- [48] Y. Wan, Y. Shi, D. Zhao, *Chem. Commun. (Camb)*. **2007**, 897–926.
- [49] H. Lin, C. Mou, *Acc Chem. Res.* **2002**, *35*, 927–935.
- [50] S. Che, A. E. Garcia-Bennett, T. Yokoi, K. Sakamoto, H. Kunieda, O. Terasaki, T. Tatsumi, *Nat. Mater.* **2003**, *2*, 801–805.
- [51] T. Yokoi, H. Yoshitake, T. Tatsumi, *Chem. Mater.* **2003**, *15*, 4536–4538.
- [52] M. P. Kapoor, A. Vinu, W. Fujii, T. Kimura, Q. Yang, Y. Kasama, M. Yanagi, L. R. Juneja, *Microporous Mesoporous Mater.* **2010**, *128*, 187–193.
- [53] R. Ishii, T. Itoh, T. Yokoyama, S. I. Matsuura, T. Tsunoda, S. Hamakawa, F. Mizukami, T. A. Hanaoka, *J. Non. Cryst. Solids* **2012**, *358*, 1673–1680.
- [54] L. Han, C. Gao, X. Wu, Q. Chen, P. Shu, Z. Ding, S. Che, *Solid State Sci.* **2011**, *13*, 721–728.
- [55] A. Coiffier, T. Coradin, C. Roux, O. M. M. Bouvet, J. Livage, *J. Mater. Chem.* **2001**, *11*, 2039–2044.
- [56] R. B. Bhatia, C. J. Brinker, *Chem. Mater.* **2000**, 2434–2441.
- [57] K. S. Finnie, J. R. Bartlett, J. L. Woolfrey, *J. Mater. Chem.* **2000**, *10*, 1099–1101.
- [58] H. T. Jang, Y. Park, Y. S. Ko, J. Y. Lee, B. Margandan, *Int. J. Greenh. Gas Control* **2009**, *3*, 545–549.
- [59] M. Bhagiyalakshmi, L. J. Yun, R. Anuradha, H. T. Jang, *J. Hazard. Mater.* **2010**, *175*, 928–938.
- [60] J. Y. Ying, C. P. Mehnert, M. S. Wong, *Angew. Chemie Int. Ed.* **1999**, *38*, 56–77.
- [61] S. L. Westcott, S. J. Oldenburg, T. R. Lee, N. J. Halas, *Langmuir* **1998**, *14*, 5396–5401.
- [62] A. Salonen, A. M. Kaukonen, J. Hirvonen, V.-P. Lehto, *Int. J. Drug Dev. Res.* **2007**, *3*, 26–33.
- [63] J.-F. Chen, H.-M. Ding, J.-X. Wang, L. Shao, *Biomaterials* **2004**, *25*, 723–727.
- [64] H. Jaganathan, B. Godin, *Adv. Drug Deliv. Rev.* **2012**, *64*, 1800–1819.
- [65] H. H. Weetall, *BBA - Enzymol.* **1970**, *212*, 1–7.
- [66] M. Grün, I. Lauer, K. K. Unger, *Adv. Mater.* **1997**, *9*, 254–257.
- [67] G. J. D. A. A. Soler-illia, **2002**, DOI 10.1021/cr0200062.
- [68] S. Huh, J. W. Wiench, J.-C. Yoo, M. Pruski, V. S.-Y. Lin, *Chem. Mater* **2003**, *15*, 4247–4256.
- [69] Y.-S. Lin, C. L. Haynes, *J Am Chem Soc* **2010**, *132*, 4834–4842.
- [70] H. Meng, M. Xue, T. Xia, Z. Ji, D. Y. Tarn, J. I. Zink, A. E. Nel, *ACS Nano* **2011**, *5*, 4131–4144.
- [71] D. Zhao, Q. Huo, J. Feng, B. F. Chmelka, G. D. Stucky, *J. Am. Chem. Soc.* **1998**, *120*, 6024–6036.
- [72] S. Kim, M.-J. Stébé, J.-L. Blin, A. Pasc, *J. Mater. Chem. B* **2014**, *2*, 7910–7917.
- [73] A. Pasc, J.-L. Blin, M.-J. Stébé, J. Ghanbaja, *RSC Adv.* **2011**, *1*, 1204.
- [74] R. Ravetti-Duran, J.-L. Blin, M.-J. Stébé, C. Castel, A. Pasc, *J. Mater. Chem.* **2012**, *22*, 21540.
- [75] S. Kim, R. Diab, O. Joubert, N. Canilho, A. Pasc, *Colloids Surf. B. Biointerfaces* **2015**, *140*, 161–168.
- [76] F. B. Haffner, M. Girardon, S. Fontanay, N. Canilho, R. E. Duval, M. Mierzwa, M. Etienne, R. Diab, A. Pasc, *J. Mater. Chem. B* **2016**, *4*, 7929–7935.
- [77] R. Wetherbee, *Sci. Compass* **2002**, *298*, 1.
- [78] W. E. G. Müller, A. Krasko, G. Le Pennec, H. C. Schröder, *Microsc. Res. Tech.* **2003**, *62*, 368–377.
- [79] D. Losic, J. G. Mitchell, N. H. Voelcker, *Adv. Mater.* **2009**, *21*, 2947–2958.
- [80] C. C. Berton-Carabin, K. Schroën, *Annu. Rev. Food Sci. Technol.* **2015**, *6*, 263–97.
- [81] E. Bye, R. Davies, D. M. Griffiths, B. Gylseth, C. B. Moncrieff, *Br. J. Ind. Med.* **1984**, *41*, 228–234.
- [82] H. Zhang, M. A. Shahbazi, E. M. Mäkilä, T. H. da Silva, R. L. Reis, J. J. Salonen, J. T. Hirvonen, H. A. Santos, *Biomaterials* **2013**, *34*, 9210–9219.
- [83] M. Il Kim, J. Kim, J. Lee, H. Jia, H. Bin Na, J. K. Youn, J. H. Kwak, A. Dohnalkova, J. W. Grate, P. Wang, et al., *Biotechnol. Bioeng.* **2007**, *96*, 210–218.
- [84] L. Hu, H. Sun, Q. Zhao, N. Han, L. Bai, Y. Wang, T. Jiang, S. Wang, *Mater. Sci. Eng. C* **2015**, *47*, 313–324.
- [85] B. Moulari, D. Pertuit, Y. Pellequer, A. Lamprecht, *Biomaterials* **2008**, *29*, 4554–4560.
- [86] H. Meng, M. Liong, T. Xia, Z. Li, Z. Ji, J. I. Zink, A. E. Nel, *ACS Nano* **2010**, *4*, 4539.
- [87] J. H. Park, D. Hong, J. Lee, I. S. Choi, *Acc. Chem. Res.* **2016**, *49*, 792–800.
- [88] N. Kupferschmidt, R. Csikasc, L. Ballell, T. Bengtsson, A. E. Garcia-Bennett, *Nanomedicine* **2014**, *9*, 1353–1362.
- [89] R. Mellaerts, C. A. Aerts, J. Van Humbeeck, P. Augustijns, G. Van den Mooter, J. A. Martens, *Chem. Commun.* **2007**, *d*, 1375–1377.
- [90] A. Doadrio, A. Salinas, J. Sánchez-Montero, M. Vallet-Regí, *Curr. Pharm. Des.* **2015**, *21*, 6213–6819.
- [91] I. Izquierdo-Barba, Á. Martínez, A. L. Doadrio, J. Pérez-Pariente, M. Vallet-Regí, *Eur. J. Pharm. Sci.* **2005**, *26*, 365–373.
- [92] F. Balas, M. Manzano, P. Horcajada, M. Vallet-reg, **2006**, 8116–8117.
- [93] K. Patel, S. Angelos, W. R. Dichtel, A. Coskun, Y. W. Yang, J. I. Zink, J. F. Stoddart, *J. Am. Chem. Soc.* **2008**, *130*, 2382–2383.
- [94] A. Popat, S. Jambhrunkar, J. Zhang, J. Yang, H. Zhang, A. Meka, C. Yu, *Chem. Commun. (Camb)*. **2014**, *50*, 5547–50.
- [95] S. R. Choi, D.-J. Jang, S. Kim, S. An, J. Lee, E. Oh, J. Kim, *J. Mater. Chem. B* **2014**, *2*, 616.
- [96] M. S. Aw, S. Simovic, J. Addai-Mensah, D. Losic, *Nanomedicine* **2011**, *6*, 1159–1173.
- [97] C. H. Tsai, J. L. Vivero-Escoto, I. I. Slowing, I. J. Fang, B. G. Trewyn, V. S. Y. Lin, *Biomaterials* **2011**, *32*, 6234–6244.

- [98] M. Popova, A. Szegedi, V. Mavrodinova, N. Novak Tušar, J. Mihály, S. Klébert, N. Benbassat, K. Yoncheva, *J. Solid State Chem.* **2014**, *219*, 37–42.
- [99] L. Rashidi, E. Vasheghani-Farahani, K. Rostami, F. Gangi, M. Fallahpour, *Iran. J. Biotechnol.* **2013**, *11*, 209–213.
- [100] É. Pérez-Esteve, M. Ruiz-Rico, A. Fuentes, M. D. Marcos, F. Sancenón, R. Martínez-Mañez, J. M. Barat, *LWT - Food Sci. Technol.* **2016**, *72*, 351–360.
- [101] N. W. Clifford, K. S. Iyer, C. L. Raston, *J. Mater. Chem.* **2008**, *18*, 162–165.
- [102] N. Gargiulo, I. Attianese, G. G. Buonocore, D. Caputo, M. Lavorgna, G. Mensitieri, M. Lavorgna, *Microporous Mesoporous Mater.* **2013**, *167*, 10–15.
- [103] G. Berlier, L. Gastaldi, E. Ugazio, I. Miletto, P. Iliade, S. Sapino, *J. Colloid Interface Sci.* **2013**, *393*, 109–118.
- [104] L. Heirlings, I. Siró, F. Devlieghere, E. Van Bavel, P. Cool, B. De Meulenaer, E. F. Vansant, J. Debevere, *Food Addit. Contam.* **2004**, *21*, 1125–36.
- [105] C. Acosta, E. Pérez-Esteve, C. A. Fuenmayor, S. Benedetti, M. S. Cosio, J. Soto, F. Sancenón, S. Mannino, J. Barat, M. D. Marcos, et al., *ACS Appl. Mater. Interfaces* **2014**, *6*, 6453–6460.
- [106] P. L. Abbaraju, A. kumar Meka, S. Jambhrunkar, J. Zhang, C. Xu, A. Popat, C. Yu, *J. Mater. Chem. B* **2014**, *2*, 8298–8302.
- [107] S. K. Jain, A. M. Awasthi, N. K. Jain, G. P. Agrawal, *J. Control. Release* **2005**, *107*, 300–309.
- [108] I. S. Carino, L. Pasqua, F. Testa, R. Aiello, F. Puoci, F. Iemma, N. Picci, *Drug Deliv.* **2007**, *14*, 491–5.
- [109] G. L. Amidon, H. Lennernäs, V. P. Shah, J. R. Crison, *Pharm. Res. An Off. J. Am. Assoc. Pharm. Sci.* **1995**, *12*, 413–420.
- [110] A. Tan, S. Simovic, A. K. Davey, T. Rades, B. J. Boyd, C. A. Prestidge, *Mol. Pharm.* **2010**, *7*, 522–32.
- [111] A. Hill, S. Geißler, M. Weigandt, K. Mäder, *J. Control. Release* **2012**, *158*, 403–412.
- [112] Y. Zhang, J. Wang, X. Bai, T. Jiang, *Mol. ...* **2012**.
- [113] S. Sambaraj, D. Ammula, V. Nagabandi, *Adv. Pharm. Bull.* **2015**, *5*, 403–409.
- [114] J. M. Kisler, A. Dähler, G. W. Stevens, A. J. O'Connor, *Microporous Mesoporous Mater.* **2001**, *44–45*, 769–774.
- [115] G. Chandrasekar, A. Vinu, V. Murugesan, M. Hartmann, *Young* **2005**, *158*, 829–833.
- [116] V. V. Cotea, C. E. Luchian, N. Bilba, M. Niculaua, *Anal. Chim. Acta* **2012**, *732*, 180–185.
- [117] S. Sapino, E. Ugazio, L. Gastaldi, I. Miletto, G. Berlier, D. Zonari, S. Oliaro-Bosso, *Eur. J. Pharm. Biopharm.* **2015**, *89*, 116–125.
- [118] S. Y. Park, M. Barton, P. Pendleton, *Food Control* **2012**, *23*, 478–484.
- [119] P. Urban, J. Jose Valle-Delgado, E. Moles, J. Marques, C. Diez, X. Fernandez-Busquets, *Curr. Drug Targets* **2012**, *13*, 1158–1172.
- [120] I. Izquierdo-Barba, M. Vallet-Regí, N. Kupferschmidt, O. Terasaki, A. Schmidtchen, M. Malmsten, *Biomaterials* **2009**, *30*, 5729–5736.
- [121] F. Liu, P. Yuan, J. J. Wan, K. Qian, G. F. Wei, J. Yang, B. H. Liu, Y. H. Wang, C. Z. Yu, *J. Nanosci. Nanotechnol.* **2011**, *11*, 5215–5222.
- [122] Z. Luo, Y. Deng, R. Zhang, M. Wang, Y. Bai, Q. Zhao, Y. Lyu, J. Wei, S. Wei, *Colloids Surfaces B Biointerfaces* **2015**, *131*, 73–82.
- [123] M. Ruiz Rico, Use of Silica Supports for Enhancing the Stability of Folates and Developing Antimicrobial Agents, UNIVERSITAT POLITÈCNICA DE VALÈNCIA, **2016**.
- [124] F. Balas, M. Manzano, P. Horcajada, M. Vallet-Regi, *J. Am. Chem. Soc.* **2006**, *128*, 8116–8117.
- [125] C. A. Aerts, E. Verraedt, A. Depla, L. Follens, L. Froyen, J. Van Humbeeck, P. Augustijns, G. Van den Mooter, R. Mellaerts, J. A. Martens, *Int. J. Pharm.* **2010**, *397*, 84–91.
- [126] P. Joyce, A. Tan, C. P. Whitby, C. A. Prestidge, *Langmuir* **2014**, *30*, 2779–2788.
- [127] Q. He, J. Shi, *J. Mater. Chem.* **2011**, *21*, 5845.
- [128] S. Y. Park, M. Barton, P. Pendleton, *Colloids Surfaces A Physicochem. Eng. Asp.* **2011**, *385*, 256–261.
- [129] S. Y. Park, P. Pendleton, *Powder Technol.* **2012**, *223*, 77–82.
- [130] M. W. Pettit, P. D. R. Dyer, J. C. Mitchell, P. C. Griffiths, B. Alexander, B. Cattoz, R. K. Heenan, S. M. King, R. Schweins, F. Pullen, et al., *Int. J. Pharm.* **2014**, *468*, 264–271.
- [131] L. Sun, X. Zhang, Z. Wu, C. Zheng, C. Li, *Polym. Chem.* **2014**, *5*, 1999–2009.
- [132] L. Sun, X. Zhang, C. Zheng, Z. Wu, C. Li, *J. Phys. Chem. B* **2013**, *117*, 3852–3860.
- [133] Z. Zou, D. He, L. Cai, X. He, K. Wang, X. Yang, L. Li, S. Li, X. Su, *ACS Appl. Mater. Interfaces* **2016**, *8*, 8358–8366.
- [134] Y. You, K. K. Kalebaila, S. L. Brock, D. Oupicky, *Chem. Mater.* **2008**, 3354–3359.
- [135] Q. N. Lin, Q. Huang, C. Y. Li, C. Y. Bao, Z. Z. Liu, F. Y. Li, L. Y. Zhu, *J. Am. Chem. Soc.* **2010**, *132*, 10645–10647.
- [136] S. Giri, B. G. Trewyn, M. P. Stellmaker, V. S. Y. Lin, *Angew. Chemie - Int. Ed.* **2005**, *44*, 5038–5044.
- [137] W. Qu, Y. Li, L. Hovgaard, S. Li, W. Dai, J. Wang, X. Zhang, Q. Zhang, *Int. J. Nanomedicine* **2012**, *7*, 4983–4994.
- [138] A. Bernardos, E. Aznar, M. D. Marcos, R. Martínez-Mañez, F. Sancenón, J. Soto, J. M. Barat, P. Amorós, *Angew. Chemie - Int. Ed.* **2009**, *48*, 5884–5887.

- [139] A. Agostini, L. Mondragon, L. Pascual, E. Aznar, C. Coll, R. Martínez-Máñez, F. Sancenón, J. Soto, M. D. Marcos, P. Amorós, et al., *Langmuir* **2012**, *28*, 14766–14776.
- [140] A. Schlossbauer, J. Kecht, T. Bein, *Angew. Chemie - Int. Ed.* **2009**, *48*, 3092–3095.
- [141] C. Coll, L. Mondragón, R. Martínez-Máñez, F. Sancenón, M. D. Marcos, J. Soto, P. Amorós, E. Pérez-Payá, *Angew. Chemie - Int. Ed.* **2011**, *50*, 2138–2140.
- [142] Y. Zhu, W. Meng, N. Hanagata, *Dalt. Trans.* **2011**, *40*, 10203.
- [143] G. Zhang, M. Yang, D. Cai, K. Zheng, X. Zhang, L. Wu, Z. Wu, *Appl. Mater. Interfaces* **2014**, 8042–8047.
- [144] C. Contado, L. Ravani, M. Passarella, *Anal. Chim. Acta* **2013**, *788*, 183–192.
- [145] J. Athinarayanan, V. S. Periasamy, M. A. Alsaif, A. A. Al-Warthan, A. A. Alshatwi, *Cell Biol. Toxicol.* **2014**, *30*, 89–100.
- [146] R. Jugdaohsingh, S. H. C. Anderson, K. L. Tucker, H. Elliott, D. P. Kiel, R. P. H. Thompson, J. J. Powell, *Am. J. Clin. Nutr.* **2002**, *75*, 887–893.
- [147] Q. He, Z. Zhang, Y. Gao, J. Shi, Y. Li, *Small* **2009**, *5*, 2722–2729.
- [148] C. Fu, T. Liu, L. Li, H. Liu, D. Chen, F. Tang, *Biomaterials* **2013**, *34*, 2565–75.
- [149] J. A. Lee, M. K. Kim, H. J. Paek, Y. R. Kim, M. K. Kim, J. K. Lee, J. Jeong, S. J. Choi, *Int. J. Nanomedicine* **2014**, *9*, 251–260.
- [150] Z. Tao, M. P. Morrow, T. Asefa, K. K. Sharma, C. Duncan, A. Anan, H. S. Penefsky, J. Goodisman, A.-K. Soud, *Nano Lett.* **2008**, *8*, DOI 10.1021/nl080250u.
- [151] F. Tang, L. Li, D. Chen, *Adv. Mater.* **2012**, *24*, 1504–1534.
- [152] M. M. Van Schooneveld, E. Vucic, R. Koole, Y. Zhou, J. Stocks, D. P. Cormode, C. Y. Tang, R. E. Gordon, K. Nicolay, A. Meijerink, et al., *Nano Lett.* **2008**, *8*, 2517–2525.
- [153] C. F. Chau, S. H. Wu, G. C. Yen, *Trends Food Sci. Technol.* **2007**, *18*, 269–280.
- [154] E. Pérez-Esteve, A. Bernardos, R. Martínez-Máñez, J. M. Barat, *Recent Pat. Food. Nutr. Agric.* **2013**, *5*, 35–43.
- [155] C.-H. Lee, L.-W. Lo, C.-Y. Mou, C.-S. Yang, *Adv. Funct. Mater.* **2008**, *18*, 3283–3292.

Chapter 2. Materials and Methods

2.1. Materials

2.1.1. Enzyme

The enzyme used in this work is a β -galactosidase, a lactase extracted from *Kluyveromyces Lactis* yeast, provided by Chr. Hansen holding company (Denmark). Ha-Lactase 5200 (commercial name) was provided as a highly purified and standardized mixture of water/glycerol (55/45 wt%, Appendix 3) containing β -Galactosidase with an average activity of 5200 the neutral lactase units (NLU/g), and proteases with an average activity of 75 PU/g. One NLU is the quantity of enzyme that releases 1.3 μ mol of *o*-nitrophenol per min at 30°C and pH 6.5. ^[1]One PU-unit of protease is defined as the amount of enzyme that releases 1 μ g of substrate per minute under reaction conditions.

2.1.2. Buffer solution

The phosphate buffer solution used for diluting the enzyme stock solution and for the preparation of the substrate solution was prepared following the procedure described by Engelen and Randsdorp ^[1]. First, two solutions of 1 mM of MgSO₄ and 5 μ M of EDTA were prepared separately. Then 10 mL of each solution were mixed with 8.8 g of KH₂PO₄ and 6.1 g of K₂HPO₄. Milli-Q distilled water was added up to 1L. The pH of the final solution was 6.5 and the buffer was kept in the fridge.

2.1.3. *In vitro* digestion solutions

Simulated gastro-intestinal digestion is widely employed in many fields of food and nutritional sciences. In this work, the *in vitro* digestion model proposed by Minekus was used ^[2] for the preparation of simulated gastric fluid (SGF) and simulated intestinal fluid (SIF). Their composition is described in Table 2. 2. The pH of the solutions was adjusted at 3 or 7, for SGF and SIF, respectively, with HCl (6M). The solutions were used in the release studies presented in Chapters 3 and 4)

Table 2. 1. Preparation of stock simulated digestion fluids solutions.

Constituents	Stock solution (M)	SGF	SIF
		Vol. of stock (mL)	
KCl	0.5	6.9	6.8
KH ₂ PO ₄	0.5	0.9	0.8
NaHCO ₃	1	12.5	42.5
NaCl	2	11.8	9.6
MgCl ₂ (H ₂ O) ₆	0.15	0.4	1.1
(NH ₄) ₂ CO ₃	0.5	0.5	-

2.1.4. Substrate

Lactase is a digestive enzyme found in the small intestine that catalyzes the hydrolysis of lactose into glucose and galactose. The enzyme lactase is also able to convert the o-nitrophenyl- β -D-galactopyranoside (ONPG) into galactose and ortho-nitrophenol (ONP). Conventionally ONP is used as a spectrophotometric substrate in enzymology due to its similarity to lactose. The ONPG solution is colorless, while the ONP compound is yellow ($\lambda_{\text{max}}=420$) in its basic form. This allows for a spectrophotometrical monitoring along the hydrolysis reaction.

2.2. Preparation methods

2.2.1. Modified meso-macroporous silica supports- β -Gal_x@SiO₂

2.2.1.1. Solid Lipid Nanoparticles (SLN) synthesis

Solid Lipid Nanoparticles (SLN) of cetyl palmitate were prepared using a method previously reported, with minor modifications [3]. Cetyl palmitate (n-hexadecylpalmitate, NHP, >99% purity) was purchased from Sigma-Aldrich. The NHP (Figure 2. 1) has a molecular mass of is 480 g/mol and a melting temperature of 54°C, is nontoxic and widely used in food industry [4].

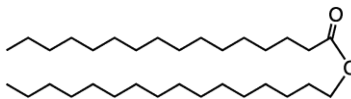


Figure 2. 1. Structure of NHP.

In a typical procedure, 2.2 g of NHP were heated at 70°C in a thermostatic bath. Once the fat has melted, it was added to 20 mL of 6.9 wt.% micellar solution of Pluronic®

P-123 also maintained at 70°C. The Pluronic® P-123 surfactant (Figure 2. 2) (poly(ethylene oxide)_x-*b*-poly(propylene oxide)_y-*b*-poly(ethylene oxide)_z triblock copolymer) has a molecular weight of 5800 g/mol and a HLB of 7-9. The poly(propylene oxide) is the hydrophobic block while poly(ethylene oxide) the hydrophilic one. The toxicity of this surfactant is very low and it is considered safe for cosmetic [5] and pharmaceutical [6] applications.

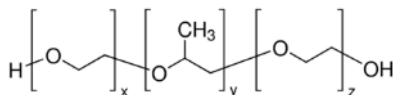


Figure 2. 2. Structure of Pluronic P 123, where x=20, y=70, z=20.

The mixture was sonicated for 3 min at 75% power with an ultrasonic device (Bandelin Sonopuls HD2200). The hot oil in water emulsion was then cooled down to room temperature under vigorous stirring to afford lipid solidification.

2.2.1.2. Preparation of meso-macroporous silica supports

The meso-macroporous silica supports were obtained through a dual templating mechanism, combining solid lipid nanoparticles and the micelles of P123 used as templates for macropores and mesopores [3,7-9], respectively as schematized in Figure 2. 3.

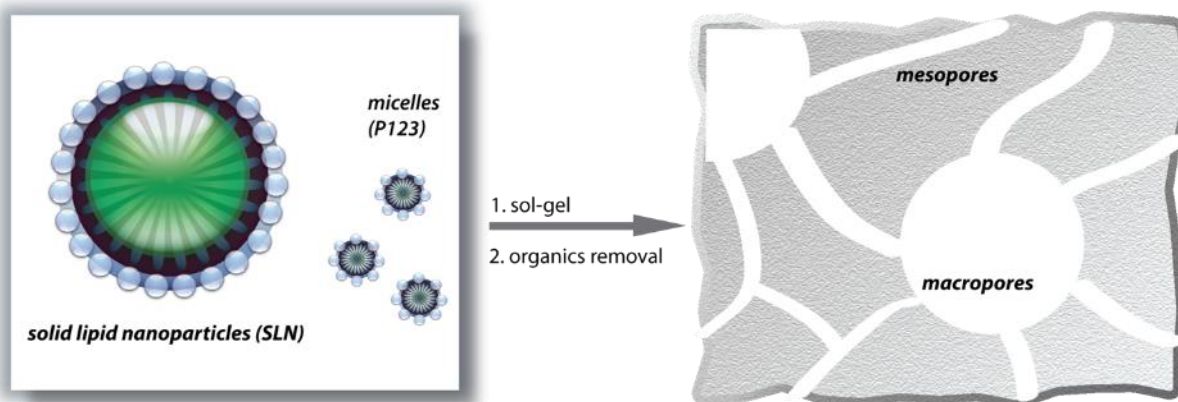


Figure 2. 3. Preparation of meso-macroporous silica supports

The synthesis of the meso-macroporous silica material was obtained through consequent hydrolysis and condensation of tetramethylorthosilicate (TMOS).[10,11] The

polymerization mechanism involves a two-step reaction and is similar to the polymerization mechanism described in Chapter 1.2 for the tetraethylorthosilicate (TEOS). The first step is the hydrolysis/initiation reaction where the hydroxyl groups are generated (Figure 2. 4 A). The second step represents the condensation reaction where the oxygen bridges between silicon atoms are formed (Figure 2. 4 B).

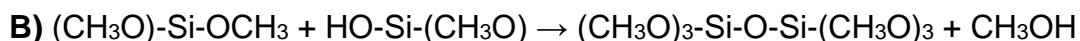
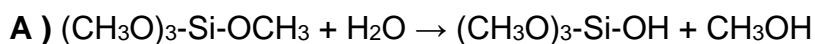


Figure 2. 4. Polymerization route of TMOS in aqueous solution.

900 mg of TMOS were added under stirring to 4 mL of SLN suspension with the surfactant to silica molar ratio (R) of 0.007. The mixture was stirred for 1 h at room temperature (RT) and then transferred into a sealed Teflon autoclave kept at 100°C for 24 h for hydrothermal treatment. Finally, the obtained gel was washed in a Soxhlet extraction setup over 24 h with ethanol to remove the surfactant and thereby to release the porosity.

2.2.1.3. Preparation of modified meso-macroporous silica supports- β -Gal_x@SiO₂

The as-obtained meso-macroporous material was then used to immobilize the β -Gal by dispersing the support in enzyme solutions of different concentrations (1.25, 2.50, 12.50 and 25.00 mg mL⁻¹). The samples were prepared by dispersing 25 mg of silica powder into 4 mL of buffer solution containing various concentrations of enzyme under gently stirring, using a vibrating table at 100 rpm for 48 h in a thermostatically controlled oven at 25 °C. After immobilization, the resultant enzyme-loaded silica materials were washed 3 times with the PBS buffer solution and centrifuged at 4000 rpm for 10 min. The final materials were labeled β -Gal_x@SiO₂, where x refers to the initial concentration of the enzyme solution used to load the silica materials.

2.2.2. Liposomes coated silica particles (LCSP)

2.2.2.1. Preparation of liposomes

The phospholipid 1,2-dioleoyl-*sn*-glycero-3-phosphocholine (DOPC) (Figure 2. 5) was used as pH responsive protective coating (see Chapter 3.2). This lipid has two oleic acids attached on the phosphatidylcholine head-group. The quaternary ammonium group has a positive charge and the phosphate group has a negative charge. This type of lipid is able to form liposomes and is naturally present in the double layer of biological membranes.

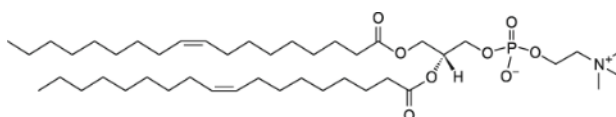


Figure 2. 5. Structure of DOPC.

Phospholipid liposomes were prepared by the lipid film hydration method. In the experiment, 390 μ l of DOPC (Avanti[®], 850375C, \geq 63 mM) were mixed in chloroform with 97 μ l Texas Red, a fluorescent dye. The chloroform was evaporated under a dry nitrogen stream to form a thin lipid film. The lipid was then hydrated with 1 ml of TRIS buffer (20 mM TRIS, 150 mM NaCl, pH 7.4) and the solution was sonicated for 30 min using an ultrasonic sonotrode, operating with a MS-72 titanium tip at 30% of the maximum power. At the end of the liposomes preparation the solution was centrifuged in order to remove the titanium particles released by the sonication tip.

2.2.2.2. Modification of porous silica particles (ESP)

A diluted solution of Ha-lactase at a concentration of 5.36 mg protein/mL was prepared from the enzyme stock solution by adding in 50:50 wt% PBS buffer (pH 6.5) and glycerol. Then, 4 mL of enzyme solution was added to 250 mg of a specific silica material KROMASIL[®] 300-10-SIL (SP), provided from AksoNobel Germany, in order to proceed the enzyme immobilization as schematized in Figure 2. 6. The mixture was left under stirring (150 rpm) at room temperature (20°C) over 3 hours. After immobilization, the resulted enzyme-loaded silica was recovered under centrifugation using a centrifuge filter (size 0.2 μ m) and washed with PBS buffer. Finally, the obtained supported enzyme catalyst was dried overnight under a fume hood at room temperature.

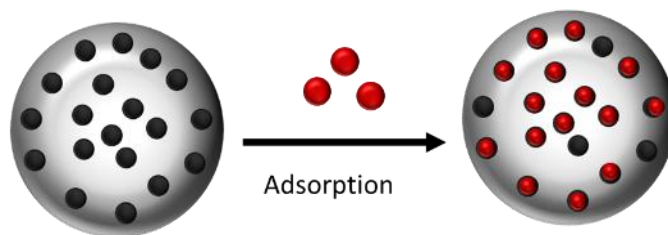


Figure 2. 6. Modification of porous silica particles

2.2.2.3. Preparation of liposomes coated silica particles (LCSP)

The LCSP were prepared as schematized in Figure 2. 7. After the adsorption of enzyme onto silica, approximately 80 mg of modified silica were dispersed in the liposomes solution and incubated for 1 hour at room temperature under stirring (150 rpm). Along incubation time, as described by Mornet e al.^[12], the pre-prepared liposomes will first adhere to mesoporous silica surface, undergo gradual deformation, break and spread on the particle surface forming a continuous bilayer phospholipid film. A final centrifugation step was performed to separate the coated silica particles (LCSP) from the remaining liposomes. After being washed with TRIS buffer 6 times, the formed LCSP were dispersed in TRIS solution and stored at 4°C.

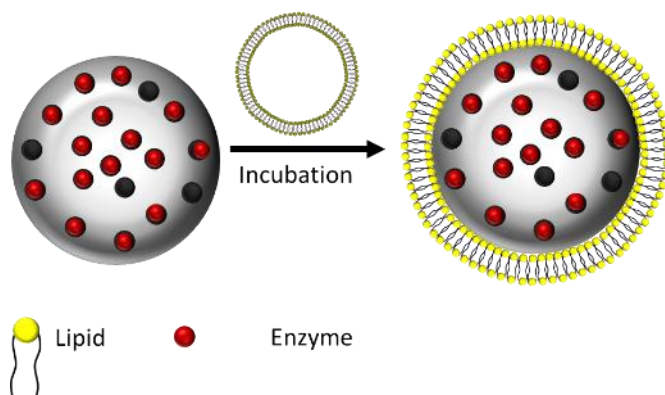


Figure 2. 7 Preparation of liposomes coated silica particles (LCSP).

2.2.3. Double emulsion type Solid Lipid Nanoparticles (SLN) synthesis

SLNs loaded β -Gal were prepared by $W_1/O/W_2$ emulsification melted dispersion method. The system was composed of shea butter as oil phase, β -galactosidase solution as the water phase 1 (W_1) and a solution of Tween 20 as water phase 2 (W_2). A schematic

representation of this preparation method for solid lipid nanoparticles preparation is shown in the Figure 2. 8. 0.600 ml of enzyme solution was added to a mixture of shea butter/PGPR (1000mg/300mg) under a vortex. To prepare the double emulsion, the inverse emulsion previously prepared was added into 10 g of aqueous solution of 20 % Tween 20 (wt%) under vortex. The sample temperature was maintained at 40°C all along the procedure. The obtained solution was cooled down slowly to 20°C under vortex in which the crystallization process of shea butter occurred and the colloidal suspension was stored at 4°C.

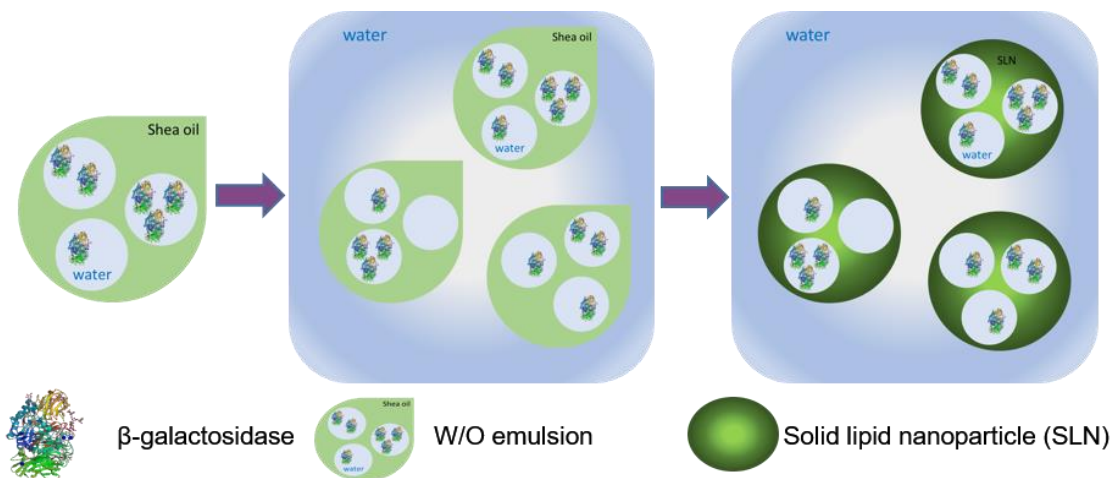


Figure 2. 8. Schematic representation of preparation method for solid lipid nanoparticles.

SLNs were prepared without organic solvents, by melt dispersion technique, using the melted lipid instead of a lipid solution in an organic solvent. The enzyme is exposed to 40 °C temperature (much lower than the unfolding temperature^[13]) for a short period of time, which reduces the possibility of enzyme degradation. Moreover, the enzyme solution contains 50% glycerol that enhances the thermal stability of β-Gal^[14].

In this formulation of the *water-in-oil-in-water* double emulsions (W/O/W), PGPR was used to stabilize the first inverse water-in-oil emulsion (W₁/O) and Tween® 20 was used to stabilize the dispersion of W₁/O emulsion in water leading to W₁/O/W₂ from which the solid lipid particles suspension is generated. The shea butter was chosen as the oil phase.

The polyglycerol polyricinoleate (PGPR) has a chemical backbone of polyglycerol grafted with pendant chains of polymerized ricinoleic acid, labeled R in Figure 2. 9. Ricinoleic acid is an unsaturated omega-9 fatty acid [15]. PGPR is already used in chocolate and chocolate base products, salad dressing and baked products [16][17][18]. This emulsifier is very lipophilic and weakly soluble in water due to the few ether and hydroxyl groups are present in the chemical backbone. Thus, PGPR is a water in oil emulsifier (HLB <1).

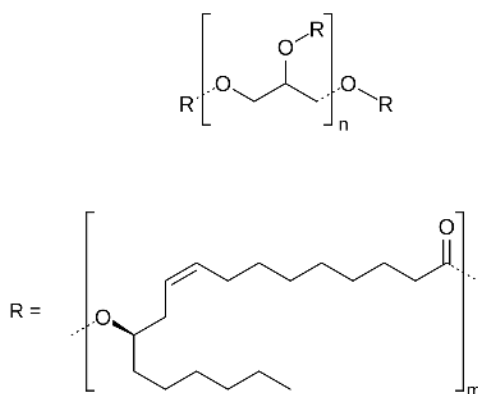


Figure 2. 9. Structure of PGRP.

The main component of shea butter are triglycerides (Figure 2. 10). The triglycerides contained in the shea butter used are derived mainly from stearic acid (36-50%) and oleic acid (40-50%) extracted from the nuts of African shea tree (*Vitellaria paradoxa*)(Appendix 2). It was provided by ieS LABO (France).

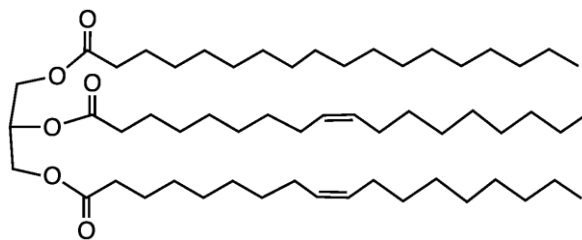


Figure 2. 10. General chemical structure of a triglyceride.

2.2.4. Preparation of hybrid materials

2.2.4.1. Preparation of hybrid alginate silica particles (ASP)

Sodium alginate was dissolved in deionized water with a final concentration of 1% wt. A 2 mL aliquot of the alginate solution was mixed with 0.735 mL of TMOS under vortex agitation. This mixture was then added drop wise into a mixture of 0.3 g PGPR and 1.5 g hexane. After one minute, in which silica polymerization is initiated, by the presence of alginate molecules^[19], 3 mL solution of 0.2 M MgCl₂ and 50% enzyme solution was added drop wise and kept under vortex agitation for 1 minute. To prevent denaturation of the enzyme in the presence of Ca²⁺, Mg²⁺ has been used. The beads, thus formed were left to crosslink with the divalent cation for a half an hour. After washing with deionized water and centrifuged on a 0.2 µm filter, the particles were lyophilized overnight.

2.2.4.2. Preparation of alginate core silica shell materials (SAM)

Sodium alginate was dissolved in deionized water with a final concentration of 1% wt. 2 mL of the alginate solution was added drop wise into a mixture of 0.3 g PGPR and 1.5 g hexane. After one minute, 3mL solution of 0.2 M MgCl₂ and 50% enzyme solution was added dropwise and kept under vortex agitation for 1 minute. After the crosslink of the alginate with the divalent cation for half an hour, 0.735 mL of TMOS was added and left to polymerize for another half an hour. After washing with deionized water and centrifuged on a 0.2 µm filter, the particles were lyophilized overnight.

2.2.4.3. Preparation of alginate particles (AP)

The procedure of alginate particles (AP) was quite similar with the preparation of SAP, except that after the crosslinking of the alginate, the emulsion was broken using isopropanol. After washing with deionized water and centrifuged on a 0.2 µm filter, the particles were lyophilized overnight.

2.3. Characterization methods

2.3.1. Protein Quantification Assay

The amount of β -galactosidase non-entrapped in the system presented in Chapters 3 and 4 was quantified with Thermo Scientific™ Pierce™ BCA Protein Assay. The Thermo Scientific™ Pierce™ BCA Protein Assay is a commercial preparation kit for the colorimetric detection and quantitation of the amount of protein in a sample. The method is based on biuret reaction, in which the reduction of copper II (Cu^{2+}) to copper I (Cu^{1+}) occurs in presence of four specific amino acids contained in the protein backbones (cysteine, cystine, tryptophan and tyrosine). Consequently, the chelation takes place between two molecules of bicinchoninic acid (BCA) and the Cu^{1+} previously formed leading to a purple-colored product absorbing visible light at $\lambda_{\text{max}}=562\text{nm}$ (Figure 2. 11) [20]. The absorbance of the water-soluble complex is linear with increasing protein concentrations in a wide range of concentrations from 0 to 2000 $\mu\text{g/mL}$. The color obtained is not only resulting from the presence of functional groups is the solution [21].

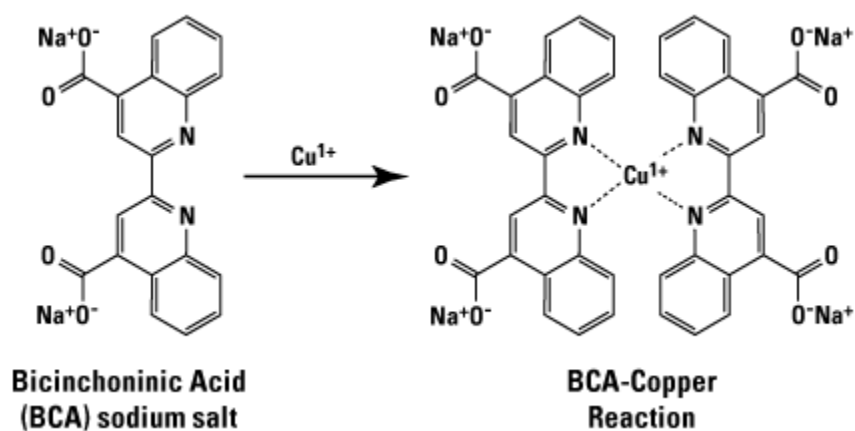


Figure 2. 11. Scheme of the chemical reaction of Cu^+ with two BCA molecules.

Usually, in the case of this method, the calibration curves are determined and reported for bovine serum albumin (BSA) as a standard reference. Thus, a series of dilutions of known concentration of BSA were prepared from the stock protein (2 mg/mL) in different media (water, simulated gastric fluid (SGF) and simulated intestinal fluid (SIF)). The slope and the intercept values of the calibration curves obtained in the three media are rather close meaning that the simulated body fluids do not change the complexation route of BCA with Cu^+ , as presented in the Figure 2. 12.

$$A_{H_2O}=0.00345[BSA]+0.14386$$

$$A_{SIF}=0.003420[BSA]+0.14533$$

$$A_{SGF}=0.00365[BSA]+0.14237$$

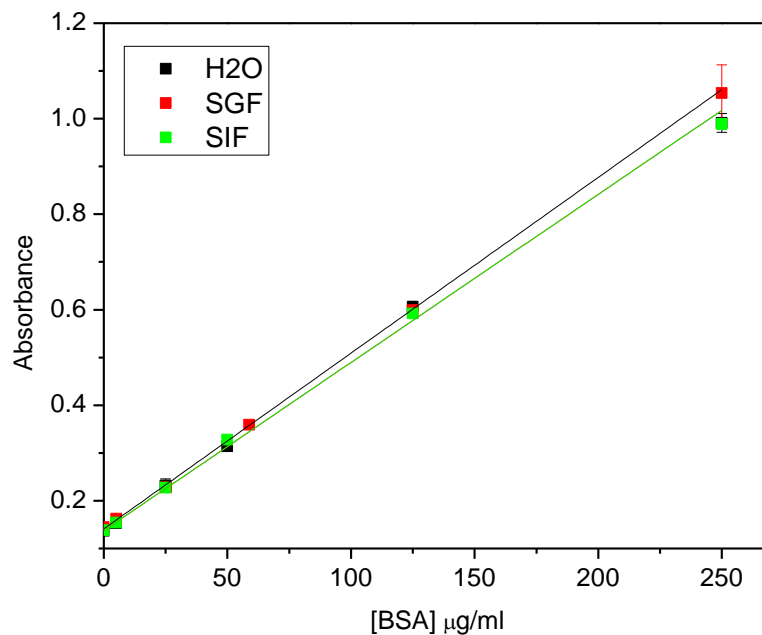


Figure 2. 12. The calibration curves obtained for chelation of BSA with Cu^+ in water, SGF and SIF.

2.3.2. Detection of enzyme and material activity

Following a typical procedure, the ONPG solution was prepared in PBS buffer, prepared two hours prior to use, at a concentration of 25 mg/L. The substrate was left to react with the enzyme for 10 minutes. The reaction was then stopped by adding a solution containing 50mM Na_2CO_3 and 7 mM EDTA. The pH shifts towards more basic values (pH 8.3), at which the ortho-nitrophenol is entirely in its base conjugated form, the ortho-nitrophenolate (Figure 2. 13 B, $\epsilon = 4.6 \text{ mM}^{-1} \text{ cm}^{-1}$ at $\lambda_{\text{max}}=420 \text{ nm}$).

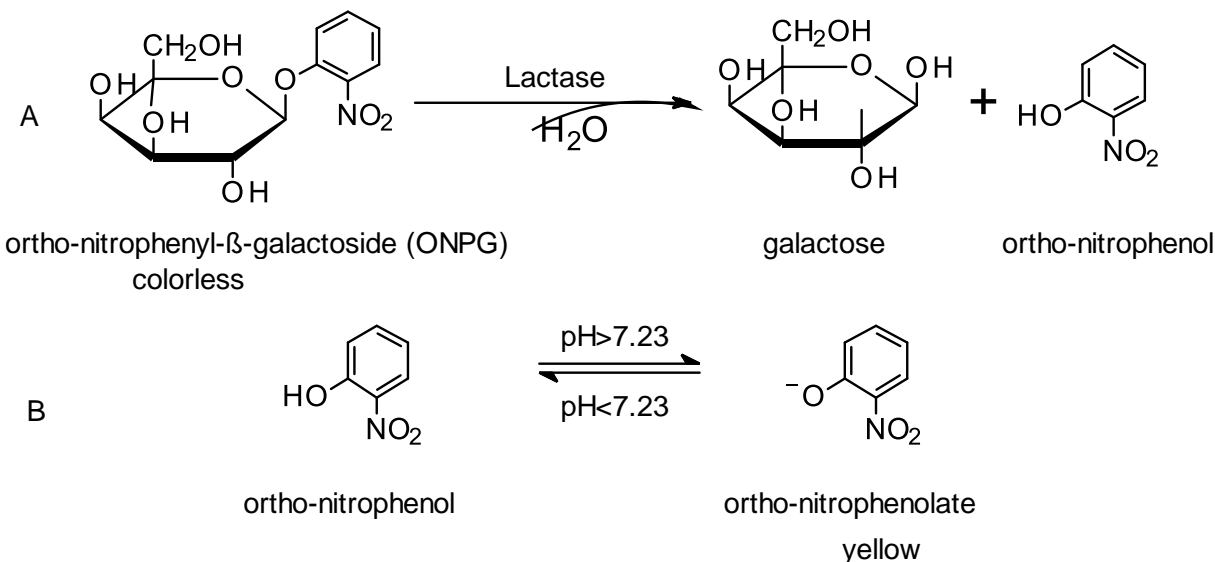


Figure 2. 13. A) Hydrolysis reaction of ONPG into galactose and ortho-nitrophenol, B) chemical shift between orthonitrophenol and orthonitrophenolat with the change of pH.

For both free and immobilized/encapsulated enzyme on silica materials the activity was defined in international units (IU), 1 IU corresponding to the amount of enzyme catalyzing the conversion of 1 μmol of substrate per minute at 25°C in Chapter 3.1 and at 30°C in Chapter 3.2 and 4.2.

In Chapter 3.1, in the case of the free enzyme, the reaction was carried out by mixing 0.5 mL of 40 mM ONPG and 0.5 mL of enzyme solution at 25°C and run over 10 min. Adding 0.5 mL of 500 mM Na_2CO_3 solution stopped the reaction. The absorbance of ONP was measured at 420 nm. For the activity of the immobilized β -Gal on meso-macroporous silica materials, 1 mg of each powder of loaded silica materials was transferred into a tube containing 0.5 mL of buffer solution, to which 0.5 mL of 40 mM of ONPG solution was subsequently added. The reaction was stopped after 10 min by adding 0.5 mL of 500 mM Na_2CO_3 solution. To remove the silica material, samples were centrifuged (4000 rpm during 30 sec) and the absorbance value of the ONP-containing supernatant was measured at 420 nm. For both free and immobilized/encapsulated enzyme on silica materials the activity was defined in international units (IU), 1 IU corresponding to the amount of enzyme catalyzing the conversion of 1 μmol of substrate per minute at 25°C.

In Chapter 3.2, the assay for the free enzyme activity was performed by mixing 2.5 ml of o-nitrophenyl- β -D-galactopyranoside (ONPG, 25 mg/L) and 0.5 ml of diluted enzyme solution (diluted 12000 times from the initial stock). The mixture was incubated at 30°C for 10 minutes before being stopped by adding 1 mL of a solution of Na₂CO₃ (50 mM). All experiments were performed in triplicate. For the activity of the immobilized β -Gal on silica particles (SP) and liposomes coated silica particles (LCSP), approximately 8 mg of SP and 100 μ l of LCSP suspension was transferred into a tube containing 1.6 mL of buffer solution (PBS), from which 0.125ml was analyzed. To this solution, 0.5 mL of ONPG solution was subsequently added. The reaction was stopped after 10 min by adding 0.25 mL Na₂CO₃ solution. To remove the silica material, samples were centrifuged (13500 rpm for 120 sec). The activity of the SP was determined at 22.4 U/mg of silica material and the activity of LCSP as 10.9 U/mg of silica. For both free and immobilized/encapsulated enzyme on silica materials the activity was defined in units (U), 1 U corresponding to the amount of enzyme catalyzing the conversion of 1 μ mol of substrate per minute at 30°C.

In Chapter 4.2, the same protocol was followed as in Chapter 3.1, with the exception that approximately 10 mg of materials were dispersed in 2 mL of buffer solution. The dilutions and the protocol remained the same.

2.3.3. Enzyme release in simulated gastro-intestinal fluid

A controlled release of the enzyme out of materials was done *in vitro* in simulated gastric fluid (SGF) and in simulated intestinal fluid (SIF). The materials were analyzed two by two, uncoated SP carrier was compared with the lipid covered silica particle (LCSP), while hybrid alginate silica particles (ASP) was compared with alginate core silica shell materials (SAM). In order to simulate the passage of the materials through the gastro intestinal tract four samples of each material were tested as presented in Table 2. 2. Each type of sample underwent four experiments under magnetic stirring at 150 rpm. In the first one the sample (LCSP1 or SP1/ ASP1 or SAM1) was kept for 1H in SGF, the second one, the carrier (LCSP2 or SP2/ ASP2 or SAM2) was kept for 2H in SGF. The third and the four experiments are a successive immersion of the sample in SGF over 2H followed by 1H or 2H in the SIF. In the case of LCSP and SP, the samples from the experiments

3 and 4 have been centrifuged before being added to the SIF (Table 2. 2). In the case of ASP and SAM, all samples were separated from the solutions by centrifugation after each hour and introduced into a new solution.

Table 2. 2. Incubation time in simulated gastro-intestinal fluids (SGF and SIF).

Experiment	Samples	Incubation treatment (time and media)
1	LCSP1 and SP1/ ASP1 and SAM1	1H in SGF
2	LCSP2 and SP2/ ASP2 and SAM2	2H in SGF
3	LCSP3 and SP3/ ASP3 and SAM3	2H in SGF followed by 1H in SIF
4	LCSP4 and SP4/ ASP4 and SAM4	2H in SGF followed by 2H in SIF

LCSP: liposomes coated enzyme-silica particles, SP: enzyme adsorbed on silica particles, ASP: hybrid alginate silica particles and SAM: alginate core silica shell materials (SAM).

All the solutions were analyzed to quantify the enzyme released and its activity.

2.3.4. Dynamic light scattering

Particle sizing distribution and their hydrodynamic radius (R_H) were obtained by dynamic light scattering (DLS) using a Malvern 3000HSA Zetasizer instrument equipped with a He-Ne laser (633 nm, 5 mW). Prior to measurement, the dispersions of SLN (used for the preparation of meso-macroporous materials in Chapter 3.1), were diluted with Millipore water until the count rate intensity was above 500 kcps. The samples were placed in disposable polystyrene cells, and the experiments were performed at constant temperature (25°C).

2.3.5. SAXS measurements

Small angle X-ray scattering (SAXS) measurements were carried out using a SAXSess mc² (Anton Paar) apparatus with slit collimation. It is coupled with an ID 3003 laboratory X-Ray generator (general electric), equipped with a sealed X-ray tube (PANalytical, CuK α radiation $\lambda = 0.1542$ nm) operating at 40 kV and 50 mA. A multilayer mirror and a block collimator provide a monochromatic primary beam. A translucent beam stop allows the measurement of an attenuated primary beam at $q=0$. Meso-macroporous materials (Chapter 3.1) were introduced into a powder cell (sandwiched in between two

Kapton foils), whereas aqueous dispersions and shea butter (Chapter 4.1) are placed in quartz capillaries of 1.5 mm of diameter. Samples are placed inside an evacuation chamber at 309 mm from the sample holder. Acquisition times are typically in the range of 30 minutes. The scattered X-ray beam is recorded by a CCD detector (Princeton Instruments, 2084×2084 pixels array with 24×24 μm^2 pixel size) in the q range from 0.09 to 5 nm^{-1} , and treated the with SAXSquant software for smearing signal correction. All data was corrected for background scattering from the respective empty cells. For the lipid dispersions, the scattering data were corrected by the water filled capillary.

2.3.6. Nitrogen sorption analysis

The pore size and the texture parameters of the bare and enzyme-loaded silica materials (Chapter 3) were determined by nitrogen sorption isotherms at 77 K using a Micromeritics Tristar device. For that purpose, all materials were degassed under vacuum over for 24 h at 20°C to remove water and CO₂ physically adsorbed at the surface of the samples. The specific surface area (S_{BET}) was determined by applying the Brunauer–Emmett–Teller (BET) theory whereas pore volume and average pore size were obtained using the Barrett–Joyner–Halenda method (BJH) applied to the desorption branch of the isotherms.

2.3.7. Microscopy

Morphology and porosity of the bare meso-macroporous silica material were observed by transmission electronic microscopy (TEM). The powder was first ground and then suspended in ethanol by sonication. A drop of the dispersion was spread out on the TEM carbon lacey grid and dried at room temperature before observation (Chapter 3.1)

Particle size of simple and double emulsions was determined by optical microscopy, using an Olympus BX51 equipped with a Toupcam camera, with a TouView software (Chapter 4.1). Droplet size, size polydispersity and morphology of prepared Pickering emulsions (Chapter 5) were evaluated by optical microscopy (Olympus BX51 microscope). The observation of the samples was carried in bright field mode.

Morphology of the bare silica material (Kromasil®)(Chapter 3.2) and hybrid alginate-silica (Chapter 4.2) were observed by scanning electronic microscopy (SEM) at an accelerating voltage of 2.0 kV and working distance of about 10 mm. The powder was spread out on the SEM carbon patch and dried at room temperature before observation.

The fluorescence microscopy measurements presented in Chapter 3.2 were performed at the Institute for Physical Chemistry, Heidelberg, Germany, using an Axio Observer inverted microscope (Carl Zeiss AG), equipped with a PlanNeofluoar 63x/1.25/PH3 antilex oil-immersion objective with a built-in lambda-quarter plate, a filter cube with the fitting filter set for Texas Red or FITC ($\lambda_{\text{excitation}} = 595 \text{ nm}$; emission 615 nm). The light source consisted of a high-pressure metal halide lamp HXP 120V. The images were recorded with an Orca ER CCD camera (Hamamatsu Photonics) with an adjusted exposure time of 50 to 300 milliseconds.

2.3.8. Fourier Transform Infrared spectroscopy – FTIR

Attenuated total reflectance Fourier transformed infrared (ATR- FTIR) spectra were collected using a IRaffinity-1 spectrometer (Shimadzu) coupled with a PIKE Technologies GladiATR accessory with a diamond crystal. The software for collecting and viewing spectra was the LabSolutions IR (Shimadzu). The absorbance spectrum of each sample has been obtained by accumulating 32 scans at 4.0 cm^{-1} of resolution. The background correction was made with the spectrum signal of the clean ATR crystal exposed to the ambient atmosphere. The bare and enzyme-loaded meso-macroporous silica materials in Chapter 3.1 and the hybrid silica materials in Chapter 4.2 were analyzed by FTIR.

2.3.9. Thermogravimetric analysis (TGA)

The enzyme adsorption efficiency was quantified by thermogravimetric analysis (TGA) using a Netzsch STA 449F1 thermobalance. Approximately 10 to 15 mg of each sample were heated up to $800 \text{ }^{\circ}\text{C}$ at $5 \text{ }^{\circ}\text{C min}^{-1}$ under air for the decomposition of organics. The results were used in the work presented in Chapter 3.

2.3.10. Zeta potential measurements

Zeta potential was measured using a Malvern Zetasizer 3000 HS instrument, based on $0.5 \text{ mg}\cdot\text{mL}^{-1}$ suspension of bare or enzyme-loaded meso-macroporous silica dispersed by sonication in a water bath in aqueous solution at pH ranging from 2.5 to 9. The bare and modified silica materials presented in Chapter 3 were analyzed by Zeta potential.

2.3.11. DSC

The calorimetric measurements (DSC) (work done at Institute for Physical Chemistry, Heidelberg, Germany) were performed using a VP-DSC calorimeter (MicroCal, Inc., Northampton, MA, U.S.A.) with a scan speed of $90^\circ\text{C}/\text{hour}$, in the temperature range $10\text{-}50^\circ\text{C}$.

Bibliography

- [1] A. J. Engelen, P. H. Randsdorp, *J. AOAC Int.* **82**, 112–8.
- [2] M. Minekus, M. Alminger, P. Alvito, S. Ballance, T. Bohn, C. Bourlieu, F. Carrière, R. Boutrou, M. Corredig, D. Dupont, et al., *Food Funct.* **2014**, *5*, 1113–24.
- [3] S. Kim, M.-J. Stébé, J.-L. Blin, A. Pasc, *J. Mater. Chem. B* **2014**, *2*, 7910–7917.
- [4] I. Zafeiri, J. E. Norton, P. Smith, I. T. Norton, F. Spyropoulos, *J. Colloid Interface Sci.* **2017**, *500*, 228–240.
- [5] S. D. Singh-Joy, V. C. McLain, *Int. J. Toxicol.* **2008**, *27 Suppl 2*, 93–128.
- [6] L.-Y. Zhao, W.-M. Zhang, *J. Drug Target.* **2017**, *25*, 471–484.
- [7] J.-L. Blin, J. Jacoby, S. Kim, M.-J. Stébé, N. Canilho, A. Pasc, *Chem. Commun. (Camb)*. **2014**, *50*, 11871–4.
- [8] S. Kim, R. Diab, O. Joubert, N. Canilho, A. Pasc, *Colloids Surf. B. Biointerfaces* **2015**, *140*, 161–168.
- [9] A. Pasc, J.-L. Blin, M.-J. Stébé, J. Ghanbaja, *RSC Adv.* **2011**, *1*, 1204.
- [10] A. E. . Palmqvist, *Curr. Opin. Colloid Interface Sci.* **2003**, *8*, 145–155.
- [11] J. Y. Ying, C. P. Mehnert, M. S. Wong, *Angew. Chemie Int. Ed.* **1999**, *38*, 56–77.
- [12] S. Mornet, O. Lambert, E. Duguet, A. Brisson, *Nano Lett.* **2005**, *5*, 281–285.
- [13] M. Sutter, S. Oliveira, N. N. Sanders, B. Lucas, A. Van Hoek, M. A. Hink, A. J. W. G. Visser, S. C. De Smedt, W. E. Hennink, W. Jiskoot, *J. Fluoresc.* **2007**, *17*, 181–192.
- [14] V. Athès, D. Combes, *Enzyme Microb. Technol.* **1998**, *22*, 532–537.
- [15] J. Kiefer, K. Frank, F. M. Zehentbauer, H. P. Schuchmann, *Biosensors* **2016**, *6*, 1–11.
- [16] E. O. Afoakwa, *Chocolate Science and Technology*, **2010**.
- [17] Nordisk Ministerråd, *Food Additives in Europe 2000 : Status of Safety Assessments of Food Additives Presently Permitted in the EU*, Nordic Council Of Ministers, **2002**.
- [18] N. T. Dunford, *Food and Industrial Bioproducts and Bioprocessing*, Wiley-Blackwell, **2012**.
- [19] S. Xu, Z. Jiang, Y. Lu, H. Wu, W. Yuan, **2006**, 511–517.
- [20] P. K. Smith, R. I. Krohn, G. T. Hermanson, A. K. Mallia, F. H. Gartner, M. D. Provenzano, E. K. Fujimoto, N. M. Goeke, B. J. Olson, D. C. Klenk, *Anal. Biochem.* **1985**, *150*, 76–85.
- [21] K. J. Wiechelman, R. D. Braun, J. D. Fitzpatrick, *Anal. Biochem.* **1988**, *175*, 231–237.

Chapter 3. Physisorption on silica

The use of enzymes as biocatalysts in industrial applications, such as food^[1], energy-biodiesel^[2] or pharmaceutical synthesis^[3] is increasing due to their high catalytic activity and selectivity. However, enzymes have a poor reusability and a low operational stability because of their sensitivity to pH and temperature. The immobilization of enzymes is one of the most promising methods to maintain enzyme performance and stability with the possibility to recover and reuse the catalyst. Supported enzymatic catalyst is also interesting to use in particular reaction conditions when enzyme is operating in organic solvent, for instance when a transesterification are required^[4-6]. Different immobilization strategies have been developed to prepare supported enzyme catalysts: entrapment, microencapsulation and cross-linked enzyme crystals (CLEC) or aggregates (CLEA)^[7]. These methods are based on physical adsorption, covalent attachment and affinity of the enzyme to the support.

Depending on the immobilization method, the chemical and physical properties of the enzyme can be altered. For example, through a covalent bonding between the enzyme and the support, the active conformation of an protein can be strongly modified and induce a decrease in the enzymatic activity^[8]. However, the physical adsorption of the enzyme generally occurs through weak forces such as hydrophobic interaction, hydrogen bonds, electrostatic, van der Waals forces or ionic interactions that do not change dramatically the native conformation and the activity of the enzyme^[9,10].

The materials employed for enzyme adsorption can be organic or inorganic but not all the enzymes can be easily immobilized on them. Investigating suitable solid supports for enzyme immobilization is still a current scientific challenge, depending on each specific enzyme and for each industrial application. The criteria to choose a suitable carrier for a given enzyme and its application include: stability (or reactivity), cost, availability and the type of the reactor in which it will be used. The surface area, the particle size, the pore size and the structure, the type of functional groups at the surface of the pores are the physico-chemical parameters that should also be considered in the choice of the support.

The most common organic carriers are synthetic or natural polymers. Natural supports used in enzyme immobilization are either pure calcium alginate [11] or in mixture with gelatin and transglutaminase [12]. Cellulose [4,13,14] and chitosan in hydrogel form [15–18], in microcrystalline form [19], or agarose gel are commonly used as supports [20]. Synthetic polymers such as poly(vinyl alcohol) [21][22], cross-linked poly(vinyl alcohol) [23], poly(N-methylolacrylamide) [24], polypropylene [25–27], poly(acrylic acid-co-acrylamide)/hydrotalcite nanocomposite hydrogels [28], poly(hydroxybutyrate) nanoparticles [29] and beads [30], poly(o-toluidine) [31] and poly(acrylonitrile) [32] are also used for enzyme immobilization.

Concerning the inorganic supports, literature reports for the immobilization of enzyme the use of metals and also many oxides such as alumina gel [11], aluminum [33] or aluminosilicates [34] (class of compounds made of aluminum, silicon and oxygen), titania sol-gel [35], gold [36,37], cordierite, mullite [38], halloysite [39], mica [40] and hydroxyapatite [41] as powder or as ceramic [42], bentonite [43] or mesoporous activated carbon [44] of different pore sizes.

Compared with the organic resin supports, the inorganic materials like amorphous silica present convenient properties for protein immobilization such as: high surface area, thermal stability, good mechanical properties, low swelling in organic solvents while withstanding high flow rates in continuous reactors. The silica materials are nontoxic, microbial resistant and they also exhibit a high biocompatibility, biodegradability. For this reasons amorphous silicon dioxide have been intensively studied as carriers [45–47]. Many amorphous porous silica materials with different morphological parameters have been extensively synthesized for its adsorption properties. The mesoporous silica SBA-15 (Santa Barbara Amorphous) presenting a hexagonal array of pores (5 to 30 nm size diameter), a large volume of meso- and microporosity ($\sim 1.0 \text{ cm}^3 \cdot \text{g}^{-1}$, $\sim 0.8 \text{ cm}^3 \cdot \text{g}^{-1}$, respectively) and a high surface area from 500 to 1400 $\text{m}^2 \cdot \text{g}^{-1}$ is an excellent support used for enzyme immobilization [48].

However, some other mesoporous silicas used for enzyme immobilization have been documented in literature: the mesoporous MCM-41 (Mobil Composition of Matter, 2

to 3 nm pore size) [49], the large to ultra large pore size MSU-H (Michigan State University, 7.6-11.9 nm pore size) [50], the FDU-12 (Fudan University Material, 8.9 nm pore size) [51], the large-pore mesoporous silica nanoparticles with a cubic Ia3d structure of pores (KIT-6, 8 nm pore size) [52], different size of mesoporous silica particles [53], the folded sheet mesoporous silica [54], silicas with small surface areas [55–57] or silica gels (particle size 0.040-0.063 nm) [58]. Finally, vesicular silica [59,60] and fumed silica [61], that have well-developed surface areas, small particles and high mechanical strength have also been investigated for the enzyme immobilization.

The affinity between the enzyme and the support is a key factor of getting an efficient enzymatic catalyst. Thus, the surface of the support is commonly modified with chemical groups that can physically interact with specific chemical groups bear by the enzyme. Usually, the grafting groups are chosen with at least two reactive groups, one that can chemically anchor on the support and the other that physically interact with the enzyme. This is the case of glutaraldehyde ($\text{CH}_2(\text{CH}_2\text{CHO})_2$) that contains two reactive aldehyde groups [36,38,62], one that can connect to the -OH groups of the support and the other with a -NH₂ groups of the enzyme. In fact, glutaraldehyde is the most common linker used for its bifunctional carbonyl groups that have high affinity to bacteria, fungi and protein.

According to the support and the enzyme immobilized, the linker can be adapted. For instance, silanes are used to modify silica materials. The most frequently used silanes are 3-amino-propyltrimethoxysilane [59,63], 3-aminopropyltriethoxy-silane [52,64,65], mercaptopropyl-trimethoxysilane or mercaptopropyl-triethoxysilane [37], n-octyltriethoxysilane [57], phenyltrimethoxy-silane, vinyltri-methoxysilane [51] and [3-(trimethoxy-silyl)propyl] octadecyl dimethyl ammonium chloride [66]. They can also be grafted on gold particles surface [37].

Polymers can be synthesized through specific monomer(s) and at different chain lengths, and besides being a class of support, they can also be used as linkers. Polymers as polyethyleneimine [67] polystyrene [19] or poly(styrene sulfonate) [68], acrylonitrile copolymers [69] or second generation polycationic dendronized polymer (de-PG2) [56] can

be employed to improve the affinity of the enzyme for the chosen support. Moreover, in some complex elaborated catalysts, enzyme–support affinity is increased by coating silica by conducting polymers as polypyrrole ^[70,71] or polyamidoamine dendrimers ^[72].

The linkers with acid-base properties like amines are also interesting to modify the support surface because hydrogen bonding is favored with enzyme. For example, diethylamine ^[73,74], diethylaminoethyl (DEAE) ^[75] or mono-aminomethyl-N-amino-ethyl ^[20] are the most commonly used amino linkers. Moreover, long chain carboxylic acid as erucic acid ^[76] or short chain carboxylic acid as itaconic acid that contain two carboxyl groups and an additional reactive carbonyl group ^[17] are also used as modifiers.

Oxygen plasma ^[4] and plasma polymerization of allyl-alcohol, allyl-amine and acrylic acid were also proposed ^[14] as a new approach for support functionalization. However, they present the disadvantage of having a high cost.

3.1. Preferential adsorption of β -galactosidase regarding Hierarchical Meso-Macro porosity of a Silica Material ²

Since their discovery in 1992 ^[77], silica mesoporous materials have been widely used in enzyme immobilization due to their tunable pore size, volume and their large specific surface area. These materials can entrap a large amount of enzymes, and the immobilization can be done either by chemisorption or physisorption. The pores are a favorable environment for enhancing the thermal and pH stability of the enzymes as well as their resistance to high salt concentrations. ^[45,78,79] However, the confinement of the enzyme in pores ^[45] and/or in a small pore size of the material, or on non-open-pore structures ^[79] can lead to a decrease of the enzymatic activity and might exhibit significant resistance to the substrate diffusion. By increasing the pore size (e.g. from meso- to macropore), one can expect an increase of the diffusion rates of substrates to the active sites of the enzyme and a larger enzyme mobility/flexibility within the cavities, resulting thus in a better enzyme activity ^[80]. Indeed, macroporous silica materials have a high mass transfer rate due to the interconnection of their broad pores, in addition to a good mechanical and thermal stability. However, even if the enzyme can be easily immobilized on this kind of materials, it can be also leached out easily, particularly when the pH of the media varies. To overcome this problem, the enzyme can be retained inside the material by crosslinking or by aggregation ^[81].

Hierarchical porous materials combine the properties of mesopores, such as high surface area and controllable pore size/volume, with those of macropores, providing high diffusion and throughput rates ^[82]. Although they are widely used in chemical catalysis ^[83], only a few examples have been reported in the literature for enzyme encapsulation. For instance, Cao et al. ^[84] used hierarchical silica spheres to encapsulate glucose oxidase by physisorption. Meso-macroporous silica materials prepared by polycondensation of sodium silicate were used to physically ^[80] and chemically adsorb β -galactosidase ^[85,86] and lipases ^[87–89]. Also, lipase was entrapped in solid lipid nanoparticles (SLN; W/O/W

² This subchapter is based on the article: I.-A. Pavel, S. F. Prazeres, G. Montalvo, C. García Ruiz, V. Nicolas, A. Celzard, D. François, L. Canabady-Rochelle, N. Canilho, A. Pasc (2017). "Effect of Meso vs Macro Size of Hierarchical Porous Silica on the Adsorption and Activity of Immobilized β -Galactosidase" *Langmuir*, 33(13), 3333–3340. <https://doi.org/10.1021/acs.langmuir.7b00134> ^[129]

type) covered by a meso-macroporous silica shell ^[90] or covalently attached to a silica foam ^[91]. The fish-in-net technique was used to entrap various enzymes (umarase, trypsin, lipase, and porcine liver esterase) inside the macroporous cages while the mesopores provided a path for the diffusion of reactants ^[92]. Using this technique, β -galactosidase and lysozyme were co-immobilized to prevent bacterial contamination of the silica matrix in the industrial production of low lactose milk dairy ^[93]. Macro-mesoporous silica spheres prepared with a micro-device were used as a support for penicillin G acylase that was covalently attached through grafted aminopropyl and glutaraldehyde chemical groups ^[94]. Recently, catalase was used to prove the efficiency of hierarchical macro/mesoporous amino-grafted silica spheres as enzyme carriers ^[95].

In the present study, β -galactosidase (β -Gal) from *Kluyveromices lactis* was immobilized into hierarchical meso-macroporous silica by physical adsorption. The enzyme adsorption pathway was investigated as a function of pore size and related to the specific activity measured for the loaded silica material.

3.1.2. Morphology and texture of bare and enzyme-loaded silica supports

The meso-macroporous silica supports were obtained through a dual templating mechanism, as detailed in Chapter 2. But briefly, the material preparation combined Solid Lipid Nanoparticles (SLN) and micelles formed by a Pluronic® block-copolymer surfactant used as templates for macropores and mesopores, respectively. The solid lipid nanoparticles were of approximately 200 nm in diameter as shown by the size distribution graph determined by dynamic light scattering (DLS) and presented on Figure 3. 1. The morphology of the meso-macroporous silica was analyzed by transmission electron microscopy (TEM).

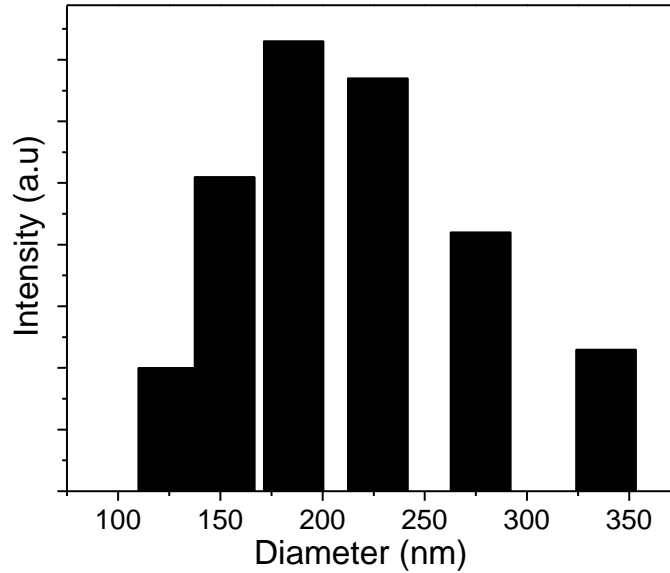


Figure 3. 1. Size distribution of SLN obtained from DLS.

TEM micrographs (Figure 3. 2) made on the silica support clearly show a dual meso-macroporosity where the mesoporosity induced by the non-ionic surfactant is imprinted in the walls of the SLN-templated macropores. This results are in agreement with our lab previous publications ^[90,96–98].

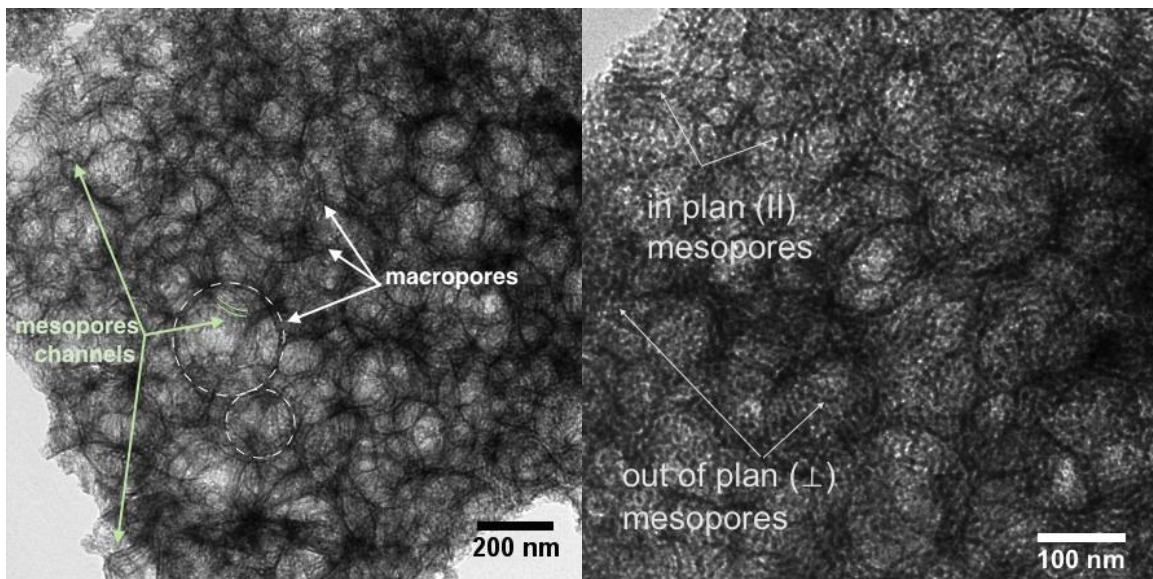


Figure 3. 2. TEM pictures of bare silica material showing the mesopores network interconnecting with macroporous walls.

In agreement with TEM micrographs, the SAXS pattern of the bare SiO₂ material presented in Figure 3. 3 confirmed the worm-like arrangement of mesopores with an average periodic Bragg distance (d_{Bragg}) of 12.4 nm. Similar pore structure where previous obtained in our lab [90,97]. As for the enzyme-loaded silica, the intensity of the diffusion peaks decreased with the increase of the concentration of the feed solution from 1.25 to 12.50 mg·mL⁻¹. As a matter of fact, when the mesoporosity is filled with organic molecules the scattering contrast consecutively decreases. This progressive extinction of the Bragg peak stopped defining the sample prepared at an enzyme concentration of 25.00 mg mL⁻¹, meaning that the corresponding material contained less β -Gal.

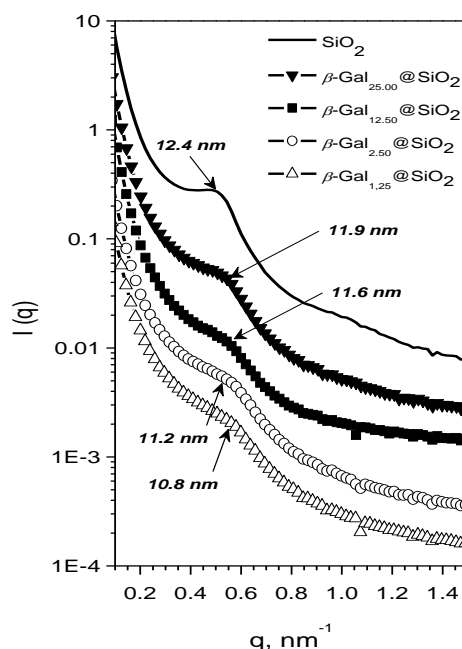


Figure 3. 3. SAXS patterns of the bare and enzyme-loaded meso-macroporous silica support materials.

Nitrogen sorption measurements were performed on bare and enzyme-loaded silica materials as shown in Figure 3. 4. Bare silica exhibited a type IV isotherm, characteristic of a mesoporous material (Appendix 1). However, at high relative pressure (p/p_0 around 0.9), a steep increase of the values of adsorbed volume was observed, suggesting the presence of macropores and/or interparticular spaces. The pore size distribution obtained by the BJH method applied to the adsorption branch of the isotherm evidenced that the average mesopore size (\emptyset) was 9 nm for the bare silica. Moreover,

the specific surface area (S_{BET}) and the pore volume (V_p) of the meso-macroporous bare material (SiO_2) were around $660 \text{ m}^2.\text{g}^{-1}$ and $1.23 \text{ cm}^3.\text{g}^{-1}$, respectively (see Table 3. 1).

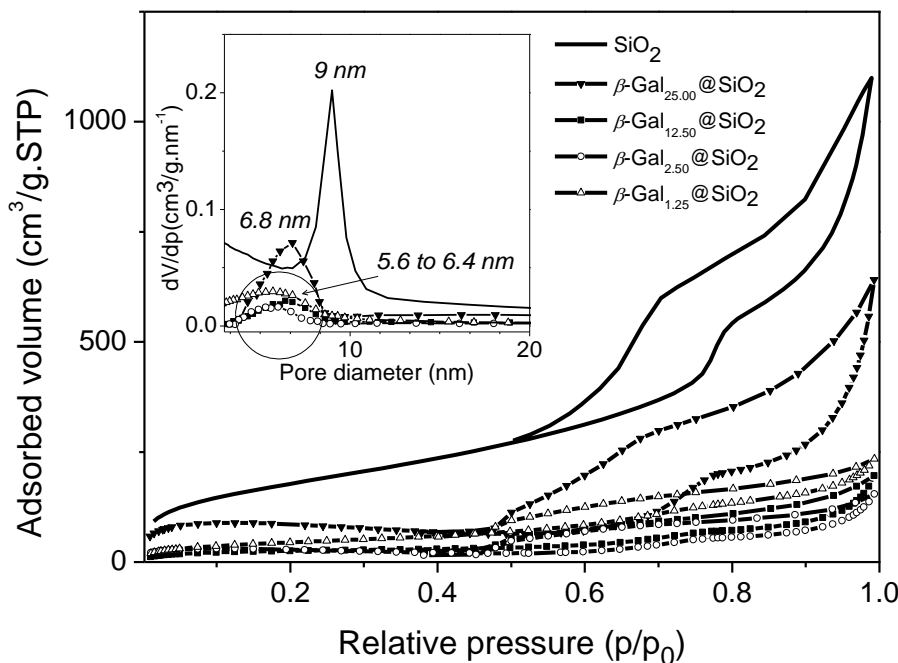


Figure 3. 4. N_2 adsorption-desorption isotherms and corresponding pore size distributions.

As expected, sorption data revealed that the values of S_{BET} , V_p and pore diameter of the $\beta\text{-Gal}$ -loaded silica materials dramatically decreased with respect to bare silica. Upon increasing the initial concentration of the feed solution from 1.25 to 12.50 $\text{mg}.\text{mL}^{-1}$, the specific surface area still decreased from $166 \text{ m}^2.\text{g}^{-1}$ (for $\beta\text{-Gal}_{1.25}@\text{SiO}_2$) to a threshold value of $85 \text{ m}^2.\text{g}^{-1}$ on average (for $\beta\text{-Gal}_{2.50}@\text{SiO}_2$ and $\beta\text{-Gal}_{12.50}@\text{SiO}_2$). Likewise, for the same range of concentration, the pore volume values dropped by half from $0.26 \text{ cm}^3.\text{g}^{-1}$ to a minimum average of $0.14 \text{ cm}^3.\text{g}^{-1}$ while the pore diameter only slightly decreased, from 6.4 to 5.6 nm. This evolution of the texture parameters indicates that, in the dilute regime, the enzyme uptake of the mesopores increased with the concentration of the feed solution. However, the material prepared with the most concentrated solution of $25.00 \text{ mg}.\text{mL}^{-1}$, $\beta\text{-Gal}_{25.00}@\text{SiO}_2$, presented significantly higher pore texture parameters with S_{BET} , V_p , and Ø of $239 \text{ m}^2.\text{g}^{-1}$, $0.52 \text{ cm}^3.\text{g}^{-1}$ and 6.8 nm, respectively. Those values remained lower than the ones of the bare silica, indicating that the enzyme was still physisorbed in the mesopores, but less than in the materials prepared with lower concentrations of enzyme.

A quantitative estimation of the variation of the silica wall thickness (ϵ) was made, by subtracting the pore diameters of each sample from the d_{Bragg} distances (see Table 3. 1). A net thickening of the material wall (from 3.4 to 5.9 nm) was observed as soon as the bare material was loaded with a diluted feed solution, 1.25 mg.mL⁻¹ to 12.50 mg.mL⁻¹. Then, just like for the other texture parameters, ϵ also decreased to 4.4 nm in the case of β -Gal_{25.00}@SiO₂ sample, indicating again a lower uptake of the enzyme in the mesopores when using higher enzyme feed solutions.

Table 3. 1. Parameters of bare and β -Gal-loaded meso-macroporous silica supports obtained from SAXS, nitrogen adsorption and thermogravimetric analysis. ^aBragg distance determined by SAXS, ^bS_{BET}: specific surface area calculated from BET theory, ^cV_p: pore volume, ^d \varnothing : pore diameter, ϵ^e wall thickness ($\epsilon = d_{\text{Bragg}} - \varnothing$), ^fmass ratio, ^gInfrared band area ratio, ^gA_{amide}:A_{SiO₂}: ratio of ATR peak areas.

	SAXS		N ₂ adsorption		ϵ^e (nm)	TGA	ATR
	d _{Bragg} ^a (nm)	S _{BET} ^b (m ² g ⁻¹)	V _p ^c (cm ³ g ⁻¹)	\varnothing^d (nm)		m _{β-Gal} : m _{SiO₂} ^f (loading, wt%)	A _{amide} :A _{SiO₂} ^g
SiO ₂	12.4	657	1.23	9	3.4	0	0
β -Gal _{1.25} @SiO ₂	10.8	166	0.26	6.4	5.1	1.17 (54)	0.11
β -Gal _{2.50} @SiO ₂	11.2	80	0.12	5.6	5.6	1.45 (59)	0.15
β -Gal _{12.50} @SiO ₂	11.6	90	0.17	5.7	5.9	1.55 (61)	0.13
β -Gal _{25.00} @SiO ₂	11.9	239	0.52	6.8	4.4	0.84 (45)	0.05

N₂ adsorption measurements can only provide information on the enzyme presence in the mesopores. To get more information on the total enzyme loading in both mesopores and macropores, thermogravimetric analysis was performed (Figure 3. 5). The respective enzyme loading for each sample is presented in Table 3. 1. It should be noted that the values of the β -Gal loading into those meso-macroporous silica materials are rather high compared to the one in organic resins [99] or hybrid materials [100]. The evolution of the loading values was in line with the trends previously observed by nitrogen sorption analysis and SAXS. Indeed, the β -Gal loading increased progressively in our case from 54 to 61 wt.% when the concentration of the enzyme solution increased from

1.25 to 12.50 mg.mL⁻¹. But when enzyme adsorption was carried out at the highest concentration (25 mg.mL⁻¹), β -Gal loading decreased down to 45 wt.%.

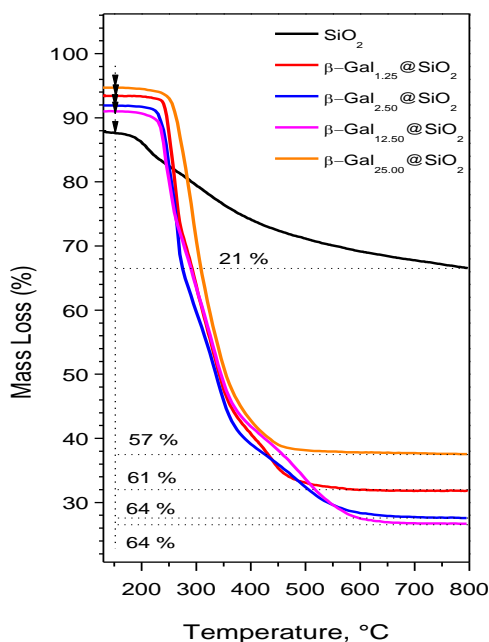


Figure 3. 5. Thermogravimetry results of bare and loaded silica meso-macroporous materials in air.

3.1.3. Interaction of β -galactosidase with the meso-macroporous material

In order to investigate the interaction of the enzyme with the meso-macroporous silica material, zeta-potential measurements and ATR-FTIR analysis were performed. Zeta-potential measurements of bare and enzyme-loaded silica materials were carried out in water at different pH values. Figure 3. 6 shows that the zeta-potential of the modified materials increased with the concentration of enzyme. At lower concentrations, the isoelectric point (pI) of the modified materials β -Gal_{1.25}@SiO₂ and β -Gal_{2.50}@SiO₂ was close to the pI of the bare silica material (2.5-3.0) and this might be explained by the presence of the enzyme mostly inside the silica mesoporous material. Indeed, no significant changes in the values of the zeta potential are observed meaning that the enzyme was not adsorbed on the external surface of the material. At higher concentrations, the pI of the modified materials β -Gal_{12.50}@SiO₂ and β -Gal_{25.00}@SiO₂ increased to 4.2-4.5, *i.e.*, close to pI of the free enzyme, 5.42 [101]. Therefore, it is

reasonable to assume that the enzyme progressively filled the mesopores and then the macropores of the silica material.

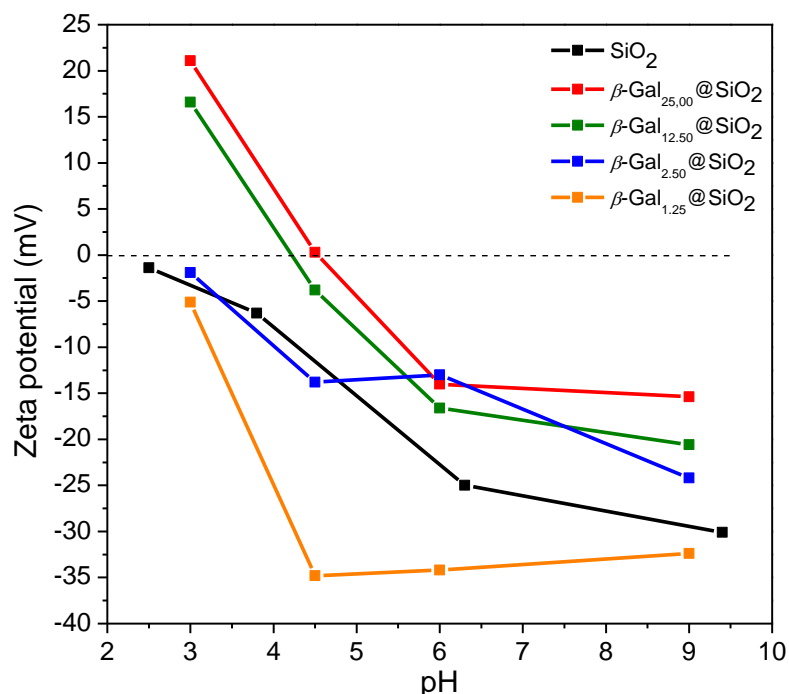


Figure 3. 6. Zeta-potential measurements for the bare and the enzyme-loaded meso-macroporous silica.

On another hand, infrared experiments were carried out and the spectra are presented in

Figure 3. 7, without any correction. ATR-FTIR spectra of the bare material shows the typical bands of silica at 1065, 960 and 800 cm^{-1} , corresponding to Si-O-Si and Si-OH stretching vibrations [102]. After enzyme immobilization, the spectra exhibited a slight displacement of these bands (from 1065 to 1053 cm^{-1} and from 960 to 956 cm^{-1} , respectively), which can be attributed to the interactions between the enzyme and the silica support. The band at 1651 cm^{-1} (C=O stretching vibration) is characteristic of the amide I, whereas the band at 1535 cm^{-1} (N-H bending vibrations) is representative of the amide II. These bands are the consequence of the immobilization of β -Gal on the meso-macroporous silica by physical adsorption. In fact, other researchers have used these bands to characterize the presence of the enzyme adsorbed on the support [103]. All the spectra, including bare silica, showed some broad bands at around 2900 cm^{-1} , characteristic of C-H vibrations and related to the presence of the surfactant (Pluronic®

P123), which was not completely removed after the Soxhlet extraction process. Indeed, thermogravimetric analysis of the bare silica evidenced a mass loss of almost 21 wt.% that corresponds to the remaining surfactant (Figure 3. 5). In agreement with the results obtained by TGA for the enzyme-loaded materials, one can also observe that the area ratios of the characteristic amide/silica bands (1651 cm^{-1} and 1058 cm^{-1} , respectively) followed the same trend as a function of the enzyme concentration in the feed solution (Table 3. 1). When using diluted solutions to immobilize the enzyme inside the meso-macroporous silica material, the loading rate increased with the concentration from 1.25 to 2.50 mg mL^{-1} , and remained constant when increasing further the initial concentration of enzyme to 12.50 mg.mL^{-1} . Interestingly, when directly immobilizing the enzyme from the stock solution at 25 mg.mL^{-1} , the amount of encapsulated enzyme was lower. Thus, a selective adsorption occurred during the loading of the meso-macroporous silica material: (1) for diluted feed solution, the enzyme is preferentially physisorbed into mesopores and the loading rate is rather high (54-61 wt.%) and (2) for a concentrated feed solution, more enzyme located into macropores but the loading rate is smaller (45 wt.%).

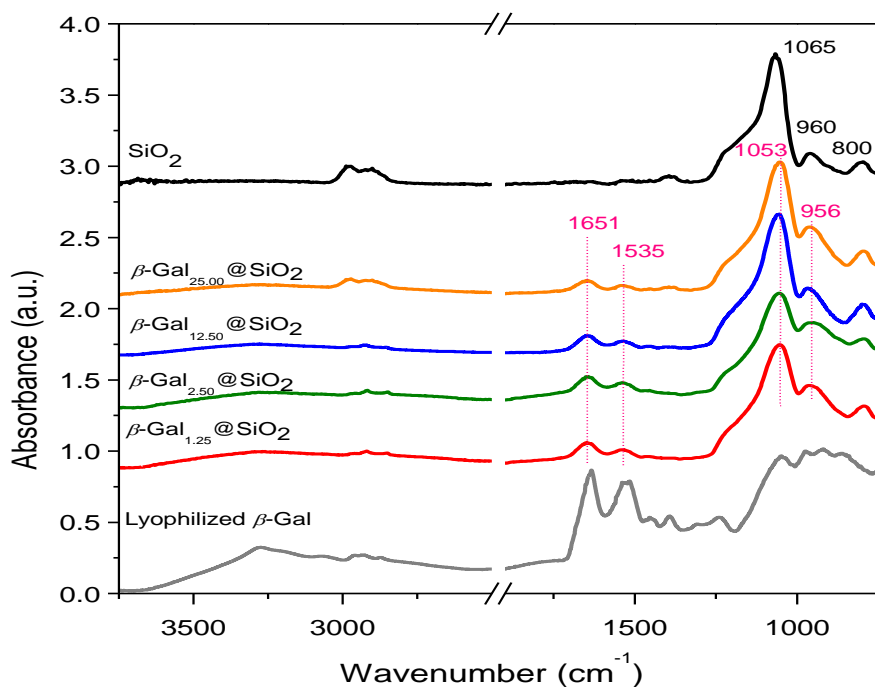


Figure 3. 7. ATR-FTIR spectra of dried enzyme, bare silica, and meso-macroporous silica materials prepared at different feed solution concentrations.

In order to rationalize the physisorption mechanism of the enzyme into the meso-macroporous silica materials, the structure and the morphology of the enzyme was further considered. Using the molecular visualization program VMD^[104], amino-acid distribution and geometrical sizes of β -Gal oligomers from *Kluyveromyces lactis* have been analysed based on the crystal structure reported previously by Pereira-Rodríguez et al. ^[105,106]. Briefly, β -Gal forms a homo-oligomer of four subunits (A–B–C–D) that can be described as a dimer of dimers. Each chain consists of 1024 residues with a molecular mass of 119 kDa. Monomers A–C and B–D form two identical dimers. The assembly of these dimers essentially occurs through interactions between monomers A and B, although there are also some contacts between monomers A and D, and monomers B and C that help stabilizing the tetramer. The dimer interfaces involve a significant proportion of hydrophobic interactions, whereas the tetramer interface results mostly from interactions between polar and/or charged residues (see Figure 3. 8). As a consequence, the energy for dissociating the tetrameric assembly into two dimers is much lower ($\sim 6 \text{ kcal.mol}^{-1}$) than the energy required to dissociate the dimer into two monomers ($\sim 20 \text{ kcal.mol}^{-1}$) ^[107]. In standard conditions, dimers and tetramers can definitely coexist and both exhibit an equal enzymatic activity^[108]. The presence of silica can however displace the equilibrium between the two structural organizations.

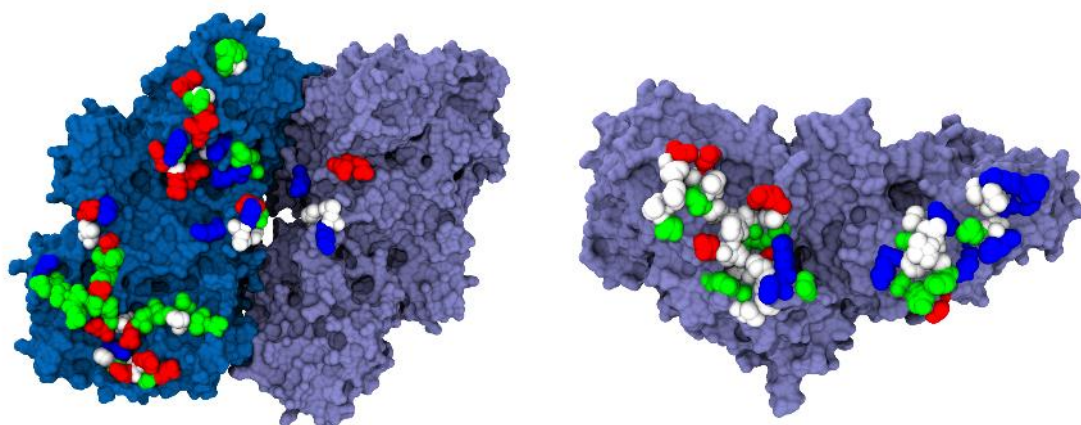


Figure 3. 8. (left) Residues of β -Gal dimer involved in the tetramerization interface and (right) residues of β -Gal monomer involved in the dimerization interface. Hydrophobic, polar, acidic and basic interfacial residues are colored in white, green, red and blue, respectively.

The planar surfaces of the tetramer expose an excess of positively charged residues (~81 basic vs 73 acidic residues), as shown in Figure 3. 9. Upon dissociation of the tetramer into two dimers, the solvent accessible surface area increases by 11% per dimer, and the number of accessible positively charged residues also steps-up. Thus, in the presence of negatively charged silanol groups, the equilibrium between the two oligomeric organizations is prone to be displaced toward the dimer.

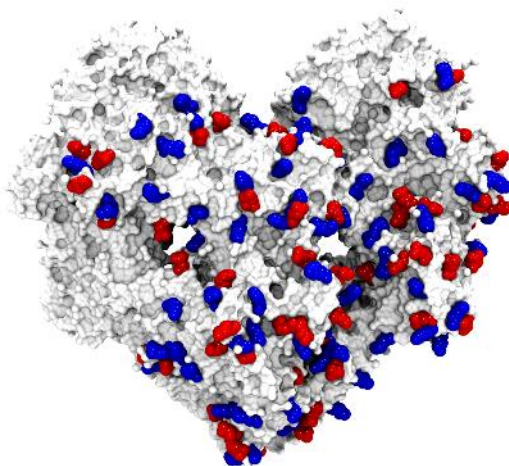


Figure 3. 9. Acidic (red) and basic (blue) surface residues of β -Gal tetramer. Only residues having a surface accessible solvent area (calculated with a probe sphere radius of 0.14 nm) larger than 0.5 nm² are represented.

Spatial extension of β -Gal *Kluyveromyces lactis* was inferred from the crystal structure of the tetramer (PDB 3OBA). Figure 3. 10, Figure 3. 11 and Figure 3. 12 show that the tetramer, the dimer and the monomer can be contained in boxes of dimensions 15.1 nm \times 17.1 nm \times 10.7 nm, 11.9 nm \times 15.6 nm \times 7.2 nm, and 7.2 nm \times 11.7 nm \times 6.3 nm respectively. Size-wise, only the monomer and the dimer are susceptible to migrate into the mesopores of the hybrid silica material (measured average diameter of 9 nm), while the bulkier tetramer can only be physisorbed in macropores. Therefore, the following mechanism of the physisorption of the enzyme in the meso-macroporous silica material can be postulated: at low enzyme concentration, silica mesopores are progressively filled when increasing the concentration of the feed solution (from 1.25 to 12.50 mg.mL⁻¹) with active dimers.

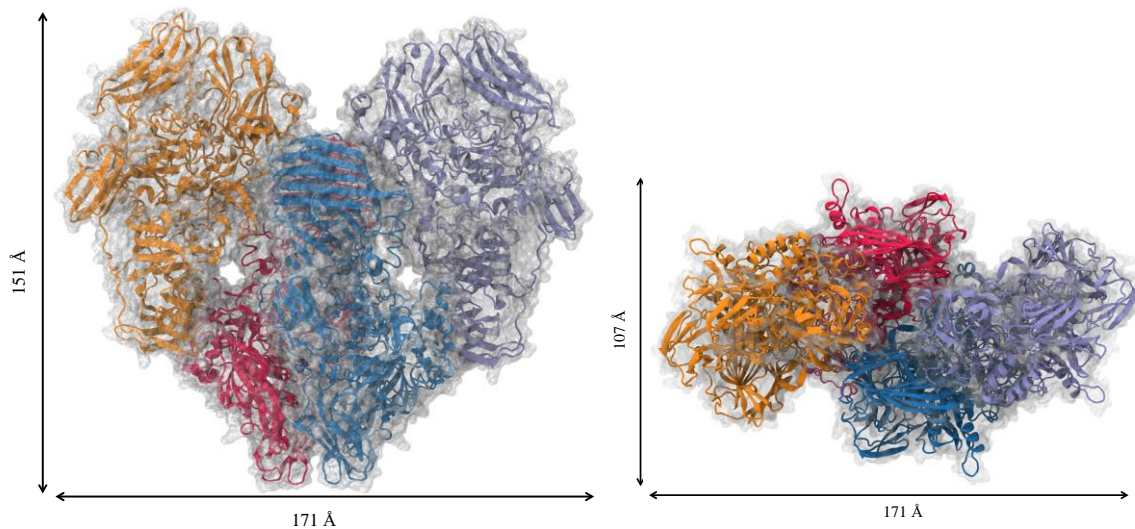


Figure 3. 10. (Left) Front and (right) side views of X-ray crystal structure of β -Gal tetramer (PDB 3OBA).

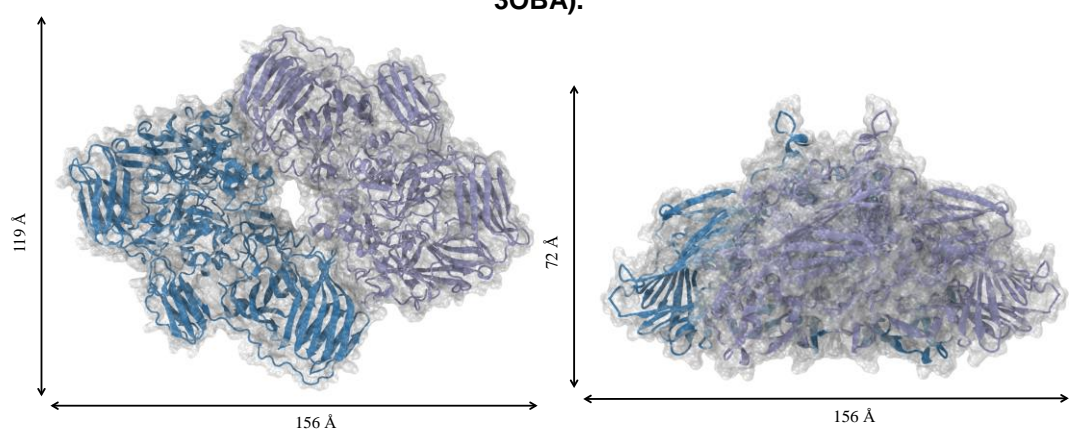


Figure 3. 11. (Left) Front and (right) side views of X-ray crystal structure of β -Gal dimer (PDB 3OBA).

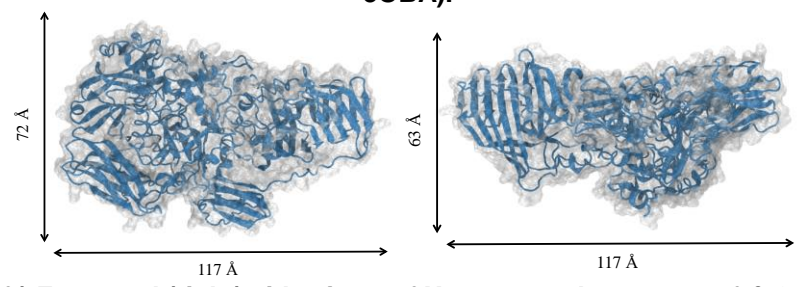


Figure 3. 12. (Left) Front and (right) side views of X-ray crystal structure of β -Gal monomer (PDB 3OBA).

However, when the feed solution reaches 25.00 mg.mL^{-1} , protein interactions leading to aggregation become important enough to limit or block the diffusion of the enzyme dimers in mesopores consistently with the lower uploading rate observed at high initial concentrations of the (Figure 3. 14)

3.1.4. Activity of free and immobilized enzyme into meso-macroporous silica materials

The enzyme activity was determined spectrophotometrically as detailed in Chapter 2. In the investigated range of concentration, the activity of free β -Gal from *Kluyveromyces lactis* was independent of the enzyme concentration. Such an effect may be explained by both the absence of association and dissociation processes and by the specific activities of various oligomers at equilibrium being identical to each other. This behavior was already observed with β -Gal from *Penicillium canescens* fungi, which also showed an equilibrium between monomers/dimers and tetramers, the active forms being dimers and tetramers [109]. The calculated specific activity of β -Gal was 104 U.mg⁻¹ of enzyme (see Figure 3. 13).

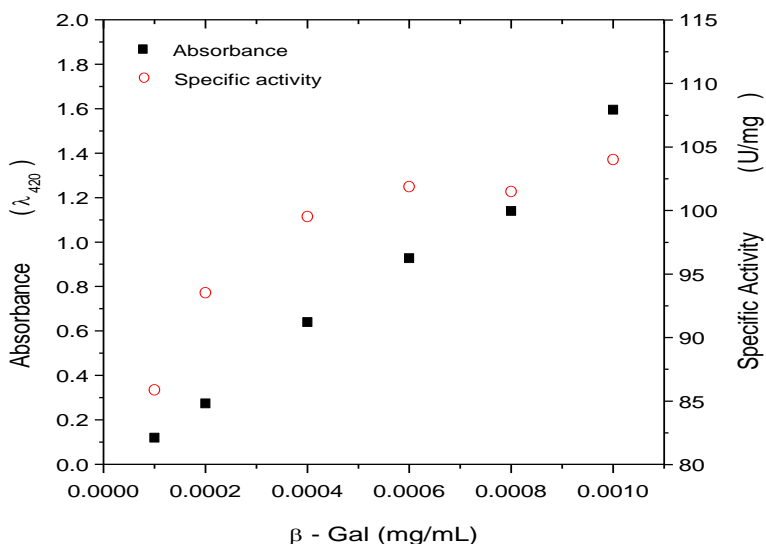


Figure 3. 13. Specific activity of the enzyme (red) and corresponding absorbance of ONP at 420 nm (black).

Upon physisorption in the meso-macroporous material, the enzyme specific activity depended on its location within the pores. When the enzyme was preferentially adsorbed (as dimers) in the mesopores, the specific activity increased with the increase of loading degree (Figure 3. 14). This behavior is often encountered for enzymes adsorbed within mesopores [110]. More interestingly, the specific activity of the enzyme physisorbed in the macropores was two times higher than that of the enzyme entrapped

into mesopores. This might be due not only to the adsorption phenomenon but also to the increased release of the substrate.

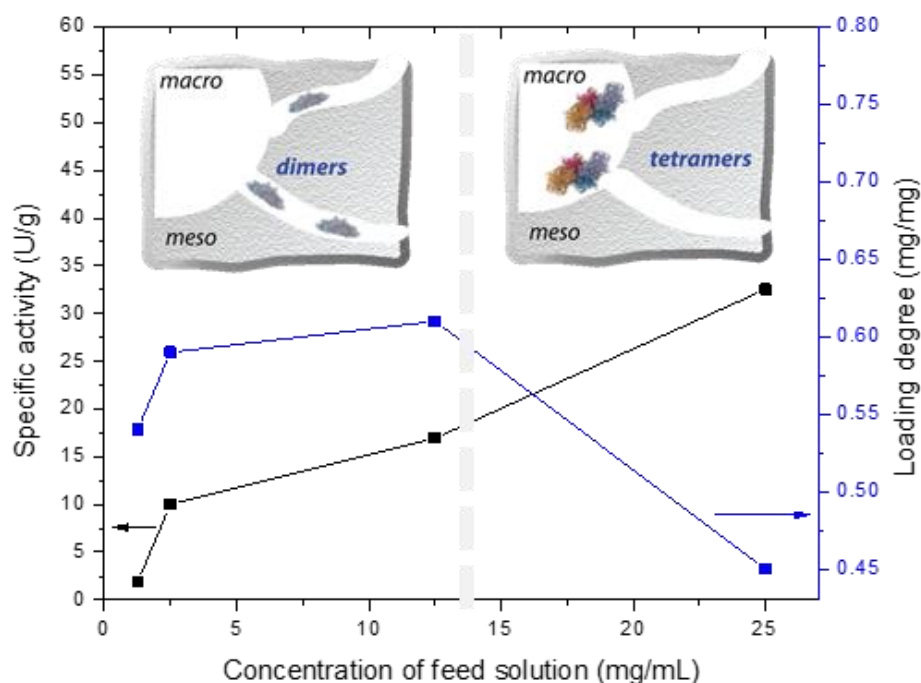


Figure 3. 14. Evolution of the specific activity and loading degree showing the preferential adsorption of the enzyme either in mesopores (meso) or in macropores (macro), depending on the initial concentration.

3.1.5. Conclusion

β -Gal from *Kluyveromyces lactis* was immobilized into hierarchical macro/mesoporous silica by physical adsorption. The support was obtained by a cooperative templating mechanism, using Pluronic® P123 micelles as porogen of mesopores on one hand, and a transcription mechanism using solid lipid nanoparticles templating macropores on the other hand. The enzyme was a tetramer, *i.e.*, a dimer of dimers with low dissociation energy in solution. The adsorption of enzyme at low concentrations in water took place preferentially in the mesopores as dimers or monomers, while the tetrameric form was adsorbed in the macropores. The enzyme immobilized in the macropores showed a higher specific activity than the one immobilized in the mesopores. Beyond food application, designed materials are of particular interest to bioconversion, bioremediation or biosensing when coupling the designed support with other enzymes.

3.2 Silica-coated liposomes for β -galactosidase delivery

The first time that mesoporous silica nanoparticles were studied as drug delivery system was in 2001 [111]. Since then, mesoporous silica nanoparticles have been widely involved in the elaboration of biomedical applications [112]. Drug delivery and bio-imaging are topics in which the use of amorphous silica is becoming popular especially because of its high drug uptake capacity. Furthermore, amorphous silica was recognized as safe by FDA [113] and authorized as an additive in Europe [114]. Particle size, shape, surface area and structure of the pores play apparently a role in biocompatibility and biotranslocation [112].

However, biocompatibility is mainly influenced by the surface properties of the solid carrier. In the case of silica materials, the silanol groups exposed on the surface can interact, denature or destroy the structure of biological molecules (cellular membrane lipids and proteins) [115]. Thus, to improve the biocompatibility and to increase the *in vivo* circulation time, the surface of the silica can be functionalized with different chemical groups, modified by polyethylene glycols (PEGs) or coated with a lipid layer [116] according to the intended medical application.

Comparing bare and lipid-coated silica nanoparticles in mice, Van Schooneveld et al. [117] observed a 10-fold improvement of biocompatibility and half-lives of blood circulation of silica. For this, a variety of therapeutic agents were encapsulated in silica-coated lipid. KLA pro-apoptotic peptide, a programmed cell death-inducing peptide used for cancer treatment, was encapsulated in mesoporous silica nanoparticles modified with dipalmitoyl phosphatidylcholine (DPPC), PEG-grafted distearoyl phosphatidylethanolamine (DSPE-PEG2000) and cholesterol lipid bilayer [118]. In oncology therapy, axitinib and celastrol [119], gemcitabine and paclitaxel [120] were co-delivered from a lipid bilayer-supported mesoporous silica nanoparticles in multi-targeted cancer therapy and pancreatic cancer, respectively. Stimuli responsive carriers have also been investigated to treat multidrug resistance [121] and cancer [122]. For example, hybrid lipid stimuli-responsive mesoporous silica nanoparticles were prepared to release doxorubicin or to carry anti-EGFR antibodies to target individual leukemia cells [123].

In the present work, β -galactosidase from *Kluyvermyces Lactis* was immobilized into low porosity silica particles by physical adsorption and coated with a pH responsive 1,2-dioleoyl-sn-glycero-3-phosphocholine (DOPC) phospholipid bilayer. As shown in the previous chapter the presynthesized meso-macroporous silica presents a bulk morphology. In order to be able to fulfill the mouth feel requirements ($< 25 \mu\text{m}$), we choose an industrial available silica, KROMASIL[®] 300-10-SIL. The adsorption and release of the enzyme was investigated *in vitro* under simulated gastrointestinal fluids.

3.2.2. Characterization of bare and enzyme-loaded silica

The morphology and structure of a commercial bare KROMASIL[®] 300-10-SIL silica particles were assessed by Scanning electron microscopy (SEM).

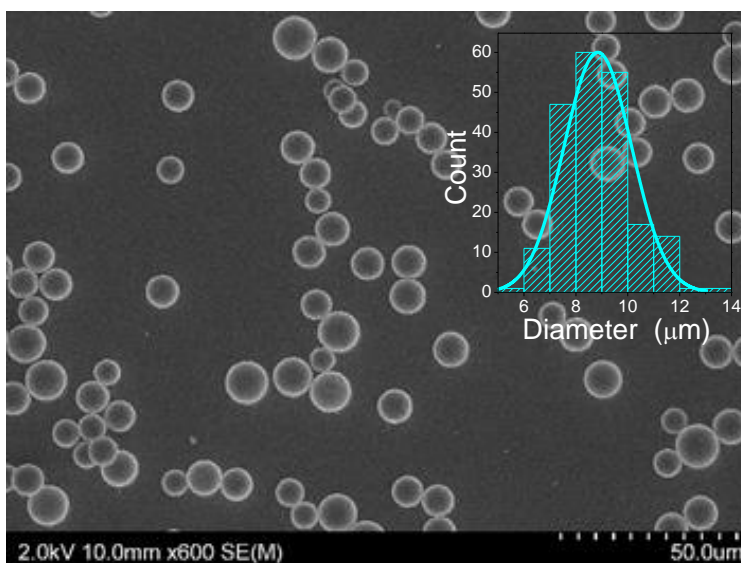


Figure 3. 15. SEM micrographs of bare silica (SP), and Size distribution of the micro-particles determined from SEM pictures.

The particles have a spherical shape with a size of $9 \pm 1 \mu\text{m}$ as determined from SEM micrographs measurements (Figure 3. 15).

Nitrogen sorption measurements were performed on bare particles (SP) and enzyme-loaded silica materials (ESP) as shown in Figure 3. 16. Bare silica exhibited a type II isotherm, with a hysteresis loop type H3, associated with the capillary condensation of the N_2 and is characteristic to the mesoporous materials with slit-shaped pores [124]. The pore size distribution obtained by the Dubinin–Radushkevich calculation

method evidenced that the bare silica material exhibits microporosity ($\varnothing < 2$ nm) and mesoporosity (average mesopore size of 25 nm). Moreover, the specific surface area (S_{BET}) and the pore volume (V_p) of the bare material were small, around $66 \text{ m}^2 \cdot \text{g}^{-1}$ and $0.33 \text{ cm}^3 \cdot \text{g}^{-1}$, respectively (see Table 3. 2). The total pore volume, $V_{0.97}$, was calculated from nitrogen adsorption at a relative pressure of 0.97. These data reveal that the micrometric silica particles have a rather low porosity. Compared with the bare silica, the β -Gal-loaded silica (ESP) have lower textural parameters values (S_{BET} , V_p and pore diameter). In fact, as summarize in Table 3. 2, the specific surface area decreased from $66 \text{ m}^2 \cdot \text{g}^{-1}$ to $15 \text{ m}^2 \cdot \text{g}^{-1}$, the volume pore (\varnothing) decreased from $0.33 \text{ cm}^3 \cdot \text{g}^{-1}$ to $0.05 \text{ cm}^3 \cdot \text{g}^{-1}$ while the mesopore diameter decreased from 25.1 to 21.5 nm. This, and the fact that the intensity of the pore size distribution significantly decrease, is an indication that the enzyme adsorbed is uptake by the mesopores and is also onto the surface of silica particles blocking the micropores.

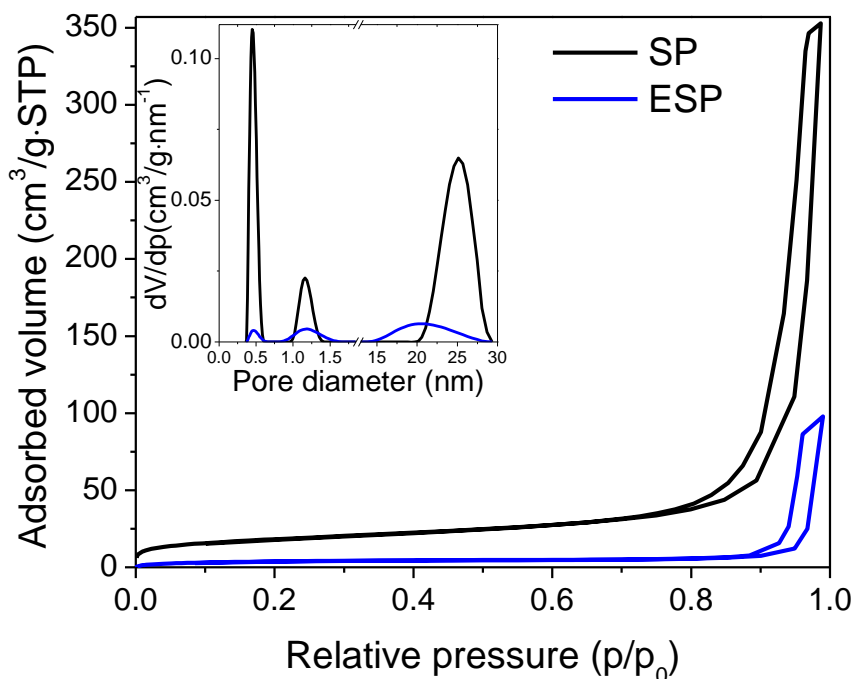


Figure 3. 16. N₂ adsorption-desorption isotherms and corresponding pore size distributions.

Table 3. 2. Summary of the textural parameters of bare (SP) and β -Gal-loaded (ESP) porous silica support obtained from nitrogen adsorption and mass loss in % obtained by TGA.

	SP	ESP
S_{BET} (m ² /g)	66	15
$V_{0.97}$ (cm ³ /g)	0.33	0.05
\emptyset (nm)	0.4/1.1/25.1	0.4/1.1/21.5
Mass loss (%)	4.1	37.5

In addition, the total enzyme loaded on the silica support was determined by UV-vis spectrophotometry, using the principle of mass conservation. The total amount of enzyme used for immobilization is equal to the cumulative amount of immobilized lactase on the silica material and the quantity remaining in the supernatant and in the washing solution. The washing water and the supernatant solutions were analyzed using the protein BCA assay method. This method provides a quantitative response of the enzyme in UV-vis spectrophotometry. The protein quantity was determined for each solution and deducted from the initial amount, thus obtaining the immobilized enzyme quantity. The calculation was performed using the Equation 3. 1:

$$\beta - Gal_{immobilized} = V_i \cdot [\beta - Gal]_i - (V_s \cdot [\beta - Gal]_s + V_{ww} \cdot [\beta - Gal]_{ww})$$

Equation 3. 1. Determination of the quantity of immobilized enzyme on SEP.

with :

- β -Gal_{immobilized}: quantity of immobilized enzyme (mg)
- V_i : volume of the initial enzyme solution (ml)
- $[\beta$ -Gal]_i: concentration of the initial enzyme solution (mg/ml)
- V_s : volume of the supernatant (ml)
- $[\beta$ -Gal]_s : enzyme concentration in the supernatant (mg/ml)
- $V_{w.w}$: volume of the washing water (ml)
- $[\beta$ -Gal]_{w.w} : enzyme concentration in washing water (mg/ml)

The amount of enzyme adsorbed on silica material was calculated at 7.5 mg enzyme/g of silica support, and the value was determined by dividing the quantity of immobilized enzyme by the quantity of silica used for the immobilization.

The immobilization yield is calculated using the following formula:

$$Yield (\%) = 100 \frac{C_i - (C_s + C_{ww})}{C_i}$$

Equation 3. 2 Calculation of immobilization yield.

where C_i is the concentration of enzyme in the immobilization solution, C_s and C_{ww} are the enzyme concentration in the supernatant and in the washing solution, respectively. The enzyme adsorption yield was calculated at $34.8 \pm 4.3\%$

Thermogravimetric analysis (TGA) was also used to quantify the amount of enzyme adsorbed on the silica material (Figure 3. 17 and Table 3.2). Two different mass loss steps were detected in the curve thermogravimetric curve obtained for the loaded silica. The first step of mass lost occurring from room temperature (RT) to 100°C can be associated with the evaporation of physically adsorbed water molecules on the loaded silica surface [125]. This phenomenon is also present in the unmodified inorganic particles (analyzed as received without further modification). A second mass loss step is detected between 100 and 450°C for the sample ESP and it corresponds to around 33% of weight loss of the total sample. This value indicates that the loaded silica bears 330 mg of organic matter per g of silica and is much higher than the amount calculated previously by the UV-vis spectrophotometric method (7.5 mg enzyme/g silica support). This can lead to the conclusion that beside enzyme, other organic species were absorbed onto the silica, probably glycerol. The source of the glycerol is the solution in which the enzyme is formulated. Its presence in the materials has a positive aspect, since the glycerol is known for protecting the enzyme against external factors that can inactivate the β -Galactosidase enzyme [126]. This can also ensure that the enzyme does not lose its activity during the absorption and the formation of the 1,2-dioleoyl-sn-glycero-3-phosphocholine (DOPC) liposomes double layer.

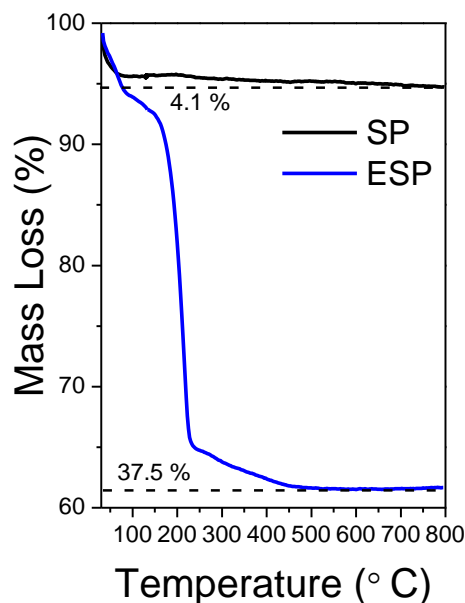


Figure 3. 17. Mass loss determined by thermogravimetric analysis made on bare (SP) and loaded silica materials (ESP) in air.

3.2.3. Characterization of liposomes coated silica particles (LCSP)

After enzyme loading, silica particles were incubated with the 1,2-dioleoyl-sn-glycero-3-phosphocholine (DOPC) lipids, resulting in the liposome-coated silica particles (LCSP), following the procedure described in Chapter 2. The presence of lipids on the surface of resulting LCSP material was confirmed by fluorescence microscopy in presence of a fluorescent dye (Texas Red).

The fluorescent microscopy experiments were made on the samples in simulated gastric fluid (SGF), simulated intestinal fluid (SIF) and in SIF containing pancreatin enzymes (and, more precisely, a mixture of amylase, lipase and protease). The preparation of stock simulated digestion fluids solutions is presented in Chapter 2. The samples were kept for 2 hours in SGF (Figure 3. 18 A) and 2 hours in SIF (Figure 3. 18 B) prior observation. As presented in Figure 3. 18 A and B, the micrometric silica particles are fluorescent. This is undoubtedly due to the presence of phospholipid bilayer around the particles since the Texas Red dye is only soluble in lipids. In addition, the silica remains covered with the lipid bilayer in SGF as well as in SIF. However, the addition of pancreatin in the SIF leads to the disappearance of fluorescence probably indicating the

removal of the lipid bilayers (Figure 3. 18 C). This experiment evidences the presence of the liposomes around the silica nanoparticles surface.

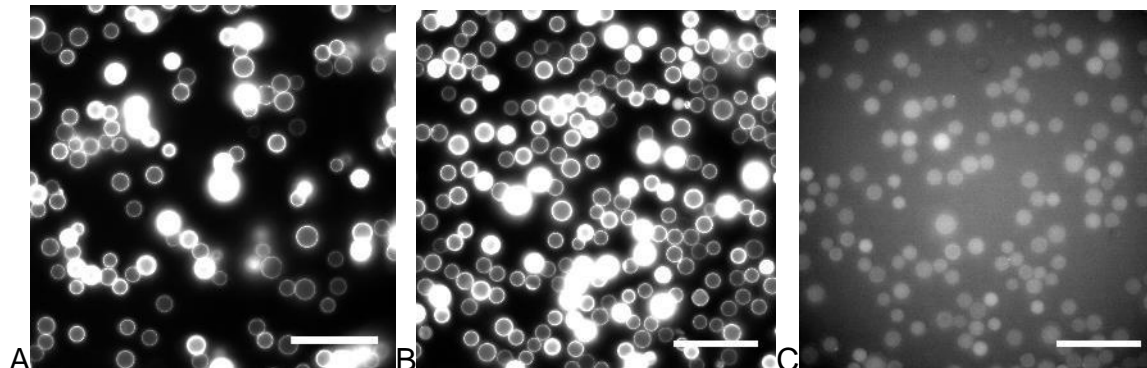


Figure 3. 18. Fluorescence microscopy images obtained for LCSP in SGF (A), SIF (B) and in SIF containing pancreatin (C) (scale bar 50 μm).

3.2.4. Enzyme activity during the immobilization and incubation

The enzyme loaded silica microparticles (ESP) initially described were dried. Approximately 85 mg of ESP were dispersed in 1 ml of TRIS buffer (pH 7.4) containing the liposomes leading to the formation of LCSP material. The liposomes that did not adhere to the surface were removed by washing the LCSP sample 7 times with the buffer. The washing waters were used to determine the quantity of the enzyme that leaked from silica during the incubation. The same principle of mass conservation was applied as in the case of the determination of the amount of enzyme present in the ESP, and the Equation 3. 3 was used.

$$\beta - Gal_{recovered} = \sum_{n=1}^7 V_n [\beta - Gal]_n$$

Equation 3. 3. Determination of the quantity of enzyme leaked from LCSP during incubation.

where $\beta\text{-Gal}_{recovered}$ (mg) is the total amount of the enzyme that was recovered in the washing waters, V_n (ml) is the volume of each washing water with the enzyme concentration $[\beta\text{-Gal}]_n$ (mg/ml)

The total amount of enzyme that was recovered in the washing water (that leaked from ESP) was determined at 0.66 mg of protein/g of silica. Thus, the amount of enzyme adsorbed into LCSP was calculated at 6.8 mg enzyme/g silica, corresponding to the total amount of enzyme immobilized on the ESP material (7.5 mg enzyme/g silica) minus the

amount of enzyme that leaked out of ESP material and minus the one that was recovered in the washing solutions.

It should also be noted that the leaked enzyme has almost the same activity as the enzyme in the initial solution used for immobilization: 5025 U/mg *versus* 5223 U/mg, respectively. The lipid incubation step did not deactivate the enzyme.

The leakage during the incubation with lipids was minimal and the specific activities of the materials were assessed by enzymatic reaction with ONPG. The specific activity of the ESP was determined at 22.4 U/mg of silica material and the activity of LCSP was measured at 10.9 U/mg of silica. The activity of LCSP material was smaller than the activity of ESP material. This was expected, since the coating with the lipid double layer decreases the diffusion of the substrate ONPG from the solution to the surface of silica where the enzyme is absorbed.

3.2.5. Enzyme release

A controlled release of the enzyme out of the uncoated ESP carrier and the lipid covered particle (LCSP), was done *in vitro* in simulated gastric fluid (SGF, pH3) and simulated intestinal fluid (SIF, pH7) as presented in Chapter 2.

In order to simulate the passage of the materials through the gastro- intestinal tract four samples of each material were tested as presented in Table 2. 2. (Chapter 2). Each type of sample underwent four experiments under magnetic stirring at 150 rpm. In the first one, the sample LCSP1 (or ESP1) was kept for 1H in SGF. In the second, the carrier LCSP2 (or ESP2) was kept for 2H in SGF. The third and the four experiments were a successive immersion of the samples LCSP3 (or ESP3) and LCSP4 (or ESP4) in SGF over 2H followed by 1H or 2H in the SIF respectively. The samples LCSP3 (or ESP3) and LCSP4 (or ESP4) from the experiments 3 and 4 have been centrifuged before being added to the SIF. The Figure 3. 19 displays the cumulative quantity of enzyme released *e.g.* after 3H in the simulated gastro-intestinal fluid, the total quantity of enzyme release is the sum of the quantity of enzyme released after 2H in SGF and the quantity of enzyme released after 1H in SIF. The values are given in Figure 3.19 are in weight percentage

(wt.%), which represents the quantity of enzyme release /initial enzyme loading per mg of silica.

A clear difference in release profiles of coated (LCSP) and uncoated (ESP) silica was observed. In SGF (pH 3), after the first hour, only a small quantity of enzyme was released from LCSP 4.6 wt.% compared with 61.2 wt.% for ESP. After 2H in SGF, the enzyme quantity released from LCSP remain 4.6 wt.% and in the case of ESP, the amount remained close to 61.7 wt.%. After 1H in SIF (pH7), the ESP carrier released in total 83.8 wt.% of enzyme that was initially absorbed. In the consecutive 2H in SIF, 96.2 wt.% of the lactase has been released. However, for LCSP, the total amount of enzyme released reached only 6.3 wt.% in the first hour of immersion in SGF and approximately the same amount as in the second hour (7.2 wt.%). According to the results obtained from the consecutive immersion test (experiment 3 and 4), it can be clearly noticed that the amount of released enzyme increased in SIF media. The silica SiO₂-bilayer interactions are controlled by van der Waals forces. At low pH, the 1,2-dioleoyl-sn-glycero-3-phosphocholine (DOPC) bilayer is fused to the surface of silica due to the favorable van der Waals forces ^[127]. As the pH value rises the electrostatic repulsion between the negatively charged silica surface and liposomes increases, and a ~1 nm water layer separates the DOPC bilayer and silica surface.^[128] As it was expected the interactions between the lipid layer and silica changed in SIF pH7 leading to the leak of the enzyme.

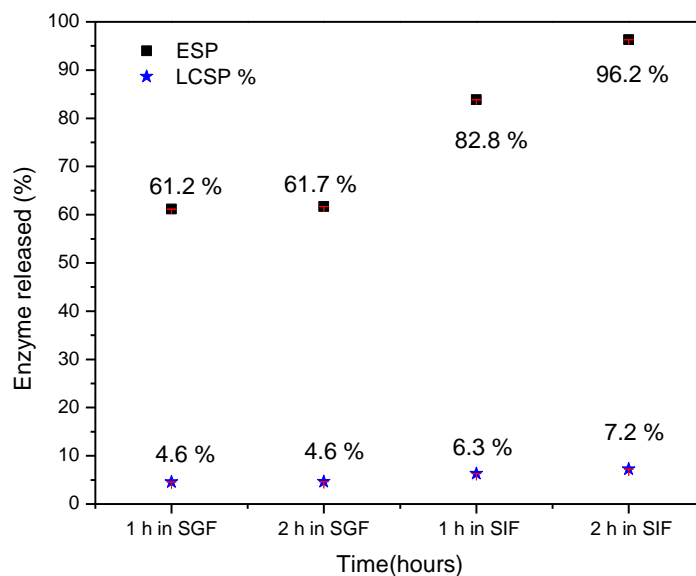


Figure 3. 19. The quantity of the enzyme release from LCSP and ESP in SGF (pH 3) and SIF (pH 7).

In order to verify if the enzyme released during the simulated digestion remains activity, the recovered solutions from *in vitro* in simulated gastric fluid (SGF) and simulated intestinal fluid (SIF) were analyzed. In terms of activity, the enzyme released from ESP and LCSP displays very different behaviors as presented in Figure 3. 20. The enzyme liberated by ESP along the experiments did not present any activity, compared to enzyme recovered from LCSP sample that was still retaining a part of its reactivity when put in SIF. When dispersed in the SIF (pH 7), the enzyme released from LCSP increased its activity progressively: from 64 U/mg in SGF the enzyme activity increased to 236 U/mg after 1H in SIF and to 351 U/mg after 2H in SIF. The conclusion that can be drawn from these results is that the lipid bilayer indeed provides protection against the acidic pH and that it works as a slow release system, which gradually liberates active enzyme.

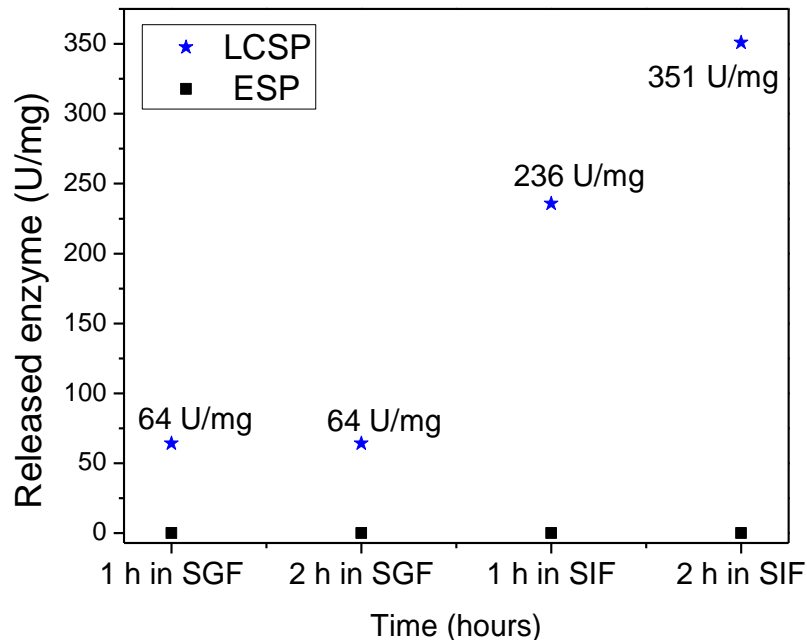


Figure 3. 20. The activity (B) of the enzyme release from LCSP and ESP in SGF (pH 3) and SIF (pH 7).

To confirm that the enzyme retains its activity during the gastric simulation, the specific activities of the materials ESP and LCSP (Figure 3. 21.) were compared with the initial ESP and LCSP. The ESP material retained only a fraction of its original activity when added to the SGF, it decreased over the time, and an insignificant increase was observed in the SIF. The final specific activity for ESP sample was calculated at 0.32 U/mg of silica. The specific activity of the LCSP sample also decreased when added in SGF, but a significant part of specific activity was retained, with a final value of 0.875 U/mg of silica. Although the specific activity variation along the four experiments has the same tendency for both LCSP and ESP catalyst, the presence of DOPC liposomes protects the enzyme from the acidic pH inactivation (SGF at pH3).

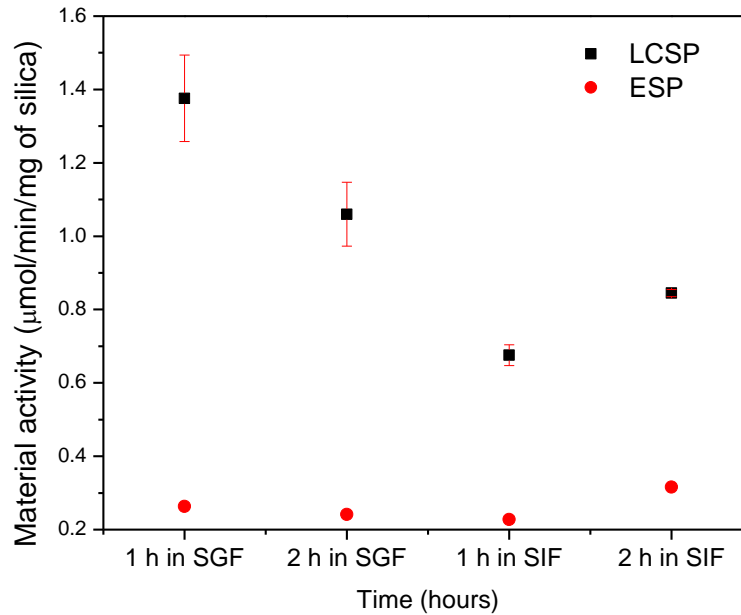


Figure 3. 21. Activity of silica materials used in the simulated gastro-intestinal digestion fluids (SGF and SIF).

3.2.5. Conclusion

β -Gal from *Kluyveromyces lactis* was immobilized into low porosity silica particles by physical adsorption and then coated with DOPC bilayers. This system presented a controlled release pattern over the pH ranges of simulated gastric and intestinal fluids. The presence of liposomes not only provides a controlled release, but also acts as a protective coating from pH inactivation in acidic pH (SGF) for the immobilized enzyme. Compared to the ESP material, LCSP sample preserved much better the activity of the enzyme (0.875 U/mg of silica vs. 0.32U/mg of silica) for a similar initial loading. Moreover, the enzyme immobilized in LCSP had, in the end of the simulated gastro-intestinal digestion experiment, the same behavior as the free enzyme, namely an increase of activity at optimal pH values. The enzyme was not denatured by the long stay in acidic pH. Although the loading in LCSP is slightly smaller than in the ESP material (6.8 vs. 7.5 mg), one can conclude that this type of immobilization could preserve the enzyme until the intestine where the lactase should be released. Thus, LCSP is a promising candidate for the delivery of enzymes, with the guarantee of safely immobilizing the enzyme intact.

The main improvement for the LCSP system that could be envisioned is an increase of its loading capacity. Since the enzyme is quite a large molecule (14 nm), a

more porous type of silica would ensure a larger amount of encapsulated enzyme. This could be achieved in the sol-gel phase, via the insertion of organic molecules. Another direction for further research is the variation of the lipids (or lipid mixtures) used in the production of the liposomes. By changing the composition of the lipids, different permeability to chemical species, in and from the carrier system, can be obtained. This would potentially lead to the tailoring of delivery systems perfectly adapted to specific triggers.

Bibliography

- [1] D. Dale, *Microencapsulation in the Food Industry*, Elsevier, **2014**.
- [2] L. Fjerbaek, K. V. Christensen, B. Norddahl, *Biotechnol. Bioeng.* **2009**, *102*, 1298–1315.
- [3] D. J. Pollard, J. M. Woodley, *Trends Biotechnol.* **2007**, *25*, 66–73.
- [4] H. A. Gulec, *Colloids and Surfaces B-Biointerfaces* **2013**, *104*, 83–90.
- [5] A. M. Klibanov, *Nature* **2001**, *409*, 241–246.
- [6] P. V. Iyer, L. Ananthanarayan, *Process Biochem.* **2008**, *43*, 1019–1032.
- [7] C. Garcia-Galan, Á. Berenguer-Murcia, R. Fernandez-Lafuente, R. C. Rodrigues, *Adv. Synth. Catal.* **2011**, *353*, 2885–2904.
- [8] L. Cao, *Curr. Opin. Chem. Biol.* **2005**, *9*, 217–26.
- [9] K. Hernandez, R. Fernandez-Lafuente, *Enzyme Microb. Technol.* **2011**, *48*, 107–122.
- [10] E. T. Hwang, M. B. Gu, *Eng. Life Sci.* **2013**, *13*, 49–61.
- [11] A. Gupta, K. Prabhu, *J. Gen. Appl. Microbiol.* **1995**, *41*, 399–407.
- [12] H. Y. Kawaguti, P. H. Carvalho, J. A. Figueira, H. Sato, **2011**, *2011*, DOI 10.4061/2011/791269.
- [13] P. M. Kosaka, Y. Kawano, O. A. El Seoud, D. F. S. Petri, **2007**, 12167–12173.
- [14] K. Labus, I. Gancarz, J. Bryjak, *Mater. Sci. Eng. C* **2012**, *32*, 228–235.
- [15] B. Krajewska, **2004**, *35*, 126–139.
- [16] M. Nasratin, A. . Hasrul, A. . Sureena, M. . Nurul Aini, A. . Ruwaida, M. . Shalyda, A. Ideris, A. . Rozaimi, J. . Sharfuddin, N. I. . Ahmad Nordin, *J. Appl. Sci.* **2010**, *21*, 2701–2704.
- [17] G. Bayramoglu, I. Gursel, M. Yilmaz, M. Y. Arica, *J. Chem. Technol. Biotechnol.* **2012**, *87*, 530–539.
- [18] M. Alatorre-meda, P. Taboada, J. Sabín, B. Krajewska, L. M. Varela, J. R. Rodríguez, **2009**, *339*, 145–152.
- [19] L. B. R. Castro, F. F. Silva, A. M. Carmona-Ribeiro, M. Kappl, D. F. S. Petri, *J. Phys. Chem. B* **2007**, *111*, 8520–8526.
- [20] M. Pešić, C. López, G. Álvaro, J. López-Santín, *J. Mol. Catal. B Enzym.* **2012**, *84*, 144–151.
- [21] A. A. Mendes, P. C. Oliveira, A. M. Vélez, R. C. Giordano, R. D. L. C. Giordano, H. F. De Castro, *Int. J. Biol. Macromol.* **2012**, *50*, 503–511.
- [22] D. Kubác, A. Čejková, J. Masák, V. Jirkú, M. Lemaire, E. Gallienne, J. Bolte, R. Stloukal, L. Martínková, **2006**, *39*, 59–61.
- [23] T. K. Ozturk, A. Kilinc, *Journal Mol. Catal. B, Enzym.* **2010**, *67*, 214–218.
- [24] J. C. Santos, G. F. M. Nunes, V. H. Perez, H. F. De Castro, **2007**, 1255–1261.
- [25] P. Torres, D. Reyes-duarte, N. Lo, M. Ferrer, A. Ballesteros, F. J. Plou, **2008**, *43*, 145–153.
- [26] E. Hita, A. Robles, B. Camacho, A. Ramírez, L. Esteban, M. J. Jiménez, M. M. Muñoz, P. A. González, E. Molina, **2007**, *42*, 415–422.
- [27] H. A. Akdogan, N. K. Pazarlioglu, *Process Biochem.* **2011**, *46*, 840–846.
- [28] Y. Zhang, T. Zhi, L. Zhang, H. Huang, H. Chen, **2009**, *50*, 5693–5700.
- [29] V. Deepak, R. Kumar, K. Kalishwaralal, S. Gurunathan, *Bioresour. Technol.* **2009**, *100*, 6644–6646.
- [30] A. A. Mendes, L. Freitas, A. K. F. De Carvalho, P. C. De Oliveira, H. F. De Castro, **2011**, *2011*, DOI 10.4061/2011/967239.
- [31] P. C. Ashly, P. V Mohanan, *Process Biochem.* **2010**, *45*, 1422–1426.
- [32] S. Sakai, Y. Liu, T. Yamaguchi, R. Watanabe, M. Kawabe, K. Kawakami, *Bioresour. Technol.* **2010**, *101*, 7344–7349.
- [33] R. Reshmi, G. Sanjay, S. Sugunan, *Catal. Commun.* **2006**, *7*, 460–465.
- [34] S. Wanjari, C. Prabhu, T. Satyanarayana, A. Vinu, S. Rayalu, *Microporous Mesoporous Mater.* **2012**, *160*, 151–158.
- [35] J. Yu, H. Ju, **2002**, *74*, 3579–3583.
- [36] M. Delvaux, S. Demoustier-Champagne, *Biosens. Bioelectron.* **2003**, *18*, 943–951.
- [37] E. J. Cho, S. Jung, H. J. Kim, Y. G. Lee, K. C. Nam, H.-J. Lee, H.-J. Bae, *Chem. Commun.* **2012**, *48*, 886–888.
- [38] K. M. de Lathouder, D. T. J. van Benthem, S. A. Wallin, C. Mateo, R. F. Lafuente, J. M. Guisan, F. Kapteijn, J. A. Moulijn, *J. Mol. Catal. B Enzym.* **2008**, *50*, 20–27.
- [39] R. Zhai, B. Zhang, L. Liu, Y. Xie, H. Zhang, J. Liu, *CATCOM* **2010**, *12*, 259–263.
- [40] U. H. Zaidan, M. B. A. Rahmana, S. S. Othman, M. Basri, E. Abdulmalek, R. N. Z. R. A. Rahman, A. B. Salleh, *Food Chem.* **2012**, *131*, 199–205.
- [41] C. Fargues, M. Bailly, G. Grevillot, L. Laboratoire, C. Ensic-cnrs, G. Bp, N. Cedex, **1998**, *16*, 5–16.
- [42] Q. Liu, X. Kong, C. Zhang, Y. Hua, **2012**, DOI 10.1002/jsfa.5997.
- [43] F. A. Erhardt, H.-J. Jördening, **2007**, *131*, 440–447.
- [44] L. J. Kennedy, P. K. Selvi, A. Padmanabhan, K. N. Hema, G. Sekaran, **2007**, *69*, 262–270.
- [45] N. Carlsson, H. Gustafsson, C. Thörn, L. Olsson, K. Holmberg, B. Åkerman, *Adv. Colloid Interface Sci.* **2014**, *205*, 339–60.
- [46] E. Magner, *Chem. Soc. Rev.* **2013**, *42*, 6213–6222.

- [47] M. Hartmann, X. Kostrov, *Chem. Soc. Rev.* **2013**, 6277–6289.
- [48] Y. Yokogawa, R. Yamauchi, A. Saito, Y. Yamato, T. Toma, *Biomed. Mater. Eng.* **2017**, *28*, 37–46.
- [49] E. Weber, D. Sirim, T. Schreiber, B. Thomas, J. Pleiss, M. Hunger, R. Gläser, V. B. Urlacher, **2010**, *64*, 29–37.
- [50] W. hua Yu, M. Fang, D. shen Tong, P. Shao, T. ning Xu, C. hui Zhou, *Biochem. Eng. J.* **2013**, *70*, 97–105.
- [51] S. B. Hartono, S. Z. Qiao, J. Liu, K. Jack, B. P. Ladewig, Z. Hao, G. Qing, M. Lu, *J. Phys. Chem. C* **2010**, *114*, 8353–8362.
- [52] M. Falahati, A. A. Saboury, L. Ma'mani, A. Shafiee, H. A. Rafieepour, *Int. J. Biol. Macromol.* **2012**, *50*, 1048–1054.
- [53] R. H. Chang, J. Jang, K. C. Wu, **2011**, *12*, 2844–2850.
- [54] T. Y. Nara, H. Togashi, C. Sekikawa, K. Inoh, K. Hisamatsu, K. Sakaguchi, F. Mizukami, T. Tsunoda, "Journal Mol. Catal. B, Enzym." **2010**, *64*, 107–112.
- [55] B. E. Grabicka, M. Jaroniec, **2010**, 385–396.
- [56] S. Fornera, T. Bauer, a. D. Schlüter, P. Walde, *J. Mater. Chem.* **2012**, *22*, 502.
- [57] M. M. Zheng, Y. Lu, L. Dong, P. M. Guo, Q. C. Deng, W. L. Li, Y. Q. Feng, F. H. Huang, *Bioresour. Technol.* **2012**, *115*, 141–146.
- [58] M. S. Bhattacharyya, A. Singh, U. C. Banerjee, *Bioresour. Technol.* **2010**, *101*, 1581–1586.
- [59] G. Zhou, K. K. Fung, L. W. Wong, Y. Chen, R. Renneberg, S. Yang, *Talanta* **2011**, *84*, 659–665.
- [60] C. Wu, G. Zhou, X. Jiang, J. Ma, H. Zhang, H. Song, *Process Biochem.* **2012**, *47*, 953–959.
- [61] M. Kramer, J. C. Cruz, P. H. Pfromm, M. E. Rezac, P. Czermak, *J. Biotechnol.* **2010**, *150*, 80–86.
- [62] L. Thudi, L. S. Jasti, Y. Swarnalatha, N. W. Fadnavis, K. Mulani, S. Deokar, S. Ponrathnam, *J. Mol. Catal. B Enzym.* **2012**, *74*, 54–62.
- [63] H. S. Mansur, R. L. Oréfice, Z. P. Lobato, W. L. Vasconcelos, E. S. Mansur, L. J. C. Machado, *Adsorption* **2001**, 105–116.
- [64] M. Falahati, L. Ma'mani, A. A. Saboury, A. Shafiee, A. Foroumadi, A. R. Badiie, *Biochim. Biophys. Acta - Proteins Proteomics* **2011**, *1814*, 1195–1202.
- [65] M. Vinoba, M. Bhagiyalakshmi, S. K. Jeong, Y. I. I. Yoon, S. C. Nam, *Colloids Surfaces B Biointerfaces* **2012**, *90*, 91–96.
- [66] D. T. Tran, C. L. Chen, J. S. Chang, *J. Biotechnol.* **2012**, *158*, 112–119.
- [67] J. J. Karimpil, J. S. Melo, S. F. D'Souza, *Int. J. Biol. Macromol.* **2012**, *50*, 300–302.
- [68] F. Xu, W. H. Wang, Y. J. Tan, M. L. Bruening, *Anal. Chem.* **2010**, *82*, 10045–10051.
- [69] T. Godjevargova, R. Nenkova, V. Konsulov, *J. Mol. Catal. B Enzym.* **2006**, *38*, 59–64.
- [70] S. W. Kwon, B. O. Jeong, E. H. Lee, Y. S. Kim, Y. Jung, **2012**, *33*, 1593–1596.
- [71] P. Xiao, X. Lv, Y. Deng, **2012**, 2719, DOI 10.1080/00032719.2012.673103.
- [72] S. Wang, P. Su, F. Ding, Y. Yang, "Journal Mol. Catal. B, Enzym." **2013**, *89*, 35–40.
- [73] H. Kawakita, K. Sugita, K. Saito, M. Tamada, T. Sugo, H. Kawamoto, *J. Memb. Sci.* **2002**, *205*, 175–182.
- [74] H. Kawakita, K. Sugita, K. Saito, M. Tamada, T. Sugo, H. Kawamoto, *Biotechnol. Prog.* **2002**, *18*, 465–469.
- [75] S. Karboune, R. Neufeld, S. Kermasha, *J. Biotechnol.* **2005**, *120*, 273–283.
- [76] Y. Z. Chen, C. T. Yang, C. B. Ching, R. Xu, *Langmuir* **2008**, *24*, 8877–8884.
- [77] J. S. Beck, J. C. Vartuli, W. J. Roth, M. E. Leonowicz, C. T. Kresge, K. D. Schmitt, C. T. W. Chu, D. H. Olson, E. W. Sheppard, S. B. McCullen, et al., *J. Am. Chem. Soc.* **1992**, *114*, 10834–10843.
- [78] S. Hudson, J. Cooney, E. Magner, *Angew. Chem. Int. Ed. Engl.* **2008**, *47*, 8582–94.
- [79] C.-H. Lee, T.-S. Lin, C.-Y. Mou, *Nano Today* **2009**, *4*, 165–179.
- [80] C. Bernal, L. Sierra, M. Mesa, *ChemCatChem* **2011**, *3*, 1948–1954.
- [81] M. Wang, W. Qi, Q. Yu, R. Su, Z. He, *Biochem. Eng. J.* **2010**, *52*, 168–174.
- [82] P. Colombo, C. Vakifahmetoglu, S. Costacurta, *J. Mater. Sci.* **2010**, *45*, 5425–5455.
- [83] C. M. A. Parlett, K. Wilson, A. F. Lee, *Chem. Soc. Rev. Chem. Soc. Rev* **2013**, *42*, 3876–3893.
- [84] S. Cao, L. Fang, Z. Zhao, Y. Ge, S. Piletsky, A. P. F. Turner, *Adv. Funct. Mater.* **2013**, *23*, 2162–2167.
- [85] C. Bernal, L. Sierra, M. Mesa, *J. Mol. Catal. B Enzym.* **2012**, *84*, 166–172.
- [86] C. Bernal, P. Urrutia, A. Illanes, L. Wilson, *N. Biotechnol.* **2013**, *30*, 500–506.
- [87] C. Bernal, A. Illanes, L. Wilson, *Langmuir* **2014**, *30*, 3557–3566.
- [88] N. Guajardo, C. Bernal, L. Wilson, Z. Cabrera, *Process Biochem.* **2015**, *50*, 1870–1877.
- [89] N. Guajardo, C. Bernal, L. Wilson, Z. Cabrera, *Catal. Today* **2015**, *255*, 21–26.
- [90] J.-L. Blin, J. Jacoby, S. Kim, M.-J. Stébé, N. Canilho, A. Pasc, *Chem. Commun. (Camb)*. **2014**, *50*, 11871–4.
- [91] N. Brun, A. Babeau-Garcia, M.-F. Achard, C. Sanchez, F. Durand, G. Laurent, M. Birot, H. Deleuze, R. Backov, *Energy Environ. Sci.* **2011**, *4*, 2840.
- [92] X. Y. Yang, Z. Q. Li, B. Liu, A. Klein-Hofmann, G. Tian, Y. F. Feng, Y. Ding, D. Su, F. S. Xiao, *Adv. Mater.* **2006**, *18*, 410–414.
- [93] H. Li, S. Li, P. Tian, Z. Wu, Z. Li, *Molecules* **2017**, *22*, DOI 10.3390/molecules22030377.
- [94] J. Zhao, Y. Wang, G. Luo, S. Zhu, *Bioresour. Technol.* **2011**, *102*, 529–35.
- [95] J. Li, L.-S. Li, L. Xu, *Microporous Mesoporous Mater.* **2016**, *231*, 147–153.
- [96] S. Kim, M.-J. Stébé, J.-L. Blin, A. Pasc, *J. Mater. Chem. B* **2014**, *2*, 7910–7917.

- [97] S. Kim, R. Diab, O. Joubert, N. Canilho, A. Pasc, *Colloids Surf. B. Biointerfaces* **2015**, *140*, 161–168.
- [98] A. Pasc, J.-L. Blin, M.-J. Stébé, J. Ghanbaja, *RSC Adv.* **2011**, *1*, 1204.
- [99] S. Gürdaş, H. A. Güleç, M. Mutlu, *Food Bioprocess Technol.* **2012**, *5*, 904–911.
- [100] T. Jesionowski, J. Zdarta, B. Krajewska, *Adsorption* **2014**, *20*, 801–821.
- [101] Z. Quinn Z.K, C. Xiao Dong, *Biochem. Eng. J.* **2001**, *9*, 33–40.
- [102] S. F. Prazeres, C. G. Ruiz, G. M. García, *Appl. Spectrosc. Rev.* **2015**.
- [103] W. Humphrey, A. Dalke, K. Schulten, *J. Mol. Graph.* **1996**, *14*, 33–38.
- [104] R. F. Pereira-Rodríguez, Ángel Leiro, M. E. Cerdán, M. I. González Siso, M. B. Fernández, *J. Mol. Catal. B Enzym.* **2008**, *52–53*, 178–182.
- [105] A. Pereira-Rodríguez, R. Fernández-Leiro, M. I. González-Siso, M. E. Cerdán, M. Becerra, J. Sanz-Aparicio, *J. Struct. Biol.* **2012**, *177*, 392–401.
- [106] A. Pereira-Rodríguez, R. Fernández-Leiro, M. I. González Siso, M. E. Cerdán, M. Becerra, J. Sanz-Aparicio, *Acta Crystallogr. Sect. F. Struct. Biol. Cryst. Commun.* **2010**, *66*, 297–300.
- [107] E. Krissinel, K. Henrick, *J. Mol. Biol.* **2007**, *372*, 774–97.
- [108] M. Becerra, E. Cerdán, M. I. G. Siso, *Biotechnol. Tech.* **1998**, *12*, 253–256.
- [109] O. S. Pilipenko, L. F. Atyaksheva, O. M. Poltorak, E. S. Chukhrai, *Russ. J. Phys. Chem. A* **2007**, *81*, 990–994.
- [110] C. Lei, T. a Soares, Y. Shin, J. Liu, E. J. Ackerman, *Nanotechnology* **2008**, *19*, 125102.
- [111] M. Vallet-Regí, A. Rámila, R. P. Del Real, J. Pérez-Pariente, *Chem. Mater.* **2001**, *13*, 308–311.
- [112] F. Tang, L. Li, D. Chen, *Adv. Mater.* **2012**, *24*, 1504–1534.
- [113] FDA, **2009**, www.accessdata.fda.gov/scripts/fcn/gras_notices/GR.
- [114] C. Contado, L. Ravani, M. Passarella, *Anal. Chim. Acta* **2013**, *788*, 183–192.
- [115] I. I. Slowing, C. W. Wu, J. L. Vivero-Escoto, V. S. Y. Lin, *Small* **2009**, *5*, 57–62.
- [116] A. E. Nel, L. Mädler, D. Velegol, T. Xia, E. M. V. Hoek, P. Somasundaran, F. Klaessig, V. Castranova, M. Thompson, *Nat. Mater.* **2009**, *8*, 543–557.
- [117] M. M. Van Schooneveld, E. Vucic, R. Koole, Y. Zhou, J. Stocks, D. P. Cormode, C. Y. Tang, R. E. Gordon, K. Nicolay, A. Meijerink, et al., *Nano Lett.* **2008**, *8*, 2517–2525.
- [118] Y. Jin, N. Zhang, C. Li, K. Pu, C. Ding, Y. Zhu, *Colloids Surfaces B Biointerfaces* **2017**, *151*, 240–248.
- [119] J. Y. Choi, T. Ramasamy, S. Y. Kim, J. Kim, S. K. Ku, Y. S. Youn, J. R. Kim, J. H. Jeong, H. G. Choi, C. S. Yong, et al., *Acta Biomater.* **2016**, *39*, 94–105.
- [120] H. Meng, M. Wang, H. Liu, X. Liu, A. Situ, B. Wu, Z. Ji, C. H. Chang, A. E. Nel, *ACS Nano* **2015**, *9*, 3540–3557.
- [121] N. Han, Q. Zhao, L. Wan, Y. Wang, Y. Gao, P. Wang, Z. Wang, J. Zhang, T. Jiang, S. Wang, *ACS Appl. Mater. Interfaces* **2015**, *7*, 3342–3351.
- [122] Z. Wang, Y. Tian, H. Zhang, Y. Qin, D. Li, L. Gan, F. Wu, *Int. J. Nanomedicine* **2016**, *11*, 6485–6497.
- [123] P. N. Durfee, Y. S. Lin, D. R. Dunphy, A. J. Muñoz, K. S. Butler, K. R. Humphrey, A. J. Lokke, J. O. Agola, S. S. Chou, I. M. Chen, et al., *ACS Nano* **2016**, *10*, 8325–8345.
- [124] J. Sun, D. Ma, H. Zhang, F. Jiang, Y. Cui, R. Guo, X. Bao, *Langmuir* **2008**, *24*, 2372–2380.
- [125] S. H. Ahn, S. H. Kim, S. G. Lee, *J. Appl. Polym. Sci.* **2004**, *94*, 812–818.
- [126] V. Athès, D. Combes, *Enzyme Microb. Technol.* **1998**, *22*, 532–537.
- [127] P. S. Cremer, S. G. Boxer, *J. Phys. Chem. B* **1999**, *103*, 2554–2559.
- [128] F. Wang, J. Liu, *Small* **2014**, *10*, 3927–3931.
- [129] I.-A. Pavel, S. F. Prazeres, G. Montalvo, C. García Ruiz, V. Nicolas, A. Celzard, F. Dehez, L. Canabady-Rochelle, N. Canilho, A. Pasc, *Langmuir* **2017**, *33*, 3333–3340.

Chapter 4. Encapsulation of β -galactosidase in responsive carriers allowing release triggered by either temperature or pH

The encapsulation strategies involve the entrapment of active agents (cells, enzymes, food ingredients) in/by the matrix of the carrier with the purpose of preventing premature release or degradation of the active moiety particularly when it should be delivered to a targeted site like intestine, as the case of this work. Encapsulation is required to protect the agent from moisture^[1], heat^[2], oxygen or light^[3] and sometimes to improve the shelf-life^[4]. However, encapsulation can also be a strategy for masking undesirable odor, taste and color or, for preventing reactions and interactions between the ingredients and the active agent. Another very important reason for choosing encapsulation is to control the delivery. In addition, encapsulation can modify the physical characteristics of the components (e.g. from liquid to solid) leading to easier handling, separation and may also confer adequate concentration and uniform dispersion in the mixture ^[5]. The use of the entrapment techniques has increased in the food industry.

The encapsulation of flavours and aromas improves the stability for volatile molecules ^[6] against evaporation and chemical reactions (interaction with food or other flavours or oxidation). Organosulfurs ^[7], herbal and plants extract ^[3] that present health benefits, are encapsulated to mask an unpleased smell. Bioactive components, such as lipids, peptides (fragments of proteins), vitamins, minerals, antioxidants, cells (probiotic) display multiple health benefits. Their encapsulation protects them from external factors during storage, and from acidic pH during their passage through gastro-intestinal track ^[8]. Probiotic bacteria are encapsulated to increase their bioavailability and functionality against a pH variation, the digestive enzymes of stomach or, to resist to mechanical stress or transport conditions ^[9].

Enzymes are used in various food industries (starch, baking, brewing, dairy, vegetables, fruits, fats and oils, fish and meat industry) mainly as processing agents. The enzymes can be added in different production steps: preparation, processing, treatment, packaging, transportation or in the storage stage ^[10]. Enzymes easily denature, thus encapsulation provides them a longer lifetime, and improves the resistance to harsh pH

and to temperature. The encapsulated enzymes present in some specific cases new catalytic properties compared with the free enzyme [6].

Various techniques can be applied to entrap enzyme, including: extrusion, coating, liposome entrapment [11], spray drying, agglomeration or multistage drying, spray chilling or spray cooling, fluidized bed granulation or coating, coacervation, inclusion complexation, centrifugal extrusion, high shear granulation, melt extrusion and melt injections, rotational suspension separation, emulsification and sol-gel encapsulation [12]. All these methods present advantages and drawbacks, but the encapsulation approach of the enzyme depends on its intended application in the food manufacture process. For example Dusterhofs et al. [13] entrapped amylase enzyme (used in the baking industry to maintain freshness of the final product during storage) via spray coating and chilling in a core-shell particle. The encapsulated enzymes were protected against temperature and the release was controlled during dough baking [2]. Using spray coating, Solomon et al. [14] investigated functional coating of lactase with acacia gum, shellac and hydroxypropylmethyl cellulose to protect the enzyme from low pH 2.

The shape of the capsule depends on the entrapment method used. Figure 4. 1 resents various forms of capsules:

- the well-defined core-shell morphology is the simplest form (mononuclear), which can be a sphere or an irregular shape
- the polynuclear capsules present multiple cores inside a shell
- the multi-wall capsules present more than one wall around the core, each wall can be made from the same material or may be different
- the matrix type, where the active agent is dispersed into a matrix (usually a polymer)

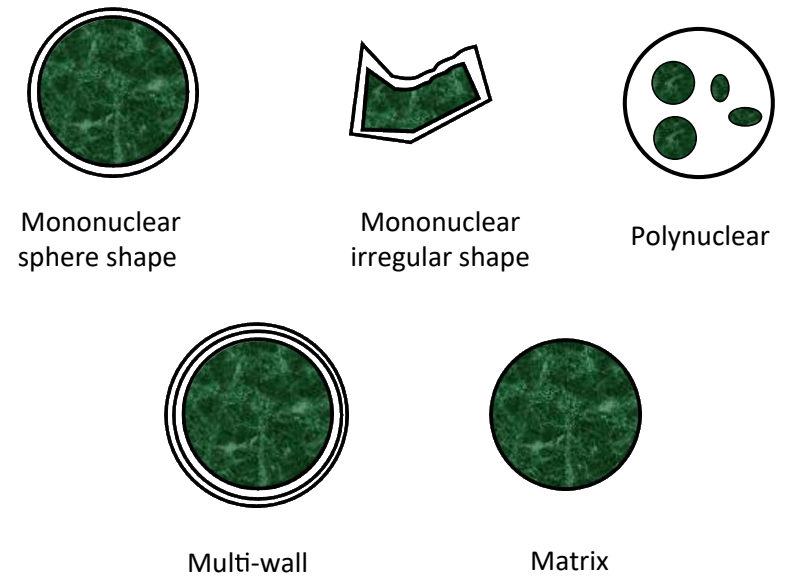


Figure 4. 1 Various forms of capsules (reproduced from [15]).

The encapsulation ingredients used in food applications must be “generally recognized as safe” (GRAS) and approved by the governmental agencies (EFSA-European Food Safety Authority and FDA-Food and Drug Administration) [6]. Obviously, the protective shell must be from a food grade material and be biodegradable.

The most used materials for encapsulation in food applications are polysaccharides and derivatives: plants exudates and extracts of acacia, mesquite gums, pectins, galactomannans, soluble soybean polysaccharides or marine extracts such as alginate and carrageenan. Starch and their derivatives –cellulose, syrups, amylose and amylopectin, dextrans and maltodextrins or polydextrose are also used for encapsulation. Another category of polysaccharides used for encapsulation, like chitosan, dextran, and xanthan, have microbial or animal origins. Other common encapsulating natural agents include: milk proteins (casein), waxes (candellina wax, carnauba wax and beeswax), fatty acids or alcohols, lipids, or phospholipids. Other organic materials that have been used for encapsulation are polyvinylpyrrolidone (PVP), paraffin oil or shellac [5].

Among the inorganic materials used for enzyme encapsulation, mesoporous silica is the most used. Silica materials exhibit a high degree of biocompatibility, biodegradability and nontoxicity, and some resistance to microbial attack. The high

surface area and tuneable pore size can encapsulate a high amount of agent and to confer a controlled release. Enzymes can be encapsulated directly into the matrix by sol-gel approach [16] or into the pores [17]. Beside bare mesoporous silica, calcium carbonates, metal-organic frameworks (MOFs), mesoporous titanium oxide, mesoporous organosilica, hybrid organic/inorganic silica, mesoporous carbon are also employed for encapsulation [6].

However, the enzyme encapsulation process requires mild conditions to minimize the effect on enzyme activity, conferring a network confinement that restricts the unfolding of the enzyme while retaining the activity. Encapsulation enables enzymes to maintain their viability for longer time, since it can protect them from inactivation factors such as inhibitors, ions, protons or radicals (Figure 4. 2), similar with their natural occurrence in cells.

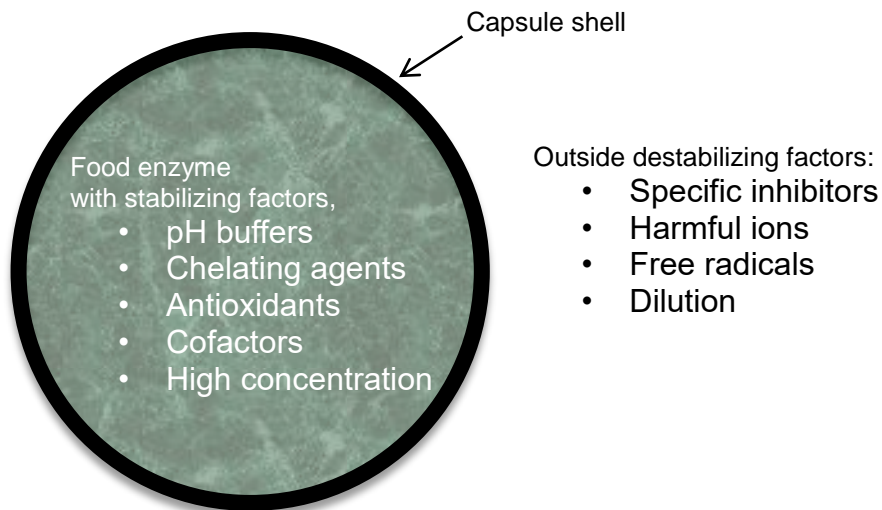


Figure 4. 2. Benefits of enzyme encapsulation in food industry (reproduced from [15]).

Another advantage of enzyme encapsulation is that the permeability of the matrices allows the transfer of small compounds (the substrate of the enzyme and the reaction products for example) while the tuneable porosity can allow the accommodation of enzymes of different sizes. The triggered release can be achieved by modifying the shell structure or the matrix [18]

Finding a suitable solution for enzyme encapsulation in the food industry, in spite of increasing demand, is still challenging. Since it requires mild reaction conditions compatible with the manipulation of biological macromolecules good physical properties of the resulting carriers in term of stability, biocompatibility and loading capacities, are difficult to achieve..

The release of the active ingredient from the carrier can be stage-specific, side-specific or triggered by external stimuli. Temperature (high or low), pH, enzyme trigger, irradiation, shear or pressure release (mechanical, mastication), osmotic shock, moisture or solvent release (via rehydration, dissolution) are used as external stimuli. Triggered release seeks to deliver the active ingredient in a different manufacture stage or a specific location within the body after food ingestion.

The design of the capsule is made according to the release mechanism. Dispersive or water-soluble materials (*e.g.* proteins, carbohydrates) are used for water trigger release. Fats, lipids and waxes are used in the capsules that have a temperature trigger release. Specific parts in the gastro-intestinal track have specific pH values and specific enzymes. A starch capsule can be used for the release of the active ingredient in the mouth, since starch is hydrolysed by amylase (present in the mouth). The protease in the stomach can disintegrate by hydrolysis a capsule made of protease. Resistant materials to the acidic pH of the stomach, denatured proteins, food polymers (*e.g.* zein, shellac) can be used for the delivery in the intestine, where the capsule becomes soluble at basic pH values.

4.1. Thermo-responsive food grade delivery system for the treatment of lactose intolerance

The solid lipid nanoparticles (SLNs) are alternative colloidal carriers to emulsions, liposomes, polymer micro- or nanoparticles. SLNs can encapsulate both hydrophobic and hydrophilic drugs, enabling thus the enhancement of drug absorption in the gastrointestinal tract ^[19]. SLNs have gained increase attention from food, cosmetic and pharmaceuticals industry.

There are different formulation procedures to prepare SLNs. In High-Pressure Homogenization (HPH) technique, a liquid is pushed with pressure through a micron size gap. Although this is an energy intensive process, it is also an efficient dispersing technique. The method starts from the dispersion of the drug in the melted lipid (5-10°C above the melting point). It can be performed either at high temperature (hot HPH) or low temperature (< RT, cold HPH).

There are two other high energy dispersive techniques are high shear homogenization and ultrasonication techniques. In both cases, the lipid particle solution is obtained by dispersion of the melted lipid in a hot aqueous phase containing surfactant as particles stabilizer. The solid lipid nanoparticles are obtained by cooling down the previous dispersion.

SLNs can also be obtained from low energy techniques such as: microemulsion, membrane contractor, phase inversion temperature, coacervation and double emulsion. In the microemulsion, the melted lipids are mixed with a hot surfactant solution. Due to the high ratio of lipid/surfactant, a microemulsion is spontaneous formed under gentle stirring^[20]. The hot microemulsion is dispersed in a high amount of cold water and the lipids solidify forming the SLNs dispersion. The membrane contractor technique employs a cylindrical membrane module. While working at the melting temperature of the lipid, in the internal channel of the membrane, a surfactant solution is circulated while the melted lipid is presses through pores ^[21]. By cooling the SLNs dispersion is formed.

Phase inversion temperature technique is another way to prepare SLNs. In fact, by changing the temperature, the HLB index of the surfactant changes, and the O/W type emulsion can change to a W/O emulsion. The SLNs formulation is formed at low temperatures.

Emulsification-solvent evaporation technique, emulsification solvent diffusion technique, solvent injection technique, supercritical fluid technique are methods that require the use of an organic solvent. The emulsification-solvent evaporation technique involves three steps. After the liposomes are dissolved in an organic solvent, they are dispersed in an aqueous solution by high-speed homogenizer. This dispersion is then passed through HPH and the SLNs nanoemulsion is obtained. The emulsification solvent diffusion technique requires the use of an organic solvent miscible with water. By dispersing the solvent solution that contains the lipids in water, under stirring, the SLNs are formed due to the diffusion of the organic solvent. The solvent injection technique is based on the same principle as emulsification solvent diffusion technique. The lipids dissolved in a water-miscible solvent, are injected in a surfactant solution [21].

Hydrophobic compounds can be dispersed directly in the lipid phase, while hydrophilic phase can be dispersed in the inner water phase of a double emulsion W/O/W. Only a few examples of lipid formulation for peptides and proteins entrapment have been reported in the literature [22].

The first example concerns the encapsulation of insulin, a model peptide, into particles of tripalmitin (Dynasan®116) [23,24] or glyceryl monostearate and cetyl palmitate [25,26], by the solvent evaporation method. Using the same procedure, catalase, an enzyme that can prevent the accumulation of toxic levels of hydrogen peroxide, was encapsulated in lecithin/triglyceride [27] and in soybean phosphatidylcholine [28]. However, the use of organic solvents has several drawbacks. It can decrease enzyme activity [29] and increase the toxicity of the final product [30].

The melted dispersion technique is a solvent free route allowing the preparation of double emulsions of W/O/W from melted lipids. The emulsification is carried out at a temperature above the melting point of the lipid. By cooling down to room temperature or

lower, the solid lipid particles are formed, leading to a colloidal suspension. Reithmeier [23] compared the solvent evaporation technique with the melt dispersion technique for the encapsulation of insulin. The best encapsulation efficiency was obtained using the W/O/W melt dispersion technique.

Thermal responsive delivery drug [31] and protein [32] systems are widely researched. They usually use polymers as the thermal responsive component. Although there are couple of groups that are investigating lipids [33] or wax [34,35] formulations thermo-responsive, up to our knowledge, this is the first time that enzyme encapsulation in SLNs has been design as a thermal trigger response system.

Used in pharmaceutical, cosmetic and food industry, shea butter was chosen as the oil phase. Being a triglyceride mainly formed with stearic and oleic acid, it presents a low melting temperature (between 25°C and 45°C) [36]. The closeness to body temperature makes shea butter a good candidate for the preparation of temperature triggered SLNs. In addition, shea butter has antioxidant and anti-inflammatory properties due to the presence of α -tocopherol and polyphenols that can enrich foods. These are investigated for the prevention of oxidation in human cells and may reduce the chance of degenerative diseases [36]. Although it is widely used in industry, only few examples have been reported in literature for the preparation of shea butter based solid lipid nanoparticles or nanostructured lipid carriers (NLC). Substances like anesthetics (lidocaine [37]), polyphenols (curcumin [38]), anti-inflammatory (nimesulide [39]), fragrances ((α)-amyl-cinnamal, cinnamal, cinnamyl alcohol, eugenol, geraniol, hydroxycitronellal, and isoeugenol [40]), moisturizing agents (sodium scetylated hyaluronate and ceramides [41]) or peptides (heptapeptide-acetyl-DEETGEF-OH) [42] have been so far encapsulated in shea butter carriers, but to the best of our knowledge there was no study concerning the encapsulation of enzymes.

In the present study, the SLNs formulated as delivery systems were obtained by the melted dispersion technique through a double W/O/W emulsion in which the β -galactosidase from *Kluyveromyces Lactis* was incorporated in the inner water phase. The

release of the enzyme was triggered by thermal response and investigated by in situ UV-Vis spectroscopy.

4.1.1. SLNs particle characterization

The SLNs preparation was described in Chapter 2. The particles shape and the emulsion texture were visualized by optical microscopy for the simple emulsion (W_1/O) and for the double emulsion ($W_1/O/W_2$) (Figure 4. 3). The water phase W_1 droplets in the double emulsion ($W_1/O/W_2$) are separated by a thin film of continuous phase (the shea butter phase), as the W_1/O emulsion is highly concentrated. The size distribution of the water droplets in the inverse emulsion W_1/O and the particle size of the double emulsion ($W_1/O/W_2$) was established using a droplet and counting from the images. The diameter of aqueous droplets where the enzyme is solubilized was determined as $0.8 \pm 0.3 \mu\text{m}$ whereas the size of the $W_1/O/W_2$ double emulsion was very polydisperse from 20 to 140 μm .

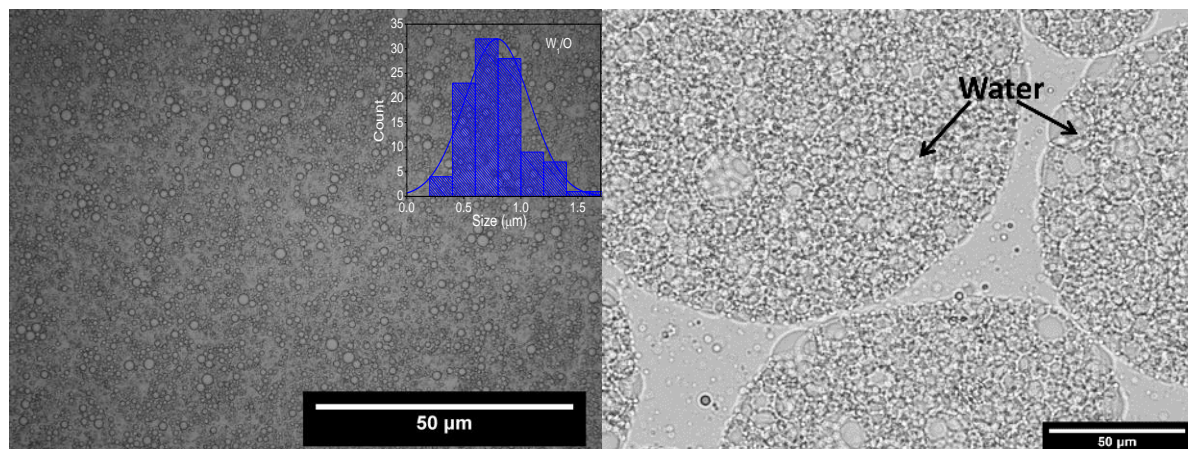


Figure 4. 3. Optical microscopy pictures and size distributions of inverse emulsion (W_1/O) (left) and optical microscopy pictures of double emulsion ($W_1/O/W_2$) (right).

Furthermore, it was found that nanometric sizing of a hard fat has an influence on its intrinsic properties such as the melting temperature (T_m), as it was demonstrated by Bunjes et al. [43] in the case of triglycerides. In addition, Haji Ali et al. [38] showed, by performing differential scanning calorimetry (DSC) experiments, that the melting temperature of shea butter shifts from 37 $^{\circ}\text{C}$ in bulk state to 33 $^{\circ}\text{C}$ once in SLN form.

The SLNs formulated in this work are slightly different since they entrap water and enzymes molecules. In order to figure out if the T_m of this type of SLN changed, differential scanning calorimetry has been also performed on bulk shea butter, on a solution of free enzyme in the presence of the SLNs (β -Gal+SLN) and on a colloidal suspension of SLNs encapsulating enzymes molecules (β -Gal@SLN) (Figure 4. 4). In the case of shea butter two melting temperatures have been detected at 15 °C and 30 °C. The physical and thermal properties of the natural lipids are given by the different compositions of triglycerides. The presence of polyunsaturated triglycerides in their structure (< 20wt%) lead to a polymorphic behavior ^[37] hence the presence of the two peaks in the bulk shea butter thermogram. In the case of SLN only one peak appears in the DSC thermogram (Figure 4. 4), corresponding to the melting of the shea butter and the rupture of the SLN. The thermograms for free enzyme in the presence of the SLNs (β -Gal+SLN) and colloidal suspension of SLNs encapsulating enzymes (β -Gal@SLN) are the same indicating that the presence of the enzyme doesn't change the structure of the SLN.

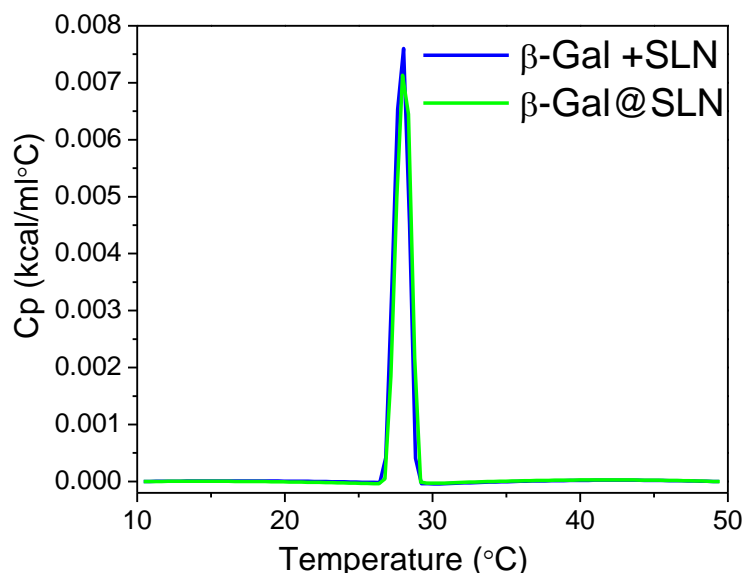


Figure 4. 4. DSC thermograms free enzyme in the presence of the SLNs (β -Gal+SLN) and colloidal suspension of SLNs encapsulating enzymes (β -Gal@SLN).

The same trend was observed from the small angle scattering data (Figure 4. 5 A) recorded for bulk shear butter between 10°C to 50°C. The presence of the broad pick at ~45 Å at low temperature (10°C) is correlated with a two-chain (2L) packed layers and the

small pick ($\sim 66 \text{ \AA}$) is correlated with triple-chain length (3L) of the triglycerides. The presence of a 3L is confirmed at 20°C and 30°C . This type of crystallinity is formed by saturated fatty acids (2L structure) and unsaturated triglycerides (3L structure)^[38]. At temperatures higher than 30°C , the peaks that correspond to 2L and 3L crystallinity disappear at high contact angle that corresponds with the melting of the lipid (Figure 4. 5 A).

The SAXS patterns obtained for the samples $\beta\text{-Gal+SLN}$ and $\beta\text{-Gal@SLN}$ (Figure 4. 5 B and C) are rather similar with each other for all the temperatures, with one peak (4.6 \AA) related to a crystalline beta phase which intensity decreases with the increase of temperature.

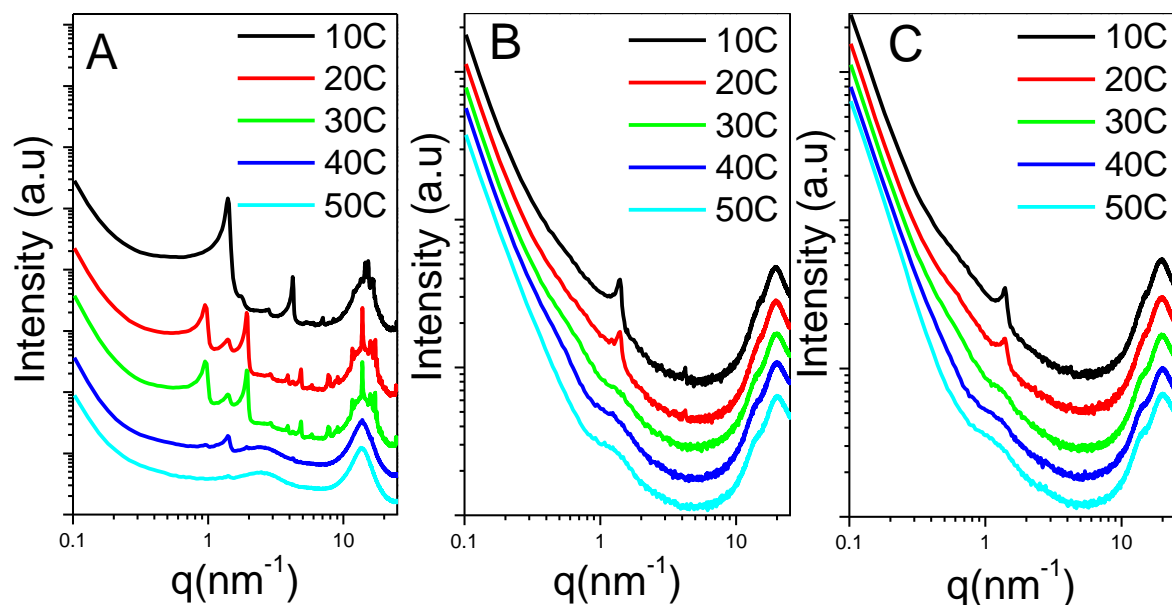


Figure 4. 5. SAXS patterns obtained for the bulk shea butter (A), free enzyme in the presence of the SLNs ($\beta\text{-Gal+SLN}$) (B), and colloidal suspension of SLNs encapsulating enzymes ($\beta\text{-Gal@SLN}$) (C).

4.1.2. *In situ* UV-visible spectroscopy of enzyme activity

The release of the enzyme out of the SLNs was performed by *in situ* UV-visible spectroscopy through the hydrolyses reaction of o-nitrophenyl- $\beta\text{-D}$ -galactopyranoside (ONPG) catalysed by the $\beta\text{-Gal}$. Preliminary experiments had to be performed in order to establish the effect of the temperature on the physical and the chemical parameters of o-nitrophenol (ONP) product: the acidic constant (pK_a) and the extinction coefficient (ϵ).

The absorbance coefficient ϵ was calculated from the Beer-Lambert law (Equation 4. 1) by measuring the adsorption of consecutive dilutions of a pre-synthesized ONP solution (0.8 mM) at λ_{410} nm at different temperatures (10, 20, 30, 40 and 45° C). The curves absorbance vs concentration (Figure 4. 6) were plotted and the slope of each straight lines represents ϵl from the Beer-Lambert equation.

$$A = \epsilon \cdot l \cdot c$$

Equation 4. 1. Beer-Lambert equation.

where ϵ is the absorption coefficient ($\text{cm}^{-1}\text{mol}^{-1}$), l is the light pass length (cm) and c is the concentration of the solution (M).

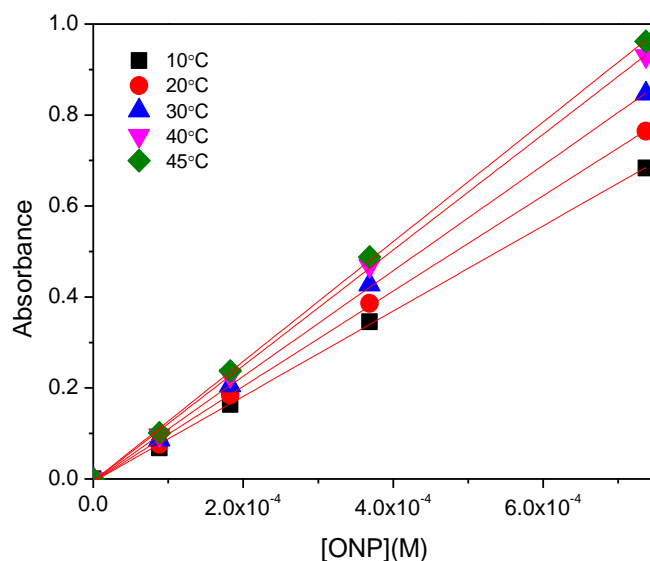


Figure 4. 6. The absorbance of different ONP concentrations at different temperatures.

The values determined for ϵ from Figure 4. 6 were taken into account to calculate the ϵ for each temperature (Figure 4. 7).

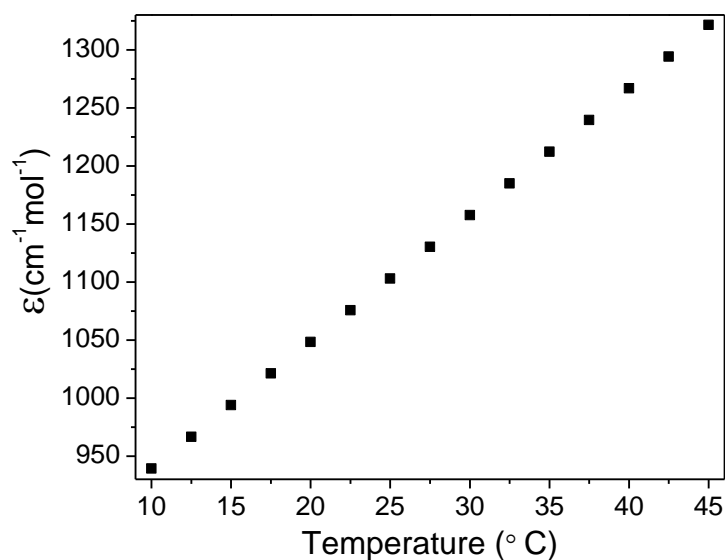


Figure 4. 7. The ϵ variation in a temperature range from 10 to 45°C.

The values for the acidic constant pK_a determined by Robinson et al. [44] were taken into account to calculate the pK_a for each temperature (Figure 4. 8).

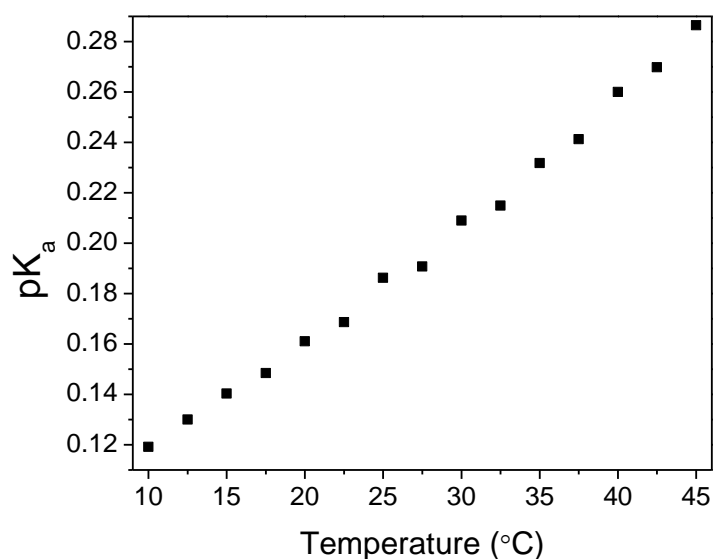


Figure 4. 8. The pK_a variation in a temperature range from 10 to 45°C.

As can be observed from Figure 4. 7 and Figure 4. 8 the temperature plays an important role. The values for pK_a increase with 140 % from 10 °C to 45 °C and the values for ϵ increase with 40 % in the range of temperature used. For this reason, UV-

visible spectroscopy results were corrected by the appropriate pK_a and ε for each temperature.

The hydrolyses of ONPG by β-galactosidase was followed *in situ* by UV-visible spectrophotometry over a thermal ramp ranging from 10°C to 45°C. A spectrum was recorded every 2.5°C for 5 minutes. More precisely, the experiment was performed as follow: 2.5 ml of ONPG solution (25 mg/L) was kept in a quartz cuvette under magnetic stirring over 5 minutes at the desired temperature. Then 0.1 ml of diluted free enzyme solution was added to tempered ONPG. The free enzyme solution was diluted 12000 times from the initial stock solution. The corrected rate formation of ONP ($V_{i_{corrected}}$) was calculated from the slope (Absorbance vs time) recorded at λ₄₁₀ nm, and corrected with the ε (Figure 4. 7) and pK_a (Figure 4. 8) values of ONP for each temperature according to the Equation 4. 2 [45].

$$V_{i_{corrected}} = V_{i_{410}} \cdot \left(\frac{1}{\epsilon} + \frac{1}{\epsilon \cdot pKa} \right)$$

Equation 4. 2. V_i correction equation.

Where $V_{i_{corrected}}$ (M/s) is the initial corrected rate for the ONP formation, $V_{i_{420}}$ (M/s) is the initial rate obtained from the UV taken at λ₄₁₀ nm, ε (cm⁻¹mol⁻¹) is the absorbance coefficient and pK_a is the ionization constant of ONP.

Figure 4. 9 displays the profiles of the initial rates of the ONP transformation catalyzed by the free enzyme (β-Gal) at different temperatures. Each experimental point represents the average of 4 repeated measurements.

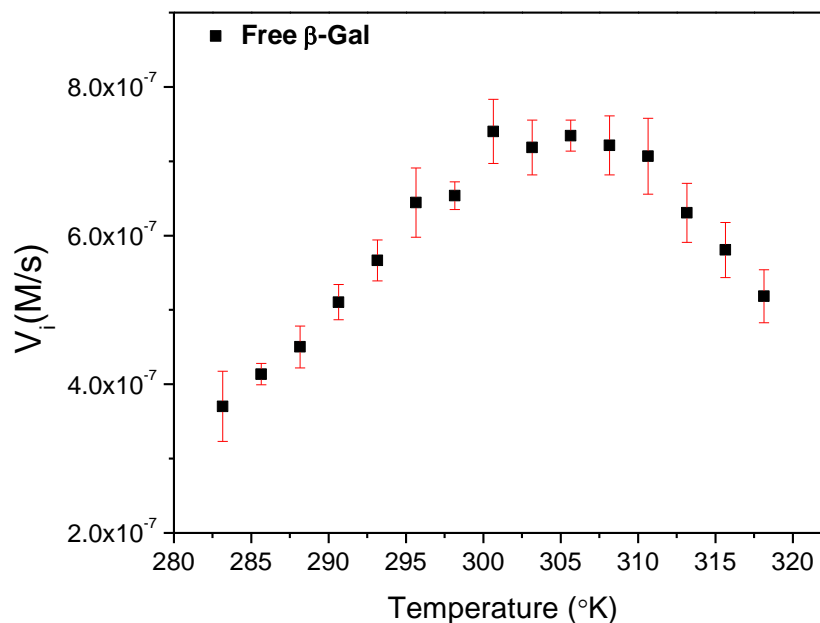


Figure 4. 9. Initial corrected rates (V_i) of free β -Gal in solution.

The effect of temperature on enzyme activity has been well established. At low temperatures, the reaction rate is slow and increases rapidly with the increase of the temperature until reaches a maximum at the optimal temperature. Before reaching the optimal temperature, the initial rate reaction catalyzed by the enzyme can be altered by the inhibition of the product resulted from the reaction. After the temperature increases beyond optimal temperature, the enzyme structure changes due to thermal inactivation [46,47] and the activity decreases. The same phenomenon is taking place for the free β -gal as presented in Figure 4. 9. The Arrhenius approach (Equation 4. 3) was used in order to better correlate the activity of the enzyme with temperature [46].

$$k = Ae^{-E_a/(RT)}$$

Equation 4. 3. Arrhenius equation.

Where k is the rate constant, A is the pre-exponential factor (a constant characteristic to the reaction, defined by the frequency of the particles collisions), R is the gas constant ($J \cdot K^{-1} \cdot mol^{-1}$) and T is the temperature (K).

Figure 4. 10 displays the $\ln(V_i)$ corrected in function of $1/T$. As can be observed the enzymatic activity increases with the increase of the temperature until 27.5 °C

followed by a region where it remains constant. After 37.5 °C the activity slowly decreases. This means that the optimal temperature for the enzyme is 37.5 °C. The degradation trend of the enzyme is a straight line and a first-order reaction in agreement with Arrhenius' equation and with the literature [48].

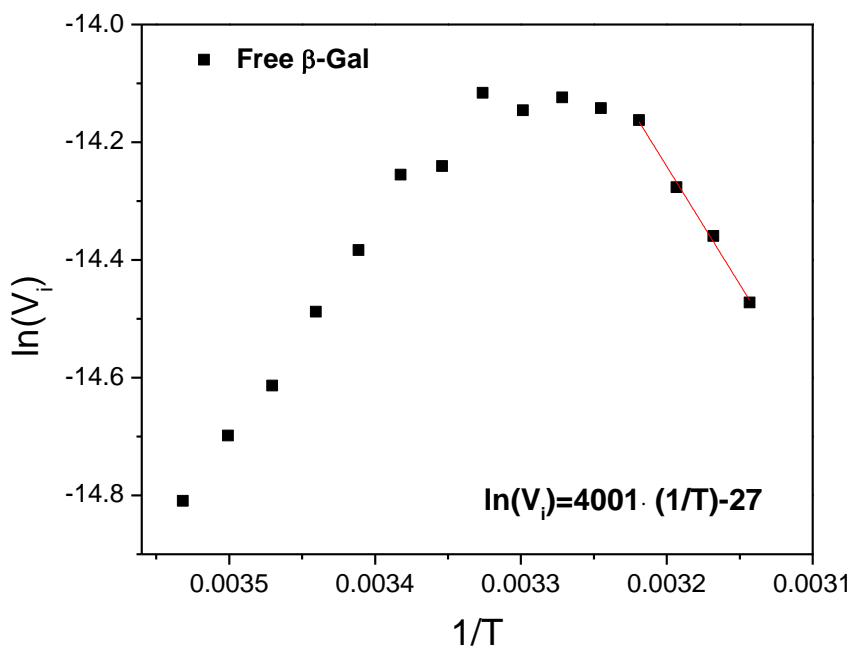


Figure 4. 10. $\ln(V_i)$ vs $1/T$ for the free β -Gal in solution.

It has been reported in literature that many proteins retained or increased their activity when absorbed on the hydrophobic surfaces [49] or on SLNs [22]. For this reason, the activity of the free enzyme in the presence of SLNs was analyzed in function of temperature. The SLNs were prepared as detailed in Chapter 2, by replacing the solution of enzyme with a mixture containing PBS/Glycerol (50/50 wt%). After the formation of the SLNs, an enzyme solution was added, having the same final concentration as the enzyme solution used for the analysis of the free enzyme.

The Figure 4. 11 displays the profiles of the initial rates of the ONP transformation catalyzed by β -Gal put in presence of SLNs (β -Gal+SLN) at different temperatures. Each experimental point represents the average of 2 repetitions. The values for these experiments were very similar and the calculated error is negligible. It can be observed that the initial rate for β -Gal+SLN has a similar trend as the initial rate for free β -Gal with an increase of more than 35% all over the temperature range.

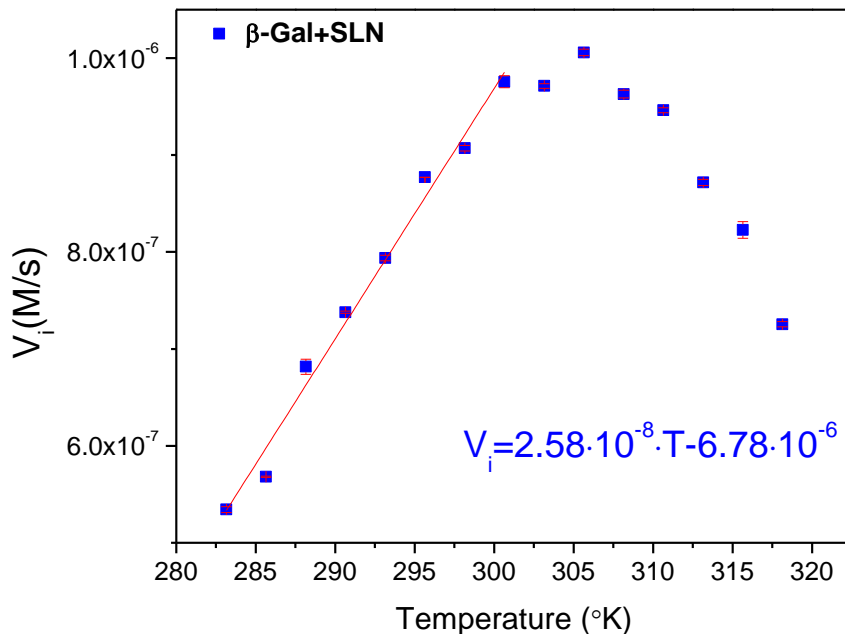


Figure 4. 11. Initial corrected rates (V_i) of β -Gal put in presence of SLNs (β -Gal+SLN).

In order to better compare the activity of the free β -Gal and (β -Gal+SLN), the $\ln(V_i)$ in function of $1/T$ graph was analyzed (Figure 4. 12).

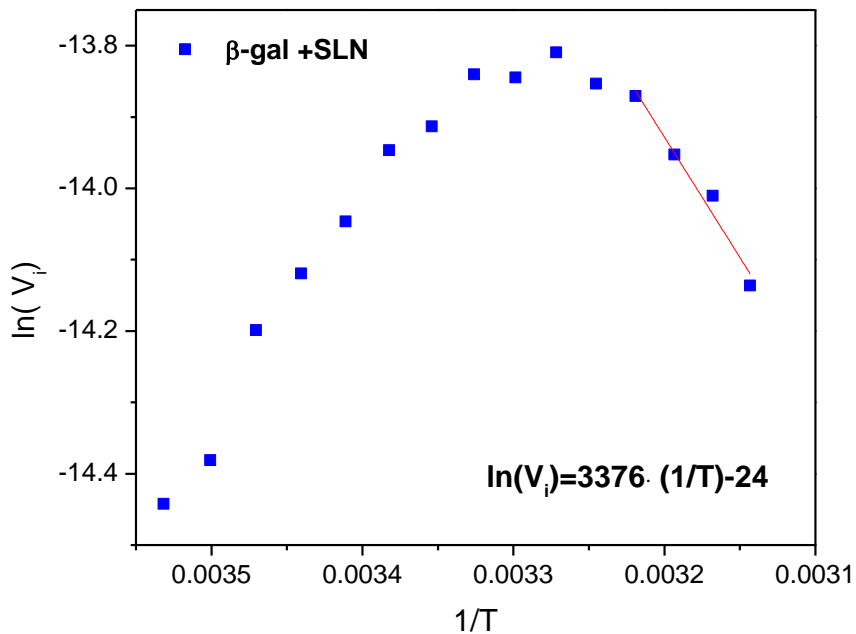


Figure 4. 12. $\ln(V_i)$ vs $1/T$ for the β -Gal put in presence of SLNs (β -Gal+SLN).

As can be observed the enzymatic activity of β -Gal+SLN has the same trend as the enzymatic activity the free β -Gal. The activity increases with the increase of the

temperature until 27.5 °C followed by a region where it remains constant. After 37.5 °C (the optimal temperature) the activity slowly decreases. Compared with the Free β -Gal, the β -Gal+SLN not only has a higher activity (by comparing the values of V_i and $\ln(V_i)$ respectively) but also has lower rate of degradation (by comparing the slope of the regions where the enzyme degrades). As it can be observed the slope for the degradation of the free β -Gal is higher ($4001 \text{ M}\cdot\text{K}\cdot\text{s}^{-1}$) compared with the slope for the degradation of β -Gal+SLN ($3376 \text{ M}\cdot\text{K}\cdot\text{s}^{-1}$).

In order to observe the effect of the encapsulation on the enzyme, the colloidal suspension of SLNs encapsulating enzymes molecules (β -Gal@SLN) was analyzed in the same way. The final concentration of the enzyme used for encapsulation was the same as the one used to analyze the free β -Gal and β -Gal+SLN.

The Figure 4. 13 displays the profiles of the initial rates of the ONP transformation catalyzed by β -Gal+SLN. Each experimental point represents an average of 3 repetitions.

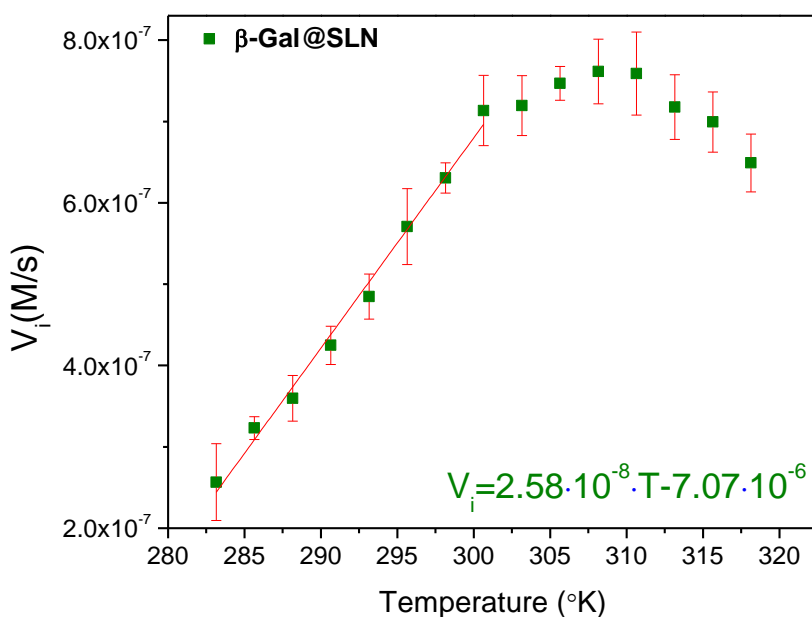


Figure 4. 13. Initial corrected rates (V_i) of the colloidal suspension of SLNs encapsulating enzymes molecules (β -Gal@SLN).

The concentration of β -Gal+SLN and the initial concentration of enzyme used to form β -Gal@SLN formulation were the same, therefore, one can assume that the enzyme

that is released from the SLNs presents the same behavior as the enzyme in the presence of SLN. It can be observed by comparing the Figure 4. 13 with Figure 4. 11, that at a temperature below 28°C, the initial rate V_i has a linear increase with the increase of the temperature for both samples. The slopes in this region, for β -Gal+SLN and for β -Gal@SLN are the same ($2.58 \cdot 10^{-8} \text{ Ms}^{-1}\text{K}^{-1}$). This indicates that in case of β -Gal@SLN no release is taking place in this region as the concentration of the enzyme is constant as in the case of β -Gal+SLN. The difference in the slopes equation is the intercept value that is smaller for β -Gal@SLN compare to β -Gal+SLN. This indicates that the enzyme quantity present in the sample β -Gal@SLN is low. The substrate (hydrophilic) does not have access to the enzyme that is entrapped in the lipids (hydrophobic) and only the enzyme that is outside the SLN (the enzyme that was not entrapped) can hydrolyse the substrate.

To quantify the amount of enzyme encapsulated in the SLNs the V_i of the enzyme in the solution of the studied samples (β -Gal+SLN and β -Gal@SLN) were compared. Starting from Michaelis-Menten equation (Equation 4. 4) and the fact that the both samples have the same behavior at low temperatures (they have the same rate constant k) the Equation 4. 5 was used to calculate the encapsulation efficiency.

$$V_i = k[E]$$

Equation 4. 4. Michaelis-Menten equation.

Where V_i is the initial speed of the reaction (M/s), k is the rate constant (M/s·mg) and $[E]$ is the concentration of the enzyme (mg/ml).

The V_i value at 20°C was taken into account to minimize the errors that can appear at 10°C due to air humidity that can influence the results. As it can be observed, the error bar of the value V_i at 10°C for β -Gal@SLN is higher than the error bar for the V_i value at 20°C. Another reason that the V_i values at 20°C were taken into consideration is because the SAXS patterns obtained for that sample (Figure 4. 5) at 10°C and 20°C are the same, proving that the crystalline structure remains the same.

The encapsulation efficiency (EE), defined as the percentage of β -Gal encapsulated in the SLN compared with the amount of enzyme used for the preparation of the formulation ($[\beta - Gal]_+$ (Equation 4. 5). This value was calculated to be $38.92\pm 3.48\%$

$$\%EE = \frac{V_{@} [\beta - Gal]_{+}}{[\beta - Gal]_{t}} * 100$$

Equation 4. 5. Encapsulation efficiency (EE).

Where %EE is the encapsulation efficiency, $V_{@}$ is the rate of the enzyme that is in the solution of the formulation β -Gal@SLN, V_{+} and $[\beta$ -Gal] $_{+}$ is the rate and the concentration of enzyme that is in the solution of the formulation β -Gal+SLN and $[\beta$ -Gal] $_{t}$ is the total enzyme concentration used.

In order to better understand the activity of β -Gal@SLN and to observe where and if a release is taking place, the $\ln(V_i)$ in function of $1/T$ graph was analyzed (Figure 4. 14).

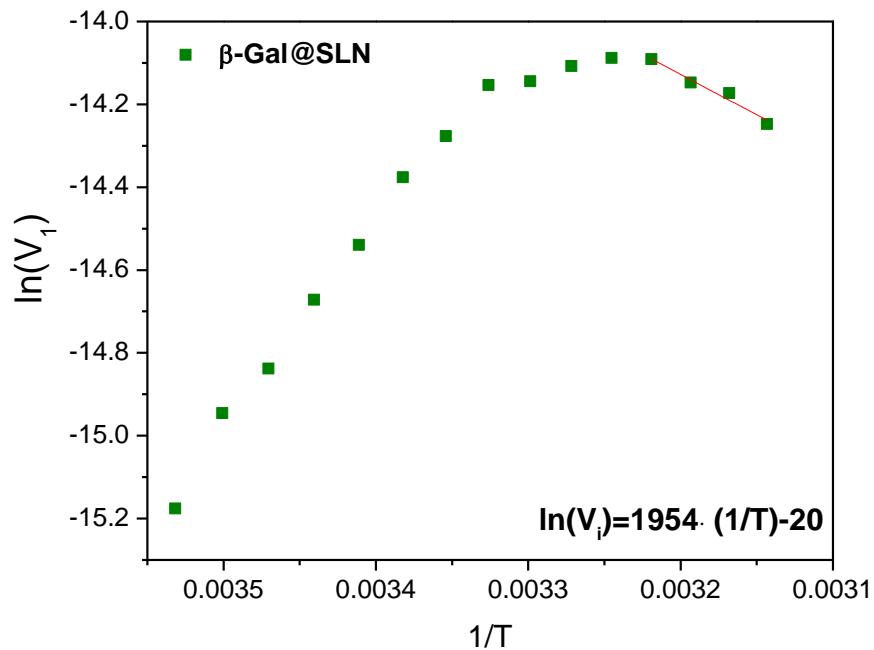


Figure 4. 14. $\ln(V_i)$ vs $1/T$ for the β -Gal@SLN.

As can be observed the enzymatic activity of β -Gal@SLN has the same trend as the enzymatic activity of the free β -Gal and β -Gal+SLN for the region 10-27.5 °C, they increases with the increase of the temperature. On a closer look, it can be observed that in the region between 27.5 °C and 37.5 °C the enzymatic activity slowly increases for β -Gal@SLN. Taking into account that β -Gal+SLN and β -Gal@SLN have the same behavior, this indicates that the enzyme starts to be released from the SLNs. The slope of the regions where the enzyme degrades, temperatures higher than 37.5 °C which represents the optimal temperature for the enzyme were compared. The slope for the degradation of β -Gal@SLN (1954 MKs⁻¹), which is correlated with the enzyme degradation, is 57% smaller than in the case of β -Gal+SLN (3376 MKs⁻¹). The interpretation of this result is that two distinct phenomena occur in the same time, the release of the enzyme combined with the partial inactivation of the enzyme.

4.1.3. Conclusions and perspectives

In this study β -Gal from *Kluyveromyces lactis* was entrapped in thermo-responsive shea butter solid lipid nanoparticles. The SLN formulation was prepared from food grade ingredients, through a safe and low energy method (melt dispersion technique) without organic solvent. The enzyme was encapsulated through a double emulsion affording a loading efficiency of 40% in the SLNs (β -Gal@SLN). According to the *in situ* experiments made under thermal variation, no release of the enzyme was detected at a temperature below 27.5°C, while the carriers are still solid. The UV-visible spectroscopy experiments made on the β -Gal+SLN sample also shown that in presence of the lipid particles, the activity of the enzyme increased by 35% on an interval from 10°C to 45°C, compared to the native activity of the free enzyme in the same range of temperatures. The enhanced enzymatic activity effect was maintained for the sample β -Gal@SLN. Concerning the enzyme release behavior observed for the formulation (β -Gal@SLN), the presence of an increase in activity in the values of V_i starting from 27.5 °C coincided with the melting temperature of the SNLs (28 °C). This means that the encapsulated enzyme in the SLNs is released with the temperature trigger. These results are encouraging for continued investigation towards the formulation of non-toxic carriers for temperature triggered release of enzymes in the human body.

In perspective, the improvement of this delivery system is tied to the melting point of the SLNs. The increase of the melting point from 28°C for the previously described SLNs to a temperature closer to the human body, 37.5°C, could be attained by the addition of a small percentage of food grade fatty acids such as palmitic or stearic acids. These lipids have a higher melting point compare to shea butter, and they present a very good compatibility with triglyceride fatty acids in general^[50]. The resulting future SLNs would present a melting point closer to the body temperature which improved the structural integrity and homogeneity of the carrier until the intestine.

4.2. pH-responsive hybrid silica-alginate carrier for lactose intolerance treatment

Alginate is a polysaccharide biopolymer recognized as biocompatible, food grade and abundant in nature. This linear polymer is an anionic block copolymer composed of 1-4-linked residues of β -D-mannuronic acid block covalently linked to the α -L-guluronic acid block. A large density of the electrostatic interactions between the carboxylate groups ($-\text{COO}^-$) of the α -L-guluronic residues and multivalent cation, like Mg^{2+} , Ca^{2+} or Fe^{3+} the mostly used, lead to the formation of a hydrogel as shown in the Figure 4. 15. The calcium alginate hydrogels are of interest to control and to target a release phenomenon specifically in the gastrointestinal tract, as this polymer is pH sensitive. In fact, at low pH (e.g. stomach), the alginate hydrogel shrinks as the carboxylate groups are been totally protonated ($-\text{COOH}$, $\text{pKa}\sim 3.5$), while above in basic pH (~ 7) the hydrogel swells since most of the carboxyl groups are negatively charged. As a consequence, the alginate chains start to repel each other and water infiltration occurs in the polymer network [51].

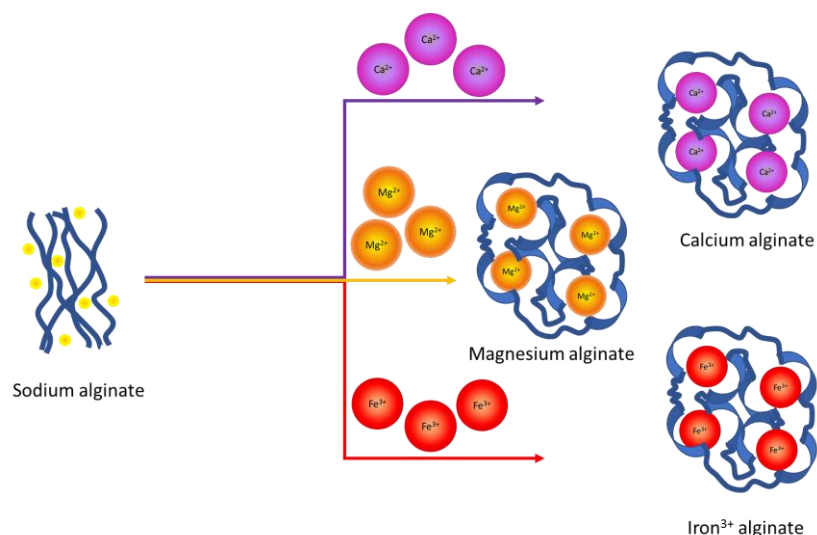


Figure 4. 15. Arrangement of alginate chains in presence of a divalent cations

The enzyme encapsulation procedure is always carried out under very mild conditions. Polysaccharides such as alginate were already utilized to entrap enzymes [53]. The only drawbacks of using a polymeric hydrogel are related to the large pores that can appear in the network which can lead to enzyme leakage [54–56] or to the diffusion of an

acidic solution inside the hydrogel that may denature the enzyme, as it may happen in the stomach.

In order to take advantage of the pH sensitive release mechanism presented by the alginate while mitigating the mass transfer phenomena associated with the polymeric matrix, we propose here the combination of mesoporous silica together with an alginate matrix in the elaboration hybrid organic-inorganic particles. The hybrid organic-inorganic composite materials could combine the advantages of both materials. Many researchers have prepared hybrid silica-polysaccharide composites for enzyme immobilization to improve the mechanical properties of alginate hydrogel. As an example, the alginate/silica biocomposites can be synthesized by impregnation of mesoporous silica particles, such as MCM-41, with alginic acid solution that contained β -galactosidase from *K. fragilis*, followed by the ionic gelation of the biopolymer. The hybrid material exhibited a higher stability upon ageing (kept one week at 5°C) compared with the alginate gel alone [57].

In this work, the β -galactosidase entrapment efficiency was studied and compared for alginate/silica hybrid particles (ASP) and alginate/silica core-shell materials (SAM). Tetramethyl orthosilicate (TMOS) was used as silica precursor, since the methanol that is released during hydrolysis-condensation of the silicon alkoxides is less harmful for the enzyme compared to ethanol, which is released when using tetraethyl orthosilicate source (TEOS) [58].

4.2.1. Particle characterization

The detailed protocol preparation of the two types of hybrid inorganic-organic samples ASP and SAM has been described in Chapter 2. Alginate beads (AP) were prepared to compare physical characteristics of the hybrid material with the organic alginate beads. Once obtained, the materials were lyophilized, as preparation for electron microscopy. The morphology and the structure of alginate, and the core-shell and the hybrid alginate silica particles were assessed by scanning electron microscopy. All the samples kept their form after the immobilization. The AP (Figure 4. 16 A) and ASP (Figure 4. 17 A) materials have a sphere-like form while in the case of SAM (Figure 4. 18 A) the alginate beads seem to be entrapped in a silica network. From the SEM micrographs, the surface of the particles can be closely observed. AP (Figure 4. 16 B) and ASP (Figure 4.

17 B) surface present a similar coarse surface indicating the presence of small particles, while the SAM (Figure 4. 18 B) surface has the appearance of a continuous network.

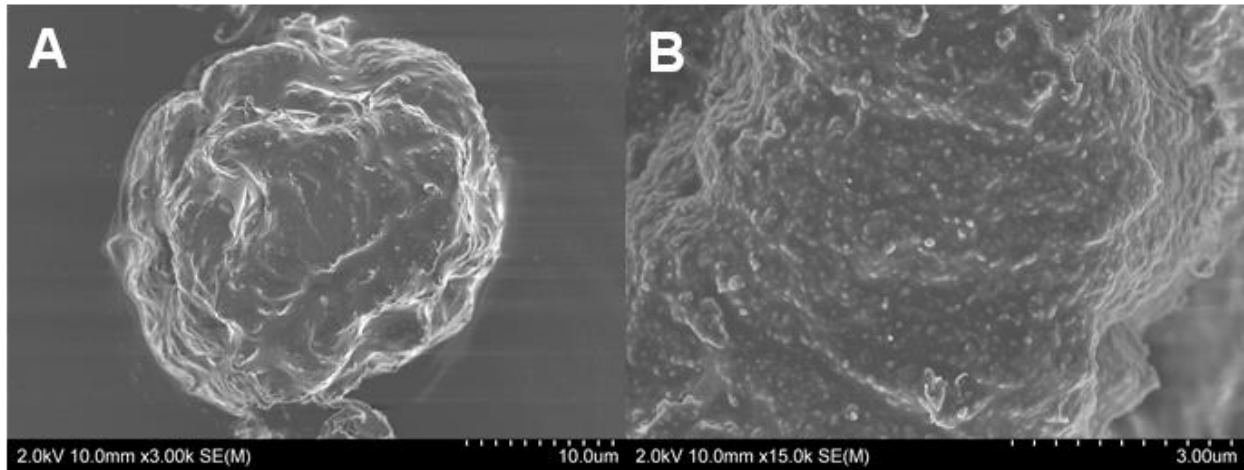


Figure 4. 16. SEM micrographs of (A) alginate particle and (B) zoom on the surface of the material.

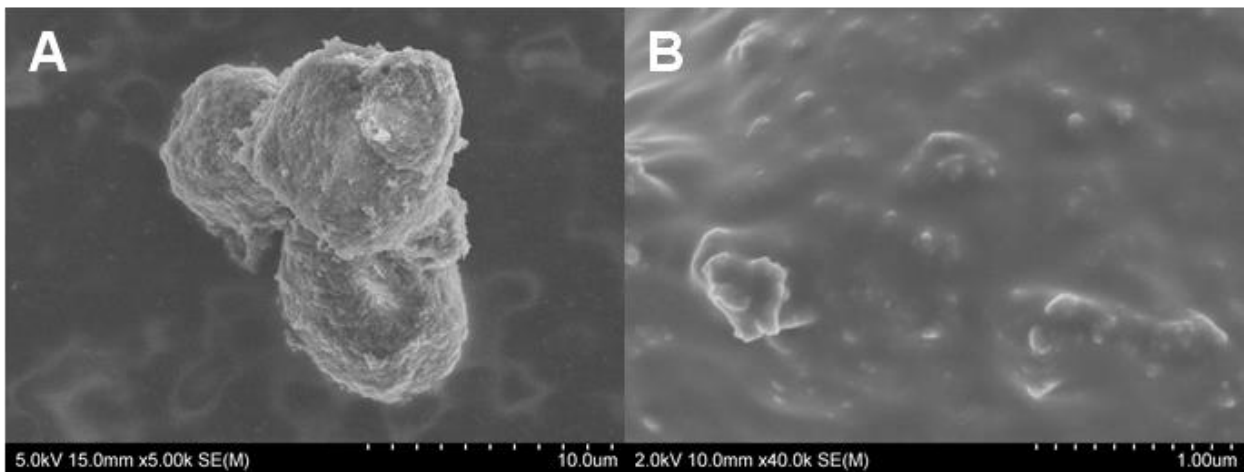


Figure 4. 17. SEM micrographs of (A) hybrid alginate-silica particle (ASP) and (B) zoom on the surface of the material.

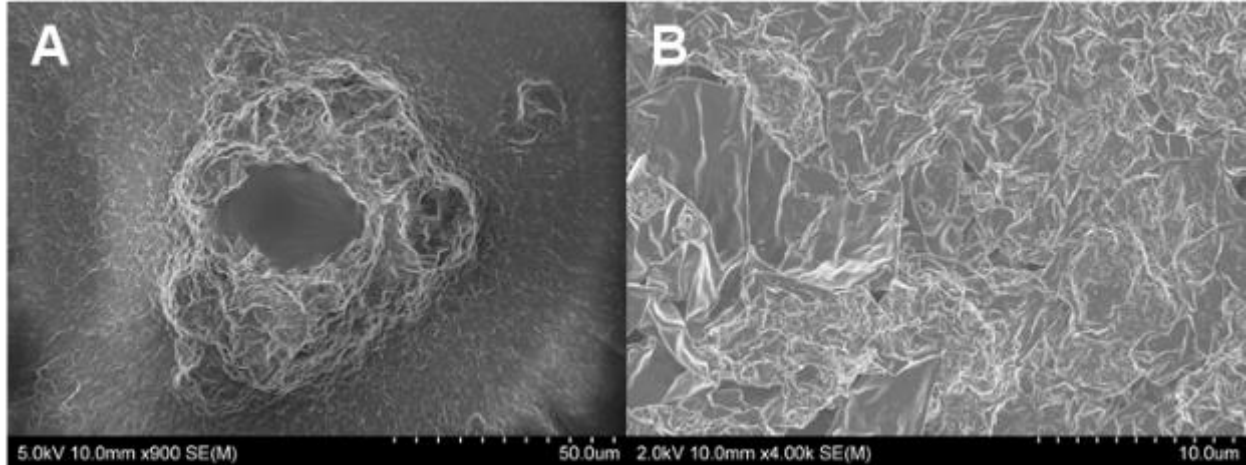


Figure 4. 18. SEM micrographs of (A) the core-shell alginate/silica materials (SAM), (B) zoom on the surface of the material.

The apparent crystals-like structures on the surface of AS and ASP were analyzed by the Energy Dispersive Spectroscopy (EDS) analysis. The imprint of magnesium is present, as are oxygen and silicon as can be observed in Figure 4. 19. As such, the small particles present on the surface of both AS and ASP are the crystallized magnesium salts.

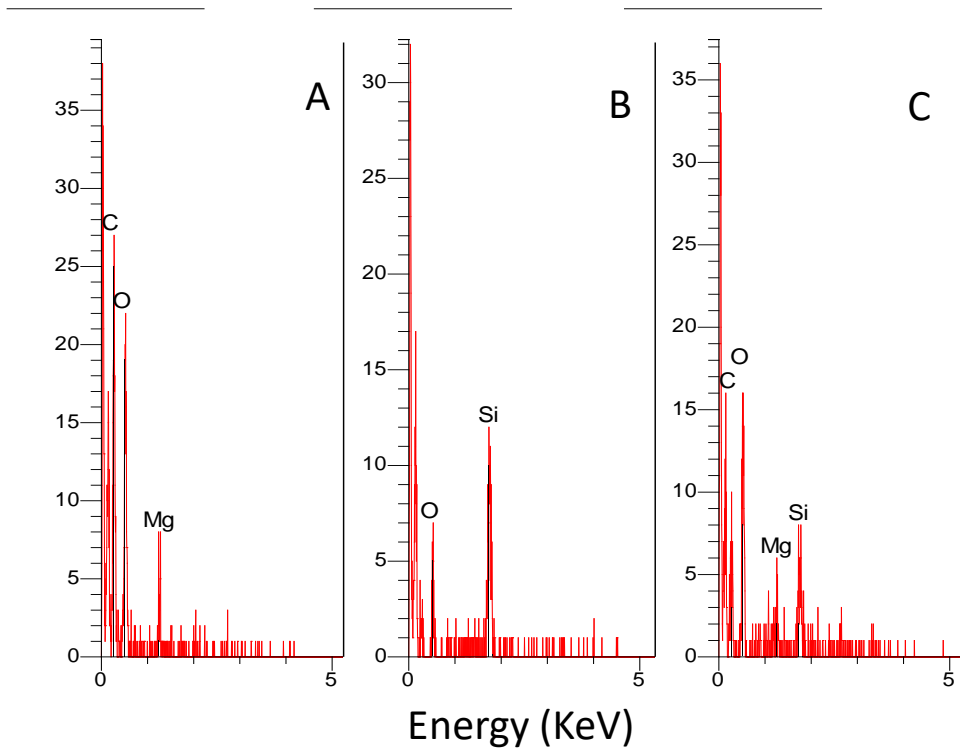


Figure 4. 19. EDS analysis on the AP surface (A) on the ASP surface (B) and on the small particles on the coarse surface.

In order to compare the silica network for ASP and SAM both materials were calcined according to the following ramp settings: 1h at 100°C, 2h at 350°C and 3h at 550°C. After the calcination, all organic compounds are removed. As it can be observed in Figure 4. 20 A the silica that resulted from the ASP forms a continuous network, with small inorganic particles (Figure 4. 20 B). As shown above, these small particles are a mixture of magnesium salt and silica that formed during the synthesis (Figure 4. 19 C). The porous sponge like structure of the silica confirms that the ASP was initially a mixture, and that the alginate and the silica polymerize together.

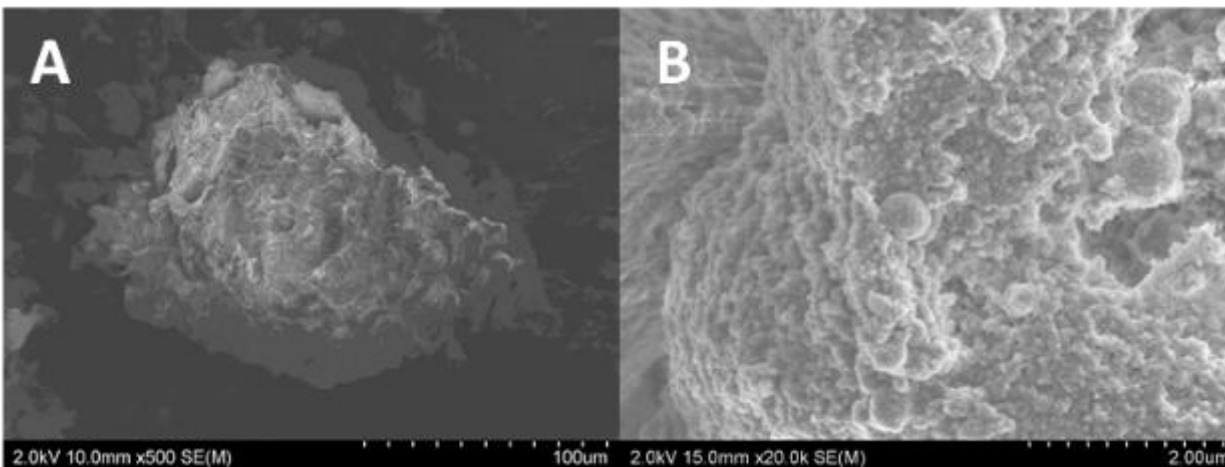


Figure 4. 20. SEM micrographs of calcined ASP (A) and zoom on the surface of the silica material (B).

Compared with the calcinated ASP that is a continuous network, the silica structure remained after calcination of SAM (Figure 4. 21) is a framework displaying sphere-shaped holes. This is the result of the removal of the alginate beads in the calcination process.

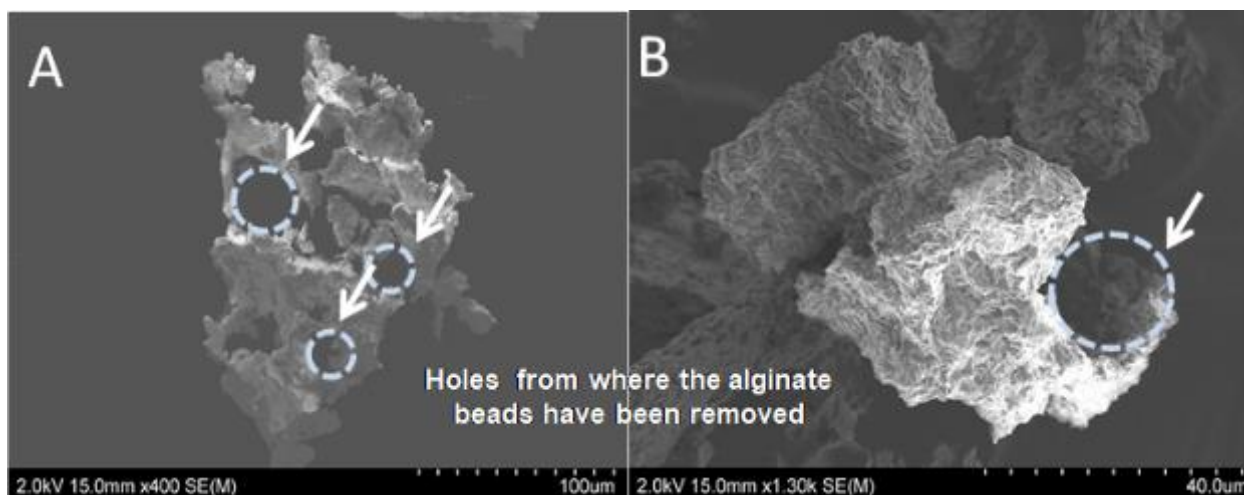


Figure 4. 21. SEM micrographs of calcined SAM (A) and zoom on the silica material (B).

Infrared experiments were carried out on the three materials, AP, ASP and SAM. The spectra are presented in Figure 4. 22 without supplementary processing.

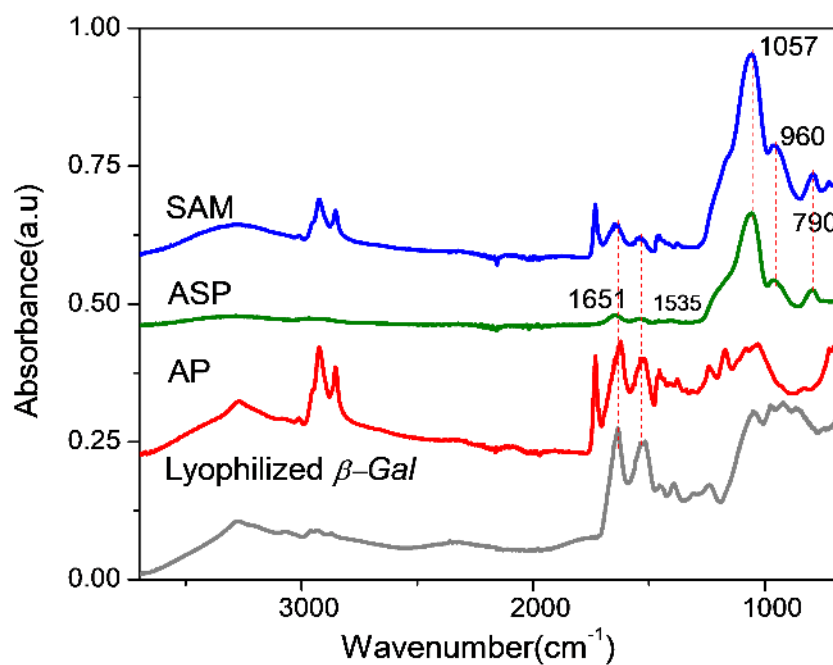


Figure 4. 22. ATR-FTIR spectra of dried enzyme, AP, ASP and SAM.

ATR-FTIR spectra of ASP and SAM display the typical bands of silica the bands at 1057, 960 and 790 cm⁻¹, corresponding to common Si-O-Si and Si-OH stretching described in literature as characteristic of silica materials. At the same time, the bands at

1057 and 790 cm^{-1} can be related to the presence of Si-O-C and C-O-C bonds^[59]. The characteristic bands of the alginate (the ones that do not overlap with the characteristic bands for the enzyme) at 1730 cm^{-1} (corresponding of C=O stretch of COOH) and at 2850 cm^{-1} and 2924 cm^{-1} (corresponding to the C-H stretch) ^[60] can be clearly seen in the SAM spectra. In the ASP spectra, these bands are less well represented, probably indicating strong interactions between silica and the alginate. The presence of 1651 cm^{-1} and 1535 cm^{-1} bands in all three materials indicate the presence of the encapsulated enzyme ^[61].

To confirm the presence of the enzyme, the three materials AP, ASP and SAM were dispersed into a solution containing 1 M NaOH, the standard used to dissolve silica networks, and 0.9 wt% of NaCl, to dissolve the alginate network. These solutions were analyzed with the BCA assays in order to quantify the amount of enzyme (E) entrapped in the different systems. The results are as following:

- in AP sample: 46.500±0.064 mg (E)/g (AP)
- in ASP sample: 106.000±0.001 mg (E)/g (ASP)
- in SAM sample: 619.000±0.006 mg (E)/g (SAM)

The simple alginate beads encapsulated the lowest quantity of enzyme. Comparing the AP and ASP, the hybrid material encapsulated more enzyme. This result is expected, according to the literature^[54], as the alginate gel has a more porous structure and the enzyme can easily leak during the washing step. The SAM material presented the highest load of enzyme. This can be due to the fact that a silica network covers the already formed alginate beads, preventing a leakage and assuring a better encapsulation.

Only the ASP and SAM materials were taken into consideration and analyzed in a simulated gastro-intestinal digestion for two reasons. The high porosity of the alginate promotes a rapid leakage and a fast inactivation of the enzyme in the acidic pH. The second reason is that the isopropanol was used to release the alginate beads from the emulsion and the enzyme most likely loses a part of its activity. That is why the AP material was only used in the physical characterization of the materials.

4.2.2. Enzyme release in gastro intestinal simulated fluids

In order to simulate the passage of the hybrid alginate-silica materials through the gastric system four samples for each ASP and SAM were prepared in separated batches, as described in Chapter 2. In a standard experiment, the silica samples were suspended consecutively in two simulated gastro-intestinal fluids for up to 2h in each: the simulated gastric fluid first (SGF) and the simulated intestinal fluid second (SIF); the suspension was kept under stirring (150 rpm). For each sample, the supernatant recovered after centrifugation, was used to quantify and determine the activity of the enzyme released, while the hybrid materials were used to determine the specific activity of the material.

Table 4. 1 displays the cumulative quantity of enzyme released e.g. after 3H in the simulated gastro-intestinal fluid, the total quantity of enzyme released is the sum of the quantity of enzyme released after 2H in SGF and the quantity of enzyme released after 1H in SIF. The values that are given in the Table 4. 1 are in weight percentage (quantity of enzyme release /initial quantity of enzyme encapsulated per mg of material).

A clear difference in release profiles of ASP and SAM materials was observed. The ASP materials have a very slow release. In SGF (pH 3) almost no release is observed, 0.002 wt % of enzyme is released after the first hour and 0.025 wt% of enzyme is released in the second hour. When added in SIF (pH 7) a steady and (still) slow release is observed, 0.114 wt % in the first hour and 0.195 wt% in the second hour. This means that only 0.205 mg of enzyme was released from 105 mg that was encapsulated per gram of silica during the simulated gastro-intestinal fluid. Conversely more enzyme is released from SAM. This is a clear difference observed from the data. During SAM incubation in SGF (pH 3), 3.83 wt % of enzyme is released in the first hour and 17.61 wt % in the second hour. The release is progressively increased in SIF (pH 7). Then 42.69 wt % is released in the first hour and 82.92 wt % is released in the second hour. This means that almost 520 mg of enzyme was released from 619 mg that was encapsulated per g of silica during the simulated gastro-intestinal fluid.

Table 4. 1. Quantity of enzyme released from ASP and SAM in SGF (pH 3) and SIF (pH 7) in wt%.

	1 h in SGF	2 h in SGF	2 h in SGF and 1h in SIF	2 h in SGF and 2h in SIF
ASP	0.002	0.025	0.114	0.195
SAM	3.83	17.61	42.69	82.92

In order to check if the enzyme released during the simulated digestion kept its activity, the recovered solutions from *in vitro* simulated gastric fluid (SGF) and simulated intestinal fluid (SIF) were analyzed. In terms of activity, the enzyme released from ASP and SAM displays very a different behavior, that are opposite compared with the released profiles. Table 4. 2 presents the enzymatic activity in U/mg of enzyme. The enzyme liberated by SAM along the experiments lost almost all its activity, having 6.7 U/mg after the first hour in SGF decreasing at 0.44 U/mg after the second hour in SGF. When the enzyme is released in SIF fluid (pH 7) the enzyme continues to remain almost inactive. Compared to the enzyme recovered from SAM, the enzyme released from ASP sample still retained part of its reactivity. When added in the acidic pH, the enzyme lost a part of its activity after the first hour continuing to decrease in the second hour when is released in SGF. In SGF (pH=7) the activity of the enzyme remains almost constant.

Table 4. 2. Activity of the enzyme (U/mg) released from ASP and SAM in SGF (pH 3) and SIF (pH 7).

	1 h in SGF	2 h in SGF	2 h in SGF and 1h in SIF	2 h in SGF and 2h in SIF
ASP	1739.131	108.74	37.56	35.75
SAM	6.70	0.44	0.33	0.45

To verify if the enzyme retains a part of its activity during the gastric simulation, the specific activities of the materials used in the experiment were compared with the initial ASP and SAM specific activities (Figure 4. 23). The same phenomenon occurred, as observed in case of the enzyme released, concerning the activity measured for the materials after their incubation in the simulate gastric system as presented in Figure 4. 23 . The graph displays the enzymatic activity of the SAM and ASP materials, compared to the activity of the free enzyme. Both SAM and ASP materials start losing their activity after the first hour in SGF (pH 3) and continue to decrease after the second hour in the acidic pH. Compared with ASP activity, the SAM activity does not increase when the

materials are inserted in a basic pH. The activity of the free enzyme follows the same trend as the activity of the SAM materials.

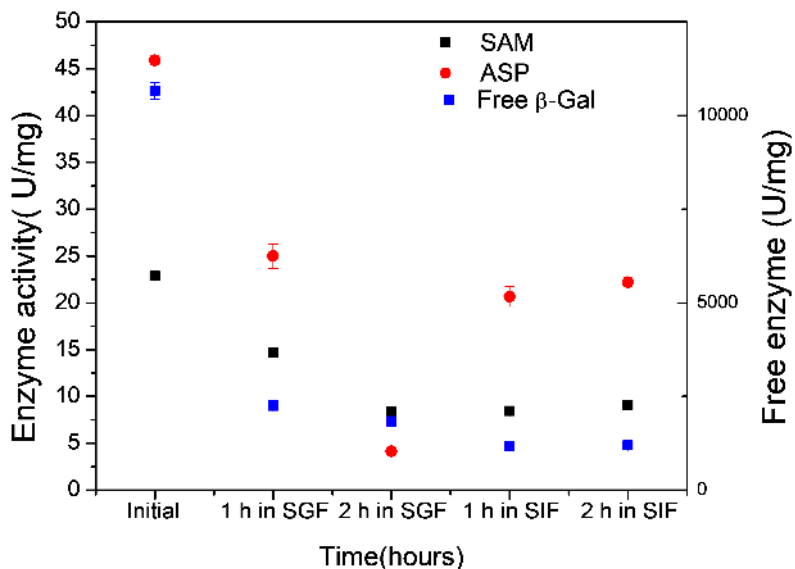


Figure 4. 23. Activity of silica materials after a stay in the simulated gastro-intestinal fluids (SGF and SIF) (on the left Y axe) compared with the activity of the free enzyme (on the right Y axe).

This concludes that, although the SAM material can encapsulate a larger quantity of enzyme and presents a better release compared with ASP materials, the SAM materials are unable to protect the enzyme from the acidic pH. The ASP materials can better protect the encapsulated enzyme, but the tight network hinders the release. The typical use of this type of materials is in catalysis, where they constitute enzyme supports. The supports provide a well-protected environment for the enzyme, hindering its leakage during the process and during the repeatability cycles [54,62]. The results of our experiments are in good accord with this fact.

4.2.3. Conclusion and perspectives

Enzyme-encapsulated core-shell alginate/silica (SAM) and hybrid alginate silica materials (ASP) were synthesized by direct emulsion (*water-in-oil* type emulsion). The encapsulated enzyme presented a higher release from SAM, but with a rapid decrease of its activity in acidic pH. In the case of SAM, the trigger pH worked correctly, the material presenting a low release in acidic pH and a high release at neutral pH, however the natural inactivation of both the released and the encapsulated enzyme in the acidic pH

occurred. The ASP encapsulated enzyme presents a slow release during the incubation in the simulated gastro-intestinal fluids, but an increase of specific activity of the material was noticed when introduced into basic pH. The activity of the ASP liberated enzyme along the 4h is much greater than in the case of SAM. The very slow liberation of the enzyme, coupled with the protection from pH inactivation propose the ASP materials as a viable biocatalyst option for the removal of lactose in the dairy industry. As a perspective towards a better triggering at basic pH values the modification of the silica composition is envisioned. For example the insertion of NH₂ moieties in the silica structure via (3-Aminopropyl)triethoxysilane (APTES) could act as basic poles for the local increase of pH. This design change might allow the protection from inactivation of the enzyme over the acidic pH range.

Bibliography

- [1] C. Bernal, L. Sierra, M. Mesa, *ChemCatChem* **2011**, 3, 1948–1954.
- [2] M. C. Horn, *Methods and Compositions for Retarding the Staling of Baked Goods*, **2003**, EP1533840 B1.
- [3] M. Vinceković, M. Viskiđ, S. Juriđ, J. Giacometti, D. Bursać Kovačević, P. Putnik, F. Donsi, F. J. Barba, A. Režek Jambrak, *Trends Food Sci. Technol.* **2017**, 69, DOI 10.1016/j.tifs.2017.08.001.
- [4] F. Kayaci, T. Uyar, *Food Chem.* **2012**, 133, 641–649.
- [5] V. Nedovic, A. Kalusevic, V. Manojlovic, S. Levic, B. Bugarski, *Procedia Food Sci.* **2011**, 1, 1806–1815.
- [6] D. Dale, *Microencapsulation in the Food Industry*, Elsevier, **2014**.
- [7] C. Acosta, E. Pérez-Esteve, C. A. Fuenmayor, S. Benedetti, M. S. Cosio, J. Soto, F. Sancenón, S. Mannino, J. Barat, M. D. Marcos, et al., *ACS Appl. Mater. Interfaces* **2014**, 6, 6453–6460.
- [8] P. de Vos, M. M. Faas, M. Spasojevic, J. Sikkema, *Int. Dairy J.* **2010**, 292–302.
- [9] M. Chávarri, I. Marañón, M. C. Villarán, *Probiotics* **2012**, 501–540.
- [10] A. K. Patel, R. R. Singhanian, A. Pandey, *Curr. Opin. Food Sci.* **2016**, 7, 64–72.
- [11] P. Walde, S. Ichikawa, *Biomol. Eng.* **2001**, 18, 143–177.
- [12] A. C. Pierre, *Biocatal. Biotransformation* **2004**, 22, 145–170.
- [13] E.-M. Dusterhoft, M. Minor, K. Nikolai, N. Hargreaves, Simon Huscroft, U. Scharf, *Encapsulated Functional Bakery Ingredients*, **2006**, US20060110494 A1.
- [14] N. A. Solomon, *Lactase Formulations*, **2013**, US20130058913 A1.
- [15] B. Gibbs, S. Kermasha, I. Alli, C. Mulligan, *Int J Food Sci Nutr.* **1999**, 50, 213–224.
- [16] R. A. Sheldon, *Adv. Synth. Catal.* **2007**, 349, 1289–1307.
- [17] N. Carlsson, H. Gustafsson, C. Thörn, L. Olsson, K. Holmberg, B. Åkerman, *Adv. Colloid Interface Sci.* **2014**, 205, 339–60.
- [18] B. Innovation, *Bioencapsulation Innov.* **2013**, 1–24.
- [19] P. Severino, T. Andreani, A. S. Macedo, J. F. Fangueiro, M. H. A. Santana, A. M. Silva, E. B. Souto, *J. Drug Deliv.* **2012**, 2012, 750891.
- [20] S. Morel, E. Ugazio, R. Cavalli, M. R. Gasco, *Int. J. Pharm.* **1996**, 132, 259–261.
- [21] P. Ganesan, D. Narayanasamy, *Sustain. Chem. Pharm.* **2017**, 6, 37–56.
- [22] A. J. Almeida, E. Souto, *Adv. Drug Deliv. Rev.* **2007**, 59, 478–90.
- [23] H. Reithmeier, J. Herrmann, A. Göpferich, *J. Control. Release* **2001**, 73, 339–350.
- [24] M. García-Fuentes, D. Torres, M. J. Alonso, *Colloids Surfaces B Biointerfaces* **2003**, 27, 159–168.
- [25] M. Trotta, R. Cavalli, M. E. Carlotti, L. Battaglia, F. Debernardi, *Int. J. Pharm.* **2005**, 288, 281–288.
- [26] M. Gallarate, M. Trotta, L. Battaglia, D. Chirio, *J. Microencapsul.* **2009**, 26, 394–402.
- [27] C. Qi, Y. Chen, Q.-Z. Jing, X.-G. Wang, *Int. J. Mol. Sci.* **2011**, 12, 4282–93.
- [28] C. Qi, Y. Chen, J.-H. Huang, Q.-Z. Jin, X.-G. Wang, *J. Sci. Food Agric.* **2012**, 92, 787–93.
- [29] I. K. Voets, W. a Cruz, C. Moitzi, P. Lindner, E. P. G. Arêas, P. Schurtenberger, *J Phys Chem B* **2010**, 114, 11875–11883.
- [30] W. Mehnert, K. Mader, *Adv. Drug Deliv. Rev.* **2001**, 47, 165–196.
- [31] M. Liu, H. Du, W. Zhang, G. Zhai, *Mater. Sci. Eng. C* **2017**, 71, 1267–1280.
- [32] K. Yong, S. Hong, **2007**, 32, 669–697.
- [33] B. J. Sun, H. C. Shum, C. Holtze, D. A. Weitz, *ACS Appl. Mater. Interfaces* **2010**, 2, 3411–3416.
- [34] M. Depardieu, M. Nollet, M. Destribats, V. Schmitt, R. Backov, *Part. Part. Syst. Character.* **2013**, 30, 185–192.
- [35] M. Nollet, M. Depardieu, M. Destribats, R. Backov, V. Schmitt, *Part. Part. Syst. Character.* **2013**, 30, 62–66.
- [36] F. G. Honfo, N. Akissoe, A. R. Linnemann, M. Soumanou, M. A. J. S. Van Boekel, *Crit. Rev. Food Sci. Nutr.* **2014**, 54, 673–86.
- [37] L. N. M. Ribeiro, M. C. Breitzkreitz, V. A. Guilherme, G. H. R. da Silva, V. M. Couto, S. R. Castro, B. O. de Paula, D. Machado, E. de Paula, *Eur. J. Pharm. Sci.* **2017**, 106, 102–112.
- [38] H. A. Hassan, M. Florentin, B. N. I. Sandrine, D. Pierrick, J. Jordane, L. Michel, *Eur. J. Lipid Sci. Technol.* **2015**, n/a-n/a.
- [39] R. P. Raffin, A. Lima, R. Lorenzoni, M. B. Antonow, C. Turra, M. P. Alves, S. B. Fagan, *J. Biomed. Nanotechnol.* **2012**, 8, 309–15.
- [40] A. Cortial, M. Vocanson, E. Loubry, S. Briançon, *Flavour Fragr. J.* **2015**, 30, 467–477.
- [41] I. P. Kaur, R. Agrawal, *Recent Pat. Drug Deliv. Formul.* **2007**, 1, 171–182.
- [42] F. Suter, D. Schmid, F. Wandrey, F. Züllig, *Eur. J. Pharm. Biopharm.* **2016**, 108, 304–309.
- [43] H. Bunjes, M. H. J. Koch, K. Westesen, *Langmuir* **2000**, 16, 5234–5241.
- [44] R. A. Robinson, A. Peiperl, **1981**, 2572, 1–2.
- [45] K. Selmeczi, C. Michel, A. Milet, I. Gautier-luneau, C. Philouze, J. Pierre, D. Schnieders, A. Rompel, C. Belle, *Chem. - A Eur. J.* **2007**, 9093–9106.
- [46] H. Zhang, L. Wang, Q. Shen, B. Wu, P. Gao, *Acta Biochim. Biophys. Hung.* **2011**, 43, 409–417.
- [47] M. E. Peterson, R. M. Daniel, M. J. Danson, R. Eisenhal, *Biochem. J.* **2007**, 402, 331–337.
- [48] Z. Quinn Z.K, C. Xiao Dong, *Biochem. Eng. J.* **2001**, 9, 33–40.

- [49] T. Zoungrana, G. H. Findenegg, W. Norde, *Prog. Biotechnol.* **1998**, *15*, 495–504.
- [50] D. Valeri, A. J. A. Meirelles, *J. Am. Oil Chem. Soc.* **1997**, *74*, 1221–1226.
- [51] Z. Zhang, R. Zhang, L. Chen, Q. Tong, D. J. McClements, *Eur. Polym. J.* **2015**, *72*, 698–716.
- [52] K. Kashima, I. Masanao, in *Adv. Desalin.*, **2012**, pp. 3–36.
- [53] T. Haider, Q. Husain, *Int. J. Biol. Macromol.* **2007**, *41*, 72–80.
- [54] Y. Lu, Z. yi Jiang, S. wei Xu, H. Wu, *Catal. Today* **2006**, *115*, 263–268.
- [55] A. Blandino, M. Maci, D. Cantero, M. Macías, *Mac, Enzyme Microb. Technol.* **2000**, *27*, 319–324.
- [56] A. Blandino, M. Macias, D. Cantero, *Proc. Biochem.* **2001**, *36*, 601–606.
- [57] T. Coradin, J. Livage, *Comptes Rendus Chim.* **2003**, *6*, 147–152.
- [58] D. Avnir, T. Coradin, O. Lev, J. Livage, *J. Mater. Chem.* **2006**, *16*, 1013–1030.
- [59] G. E. Chernev, B. I. Samuneva, P. R. Djambaski, I. M. M. Salvado, H. V. Fernandes, *Cent. Eur. J. Chem.* **2006**, *4*, 81–91.
- [60] G. Lawrie, I. Keen, B. Drew, A. Chandler-Temple, L. Rintoul, P. Fredericks, L. Grøndahl, *Biomacromolecules* **2007**, *8*, 2533–2541.
- [61] I.-A. Pavel, S. F. Prazeres, G. Montalvo, C. García Ruiz, V. Nicolas, A. Celzard, F. Dehez, L. Canabady-Rochelle, N. Canilho, A. Pasc, *Langmuir* **2017**, *33*, 3333–3340.
- [62] S. Xu, Z. Jiang, Y. Lu, H. Wu, W. Yuan, **2006**, 511–517.

General Conclusions and Perspectives

Designing biocatalyst and smart enzyme delivery systems remains a challenge for the food industry. Thus, the main goal of this PhD work was to investigate new formulation methods, to design bio-responsive carriers of interest for catalysis in food production, and for the elaboration of solid dairy lactase supplements.

This work presented the investigation pathways and the interpretation results of the chemical properties and responsive behaviors of four different carriers for the β -galactosidase immobilization. The formulation routes chosen were mainly based on two types of enzyme immobilization strategies: the physical adsorption and the entrapment. All the carriers obtained apply to two types of physiological stimuli, either the pH found in the small intestine or to body temperature.

Among the organic and inorganic matrix supports, the physical adsorption of enzymes was widely done on amorphous silica supports since 2001. Porosity is a parameter that can afford a high loading material. That is why, as discussed in Chapter 3, amorphous silica materials with hierarchical meso-macroporosity were used as β -galactosidase supports building the design and fabrication of a bio-catalyst. A series of enzyme-supported catalysts were prepared from different concentrations of free β -galactosidase (e.g. enzyme feed solutions). The enzymatic activity of the bio-catalyst was determined as a function of the loading degree. Surprisingly, it was observed that a selective adsorption of the enzyme in hierarchical meso or macropores occurred. Based on enzyme dimensional simulations it was hypothesized that, at low enzyme feed solution concentrations, the adsorption of the lactase took place preferentially in the mesopores as dimers or monomers, while the tetrameric form was adsorbed in the macropores. Consequently, a bio-catalyst prepared from high concentration enzyme feed solution yielded the lowest loading degree. However, this catalyst presented the highest enzymatic activity.

In Chapter 3, another silica based carrier was designed as a pH responsive system, that would retain the lactase in the gastric fluid but to release it in the small intestine fluid, based on the change in pH. β -galactosidase was physically adsorbed on

low-porosity micrometric silica beads. The beads were then covered by a biocompatible coating of 1,2-dioleoyl-*sn*-glycero-3-phosphocholine (DOPC) liposomes. This formulation strategy afforded liposome-coated silica particles with a controlled release pattern over gastric to intestinal pH (pH3 to pH7). Interestingly, the presence of liposomes also proved to be a protective coating against acidic pH, preventing the denaturation of the adsorbed enzyme. The obtained results recommend employing this type of formulation as a promising carrier for the release of lactase in the small intestine.

Chapter 4 covered the formulation of stimuli-responsive carriers prepared in the context of enzyme entrapment strategies. The first approach was to entrap lactase in food-grade solid lipid nanoparticles (SLN) through a water/oil/water double emulsion. The advantage of using a low melting point solid lipid, shea butter, conferred a thermal response to the carrier. The carrier would melt slowly around body temperature affording the release of the enzyme. The enzyme was encapsulated into this type of nanoparticles (up to 40% loading efficiency), via the inner water phase of a double emulsion. This procedure limits its diffusion and ensures its protection. The enzyme release kinetic was followed by in situ UV-vis spectrophotometry under a thermal range control (10°C to 45°C), an innovative way according to literature. The enzymatic activity of three types of samples (free β -Gal, β -Gal+SLN, β -Gal@SLN) were measured in order to determine the thermal threshold release and the activity of the enzyme in presence of the SLN. By this analytical method, the starting temperature release was detected at 27.5°C. The activity of the enzyme freed from the SLN, increased by 35% compared to free enzyme. Given the precise temperature of release and the reproducibility of the results, such a carrier could be adjusted for body temperature triggered release, and further, could serve as a reliable delivery system for β -Galactosidase.

The entrapment of lactase in a hybrid carrier that combined alginate gels and silica was investigated and the results were presented in the second part of Chapter 4. This approach aimed to design a high loaded pH responsive carrier, that can protect the enzyme from the gastric fluids, while allowing its delivery in the small intestine. The protection and release properties of two types of carriers prepared via emulsions were investigated and compared, core-shell alginate/silica and hybrid alginate-silica materials. According to the results, the hybrid alginate-silica carrier presented a slower release of

the enzyme. It displayed a higher activity and a good prevention against acidic pH inactivation.

The different types of carriers obtained by the defined formulation strategies are promising candidates in overcoming some challenges of the food industry. There are some general perspectives can still be explored in order to improve this work. Regarding silica supported enzyme catalyst incased in the phospholipid liposome layer, the main drawback of that carrier is its weak loading degree. This point could be improved by using porous silica supports presenting higher pore sizes relative to the enzyme dimension. Another strategy could be changing the lipid nature or type. This type of carrier may allow a triggered release, based on body temperature.

In the case of the SLN based carrier, the improvement of this delivery system is tied to the melting point of the lipid (mp). A very good correlation between this and enzyme release was already achieved. The increase from 32.5°C melting point of shea butter to 37.5°C, human body temperature could be attained by the addition of a small percentage of fatty acid. Palmitic or stearic acids have high melting points, they are safe for human consumption and present a very good compatibility with other fats. The resulting SLNs would present a higher overall melting point and would keep their structural integrity and homogeneity.

Another strategy would be the formation of a shell of silica around the SLN. An interesting opportunity is to replace the surfactant for the formation of the double emulsion with silica nanoparticles, to form a Pickering emulsion. A Pickering emulsion is the emulsion stabilized by solid particles, such as silica nanoparticles. The particles act by being adsorbed irreversibly at the interface of two phases and reduce the interfacial tensions.

A brief exploration of this principle has already been done, applied directly on this subject by using silica nanoparticles to stabilize SLNs. Thus, in order to form an inverse emulsion, the silica nanoparticles had to be partially hydrophobized. For this, stabilizing HDK[®] T40 hydrophilic fumed-silica nanoparticles (NPs) purchased from Wacker (Germany), were modified with stearic acid. Using the modified NPs and a hard oil at room temperature, Witocan P (kindly provided by Palsgaard) a solid lipid nanoparticles dispersion, stabilized by NPs was obtained, as shown the figure below. This type of SLN

Pickering-like stabilized suspension, presented a very good preservation of structural integrity, which is the first criterium of enzyme entrapment. As a preliminary result, this finding is very encouraging towards this strategy.

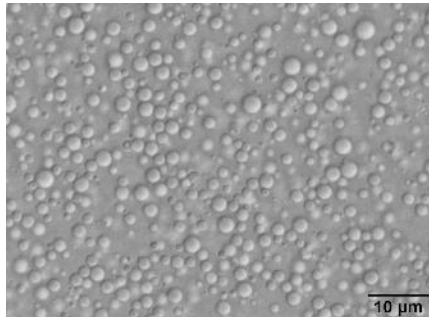


Figure 1. Witocan P solid lipid nanoparticles dispersion stabilized by Pickering emulsion

This work aims to prove that enzymatic catalysis is a thing of the present, and that it can be adapted to any specific challenges. During this project, we tried to showcase the variety and richness of possibilities of encapsulation techniques. Four distinct types of systems have been designed and characterized, with the goal to emphasize how each certain method can accommodate different requirements of the material. My hope is that this work will contribute to the further development of supported enzymatic catalysis and to that of smart foods.

Conclusions générales et perspectives

La conception de biocatalyseurs et de systèmes intelligents pour la libération d'enzymes, restent un défi pour l'industrie alimentaire. Ainsi, l'objectif principal de ce travail de doctorat était d'élaborer de nouvelles méthodes de formulation pour la conception de transporteurs bio-sensibles d'intérêt pour la catalyse de la réaction d'hydrolyse du lactose et ainsi élaborer des suppléments solides de lactase pour l'industrie agroalimentaire.

Ce travail a montré les voies de recherche et la caractérisation des propriétés chimiques et les comportements bio-sensibles de quatre systèmes de transport conçu pour l'immobilisation de β -galactosidase. Tous les systèmes de transport obtenus présentent des réponses à deux types de stimuli physiologiques, soit la température soit le pH. De plus, les voies de formulation choisis étant dictées par deux types de stratégies d'immobilisation d'enzyme : l'adsorption physique et l'emprisonnement.

Parmi les matrice supports, organiques et inorganiques, l'adsorption physique des enzymes était faite largement sur les supports de silice amorphe depuis 2001. Le degré et la nature de la porosité sont des paramètres qui permettent d'atteindre un taux d'adsorption important dans le matériau. C'est pourquoi, comme discuté au chapitre 3, les matériaux de silice amorphe avec une méso-macro porosité hiérarchique, ont été utilisés comme support pour l'élaboration d'un biocatalyseur. Une série de catalyseurs supportés a été préparée à partir de différentes concentrations de β -galactosidase (solutions « feed » d'enzyme). L'activité enzymatique du catalyseur a été déterminée par rapport au degré d'adsorption en enzyme. Curieusement, une adsorption sélective d'enzyme dans les méso-macro pores hiérarchiques a eu lieu. A partir de simulations dimensionnelles de l'enzyme, les hypothèses suivantes ont été émises : à une concentration faible de solution enzymatique l'adsorption de la lactase se passe préférentiellement dans les mésopores sous la forme de dimers ou de monomères, alors que la forme tétramérique est préférentiellement adsorbée dans les macropores à plus haute concentration. En conséquence, un biocatalyseur préparé à une concentration élevée en enzyme présentait le degré minimum de chargement, néanmoins ce catalyseur avait une plus grande activité enzymatique étant donné que le tétramère est la forme la plus active.

Dans le chapitre 3, un autre transporteur à base de silice a été conçu pour être sensible au pH physiologique, et protéger la lactase dans le fluide gastrique mais permettre sa libération dans l'intestin grêle. Ainsi, après l'adsorption physique sur des billes micrométriques de silice avec une faible porosité, les billes ont été couvertes par une couche biocompatible de liposomes à base de 1,2-dioleoyl-*sn*-glycero-3-phosphocholine (DOPC). Cette stratégie de formulation a généré des particules de silice enrobées de liposomes, montrant une libération contrôlée au pH intestinal (pH7). De façon intéressante d'après les résultats, la présence des liposomes a joué le rôle d'une couche protectrice à pH acide, empêchant ainsi la dénaturation de l'enzyme immobilisée. A partir des résultats obtenus, ce type de formulation peut conduire à l'élaboration d'un transporteur prometteur pour la libération de la lactase dans l'intestine.

Le chapitre 4 décrit la formulation de transporteurs dans lesquels la stratégie d'emprisonnement de l'enzyme a été choisie. La première approche était tout d'abord l'emprisonnement de la lactase dans les nanoparticules solides lipidiques (SLNs) par une double émulsion eau/huile/eau. L'usage de SLN assurait la libération de l'enzyme par un stimuli thermique, la température du corps humain. Le taux d'encapsulation dans les nanoparticules a été déterminé allant jusqu'à 40% dans la phase intérieure de l'émulsion double qui limite sa diffusion et assure sa protection. La cinétique de libération de l'enzyme a été suivie in situ par spectrophotométrie UV-vis dans un intervalle de température allant de 10°C to 45. Cette méthodologie a été très peu explorée d'après la littérature. L'activité enzymatique pour trois types d'échantillons (β -Gal libre, β -Gal+SLN, β -Gal@SLN), a été mesurée pour déterminer la limite thermique de libération et l'activité de l'enzyme en présence des SLNs. Par cette méthode analytique, le début de libération a été détectée à 27.5°C et l'activité de l'enzyme libre en présence des SLNs a été quantifiée à 35% supérieur à l'enzyme seule en solution. D'après ces résultats, un tel transporteur pourrait être reformulé pour obtenir une libération de la de β -Galactosidase à la température du corps.

Finalement, l'emprisonnement de la lactase dans un transporteur hybride qui combine l'alginate et la silice a aussi été étudié et présenté dans le Chapitre 4. Cette approche a visé la conception un transporteur hautement chargé en enzyme qui répondrait au pH pour ainsi protéger l'enzyme du fluide gastrique mais permet sa livraison

dans l'intestin. Les propriétés de protection et de libération pour deux types de transporteurs également produits à partir d'émulsions ont été investigués et comparés. Les deux types de transporteurs sont les suivants : core/shell alginate/silice et hybride alginate-silice. D'après les résultats, le transporteur hybride alginate-silice a présenté une libération plus lente de l'enzyme, une activité supérieure et une meilleure protection contre le pH acide que le système core/shell alginate/silice.

Les deux types de transporteurs fabriqués par la voie d'émulsion sont prometteurs pour remplir les défis de l'industrie alimentaire. Cependant, les perspectives suivantes peuvent être explorées pour améliorer ce travail.

Concernant l'enzyme supportée par les billes de silice enrobées de la couche de liposomes phospholipidiques, l'inconvénient majeure de ce transporteur est le faible degré d'adsorption d'enzyme. Ce point pourrait être amélioré par l'usage de supports sphériques avec un volume libre plus important et une dimension de pores supérieure à la taille de l'enzyme.

En perspective, l'amélioration dans le cas des transporteurs à base de SLNs est liée du point de fondre. Une très bonne corrélation entre la température de fusion et la libération de l'enzyme a été déterminé. L'incrément de 4°C, du point de fusion du beurre de karité par l'ajout d'acide gras tels que l'acide palmitique ou l'acide stéarique, permettrait d'induire le relargage de l'enzyme à la température du corps humain. Les SLNs résultants présenteraient un point de fusion global plus élevé tout en gardant leur homogénéité et intégrité structurale.

Une autre stratégie pour favoriser l'adhésion des SLN à l'intestin serait la formation d'une couche de silice autour des SLN. Une voie facile est le remplacement du surfactant pour la formation de la double émulsion par des nanoparticules de silice, pour former une émulsion Pickering. Une émulsion Pickering est une émulsion stabilisée par des particules solides, comme les nanoparticules de silice. Les particules sont absorbées irréversiblement à l'interface entre les deux phases liquides, réduisant ainsi les tensions interfaciales.

Une courte exploration a été faite en utilisant des nanoparticules de silice hydrophiles de type HDK[®] T40. Cependant pour former une émulsion inverse les particules de silice ont été hydrophobisées au préalable par des chaînes d'acide

stéarique. Dans ce travail d'exploration, les SLNs ont été préparés à partir de WitocanP (également une graisse solide à température ambiante). Puis une dispersion de SLNs stabilisés par des nanoparticules a été obtenue comme présenté dans la figure ci-dessous. La suspension obtenue était très stable ce qui présage un emprisonnement efficace de l'enzyme dans les SLN.

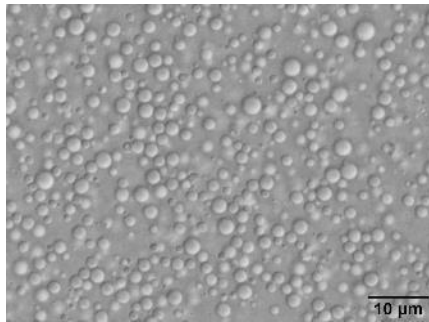


Figure 1. Witocan P dispersion de nanoparticules lipidiques solides stabilisées par le principe de l'effet Pickering

Ce travail aspire à démontrer que la catalyse enzymatique est une chose pour maintenant, et qu'elle peut être adaptée pour des défis caractéristiques. Durant ce projet, on a essayé à présenter une variété des possibilités pour l'encapsulation des enzymes. Quatre types de systèmes ont été conçu et caractérisés, avec le but a souligné comme chaque méthode particulière peut être accommodé les demandes particulières de chaque matériau. Mon espoir est que ce travail va contribuer pour le développement futur de la catalyse enzymatique et pour la nourriture intelligente (smart foods).

Appendix 1 Techniques of characterization

DLS

Dynamic light scattering (DLS) (also known as Quasi- Elastic Light Scattering or Photon Correlation Spectroscopy) is a technique allowing the evaluation of particle size and size distribution of emulsions, micelles, polymers, proteins, nanoparticles and colloids. The sample is illuminated by a laser beam and the time-dependent fluctuations of the scattered light are detected at a known scattering angle θ (90° in our case) by a photon detector. The particles undergo a random motion due to thermal agitation (or Brownian motion) leading to the scattering of light in all directions. This motion results in fluctuations of the distances between the particles, and hence also in fluctuations of the phase relations of the scattered light waves. Additionally, the number of particles within the scattering volume may also vary in time. All the fluctuating scattered intensity is recorded and mathematically treated to plot a so-called correlation function from which a diffusion coefficient (D) of the scatters is determined. Then with the Stockes-Einstein equation, the hydrodynamic radius (R_H) of the particles is calculated:

$$R = \frac{k_b T}{6\pi\eta D}$$

with k_B the Boltzmann constant, T the absolute temperature, η the viscosity of the continuous medium and D the diffusion coefficient.

Small angle X-ray scattering (SAXS)

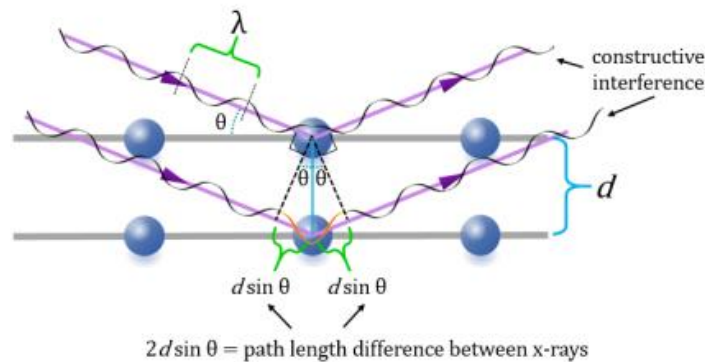
Small angle X-ray scattering (SAXS) is a technique able to indirectly define the size, the shape and the internal structure of samples being powder, fibers, colloidal dispersions of solid particles, peptides, polymers or nanostructured systems. The dimensional detection size range extends from 1 to 100 nm. This technique is based on the differences of scattering intensity induced by electron densities variation between the scatters and the continuous medium. The diffusion intensity curves $I(q)$ is usually represented as a function of the scattering vector, q

$$q = \frac{4\pi \sin \theta}{\lambda}$$

where θ is the scattering angle and λ is the X-ray beam wavelength. The diffusion of the X-ray waves gives a scattering pattern following Bragg's law. When an intense scattering is observed at small angles it means that the distance between the electrons is large. If there is a periodic arrangement in the sample or a monodisperse size, a multiple scattering pattern is recorded.

$$2d_{h,k,l} \sin \theta = n\lambda$$

where $d_{h,k,l}$ is the repetition distance, θ is the diffraction semi-angle, n is the reflection order, λ is the X-ray wavelength.



The dimensional and structural parameters of the studied system are given by the relationship between the repeat distances determined mathematically from the Bragg reflection patterns.

Nitrogen sorption analysis

Adsorption is a surface phenomenon consisting of the physical adhesion of atoms, ions, or molecules from a gas, liquid, or dissolved solid (adsorbate) to a surface (adsorbent) through Van der Waals forces.

The nitrogen adsorption-desorption technique provides information about the

texture characteristics of a solid e.g. surface area, pore size and pore size distribution. Usually, the probing adsorbate used is N₂ with a boiling temperature of 77K. Under controlled pressure, the gaseous molecules adsorbed to the material in layers. According to Brunauer, Emmett and Teller theory (BET) which is an extension of Langmuir theory, adsorbate gas molecules are more realistically adsorbed in multilayers.

The quantity of adsorbed gas is plotted as a function of the equilibrium pressure (P/P_0). According to IUPAC the isotherms are classified according to six types:

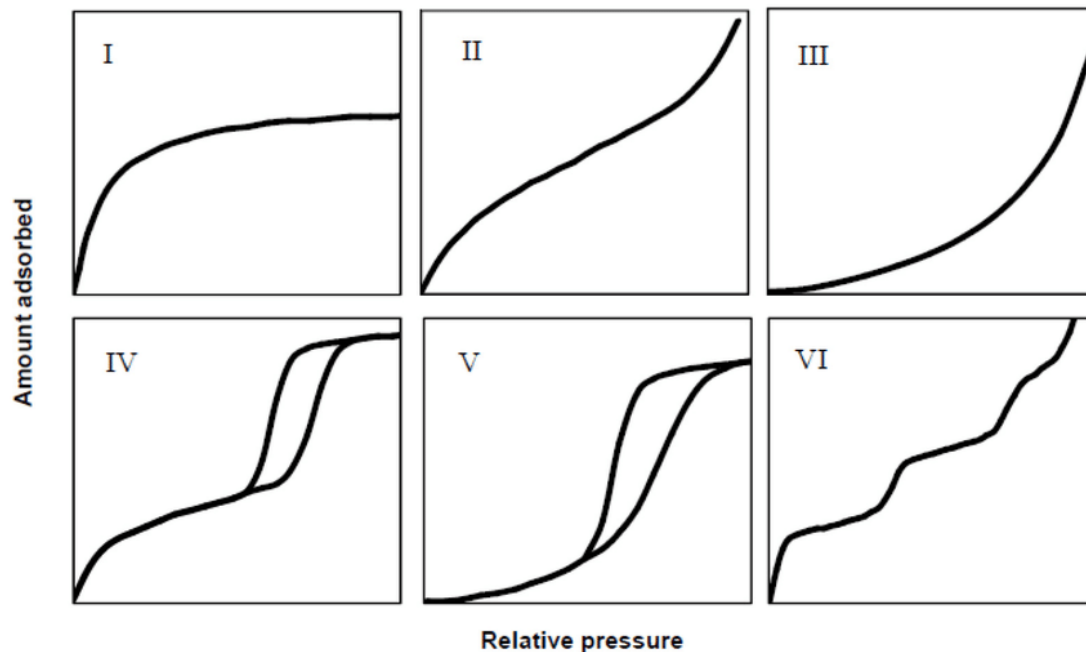


Figure Appendix 1 -1 Isotherms physisorption (IUPAC classification)^[335]

I- Type I isotherm indicates that the molecules of the adsorbate form a monolayer. It rises sharply at low relative pressures and reaches a plateau: the amount of gas adsorbed by the unit mass of solid reaches a limited value, as the relative pressure (P/P_0) is almost 1. This type of isotherm indicates the existence of micropores.

- Type II isotherm indicates an unrestricted monolayer-multilayer formation after the formation of a monolayer at low relative pressure, and is found for non-porous or macroporous adsorbents.

- Type III isotherm is not common and shows that no monolayer is formed at the surface of the solid (unrestricted multilayer). This type of isotherm is characteristic of a weak adsorbent-adsorbate interaction because the interactions between adsorbed molecules are stronger compared with the interactions between the adsorbent surface and adsorbate.

- Type IV isotherm indicates the existence of mesopores. At relatively small pressure the fast increase of the adsorbed nitrogen quantity corresponds to the adsorption of a monolayer. The presence of the mesopores (2-5 nm) can be observed at higher relative pressures when the adsorbed volume is translated by a capillary condensation phenomenon, followed by a plateau. Because of this phenomenon (irreversible nature of the capillary condensation), a hysteresis loop appears when the nitrogen starts the desorption process.

- Type V isotherm is attributed to monolayer-multilayer adsorption, it follows the same path as Type II isotherms but, it also exhibits a hysteresis loop due to capillary condensation, which is associated with the mechanism of pore filling and emptying.

- Type VI isotherm is associated with layer-by-layer adsorption on a highly uniform non-porous surface. The step-height represents the monolayer capacity for each adsorbed layer and, in the simplest case, remains nearly constant for two or three adsorbed layers.

The specific surface area, can be calculated from adsorption-desorption isotherms using the following algorithm

The Brunauer-Emmett-Teller equation is used to determine surface area of the porous material from the monolayer volume capacity (V_m):

$$\frac{P}{V(P_0 - P)} = \frac{1}{V_m C} + \frac{(C - 1)P}{V_m C P_0}$$

With V the adsorbed volume at a pressure P ; V_m is the monolayer volume; P_0 is the saturating vapor pressure of the adsorbate gas; C is constant.

$$S_{BET} = \frac{V_m}{V_{mol}} N_a \sigma$$

where σ is the molecular cross-sectional area (16.2 \AA^2 for N_2 at 77 K); V_m is the molar gas volume; N_a is Avogadro number.

The pore size distribution is calculated using the BJH method (Barrett, Jayne and Halenda). This theory is based on the phenomenon of capillary condensation which appears in the mesopores, and by applying the Kelvin law, which links the pressure P at which the condensation happens to the curvature radius of the meniscus of the formed liquid.

$$\ln \frac{P}{P_0} = - \frac{\gamma V_m}{(r_0 - t) RT}$$

where γ is the surface tension at a temperature T ; r_p is the pore radius; t is the thickness of the adsorbed layer.

This calculation is applied to the adsorption branch of the isotherm. The pore size range that can be detected by this technique is between 1.8 and 50 nm.

Appendix 2 Shea butter technical sheet



INTEREXPORT SERVICES

Fiche technique / Technical specifications Beurre de KARITE raffiné/ Refined SHEA butter

Date : 28/03/2012
Reference **ies LABO** HV014

Mode d'extraction / Extraction process : Extrait par pression puis raffiné
Obtained by pressure and refined

Origine / Origin : AFRIQUE / AFRICA

Aspect / Appearance : Solid couleur crème/Solid colour cream

Nom INCI / INCI name : BUTYROSPERMUM PARKII BUTTER

Nom CTFA /CTFA name : BUTYROSPERMUM PARKII (SHEA) BUTTER

N° CAS / CAS number : 194043-92-0

N° EINECS / EINECS number : -

Durée de vie recommandée / Shelf life : 2 ans / 2 years

CARACTERISTIQUES/CHARACTERISTICS	Valeur/Value
Indice d'acide / Acid index (mgKOH /g).....	max 2
Indice de peroxyde / Peroxide index (még O ² /kg).....	max 5
Indice d'iode / Iodine value (gI ₂ /100g).....	51 - 72
Teneur en insaponifiable / Unsaponifiable matter	% min 4
Point éclair / Flash point	°C >290
Point d'ébullition / Boiling point	°C >200
Point de fusion / Melting point	°C 32 - 44

COMPOSITION EN ACIDES GRAS/COMPOSITION IN FATTY ACIDS	%
C12:0 Acide laurique / Lauric acid	max 1
C14:0 Acide myristique / Myristic acid	max 1
C16:0 Acide palmitique / Palmitic acid	3 - 10
C18:0 Acide stéarique / Stearic acid	36 - 50
C18:1 Acide oléique / Oleic acid	40 - 50
C18:2 Acide linoléique / Linoleic acid	3 - 8
C18:3 Acide linoléique / Linolenic acid	max 1
C20:0 Acide arachidique / Arachidic acid	max 3
C20:1 Acide gadoléique / Eicosenoic acid.....	max 1
C22:0 Acide béhénique / Behenic acid	max 1
C24:0 Acide lignocérique / Tetracosenoic acid	max 1

Huiles végétales – Producteur d'extraits végétaux et de macérats huileux – Producteur BIO depuis 1995
Zone artisanale – F 04 700 ORAISON Tél. 33 4 92 72 55 55 Fax. 33 4 92 72 55 56.

E-mail: info@ieslabo.com www.ieslabo.com

SAS au capital de 37 740€ - APE 2042 Z - SIRET 334 042 496 00060 - TVA FR 33 334 042 496



Ha-Lactase 5200

Product Information

Version: 3 PI-GLOB-EN 03-14-2014

Color:	Light brown	Form:	Liquid
Solubility:	Water soluble	Odor:	Characteristic
pH:	6.50 - 8.00	Density:	1.10 - 1.20

The product may exhibit batch-to-batch color variations. This has no influence on the activity.

Formulation

Glycerol %: ≥ 45 %

Microbiological quality

Total count:	< 100 cfu/ml	Yeast and mould:	Negative in 1 ml
Clostridia:	< 1 cfu/ml	Coliform bacteria:	Negative in 5 ml
Escherichia coli:	Negative in 25 ml	Salmonella:	Negative in 25 ml
Listeria:	Negative in 25 ml	Staphylococcus aureus:	Negative in 1 ml

Conformity

Protease side activity PU/g: $\leq 75,00$ PU/G

Comments

Methods are available on request.

Our fermentation produced enzymes are tested for the relevant mycotoxins and metabolites according to JECFA's General Specifications for Enzymes.

This product complies with the recommended purity specifications for food-grade enzymes given by the Joint FAO/WHO Expert Committee on Food Additives (JECFA) and the Food Chemical Codex (FCC) with heavy metal specifications for Lead (≤ 5 ppm), Cadmium ($\leq 0,5$ ppm), Mercury ($\leq 0,5$ ppm) and Arsenic (≤ 3 ppm).

Certificate of Analysis

A Certificate of Analysis (CoA) will normally accompany the goods.

Technical Data

Temperature

The desired degree of hydrolysis can be obtained by selecting the appropriate temperature, time and dosage for the reaction. The optimal temperature is between 35-45°C (95-113°F). The enzyme is denatured at temperatures above 50°C (122°F).

Figure 1 illustrates the influence of temperature on activity using whey permeate substrate. It is often preferable to carry out hydrolysis at low temperatures to minimize microbial spoilage.

Figure 2 illustrates the degree of hydrolysis obtained in milk at 5°C (41°F) for 24 hours at different dosages of lactose. The reaction time may be reduced at higher temperatures. A hydrolysis of 80-90% is observed within 2-4 hours at 40°C (104°F) using a dosage of 2000 NLU/L.

www.chr-hansen.com

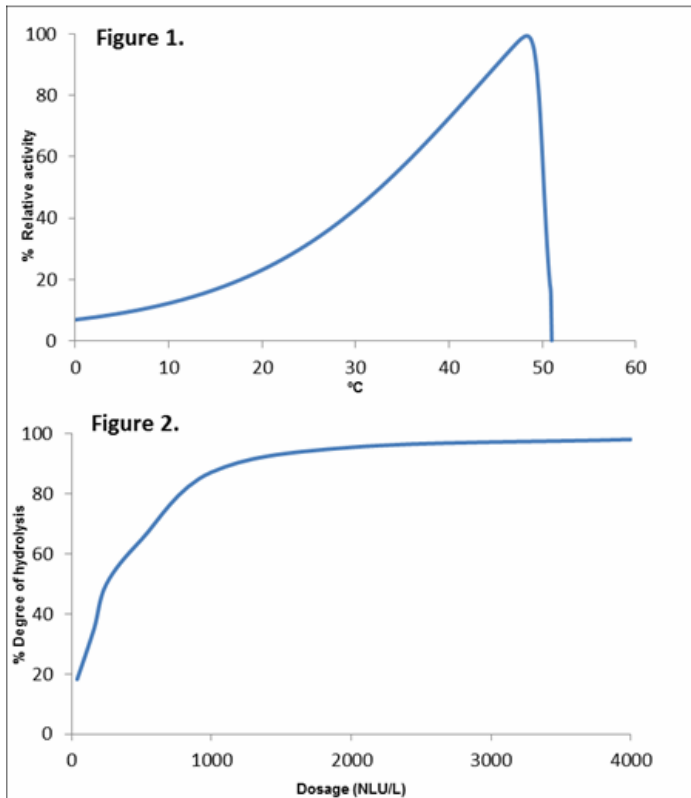
Page: 3 (7)

The information contained herein is presented in good faith and is, to the best of our knowledge and belief, true and reliable. It is offered solely for your consideration, testing and evaluation, and is subject to change without prior and further notice. There is no warranty being extended as to its accuracy, completeness, currentness, non-infringement, merchantability or fitness for a particular purpose. To the best of our knowledge and belief, the product(s) mentioned herein do(es) not infringe the intellectual property rights of any third party. The product(s) may be covered by pending or issued patents, registered or unregistered trademarks, or similar intellectual property rights. Copyright © Chr. Hansen A/S. All rights reserved.

Ha-Lactase 5200

Product Information

Version: 3 PI-GLOB-EN 03-14-2014



pH

Ha-lactase is a neutral lactase. The pH optimum is between pH 6.0 - 7.0. The enzyme is significantly inhibited at pH values below 5.5.

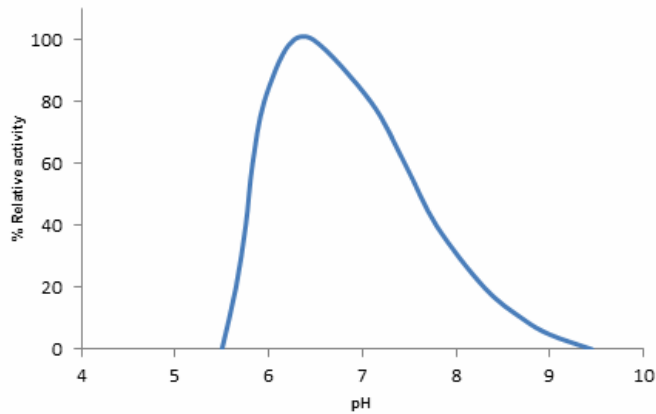
The figure illustrates the influence of pH on activity using whey permeate substrate.

Temp: 40°C (104°F), Dosage: 800 NLU/L, Substrate: Whey permeate (5% lactose)

Ha-Lactase 5200

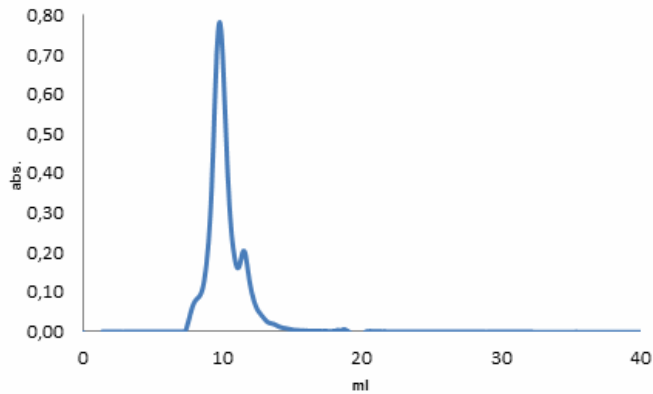
Product Information

Version: 3 PI-GLOB-EN 03-14-2014



Purity

This product is one of the purest lactase products available on the market.



Technical support

Chr. Hansen's Application and Product Development Laboratories and personnel are available if you need further information.

Dietary Information

www.chr-hansen.com

Page: 5 (7)

The information contained herein is presented in good faith and is, to the best of our knowledge and belief, true and reliable. It is offered solely for your consideration, testing and evaluation, and is subject to change without prior and further notice. There is no warranty being extended as to its accuracy, completeness, currentness, non-infringement, merchantability or fitness for a particular purpose. To the best of our knowledge and belief, the product(s) mentioned herein do(es) not infringe the intellectual property rights of any third party. The product(s) may be covered by pending or issued patents, registered or unregistered trademarks, or similar intellectual property rights. Copyright © Chr. Hansen A/S. All rights reserved.



Ha-Lactase 5200

Product Information

Version: 3 PI-GLOB-EN 03-14-2014

Kosher:	Kosher Pareve Excl. Passover
Halal:	Certified
Vegetarian:	Yes

Handling precautions

For detailed handling information, please refer to the appropriate Safety Data Sheet. Enzymes may cause irritation upon inhalation or skin contact among sensitive individuals. The use of personal protection equipments such as gloves, goggles and respiratory equipment can prevent sensitisation. For additional guidelines refer to 'Guide to the safe handling of microbial enzymes preparations' published by the Association of Manufacturers and Formulators of Enzyme Products (AMFEP) and 'Working Safely With Enzymes' by the Enzyme Technical Association (ETA).

According to EU legislation, disposal of packaging material of this product should be treated as hazardous waste. Alternatively, or for non EU countries, packaging may be disposed of as normal waste by rinsing with plenty of water to ensure no enzyme residues are present.

Legislation

This product complies with JECFA- (FAO/WHO) and FCC-recommended specifications for food-grade enzymes. The application of enzymes in food processing is governed by general food laws and by Reg. (EC) No 1332/2008. However, the approval system provided by Reg. 1332/2008 is not yet fully operational. Chr. Hansen A/S will ensure EU approval in due time. Meanwhile, please check for local/national rules or regulations as national requirements may apply.

The product is intended for use in food.

Labeling

The product is a processing aid. There are no legislative requirements for labelling processing aids on final food products.

Trademarks

Product names, names of concepts, logos, brands and other trademarks referred to in this document, whether or not appearing in large print, bold or with the ® or TM symbol are the property of Chr. Hansen A/S or used under license. Trademarks appearing in this document may not be registered in your country, even if they are marked with an ®.

Additional information

The following application sheets are available upon request:

- Ha-lactase™ - Milk
- Ha-lactase™ - Fermented milk products
- Ha-lactase™ - Dulce de leche
- Ha-lactase™ - Ice cream

www.chr-hansen.com

Page: 6 (7)

The information contained herein is presented in good faith and is, to the best of our knowledge and belief, true and reliable. It is offered solely for your consideration, testing and evaluation, and is subject to change without prior and further notice. There is no warranty being extended as to its accuracy, completeness, currentness, non-infringement, merchantability or fitness for a particular purpose. To the best of our knowledge and belief, the product(s) mentioned herein do(es) not infringe the intellectual property rights of any third party. The product(s) may be covered by pending or issued patents, registered or unregistered trademarks, or similar intellectual property rights. Copyright © Chr. Hansen A/S. All rights reserved.

Ha-Lactase 5200

Product Information

Version: 3 PI-GLOB-EN 03-14-2014

GMO Information

In accordance with the legislation in the European Union* we can state that Ha-Lactase 5200 does not contain GMOs and does not contain GM labeled raw materials**. In accordance with European legislation on labeling of final food products** we can inform that the use of Ha-Lactase 5200 does not trigger a GM labeling of the final food product. Chr. Hansen's position on GMO can be found on: [www.chr-hansen.com/About us/Policies and positions/Quality and product safety](http://www.chr-hansen.com/About-us/Policies-and-positions/Quality-and-product-safety).

* Directive 2001/18/EC of the European Parliament and of the Council of 12 March 2001 on the deliberate release into the environment of genetically modified organisms and repealing Council Directive 90/220/EEC.

** Regulation (EC) No 1829/2003 of the European Parliament and of the Council of 22 September 2003 on genetically modified food and feed.

Regulation (EC) No 1831/2003 of the European Parliament and of the Council of 22 September 2003 concerning the traceability and labeling of genetically modified organisms and the traceability of food and feed products produced from genetically modified organisms and amending Directive 2001/18/EC.

Allergen Information

List of common allergens in accordance with the US Food Allergen Labeling and Consumer Protection Act of 2004 (FALCPA) and EU labeling Directive 2000/13/EC with later amendments	Present as an ingredient in the product
Cereals containing gluten* and products thereof	No
Crustaceans and products thereof	No
Eggs and products thereof	No
Fish and products thereof	No
Peanuts and products thereof	No
Soybeans and products thereof	No
Milk and products thereof (including lactose)	No
Nuts* and products thereof	No
List of allergens in accordance with EU labeling Directive 2000/13/EC only	
Celery and products thereof	No
Mustard and products thereof	No
Sesame seeds and products thereof	No
Lupine and products thereof	No
Mollusks and products thereof	No
Sulphur dioxide and sulphites at concentrations of more than 10 mg/kg or 10 mg/litre expressed as SO ₂	No

* Please consult the EU Labeling Directive 2000/13 Annex IIIa for a legal definition of common allergens, see European Union law at: www.eur-lex.europa.eu